

Nitrogen and Sulphur biogeochemistry in a High Arctic glacial watershed: an investigation with isotopic tracers and solute chemistry



Arif Husain Ansari
Department of Geography
The University of Sheffield

June 2012

Thesis submitted for the degree of Doctor of Philosophy

Table of Contents

Nitrogen and Sulphur biogeochemistry in a High Arctic glacial watershed: an investigation with isotopic tracers and solute chemistry	i
Acknowledgements.....	2
CHAPATER 1: INTRODUCTION	3
1.1 Significance of this study	3
1.2 Aim of the study.....	4
1.3 Thesis outline	6
CHAPTER 2: NITROGEN AND SULPHUR BIOGEOCHEMICAL CYCLING IN HIGH ARCTIC: A REVIEW	7
2.1 Nitrogen Biogeochemistry	7
2.1.1 Introduction	7
2.1.2 Source of fixed nitrogen to the Arctic.....	9
2.1.2.1 Atmospheric input.....	9
2.1.2.1.1 Stratospheric input	10
2.1.2.1.2 Tropospheric input	12
2.1.2.2 Geological nitrogen.....	13
2.2 Sulphur Biogeochemistry	16
2.2.1 Introduction.....	16
2.2.2 Source of sulphur in the Arctic	17
2.2.2.1 Atmospheric input.....	17
2.2.2.1.1 Biogenic	17
2.2.2.1.2 Volcanic emission, sea spray and dust.....	18
2.2.2.1.3 Anthropogenic.....	18
2.2.2.2 Geological sulphur	19
2.3 Deposition of atmospheric nitrogen and sulphur	19
2.4 Post-deposition processes.....	22
2.5 Snow and supraglacial ice biogeochemistry	24
2.6 Subglacial and Proglacial runoff biogeochemistry	26
2.7 Stable isotopes in biogeochemical studies	30

2.7.1 Stable isotope composition of major N and S sources in High Arctic	31
2.7.2 Fractionation	34
2.7.2.1 Kinetic fractionation	35
2.7.2.2 Equilibrium fractionation	35
2.8 Nitrogen based biological processes responsible for isotopic fractionation	35
2.8.1 Nitrogen fixation	35
2.8.2 Assimilation	36
2.8.3 Mineralisation and Nitrification	36
2.8.4 Denitrification	38
2.8.5 Dissimilatory nitrate reduction to ammonia (DNRA)	38
2.8.6 Anammox	39
2.9 Sulphur based biological processes responsible for isotopic alterations	39
2.9.1 Sulphide oxidation	39
2.9.2 Sulphate reduction	40
CHAPTER 3: FIELD SITE AND METHODOLOGY	41
3.1 Svalbard climate and its importance in research context	41
3.2 Field Site: Glacier Midtre Lovénbreen	45
3.2.1 Geology	47
3.2.2 Ecology	49
3.2.3 Glacier structure	51
3.2.4 Mass Balance	52
3.2.5 Hydrology	53
3.3 Sampling	54
3.3.1 Sampling sites and sampling frequency	54
3.3.2 Winter deposition sampling	57
3.3.3 Summer stream sampling	57
3.3.4 Sample preservation	57
3.3.5 Real time stream monitoring	58
3.4 Chemical analysis	60
3.4.1 Dissolved Organic Carbon (DOC)	60
3.4.2 Total dissolved nitrogen (TDN) and dissolved organic nitrogen (DON) by Thermalox analyser	61

3.4.3 Dissolved organic nitrogen (DON) by persulphate oxidation method.....	62
3.4.4 Major ions	63
3.4.5 Dissolved silicate (SiO ₂)	64
3.5 Analysis of stable isotopic tracers.....	65
3.5.1 Denitrifier method for δ ¹⁵ N-NO ₃ and δ ¹⁸ O-NO ₃ analysis using GC-IRMS	65
3.5.2 δ ³⁴ S-SO ₄ and δ ¹⁸ O-SO ₄ analysis.....	65
3.5.3 δ ¹⁸ O-H ₂ O Analysis.....	66
3.6 Rock dissolution experiments	66
3.6.1 Dissolution experiments.....	67
3.6.2 Adsorption experiment.....	68
CHAPTER 4: RESULTS.....	70
4.1 Ny Ålesund Meteorology	70
4.2 Hydrological conditions	72
4.3 Snow solute chemistry	73
4.3.1 Year 2009.....	75
4.3.2 Year 2010.....	76
4.4 Stream nitrogen and sulphur dynamics	77
4.4.1 Year 2009.....	79
4.4.1.1 Spatio-temporal nitrogen dynamics	81
4.4.1.2 Spatio-temporal sulphate dynamics	83
4.4.2 Year 2010.....	86
4.4.2.1 Spatio-temporal nitrogen dynamics	91
4.4.2.2 Spatio-temporal sulphate dynamics	92
4.5 Isotopic characterisation.....	96
4.5.1 Year 2009	96
4.5.1.1 δ ¹⁵ N, δ ¹⁸ O-NO ₃ and δ ¹⁸ O-H ₂ O of snow and streams.....	96
4.5.1.2 δ ³⁴ S-SO ₄ and δ ¹⁸ O-SO ₄ of streams	98
4.5.2.1 δ ¹⁵ N, δ ¹⁸ O-NO ₃ and δ ¹⁸ O-H ₂ O of snow and streams.....	100
4.5.2.2 δ ³⁴ S-SO ₄ and δ ¹⁸ O-SO ₄ of streams	103
4.6 Dissolution experiment results	104
4.6.1 Rock nitrogen, sulphur and their isotopic composition	104

4.6.2 Dissolved inorganic nitrogen and other ions release from rock dissolution	104
4.6.3 Nitrogen adsorption efficiency of the rocks.....	106
4.7 Summary	107
CHAPTER 5: DISSCUSSION.....	109
5.1 Snow nitrogen sources, abundance and their annual variability	109
5.1.1 Isotopic insights	109
5.1.2 Dissolved organic nitrogen	112
5.2 Snow sulphur sources, abundance and their annual variability	115
5.2.1 Isotopic insights	115
5.3 Spatio-temporal stream nitrogen dynamics.....	116
5.3.1 Year 2009.....	117
5.3.1.1 Subglacial nitrogen biogeochemical cycling	119
5.3.1.2 Proglacial nitrogen biogeochemical cycling	124
5.3.2 Year 2010.....	126
5.3.2.1 Downstream nitrogen changes	129
5.3.3 Nitrogen release from rock weathering.....	131
5.4 Stream sulphur dynamics	132
5.4.1 Source and production pathways of sulphate.....	133
5.4.2 Spatio-temporal stream sulphate dynamics.....	137
5.5 Summary	139
CHAPTER 6: CONCLUSION.....	141
6.1 Summary comments and conceptual model.....	141
6.1.1 Nitrogen biogeochemical cycling	141
6.1.2 Sulphur biogeochemical cycling.....	144
6.2 Recommendations for future work.....	146
BIBLIOGRAPHY	147
APPENDIX.....	194

Table of Figures

Figure 2.1. Dynamical aspects of stratosphere-troposphere exchange	11
Figure 2.2. SO _x and NO ₃ deposition in the Arctic during 2006 (adapted from AMAP assessment 2006: Acidifying Pollutants, Arctic Haze, Acidification in the Arctic, Figure 3.20)	21
Figure 2.3. (a) δ ¹⁵ N and (b) δ ³⁴ S distribution in various ecosystems	33
Figure 2.4. A schematic diagram of oxygen atom incorporation from O ₂ and H ₂ O during nitrification and denitrification	37
Figure 3.1. Svalbard Map and its position on globe	42
Figure 3.2. North Atlantic Oscillation showing positive and negative mode circulation pattern. 44	
Figure 3.3. Glacier Midtre Lovénbreen situated on Ny Alesund, Svalbard	46
Figure 3.4. Geological map of the Midtre Lovénbreen glacier.....	48
Figure 3.5. Physically active, intermittent and inactive zone in Midtre Lovénbreen catchement. 50	
Figure 3.6. Midtre Lovénbreen map of 2009 sampling set up. UPW is the upwelling site and MLE1 and MLW1 are the downstream sites on the eastern and western streams respectively. SG1-SG5 are supraglacial sites.....	55
Figure 4.1. Meteorological conditions at the Ny Alesund during 2009 and 2010.....	71
Figure 4.2. Daily average discharge variations at MLE1 and MLW1 during summer 2009	72
Figure 4.3. Daily average discharge variations at MLE1 and MLW1 during summer 2010	73
Figure 4.4. Altitudinal variations of Ca ²⁺ , Mg ²⁺ , Cl ⁻ , SO ₄ ²⁻ concentrations in the 2009 snow	75
Figure 4.5. Altitudinal variations of Ca ²⁺ , Mg ²⁺ , Cl ⁻ , SO ₄ ²⁻ concentrations in the 2010 snow....	77
Figure 4.6. Panels (a), (b) and (c) shows the temporal variation of Mg ²⁺ , Na ⁺ , and Cl ⁻ at MLE1, MLW1 and UPW sites respectively during 2009	80
Figure 4.7. Panels (a), (b) and (c) shows temporal variation of NO ₃ ⁻ -N, Cl ⁻ and DOC at MLE1 MLW1 and UPW during summer 2009.....	82
Figure 4.8. Spatial and temporal variations of NO ₃ ⁻ -N/Cl ⁻ concentration ratio in the stream water at MLE1, MLW1, UPW during summer 2009	83
Figure 4.9. Temporal variations of Ca ²⁺ / SO ₄ ²⁻ molar ratios and non-snow, snow SO ₄ ²⁻ at the (a) MLE1 and (b) MLW1 and (c) UPW and the temporal variations of Ca ²⁺ , K ⁺ , SO ₄ ²⁻ at the (d) MLE1, (e) MLW1, and (f) UPW during summer 2009.....	85

Figure 4.10. Spatial and temporal variations of Mg^{2+} and Si in the eastern stream during summer 2010	89
Figure 4.11. Spatial and temporal variations of Na^+ and Cl^- in the eastern stream during summer 2010.....	89
Figure 4.12. Spatial and temporal variations of Mg^{2+} and Si in the western stream during summer 2010.....	90
Figure 4.13. Spatial and temporal variations of Na^+ and Cl^- in the western stream during summer 2010.....	90
Figure 4.14. Spatial and temporal variation of NO_3^- -N, NH_4^+ -N, DON, and DOC/DON in the eastern stream during summer 2010	91
Figure 4.15. Spatial and temporal variations of NO_3^- -N, NH_4^+ -N, DON, and DOC/DON in the western stream during 2010.....	92
Figure 4.16. Spatial and temporal variations of Ca^{2+} , SO_4^{2-} , K^+ in the eastern stream during 2010	93
Figure 4.17. Spatial and temporal variations of Ca^{2+} , SO_4^{2-} , K^+ in the western stream during 2010	94
Figure 4.18. Spatial and temporal variations of snow, non snow derived SO_4^{2-} and Ca^{2+}/SO_4^{2-} molar ratio in the eastern stream during summer 2010	95
Figure 4.19. Spatial and temporal variations of snow, non-snow derived SO_4^{2-} and Ca^{2+}/SO_4^{2-} molar ratio in the western stream during 2010.....	95
Figure 4.20. $\delta^{15}N$ - NO_3 versus $\delta^{18}O$ - NO_3 plot for the snow and stream samples during 2009	98
Figure 4.21. $\delta^{34}S$ - SO_4 Vs SO_4^{2-} plot for 2009 and 2010 summer stream samples. The two circles represent the two types of SO_4^{2-} regime: one pre DOY 196 and other post DOY 196 during summer 2009	99
Figure 4.22. Temporal variations of stream's $\delta^{18}O$ - SO_4 during summer 2009	99
Figure 4.23. $\delta^{15}N$ - NO_3 versus $\delta^{18}O$ - NO_3 plot for the snow and stream samples during 2010 ...	101
Figure 4.24. $\delta^{15}N$ - NO_3 and $\delta^{18}O$ - NO_3 spatial and temporal variation in the eastern stream during summer 2010.....	102
Figure 4.25. $\delta^{15}N$ - NO_3 and $\delta^{18}O$ - NO_3 spatial and temporal variation the western stream during summer 2010.....	102

Figure 4.26. Spatial and temporal variations in $\delta^{34}\text{S-SO}_4$ and $\delta^{18}\text{O-SO}_4$ in the eastern stream during 2010	103
Figure 4.27. $\text{NH}_4^{+}\text{-N}$ and $\text{NO}_3^{-}\text{-N}$ release from the three Midtre Lovenbreen rocks	105
Figure 4.28, NH_4^{+} adsorption isotherm curve for the three major rocks from the Midtre Lovenbreen	106
Figure 5.1. $\delta^{15}\text{N-NO}_3$ versus $\delta^{18}\text{O-NO}_3$ variations at Midtre Lovenbreen. Individual data points are from the present study, while the larger annotated rectangles represent the domain of graph occupied by results from previous work at this site (“Snow”, “Supraglacial streams” and “Subglacial upwelling”). The shaded rectangle (“Bacterial”) depicts the predicted composition of microbially produced NO_3^{-}	110
Figure 5.2. Mean atmospheric temperature variation in Ny Alesund during summer 2009 and 2010.....	118
Figure 5.3. Schematic diagram of average discharge weighted total dissolved nitrogen (TDN) concentration in the subglacially routed eastern stream (between DOY 198 and DOY 250)...	120
Figure 5.4. $\delta^{15}\text{N-NO}_3$ versus $\delta^{18}\text{O-NO}_3$ variation at the three stream sites and in the snowpacks. The shaded rectangle (“Bacterial nitrate”) depicts the predicted composition of microbially produced NO_3^{-} , while the grey arrow shows a hypothetical denitrification vector.....	125
Figure 5.5. Daily mean temperature variation of eastern stream water during summer 2009 and 2010.....	127
Figure 5.6. $\delta^{15}\text{N}$ versus $\delta^{18}\text{O}$ of snow and stream NO_3^{-} during 2010. The grey line between snow and bacterial n member show the possible mixing of two NO_3^{-} sources, whilst the other grey line represents the possible denitrification of mixed NO_3^{-} in subglacial system	128
Figure 5.7. Schematic diagram of average discharge weighted total dissolved nitrogen (TDN) concentration in the subglacially routed eastern stream (between DOY 186 to DOY 227, 2010)	129
Figure 5.8. Schematic diagram of average discharge weighted total dissolved nitrogen (TDN) concentration in the western (between DOY 186 to DOY 227, 2010).....	129
Figure 5.9. $\delta^{18}\text{O-SO}_4$ Vs $\delta^{34}\text{S-SO}_4$ plot for the stream sites during summer 2009 and 2010 .	134
Figure 5.10. Relationship between Ca^{2+} and SO_4^{2-} of Midtre Lovenbreen proglacial streams ..	136
Figure 6.1. Conceptual model of dissolved available nitrogen in Midtre Lovenbreen.....	143
Figure 6.2. Conceptual model of dissolved sulphur in Midtre Lovenbreen	145

List of Tables

Table 2.1 Stable isotopes of N, O and S	30
Table 3.1. Operatic condition of the Thermalox TC/TN analyser	61
Table 3.2. Operatic condition of the Thermalox TC/TN analyser	62
Table 3.3. Operating conditions for cations.....	63
Table 3.4. Operating conditions for anions.....	63
Table 4.1. Average concentrations (\pm standard deviation) of solute and their ratio against Cl^- in snow [SSR = Sea Salt Ratio (Wilson, 1975) and n = number of samples].....	74
Table 4.2. Average concentration of solute and their ratio against Cl^- at UPW, MLE1, and MLW1 during summer 2009	78
Table 4.3. Average concentrarion of ions, DOC, DON with standard deviation at the stream sites during 2010	87
Table 4.4. Average of ionic ratios with standard deviation at the stream sites durinf summer 2010	88
Table 4.5. Average of stable isotope composition of NO_3^- , SO_4^{2-} , H_2O in snow and stream samples during 2009	96
Table 4.6. Average stable isotope composition of NO_3^- , SO_4^{2-} , H_2O in snow and stream samples during 2010	100
Table 4.7, The content of nitrogen, sulphur and its respective isotope signature for the six major meta-sedimentary rocks collected from the Midtre Lovenbreen catchment (Wynn, 2004)	67
Table 4.8, Release of major ions during the dissolution of three abundant meta-sedimentary rocks from Midtre Lovenbreen	105

Table AI. Solute chemistry of five supraglacial snowpit samples collected in early June 2009	194
Table AII. Solute chemistry parameters of five supraglacial snowpit samples collected in late May	194
Table AIII. Solute chemistry parameters of the MLE1, MLW1, and UPW during summer 2009	194
Table AIV. Solute chemistry at the seven proglacial stream sites during summer 2010	196
Table AV. Isotopic compositions of five isotopic composition of five supraglacial snowpit samples collected in late spring 2009 and 2010.....	197
Table AVI. Isotopic compositions of stream samples during summer 2009	198
Table VII. Isotopic compositions of streams during summer 2010.....	198

Abstract

This study covered two Arctic summer seasons (2009 and 2010). The first focussed upon temporal dynamics of N and S biogeochemistry, whilst the second study was more focussed upon spatial dynamics. Further lab-based rock dissolution and adsorption experiments were conducted and integrated with stream chemistry data to understand geological controls upon catchment scale N and S biogeochemistry.

This study reveals DON as the major component of nitrogen pool (ca. 42-70%) in the snow, followed by NO_3^- -N (ca. 18-34%) and NH_4^+ -N (ca. 17-24%). However, the composition changes annually. DON largely comes from marine biogenic sources and during the summer plays a major role in subglacial biogeochemical cycling (i.e. a substrate for NO_3^- -N production). Isotopic evidence suggests that in both subglacial and proglacial streams NO_3^- -N production and removal processes occur simultaneously. Furthermore, rock dissolution experiments demonstrate that geological nitrogen can be a source of the additional NO_3^- -N seen in subglacial runoff and proglacial streams. However N content, composition, biogeochemical processes and their detectability in Arctic streams varies each year due to climatic conditions.

This study also reveals that; sea-salt, anthropogenic and di-methyl sulphide (DMS)-derived SO_4^{2-} are three major sources to Arctic snow SO_4^{2-} and their relative fraction vary annually. In the proglacial streams, aerobic biological oxidation of sulphide minerals seems the most plausible SO_4^{2-} production mechanism. The ionic data of the subglacial runoff and proglacial streams demonstrate that sulphide oxidation was more important in the subglacial environment than in open proglacial streams. The coupling between sulphide oxidation – calcite weathering was more significant in the proglacial streams.

Acknowledgements

It is a great pleasure to thank all those peoples who have supported in various ways to make this thesis possible.

First and foremost I would like to express my deep gratitude to my advisors Prof. Andrew Hodson and Dr. Tim Heaton for their continuous support and encouragement during my PhD study and research. I could not have imagined having better advisors and mentors for my PhD study.

I would like to thank all those people who have provided their invaluable support in field work as well as laboratory works. The help of Dr. Tris Irwvine Fynn, Aga Nowak, Mats Björkman in sample collection, during my field work was immense. I am also thankful to Nick Cox, station manager at NERC British Arctic Station (Ny Ålesund, Svalbard) for providing the necessary logistical support. I would like to thank William Crow, Kath Taylor, Claire Plant (University of Sheffield), Dr. Tim Heaton (NERC Isotope Geosciences Laboratory, Nottingham) Dr. Jan Kaiser, Dr. Alina Marca-Bell and Laura Campisi (University of East Anglia) for their generous support in the laboratory whilst providing me basic training on the various instruments and techniques used in this study, as well as for analysing some of the samples.

This work was supported by NSINK project (EU Marie Curie action plan, project no: R/123386).

CHAPTER 1: INTRODUCTION

“Hidden in wonder and snow, or sudden with summer, this land stares at the sun in a huge silence endlessly repeating something we cannot hear. inarticulate, arctic, not written on by history, empty as paper, it leans away from the world with songs in its lakes older than love, and lost in the miles.”

(Frank Scott)

1.1 Significance of this study

Since the late 20th century polar sciences have become a promising tool for investigating global climate change. Recently, research in the Polar Regions has become an increasingly more advanced component of all branches of the earth system science (atmosphere, lithosphere, hydrosphere and biosphere). Polar sciences are also used as a forensic tool to study Martian climate and geomorphology. Recent studies are also helping to understand how changes in Polar environments are connected to anthropogenic activities taking place miles away at lower latitude. For example, the ever increasing demand of a growing human population has led to the intensification of agriculture, industrialization and fossil fuel consumption, causing backlashes in the form of increasing airborne reactive nitrogen and sulphur and their extensive redistribution (Barrie and Hoff 1985; Barrie et al., 1985; Mosier et al., 2001). This is evident from increased deposition of nitrogen and sulphur to remote, fragile and relatively pristine environments such as those of the Arctic. That has led to increased acidification of Arctic snow, ice and fresh water bodies, since the industrial revolution (Barrie et al., 1985; Barrie et al., 1989).

In addition, many high latitude terrestrial ecosystems are considered nitrogen limited (Chapin and Shaver, 1996) with the input of nitrogen being through fixation, predominantly by cyanobacteria, which is thought to account for between 25% to 70% of the total annual ecosystem nitrogen input (Chapin & Bledsoe, 1992). Therefore even small increase in wet and dry deposition of nitrogen may represent significant additional contributions (Tye et al., 2005). At the same time evidence of biological activity in snow, ice, moraine and soil environments has been recorded in the Polar Regions. This brings a realisation that biological, chemical and physical changes in the Arctic environment occur in direct response to global climate change. Hence the study of ecosystem response to climate and pollution drivers is a very urgent research priority.

Many appreciable efforts have been made by researchers to describe the nitrogen and sulphur cycles in fragile High Arctic ecosystems. However the nitrogen and sulphur cycles are still far from being properly understood, and so this area still presents a very good opportunity to examine the sensitivity of this environment to the impact of anthropogenic activity. The present study therefore seeks to have a better understanding of the contribution of glacial microbial habitats to the High Arctic nitrogen and sulphur cycles, and then to indicate the likely direction of change in the ecosystem as a consequence of climate and atmospheric inputs of nitrogen and sulphur.

1.2 Aim of the study

Based on the previous work, the aim of this study is to improve the understanding of the fate of atmospheric and geologic nitrogen and sulphur in High Arctic glacial ecosystems by using stable isotopic tracers (^{15}N , ^{18}O , ^{34}S), catchment scale nutrient budgets and major ion chemistry. To achieve this aim the following objectives were set up:

- a) Isotopic characterization of the nitrogen sources to snowpack, subglacial and proglacial melt waters and sediment at different stages of annual cycle.
- b) Develop a flow-chart for total dissolved nitrogen flux from glacial to proglacial watershed to reveal their potential zone of sources and sinks.
- c) Carry out lab-based rock dissolution experiment to understand the NO_3^- and NH_4^+ release and therefore their significance in the local nitrogen biogeochemical cycling.

1.3 Thesis outline

This thesis comprises of 6 Chapters. Chapter 1 highlights the aims of study and its importance in the present scenario of climate change. Chapter 2 presents a review of the previous works done on atmospheric inputs of nitrogen and sulphur to the High Arctic glacial ecosystems, and subsequent biogeochemical processing especially during summer melt. This also includes the use of stable isotopes in order to identify and differentiate the major biological and abiological processes. Chapter 3 describes the field site location, its strategic importance, climate, ecology, hydrology and glaciology, the methodology used for sampling and chemical analysis, and the experiments employed to fulfil this study. Chapter 4 presents the hydro-meteorological data and the results of the chemical and isotopic analysis of snow, stream water and sediments collected during field work. Chapter 5 discusses these results in order to explain the major sources-sinks and related biochemical process involving of nitrogen and sulphur. This chapter further discusses the spatial and temporal variability in the nitrogen and sulphur based biogeochemical process as well as the impact of annual change in hydro-meteorological conditions. Chapter 6 outlines the concluding remarks from the study and suggests some pointers for further research.

CHAPTER 2: NITROGEN AND SULPHUR BIOGEOCHEMICAL CYCLING IN HIGH ARCTIC: A REVIEW

This chapter discusses the previous work on nitrogen and sulphur biogeochemical cycling in the High Arctic. Section 2.1 and 2.2 present the possible sources of nitrogen and sulphur respectively in High Arctic terrestrial ecosystems. Major depositional and post-depositional processes that normally take place in the study area are discussed in Section 2.3 and 2.4. Then a review of nitrogen and sulphur biogeochemical cycling in snow and ice is presented in section 2.5 before glacial streams are considered in section 2.6. Finally, Section 2.7 presents review upon N and S stable isotope biogeochemistry.

2.1 Nitrogen Biogeochemistry

2.1.1 Introduction

Nitrogen is an important structural and functional component of many necessary compounds, particularly proteins, which collectively represent a large portion of living biomass on the Earth. However a large portion of free gaseous nitrogen in the atmosphere has limited reactivity in normal conditions because of the triple bond between the two nitrogen atoms ($N \equiv N$) (Gambarotta, 1995). This is why nitrogen is often a limiting nutrient in the condensed phase. Further, due to different productivity in different climatic conditions, their respective biomass nitrogen contents are also variable. For example, because of higher productivity, biomass nitrogen content in tropical regions is generally higher than polar regions (Jaffe, 1992).

In most natural systems, available or fixed nitrogen is usually the limiting factor among the nutrients for plant growth. Conversion of free N₂ into bio-available forms is achieved via three well known pathways, biological (mostly by cyanobacteria and some plants), chemical (nitrogen fertilizers made by humans; Haber-Bosch process) and physical (by lightning). Biological fixation is the most significant pathway followed by chemical fixation by humans. The increasing demand of a growing population led to the invention and the massive use of nitrogen fertilizers during the 20th century thereupon causing a tremendous increase of various nitrogen species in the biosphere. According to Smil (1997), without use of this nitrogenous fertilizer, Earth could not have supported its current population. At the same time, the widespread use of fossil fuels releases not only carbon dioxide, but nitrogen oxides (NO_x) as well. However, global creation of NO_x through fossil fuel combustion has been found constant at about 25 Tg N yr⁻¹ from 1995 to 2000 (Cofala et al., 2007). The combined effect of these two anthropogenic processes, agriculture and fossil fuel combustion, is similar in magnitude to natural nitrogen fixation (Galloway et al., 1995; Jaffe, 2000). Substantial impacts of this NO_x increase in biosphere are evident in a number of areas, including photochemical smog, acid precipitation, stratospheric ozone chemistry, regional eutrophication, and ecosystem diversity.

In the Arctic, the largest proportion of total fixed nitrogen is considered to be sourced through biological fixation by free living cyanobacteria and microbes living in association with bryophytes and fungi (Solheim et al., 1996). Atmospheric input is considered as the second largest source of fixed nitrogen, which mostly originates from industrial emission and other anthropogenic activity in north Eurasia and America (Barrie, 1986; Law and Stohl 2007). The climatic set up during late winter and early spring helps to bring this polluted air mass to the Arctic (see Section 3.1). Snow core records from the Arctic have demonstrated a continuous net increase in atmospheric nitrogen input during rapid industrialisation (since 1900) in Europe and America (Smiöes and Zagorodnov, 2001). However, a slight decrease has been recorded since 1990 probably because of better control on emission. This atmospheric input is also very much variable, depending upon climatic conditions: for example

episodic nitrogen enrichment was documented in Svalbard during June 1999 (Hodson et al., 2010a). In addition some rocks also carry relatively significant amount of fixed nitrogen in its lattice (Rayleigh, 1939; Hutchinson, 1944; Holloway et al 2001) but its release rate to the open environment remains questionable to be a serious point source. In such conditions Arctic ecosystems become very much sensitive to even a small increase or decrease in the above sources of available nitrogen. During summer when the snow starts melting, the interaction between deposited (through wet and dry deposition) nitrogen and Arctic glacial ecosystems reaches a significant level (Gooseff et al, 2004; Hood et al., 2009; Hodson et al., 2010b). Biological activity can vary depending upon spatial and temporal changes in production. For example, Hodson et al., (2005b) and Wynn et al., (2006, 2007) indicated Midtre Lovénbreen subglacial system acts as a NO_3^- source during summer, and a sink during winter. Since, the provenance and fate of nitrogen in active proglacial streams lacks knowledge, so biotic and abiotic nitrogen speciation in this area is still far from being understood and needs to be established in order to prepare a nitrogen budget.

2.1.2 Source of fixed nitrogen to the Arctic

2.1.2.1 Atmospheric input

In the Arctic wet and dry deposition of atmospheric nitrogen species are considered one of the major sources of available nitrogen to terrestrial ecosystems. This atmospheric deposition mostly takes place during early and late winter when the meteorological set up become favourable to transport larger amount of polluted air mass from heavily populated and industrial part of the Eurasia and North America (Barrie and Hoff, 1985; see Section 3.1). Nitrogen through these air masses is carried both in the form of organic [i.e. Peroxy-acetylene nitrate (PAN), Peroxypropionyl nitrate (PPN)] and inorganic species (i.e. NO_x , NH_4^+). But in long range transport, organic species have been identified as being more persistent than inorganic ones (i.e. NO_3^- , NH_4^+) because of their less effective removal from the atmosphere (Singh and Hanst,

1981; Gorzelska and Galloway, 1990; Matsumoto and Uematsu, 2005). Usually the transport takes place via the troposphere as well as the stratosphere, however the largest portion travels through the lower middle troposphere (between 0 to 3.5 km; Barrie et al., 1988). From the isotopic studies of snow NO_3^- it has been suggested that stratospheric origins or long range tropospheric transportation might cause mass-dependent isotope fractionation, resulting in a relatively light ^{15}N signature (-2 to -20‰ ; Heaton et al., 2004; Wynn et al., 2007). To explain this lighter ^{15}N signature in the Arctic atmosphere and snow, another theory has been put forward by Morin et al., (2008), according to which photolytic recycling of snow NO_3^- regulates the $\delta^{15}\text{N-NO}_3$ value both in snow and the atmosphere. During summer, photolysis of NO_3^- in upper snow releases the lighter $^{14}\text{NO}_x$ into the atmosphere, leaving snow NO_3^- enriched in ^{15}N (ca. $\delta^{15}\text{N-NO}_3$ -1‰). Subsequent re-deposition of the released $^{14}\text{NO}_x$ in the following winter-spring then enriches the snow NO_3^- with ^{14}N leading to $\delta^{15}\text{N}$ values (ca. -15‰). Nonetheless, these hypotheses remain an issue of active debate and need more evidence to become established. The $\delta^{18}\text{O-NO}_3$ values of Ny Ålesund snow generally ranges between $+50\text{‰}$ and $+70\text{‰}$ (Wynn et al., 2007) which is derived from the probable reaction of NO_x with tropospheric ozone (Johnston and Theimens, 1997) in the atmosphere.

2.1.2.1.1 Stratospheric input

Air mass exchange between stratosphere and troposphere has been evident (Holton et al., 1995) and is of great interest in the debate over light $\delta^{15}\text{N}$ values in Arctic snow. The two atmospheric regions are separated by the tropopause, which has the lowest temperature lapse rate of about 2°K km^{-1} . This tropopause has surface potential temperature of about 380°K , found at a height of 15-18 km in tropics (Holton et al., 1995). But in the pole it slopes downwards up to 6-8 km and has a potential temperature of $290\text{-}320^\circ\text{K}$. Warm air in the tropics upwells and penetrates into stratosphere (Plumb et al., 1996), and here it moves towards poles. Rossby and gravity waves also play a significant role in pushing the air masses towards the poles (Figure

2.1). These waves act as a suction pump to draw up tropical upper troposphere air masses and push them polewards and finally downwards (Brewer et al., 1949). However, it has been suggested that such transport is slow because air must cross isentropic surfaces, which require diabatic cooling (Holten et al., 1995). In the Polar Regions these air masses start to subside into the troposphere (Holton et al., 1995). Transport from the stratosphere to the troposphere is comparatively faster but the transport of air from the troposphere to the stratosphere requires energy for adiabatic cooling, which is normally unusual in polar region except in the case of volcanic eruption.

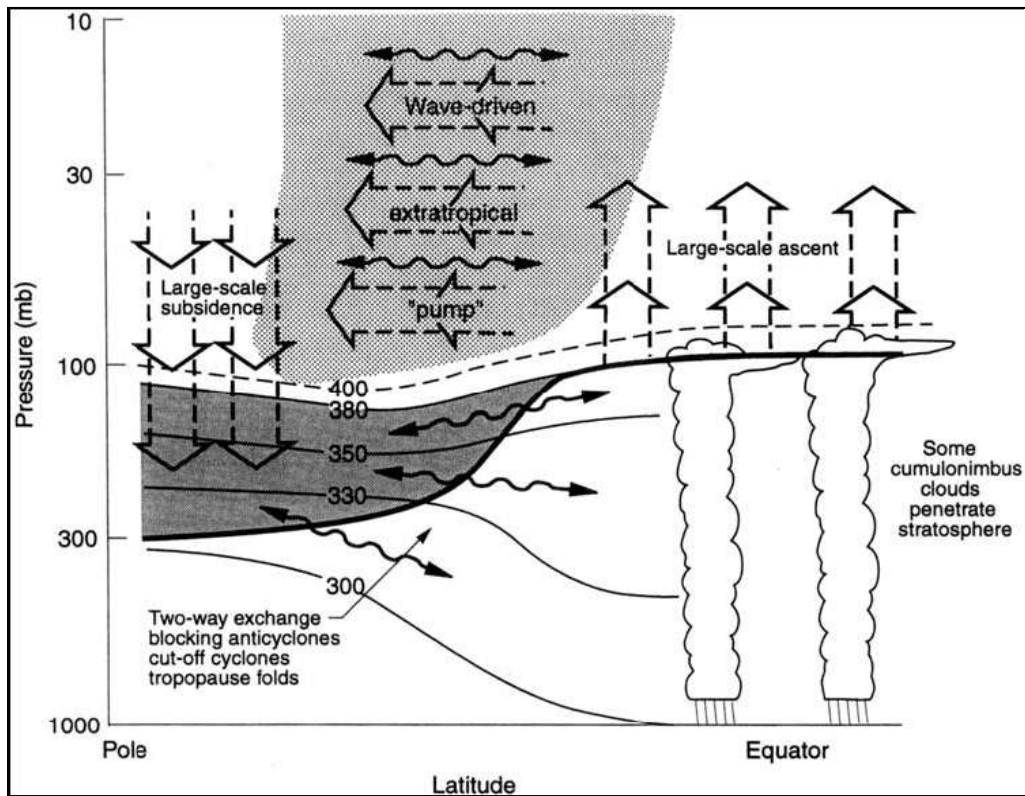


Figure 2.1. Dynamical aspects of stratosphere-troposphere exchange [adapted from Holton et al. (1995) Figure 3].

The principal reactive nitrogen species in the lower stratosphere are HNO_3 , NO , NO_2 , N_2O_5 , and ClONO_2 which control the nitrogen and ozone chemistry in this

region, of which $\text{HNO}_3 \cdot 3\text{H}_2\text{O}$ and $\text{HNO}_3 \cdot 2\text{H}_2\text{O}$ are most likely found in solid state (Temp < 200°K) and others are found in gaseous state.

Polar stratospheric clouds (PSC) have a well recognized role in stratospheric chemical input of HNO_3 and O_3 to the troposphere and finally into the Arctic terrestrial ecosystem. PSC mostly form in the winter / early spring at temperatures below 200°K (Solomn et al. 1999). In this process the most likely species of nitrogen, which can move from the stratosphere to the troposphere is $\text{HNO}_3 \cdot 3\text{H}_2\text{O}$ [Nitric Acid Trihydrate (NAT)] particles. This removal process is referred as stratosphere denitrification, which slows down the inactivation of Cl free radicals and enhances ozone destruction in the winter/spring season (Barrie et al., 1988; Solberg et al. 1996). Denitrification in the Arctic vortex in winter depends upon the size and therefore falling rate, spatial and temporal extent of sedimenting particle populations (Fahey et al., 2001).

2.1.2.1.2 Tropospheric input

At present local sources of pollution near the Arctic are spatially limited. They include volcanic emissions in Alaska and Kamchatka; anthropogenic emissions from North Western Eurasia (Law et al., 2007). Due to the seasonal movement of High Arctic pressure belt and landmass topography, Northern Eurasia is the major source region for the Arctic haze pollution. Local environmental conditions of densely populated areas on the East coasts of Asia and North America make their air masses too warm and moist to directly penetrate the polar dome, but these air masses can ascend to the Arctic middle or upper troposphere. However, Greenland, because of its high elevation, is exposed to pollution from Southeast Asia and North America more strongly than is the rest of the Arctic (Stohl et al., 2006).

The principal reactive nitrogen species reported in the troposphere of high latitude region are $\text{NO}_y = \text{NO}_x$ (NO, NO_2), N_2O_3 , N_2O_5 , HNO_2 , HO_2NO_2 , HNO_3 , PAN,

PPN and other organic nitrates (Jaffe et al., 1991). These measurements show that NO_y has maximum concentration in spring, of which PAN has longest life time at low temperature. Therefore, it has been suggested that PAN acts as a carrier for long range nitrogen transport in the troposphere. The lifetime of these nitrogen species also depends upon ultraviolet radiation, temperature and HO_x in the ambient environment (Lelieveld et al., 2004).

2.1.2.2 Geological nitrogen

It is well evident that considerable amount of nitrogen exists within igneous and sedimentary rocks in organic forms, and NH_4^+ is predominant inorganic form (Rayleigh, 1939; Hutchinson, 1944; Stevenson, 1962). NH_4^+ is usually held with secondary silicate minerals in sedimentary rocks and in igneous rocks, and is mostly found intact in K-bearing primary minerals (Stevenson 1962). Holloway et al. (1998) described geological nitrogen as a probable source of missing nitrogen documented in many ecosystem biogeochemical studies.

Although, fixed nitrogen on the Earth is found as NH_4^+ , NO_x and within organic molecules that can easily be used by biological organisms for their metabolic activity and growth, but, the majority of nitrogen (ca. 80%) on the Earth exists as biologically unavailable free N_2 molecule in the atmosphere and most of it had been generated via volcanic outgassing during early development of the planet (Rayleigh 1939; Hutchinson 1944; Rubey 1951; Mancinelli & McKay 1988). The **development of fixed nitrogen** production and subsequent evolution of N cycle can be divided into three phases: **1) Pre-biotic phase:** during this phase CO_2 , N_2 and water vapour were the major constituents, that existed in the Earth's environment and produced NO via photochemical reaction (lightning). This NO was transferred and stored in oceans and terrestrial systems by rain water as HNO_3 and HNO_2 . **2) Anaerobic phase:** during this phase early life on the Earth primarily used NH_4^+ for metabolism and as soon as NH_4^+ became limited organisms developed

ammonification in order to maintain N supply. Therefore, ammonification can be considered as the earliest biological process evolved in nitrogen biogeochemical cycling on the Earth (Mancinelli and McKay 1988). Subsequently, denitrification process was evolved as an alternative way of energy production by organisms and presence of relatively high amount of NO_3^- in ancient oceans encouraged this biogeochemical evolution. **3) Aerobic phase:** as a result of photosynthesis activity O_2 started building up in atmosphere that led to the evolution of nitrification process and later on increasing production N demand established the base biological nitrogen fixation evolution (Mancinelli and McKay 1988).

As a result of increased primary production during the aerobic phase, organic matter appears to have been deposited on the ocean floor and subsequent tectonic activities has formed sedimentary rocks and have trapped considerable amounts of organic matter. Therefore, a sedimentary rock generally contains more nitrogen than igneous rocks (Krohn et al., 1988; Williams et al., 1993; Hall et al., 1996). Further diagenesis and metamorphism determines the nitrogen content and speciation within the rocks. Organic matter within the rocks, matures at higher temperature ($> 200^\circ\text{C}$) and releases nitrogen as N_2 and NH_3 gas that can change the isotopic signature of the rock nitrogen (Haendel et al 1986). However, high amount of NH_4^+ (> 200 ppm) in metasediments is considered a biosignature since NH_4^+ yield via the abiological pathway is unable to reach such levels (Boyd and Philippot 1998; Itihara and Suwa, 1985; Papineau et al., 2005).

Due to its similarity with K^+ in ionic structure, NH_4^+ can reincorporate by replacing K^+ in mineral structures (Khan and Baur, 1972). This cation exchange capacity of K^+ containing rocks consequently promotes nitrogen retention. Scalen (1959) calculated the mean value of nitrogen in igneous rocks as 12 mg kg^{-1} and on the basis of isotopic studies he also pointed out that NH_4^+ can replace K^+ from the silicate lattice. In a recent study, the average concentration of nitrogen in the Earth's crust was estimated $1.27 \pm 1 \text{ mg kg}^{-1}$ (Allègre et al., 2001) which amounts to 20% of the global nitrogen pool (Schlesinger, 1997). Further, soil scientists classified the

crustal inorganic nitrogen into two categories (Bremner and Harada, 1959); **i) available nitrogen** which can be extracted by 1N KCl solution, **ii) fixed nitrogen** that cannot be extracted by 1N KCl solution. According to Stevenson (1962) available nitrogen in the rocks generally constitutes about 20% of whole rock nitrogen. Based upon the comparative study of soil and its parent rock nitrogen content, Holloway and Dahlgren, (1999) hypothesised a considerable nitrogen loss occurred over the last 1000 years. Further Holloway et al (2001) demonstrated the release of considerable nitrogen from rock during a leaching experiment and stated geological nitrogen as a potential stakeholder in terrestrial nitrogen biogeochemical cycling.

2.2 Sulphur Biogeochemistry

2.2.1 Introduction

Sulphur is one of the major elements (14th most abundant) upon the Earth and exists in a wide range of oxidation states (-2 to +6), making it an important constituent of life. Similar to nitrogen, sulphur in its reduced state forms the structure of some very important amino acids and enzymes. It is commonly emitted by volcanic emissions and is present on the Earth's surface usually either as metal sulphides (i.e. FeS₂, HgS, PbS, ZnS etc.) or sulphate salt [i.e. Gypsum (CaSO₄·2H₂O), Barite (BaSO₄ etc.)]. Due to low solubility in natural water, metal sulphides in oxygenated aquatic ecosystems usually remain below detection. However SO₄²⁻ is often the second most abundant anion found in aquatic ecosystems and therefore regulates the pH of aquatic environments to a large extent (Charlson et al., 1992). SO₄²⁻ is also known as a very active optical molecule that scatters lower wavelengths of light very efficiently and consequently helps to reduce the net insolation that reaches the Earth's surface. Being an efficient cloud condensation nucleus (CCN), SO₄²⁻ also helps with rain formation and so it is also known as a cooling agent.

Anthropogenic activity has disturbed the natural cycle of many major elements by a significant level. Sulphur perturbation is among them (Charlson et al., 1992). Fossil fuel burning, oil refineries and metal smelting are the major anthropogenic processes which contribute sulphur to the Earth's atmosphere. 20th century ice core records from Svalbard show that 30 to 55% of the non-geological sulphate is sourced from the oxidation of marine biogenic DMS, followed by 10 to 20% from anthropogenic sources, and 15% sea salt (Moore et al., 2006). Further, due to meteorological forces, the largest fraction (94%) of anthropogenic sulphur in the Arctic is transported from Eurasia while much less is transported from North America (Barrie et al., 1989). SO₄²⁻ is the major anion responsible for the acidic nature of winter snow in the Arctic. Further, during summer the melting of this acidic snow enhances the chemical weathering of rock debris, which has an impact upon the

biogeochemistry of the subglacial and proglacial environments (Hodson et al., 2000). Like NO_3^- , SO_4^{2-} also acts as a major oxidising agent in these environments.

2.2.2 Source of sulphur in the Arctic

2.2.2.1 Atmospheric input

2.2.2.1.1 Biogenic

Di-methyl sulphide (DMS) from marine algae is a major biogenic sulphur source (Andreae, 1985, 1986; Bates et al., 1992; Legrand and Mayewski, 1997) and is produced by the degradation of di-methyl sulphonio-propionate (DMSP), formed by marine algae and fresh water cyanobacteria. Due to similarity of intracellular DMSP structure with glycine betaine, it has also been suggested to be an osmoregulatory molecule in host cells (Vairavamurthy et al., 1985; Dickson and Kirst, 1986). Further, Kirst et al., (1991), investigated DMSP in some ice algae and also suggested a role in the cryoprotection machinery of psychrophilic microbes. In the Arctic atmosphere, DMS concentration increases throughout the summer and reaches its peak level around August (100-300 pptv; Ferek et al., 1995). DMS in the atmosphere undergoes photo-oxidation by OH, XO radicals (X = halogen element) and NO_3^- eventually producing non-sea-salt SO_4^{2-} . H_2S and carbonyl sulphide (OCS) are the other major biogenic sulphur forms, of which OCS is the most stable (life time > 1year) and abundant organic sulphur species in the troposphere (Lehmann and Conrad, 1996). H_2S is produced mostly by microbial reduction of sulphate in anaerobic conditions, therefore soil and intertidal flats are most likely to contribute H_2S to the atmosphere. However H_2S produced in deep oceanic sediments is very unlikely to reach the atmosphere unless a strong storm shakes the whole water column or strong upwelling takes place (Nielsen, 1974).

2.2.2.1.2 Volcanic emission, sea spray and dust

Volcanic emissions and biomass burning are sporadic natural sources of sulphur. These emissions contain SO_2 and H_2S as major sulphur species. Sea spray is generally the major source of SO_4^{2-} in the coastal areas. However, its abundance varies depending upon distance from the sea and predominant meteorological conditions. Further, sea-salt distribution in nearby coastal areas doesn't show significant $\delta^{34}\text{S}$ - SO_4 fractionation effects, consequently the isotopic value of deposited sea-salt SO_4^{2-} remains unchanged (+20‰; Luecke and Nielsen, 1972).

Geological dust is another potential natural source of sulphur in the Arctic atmosphere. CaSO_4 and MgSO_4 are most likely species from this sourcing. According to Nielsen et al. (1991) dust generated SO_4^{2-} in the Arctic are mostly derived from sedimentary rocks. However, Svalbard is mostly covered with snow during winter-spring and excludes the possibility of local dust formation. Therefore, long range transport from the loess deposits in Central Europe (Danube basin), Asia (Gobi and Takla Makan) and Africa (Sahara) are considered probable source for glacial sulphur and other elements generally recorded from Spitsbergen snow (Pacyna and Ottar, 1989). These regions often experience strong wind storm and low rainfall during spring which induce loess particle transport in upper atmosphere towards the Arctic by air mass circulation (Watts, 1969).

2.2.2.1.3 Anthropogenic

Higher conductivity and acidity in Arctic snow and ice caps is mostly caused by SO_4^{2-} and NO_3^- deposition from the troposphere, largely originated from Eurasia by industrial emissions and carried by the aforesaid atmospheric transport process discussed in section 3.1. The residence time of sulphur species, SO_2 in the Arctic depends upon dry deposition and oxidation rates, both of which vary seasonally. According to Barrie and Hoff, (1985), the SO_2 life time in the Arctic lower middle

troposphere during late fall is 14-20 days, 16-32 days in mid-winter and 10-19 days in the April. However, more recent studies have reported a rather short life time (ca. 2 days) (Eisinger and Burrows, 1998; Lee et al., 2011). Therefore it has been suggested that the largest fraction of sulphur is transported through this part of the atmosphere into the Arctic. Furthermore, 67% of this transported sulphur are gaseous SO₂ and the rest is in the form of particulate SO₄²⁻ (Barrie et al., 1988). Using the Danish Eulerian Hemispheric Model, Christensen (1997), suggested that Norilsk smelting complex in the Siberia is the major sulphur pollution source in the Arctic. However, local sulphur produced by coal mining in parts of Svalbard (i.e. Barentsburg, Longyearbreen, Pyramiden and Sveagruva) are considered to be limited (Simões and Zagorodnov, 2001).

2.2.2.2 Geological sulphur

Normally sulphur in sedimentary rocks is mostly sourced either from rainout deposition of volcanic gases, weathering of igneous rocks or sea-salt. But, contrary to nitrogen, sulphur in sedimentary rocks is mostly found in the inorganic form, i.e. sulphide and SO₄²⁻ (Azmy et al., 2001; Hurtgen et al., 2002, 2004; Kah et al., 2004; Gellatly and Lyons, 2005). Their relative amount of sulphur in the rock and its isotopic signature are determined by environmental conditions and the biological activity that dominated during sedimentation period (Chambers, 1982; Fry et al., 1991; Saelen et al 1993; Johnston 2008).

2.3 Deposition of atmospheric nitrogen and sulphur

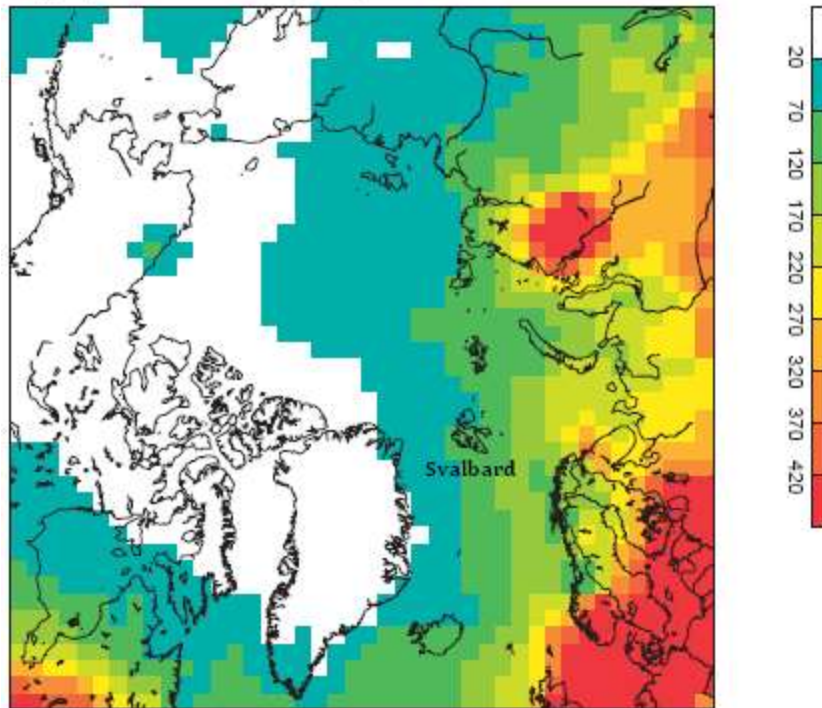
The established processes delivering NO₃⁻ and SO₄²⁻ to the High Arctic snow are; **1. wet deposition**, which can be subdivided into two different phenomena; **a) solutescavenging** (*washout*); **b) nucleation** (*especially SO₄²⁻*); **2. dry deposition** of inorganic and organic species. Beine et al. (2003) in Ny-Ålesund, Svalbard suggested

that wet precipitation (snow fall) is the major source of aerosol deposition while dry deposition also contributes a significant fraction.

Aerosol size distribution over Ny Ålesund changes from sub-micrometer (depositional mode) in spring to nanometer range (Aitken mode) in summer (Strom et al., 2003). However, particle, size distribution and their deposition are probably controlled by meteorological factors over a long range air-mass transport. Land topography also influences the transport of air-masses and subsequently higher elevation areas receive higher deposition than lower altitude areas (Lovett and Kinsman, 1990) because precipitation (snow as well as rain) is generally greatest at higher altitude. In addition based upon vertical profile of temperature gradient Yamagata et al. (2009) suggested that due to lower temperature, aerosols scavenging at higher latitude should be more efficient than at lower altitude. However, in a situation where aerosol concentration increases with increasing elevation, the “**seeder feeder**” phenomenon is considered to be a dominant mechanism, in which rains dropping from higher altitude clouds wash out the condensed aerosols from lower clouds (Choularton et al., 1988; Fowler et al., 1988).

Impaction of aerosol on the snow surface and the subsequent diffusion within it are the most likely mechanisms of dry deposition (Harder et al., 1996). The wet and dry depositions generally take place simultaneously, however the relative contribution of each may vary with space and time (Harder et al., 1996). According to the *Arctic Monitoring Assessment Programme (AMAP) 2006 report*, NO_3^- deposition in the Svalbard archipelago typically ranges between 20 to 70 $\text{mg m}^{-2} \text{yr}^{-1}$ and SO_x deposition ranges between 70 to 120 $\text{mg m}^{-2} \text{yr}^{-1}$ (Figure 2.2). This shows that in the present situation the snow acidity in the Arctic environment is equally contributed from atmospheric NO_3^- and SO_x deposition.

SO_x deposition in 2000, mg/m²/yr



NO₃ deposition in 2000, mg/m²/yr

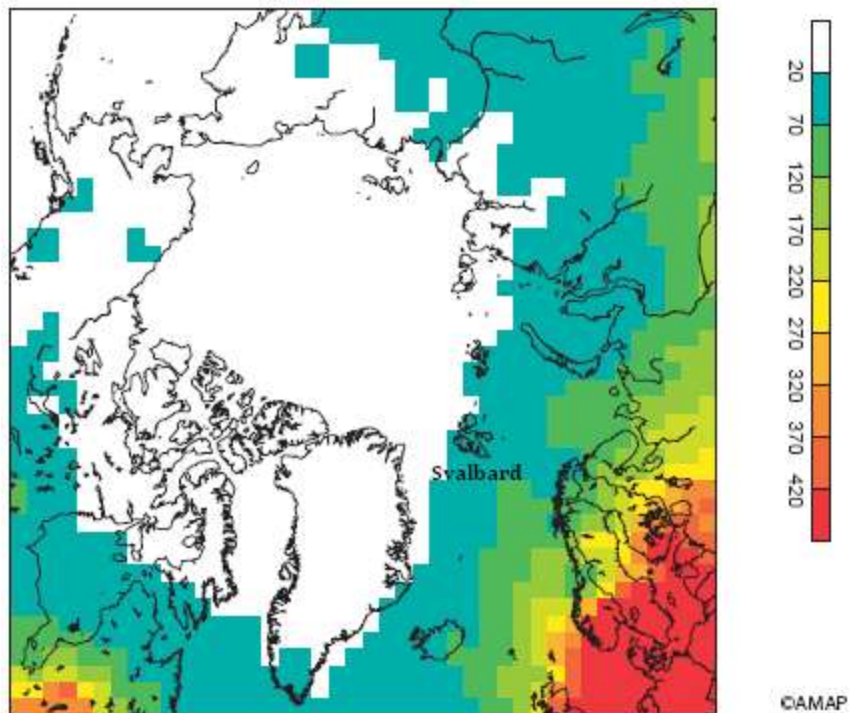


Figure 2.2. SO_x and NO₃ deposition in the Arctic during 2006 (adapted from AMAP assessment 2006: Acidifying Pollutants, Arctic Haze, Acidification in the Arctic, Figure 3.20)

Snow NO_3^- and SO_4^{2-} loading is therefore generally influenced by the following factors:

- Sea salt deposited by wind turns the snow surface alkaline (Stumm and Morgan, 1970) and this alkaline snow surface act as a trap for HNO_3 . Deeper layers of snow can remain acidic and thus any HNO_3 released may be easily trapped by the alkaline surface snow layer. Therefore, snowfall during seasons with low Ca^{2+} and Na^+ concentrations in aerosol (summer) generally dilute the net annual solute loadings in snow (Hutterli et al., 2007).
- It is also generally assumed that low snow accumulation during high aerosol presence is very likely to result in high solute concentration in snow where dry deposition become more important (Harder et al., 1996).
- The other factors which can also influence the dry deposition are wind circulation pattern, snow microstructure (regulate the effective filtration of wind aerosol passing through this structure) and surface roughness (Waddington et al., 1996).

2.4 Post-deposition processes

Post-deposition processes have been studied by several researchers tracking solutes (especially NO_3^-) in glaciers. It is well known that snows undergo many metamorphic changes due to melt–freeze cycles, which leads their physical and structural properties with melt water percolation, water vapour movement, and crystal growth (Röthlisberger et al., 2002). Such processes also affect the distribution of chemical species within snow.

According to Abbatt (1997) HNO_3 dissolution on snow surface is generally higher at colder temperature, whilst a rise in temperature also helps to release the HNO_3 from snow. However, the recorded release rates tend to only 25% of uptake. According to Röthlisberger et al. (2002) the release of deposited NO_3^- and SO_4^{2-} can be reduced by alkaline metals transported with dust and sea-salt, and subsequent salt formation [e.g. CaSO_4 , $\text{Ca}(\text{NO}_3)_2$, etc. (see Section 2.4)]. Röthlisberger et al., (2002) also suggested that a high SO_4^{2-} environment can reduce the NO_3^- solubility in snow by producing H^+ (the “common ion effect”). Volatile organic compounds can diffuse through and be lost from snow (Leggett & Hogan, 1994), but the evidence for less volatile inorganic species is not as clear. Hogan et al. (1985) suggested that NO_3^- and SO_4^{2-} losses could be because of vapour migration within the snow. Further, Neubauer & Heumann (1988) also observed NO_3^- loss in Polar snow and attributed this to surface photochemical reactions. Later on Morin et al. (2008) proposed photolysis as a significant mechanism of NO_3^- recycling in the upper few centimeters of the snow surface during spring and summer (see Section 2.2.2.1), with NO_3^- loss from snow being directly proportional to solar illumination. Although such studies are lacking for SO_4^{2-} , but photolysis can also be a possible mechanism for the snow SO_4^{2-} recycling (Rinsland et al., 1995; Vaida et al., 2003).

In addition, it should be noted that most pathways through snow are characterized by complex biological, chemical and physical changes that are still to be studied. A positive correlation found between particulate loads and biomass in the snow column (Yao et al., 2006) represents that aeolian deposition directly determines the microbial loads in snow. However, post-depositional metabolic activity and community distribution in snow depends upon micro-physio-chemical environments within the column (i.e. light intensity, nutrients, hydrological conditions and predominant temperature) (Xiang et al., 2009a). For example, phototrophs generally inhabit the surface layer of snow because of better light availability (Xiang et al., 2009b). During summer, increases in temperature and water content provide a suitable opportunity for this microbiota to increase their metabolic activity and growth. Therefore, recycling of N, S and other elements mean that it is possible for final

concentrations of NO_3^- and SO_4^{2-} in snow to be very different from original deposition.

During snowmelt, the distribution of solute varies with time, for example, the initial 30% of melt water can remove 50% to 80% of the total solute present in the original snow before melt (Johannessen and Henriksen, 1978). Davies et al. (1982) reported a preferential elution phenomenon, where some ions are removed preferentially over others in the melting water. The preferential order of elution depends upon the age of snow and possibly also depends upon melt freeze cycling. Hewitt et al., (1989) tried to explain this preferential elution on the basis of snow grain development and its metamorphosis. During snow metamorphosis some individual snow grains grow in size at the expense of others (Colbeck, 1987) and in doing so exclude chemical constituents at different rates from the ice crystals. This results in greater heterogeneity of snow grain with respect to their chemical constituents. When the snow containing these mature grains starts melting, it leads to the sequential exclusion of different ions. It has been found that generally SO_4^{2-} and NO_3^- appear in melt water fraction before Cl^- (Cragin et al., 1996). These processes consequently result high ionic concentrations in initial spring time melt water (Cragin et al., 1993).

2.5 Snow and supraglacial ice biogeochemistry

Within the last decade there has been an increase in evidence for the presence of life within extreme environments, including glaciers, which were previously assumed abiotic in nature (Hodson et al., 2008). Most of the biomass within glacial snow and ice exists in the form of microbiota that is allochthonous in nature and transported by wind from different sources (Xiang et al., 2009a). Microbes, which are transported from relatively different environmental conditions adapt to glacial conditions and multiply. Therefore, significant microbial diversity has been recorded from glaciers by various research workers (e.g. Sävström et al., 2002; Amato et al., 2007; Larose et al., 2010).

Microbes at subzero temperatures develop a micro-environment around them to help survive. Some of them produce polyols and soluble carbohydrates and release them around their cell wall to act as cryoprotectants (Gounot, 1986; Monteil and Cowan, 1993). Membrane fluidity is also enhanced by increasing the amount of unsaturated fatty acids (Amico et al., 2006). At the same time enzymes and other molecules in these so called **psychrophilic microbes** are adapted to work at low temperature (Christner et al., 2003). Though biological activity within dry snow and ice is relatively very low, Amoroso et al. (2010) have argued the occurrence of non-photochemical release of NO_x from snows as a result of biological production. Furthermore, Miteva et al. (2007) experimental observations of nitrification at -30°C by *Nitrosomonas cryotolerans*, were taken as supportive of the above argument. Similarly, various other culture incubation experiments have been used to demonstrate biological activity at subzero temperature, for example DNA and protein synthesis was observed by Carpenter et al. (2000) between -13°C to -17°C temperature and an increase in ATP concentration was observed from -15°C to -80°C as an indicator of active metabolism (Amato & Christner, 2009).

Based upon incubation experiments and molecular work, Price & Sowers (2004) suggested that there is no evidence for a definite minimum temperature for metabolism and all microbes (from permafrost, sediment, soil, water) have similar metabolic rates at the same temperature. This infers temperature is a more important controlling factor for metabolism than liquid phase availability. Later, investigating the mechanism for necessary element supply to microbial survival within dry snow or ice (in the absence of liquid phase) Rhode and Price (2007) proposed the idea of gaseous diffusion into solid ice. According to which dissolved small gaseous molecules (CO₂, O₂, N₂, CO, CH₄, and H₂S) may diffuse through the snow/ice lattice and subsequently become available to microbes for nutrient synthesis and metabolic incorporation.

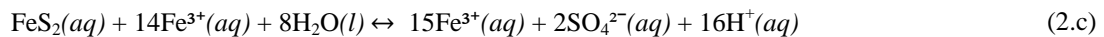
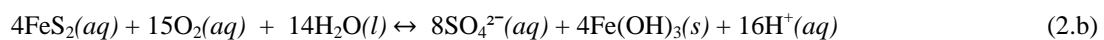
The most active and studied biological niche in the glacial ecosystem is the cryoconite hole (Anesio et al, 2010; Edwards et al 2011). These are generally formed by allochthonous particulate matter in supraglacial holes of several millimetres to a few meters in diameter. The structure of cryoconite holes includes abundant dark material, causing greater solar heat absorption than the surrounding area, resulting in a tube like structure. Cryoconite aggregates (the debris within the hole) contain highly diverse microbial communities that include cyanobacteria, rotifers, tardigrades, and ciliates (Porazinska et al., 2004; Foreman et al., 2007; Cameron et al., 2012). Some of these microbes release sticky organic substances which help to trap other particulate matter flowing with water through the holes. The trapped particulate debris could be a source of food for microbial life within cryoconite. During summer melt, this small ecosystem becomes eutrophic in relative terms and the photosynthesis and respiration rate reach levels that are found with tropical soils (Anesio et al., 2009; Telling et al., 2011). The presence of heterocystous cyanobacteria is diagnostic of nitrogen fixation (Fogg, 1974) though other cyanobacteria may also be diazotrophic. More recently Telling et al. (2011) have demonstrated that cryoconite is capable of nitrogen fixation when nitrogen availability becomes limited (for example long after the retreat of nutrient rich snow).

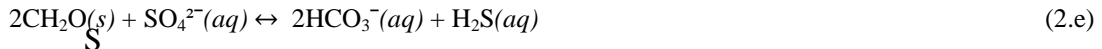
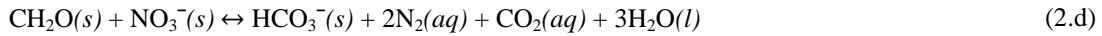
2.6 Subglacial and Proglacial runoff biogeochemistry

The subglacial system of polythermal glaciers has been studied as potential zone for biological activity (Sharp et al., 1999; Skidmore et al., 2000; Tranter et al., 2005; Kaštovská et al., 2007; Christner et al. 2008; Hodson et al, 2008). This is because parts of the bed of many polythermal glaciers remain at the pressure melting point all year, providing liquids for solute transfer and chemical weathering of rock debris. Furthermore, a recent study has demonstrated that the rocks from the glacier catchment having the capability to provide nutrients for biological growth (Borin et al., 2010) resulting the generation of nutrients that can fuel biological activity at the glacier bed. Although the absence of light in this environment is not ideal for

photosynthetic autotrophs, chemautotrophs and heterotrophs can maintain a life lineage. Skidmore et al., (2000) isolated and managed to culture aerobic heterotrophs, anaerobic NO_3^- reducers, SO_4^{2-} reducers and methanogens. Since then many lines of evidence have been presented by other research workers, all indicating the existence, activity and diversity of life within subglacial systems (Foght et al., 2004; Bhatia et al., 2006; Christner et al., 2008). During winter the subglacial system is mostly charged by subglacial pressure melting however, in summer season it can have one more major water source: supraglacial melt water, which reaches the subglacial system through small interconnected channels or open crevasses. Gradual melt of the supraglacial snow and development of efficient drainage by ice-melt decreases the subglacial hydrological pressure. Subglacial runoff water is often characterised by high solute and sediment load relative to other glacial discharge, due to greater interaction between water, sediment and rocks. According to Tranter et al., (2005) meltwater flowing through narrow distributed englacial-subglacial channels, where water pressure remains high, is more prone to becoming hypoxic/anoxic by oxygen consuming microbially catalysed weathering reactions (for example, organic matter decomposition and sulphide oxidation; Equation 2.a and 2.b). However, in wider channelized flowpath, where good ventilation spaces are available, water is unlikely to become hypoxic / anoxic and aerobic biogeochemical processes are expected to prevail.

Some studies have inferred active nitrification and denitrification beneath the glaciers (Hodson et al., 2005a; Wynn et al., 2006; 2007; Skidmore et al., 2010). Under oxic conditions microbes converts NH_4^+ to NO_3^- (Figure 2.4) and under anoxic condition NO_3^- becomes the primary electron acceptor for microbial degradation of organic matter (Equation 2.d) to produce energy for their metabolic needs.





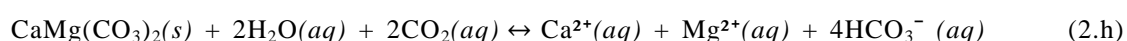
1

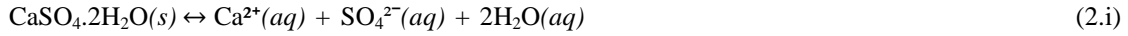
Sulphide oxidation also takes place under anoxic condition where Fe^{3+} acts as an electron acceptor (Bottrell and Tranter, 2002) and oxygen is sourced from water molecule (H_2O) (Equation 2.c). Further, SO_4^{2-} reduction (Equation 2.e) is among the discernable process in subglacial environment, (Wadham et al., 2004) though many studies suggest that abundant dissolved SO_4^{2-} and anaerobic conditions do not necessarily host SO_4^{2-} reduction activity (Tranter et al., 2002; Foght et al., 2004; Skidmore et al., 2005; Boyd et al., 2010). In the lack of SO_4^{2-} or its reduction activity, methanogenesis (Equation 2.f) generally becomes the major carbon removal process in anaerobic conditions (Lovely and Klug, 1983; Conard, 1996) which is evident in the glacial sediments and subglacial environment (Khalil and Rasmussen, 1990; Weitmeyer and Buffett, 2006; Wadham et al., 2008).

The glacier forefield host similar biogeochemical reactions as those generally observed in the subglacial system, though it can be spatially variable (Sigler and Zeyer, 2002; Sigler et al., 2002; Gooseff et al., 2004; Wadham et al., 2007; Clilverd et al., 2008; Duc et al., 2009; Bárcena et al., 2010; Borin et al., 2010). As summer temperatures increase, proglacial permafrost melts and subsequently active layer depths increase to provide more space opportunities for biogeochemical processes (Frey and McClelland, 2009). This further increases the interaction between streams and the hyporheic zone, causing variation in downstream hydrochemistry (Gooseff et al., 2004; McKnight et al., 2004; Hood and Berner, 2009). Furthermore, it has been hypothesised that due to low temperature and waterlogged anaerobic conditions, permafrost layers have stored a large amount of organic matter from last glacial maxima (Davidson and Janssens, 2006; Schuur et al., 2008). Thus, permafrost degradation during summer has potential to exfiltrate such stored organic matter into the active near surface environment.

NH_4^+ is a short lived species in oxic conditions and relatively immobile because: 1) adsorption onto negatively charged mineral surfaces (Williams and Ferrell, 1991) and, 2) preferential uptake by microbes (Kirchman, 1994). NO_3^- is more stable, relatively long-lived and mobile, making it tracers of the biogeochemical systems in glaciers (Kirk and Kronzucker, 2005). In general, the Cl^- ion is described as the most conservative anion in stream systems due to the absence of any significant source or sink in the flowpaths occupied by meltwater runoff. Tranter et al. (1996) showed how Cl^- can therefore be used as snowmelt tracer. SO_4^{2-} is one of the major ions and a key player in proglacial biogeochemistry, where pyrite rocks are in abundance. 75 to 95% of SO_4^{2-} in high Arctic glacial streams is typically derived from the oxidation of sulphide minerals (Wynn, 2004), although the relative contribution of biotic and abiotic oxidation is still a matter of debate. Sulphide oxidation in water generates H^+ that promotes carbonate dissolution resulting in higher PCO_2 than the atmosphere (Schippers and Jørgensen, 2001; Schippers and Jørgensen, 2002). Hence, such glacial runoff can act as a net source of CO_2 . Oxidation of organic matter by microbes also helps to maintain the HCO_3^- concentration in glacial streams (Skidmore et al., 2010).

Besides physical erosion, cation weathering is also strongly influenced by carbonate and silicate hydrolysis (Sharp et al., 1995; Skidmore et al., 2010). Several studies have demonstrated that high Arctic glacial streams and sediment pore waters are generally dominated by Ca^{2+} followed by Mg^{2+} , sourced by carbonate weathering [i.e. calcite, dolomite etc: see Equation 2g-2i (Cooper et al., 2002; Wynn, 2004)]. Ca^{2+} and Mg^{2+} produced this way may also precipitate as carbonate during evaporation or on its discharge into the sea, therefore promoting atmospheric CO_2 drawdown (Sharp et al., 1995; Hodson et al., 2000; Tranter et al., 2002). Na^+ concentrations in streams generally surpass K^+ because average crustal rocks carry more Na^+ than K^+ (Krauskopf, 1979), and its smaller size enhances mobility through sediments.





2.7 Stable isotopes in biogeochemical studies

Isotopes are atoms of an element having the same number of electron and proton, but different atomic mass due to a different number of neutrons. For example, nitrogen has two isotopes ^{14}N , ^{15}N . Isotopic composition in natural reservoirs change with time because of radioactive decay of unstable isotopes, cosmic ray interactions and human operated nuclear activity. Stable isotopes are those atoms or nuclei that do not disintegrate on geological time scales.

Isotopes are generally termed using the element name preceded by its atomic mass in superscript before element (for example, ^{14}N , ^{15}N) and are reported in delta notation (δ), which is calculated using the following equation:

$$\delta = R_{\text{sample}} / R_{\text{standard}} - 1 \quad (2.j)$$

Here R represents abundance ratio of the less frequent isotope (^{15}N , ^{18}O , ^{34}S) to the most frequent isotope of the same element (^{14}N , ^{16}O , ^{32}S) in the sample and standard, respectively. Delta values are usually multiplied by 1000, to express them in per mille (‰, part per thousand). Further details are shown in Table 2.1.

Stable isotope compositions of various reservoirs are generally fixed and changed in a known direction by different biological, physical and chemical processes. Therefore, it has become a promising scientific tool in biogeochemical studies, with nitrogen and sulphur cycling being among the most widely studied ones. Recent developments in mass spectrometry and improved methodology have also increased the use of stable isotopes in almost all sections of science.

Table 2.1 Stable isotopes of N, O and S (Hoefs, 2009)

Element	Stable Isotopes	Natural abundance	Reference
Nitrogen	¹⁴ N	99.634%	Atmospheric N ₂
	¹⁵ N	0.37%	(AIR)
Oxygen	¹⁶ O	99.763%	Vienna Standard Mean Ocean
	¹⁷ O	0.0375%	Water (VSMOW) or Vienna
	¹⁸ O	0.1995%	Pee Dee Belemnite (VPDB)
Sulphur	³² S	95.02%	Canon Diablo Troilite (CDT)
	³³ S	0.75%	
	³⁴ S	4.21%	

2.7.1 Stable isotope composition of major N and S sources in High Arctic

The isotopic composition of atmospheric N₂ gas is always found constant with near zero $\delta^{15}\text{N}$ value, irrespective of time and place (Mariotti, 1983) making it a widely accepted standard for natural ¹⁵N abundance. The $\delta^{15}\text{N}$ of NO_x and NH₃ produced by fossil fuel combustion and livestock farming generally range from -2‰ to +13‰ and from -8‰ to +13‰ respectively (Peterson and Fry, 1987; Kendal et al., 2007). However, isotopic compositions of NO_x and NH₄⁺ in atmospheric precipitation are generally found more negative [(-20‰ to +3‰ and from -18‰ to +8‰ respectively) Peterson and Fry 1987; Heaton et al., 2004]. Several rocks from Midtre Lovénbreen glacier in Svalbard have also been characterised for its nitrogen content (Wynn, 2004) and their $\delta^{15}\text{N}$ varies between -1.6‰ and +7.7‰.

Sea-salt $\delta^{34}\text{S-SO}_4$ is generally very close to +20‰; (Luecke and Nielsen, 1972) while DMS oxidised $\delta^{34}\text{S-SO}_4$ ranges from +14‰ to +22‰ (Calhoun et al al., 1991; McArdle and Liss, 1995; Patris et al., 2000b). However the $\delta^{34}\text{S}$ value of

anthropogenic sulphur emission (fossil fuel burning and sulphide ore smelting) vary greatly (-40‰ to $+30\text{‰}$), whereas $\delta^{34}\text{S}$ signature of SO_2 produced by fossil fuel combustion generally lies between -1‰ and $+5.4\text{‰}$ (Nielsen, 1974). Anthropogenic $\delta^{34}\text{S}$ - SO_4 from Greenland snow has been found to be uniformly around $+3\text{‰}$ (Kreutz and Sholkovitz, 2000; Pruett et al., 2004). Sulphide associated with sedimentary rocks also varies in a broad range ($+60\text{‰}$ to -60‰) but negative $\delta^{34}\text{S}$ values are more frequent and give an average of $\delta^{34}\text{S} = -12\text{‰}$ for the sedimentary rocks (Kah et al., 2004). Volcanic emissions contain SO_2 and H_2S as major sulphur species with $\delta^{34}\text{S}$ signature ranging around -10‰ to $+10\text{‰}$ (Nielsen, 1991). However, non eruptive emissions produce $\delta^{34}\text{S}$ signatures in a small range (0‰ to $+2.6\text{‰}$; Newman et al., 1991).

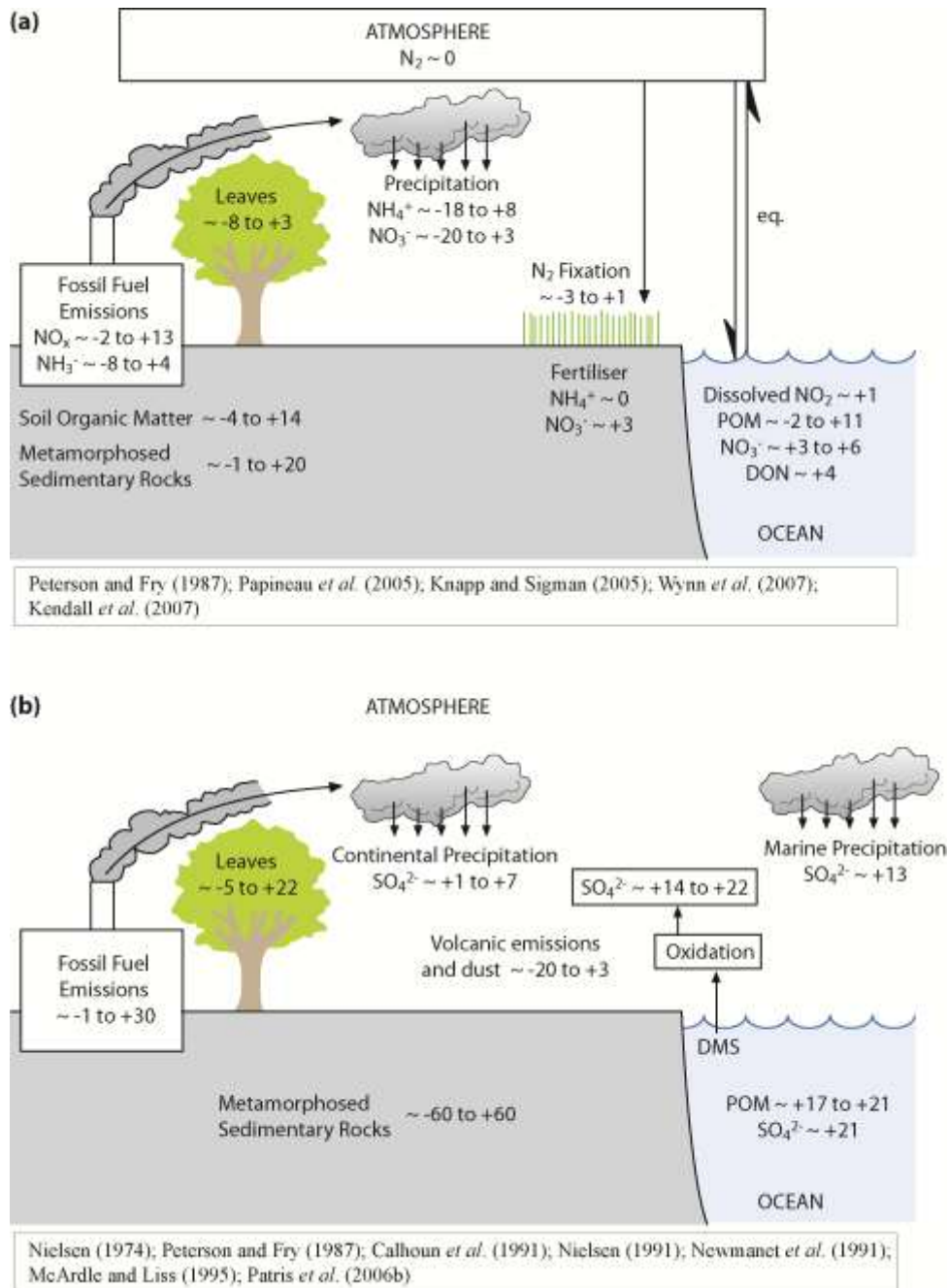


Figure 2.3. (a) $\delta^{15}\text{N}$ and (b) $\delta^{34}\text{S}$ distribution in various ecosystems. This figure is adapted from Peterson and Fry (1987).

2.7.2 Fractionation

Since isotopes have the same number of electrons, their atoms almost have identical chemical properties, and so they follow similar processes in biological as well physical systems. But, due to different mass of these nuclei, their reaction rates differ and cause a partial segregation of isotopes with variable ratios. This phenomenon of isotopic separation is known as isotopic fractionation. Three kinds of fractionation have been observed in natural systems (Hoefs, 2009).

1. Kinetic fractionation
2. Equilibrium fractionation
3. Mass independent fractionation

Isotopic fractionation is expressed as a fractionation factor (α), which is defined as the ratio of heavy to light isotopic ratio of product to reactant.

$$\alpha = \frac{R_{product}}{R_{reactant}} \quad (2.k)$$

If $\alpha > 1$, the product will be heavier in isotopic composition than the reactant and vice-versa.

The magnitude of isotopic segregation is expressed as isotope enrichment factor (ϵ in ‰).

$$\epsilon_{product-reactant} \approx \delta_{product} - \delta_{reactant} \quad (2.l)$$

$$\epsilon (\text{‰}) \approx (\alpha - 1) \times 1000 \quad (2.m)$$

2.7.2.1 Kinetic fractionation

Mass dependent isotopic fractionation takes place in unidirectional processes, where equilibrium is not attained. This kind of fractionation is found in many biogeochemical reactions. Lighter isotopes react faster and get concentrated in the product, while reactants become rich in heavier isotopes (Kendal and Caldwell, 1998).

2.7.2.2 Equilibrium fractionation

Partial separation of isotopes between two or more substances in chemical equilibrium reactions is known as equilibrium fractionation. Equilibrium fractionation is strongest at low temperature (Kendal and Caldwell, 1998).

Reduction in vibrational energy is thought to be the major cause of equilibrium isotopic fractionation, when heavier isotopes are substituted for lighter ones. This results a higher concentration of heavier isotopes in substances where vibrational energy is most sensitive to isotopic substitution, i.e. those with highest bond force constant. In case of phase change heavier isotope enrichment consequently occurs in dense material (Kendal and Caldwell, 1998).

2.8 Nitrogen based biological processes responsible for isotopic fractionation

2.8.1 Nitrogen fixation

The process of conversion of free atmospheric nitrogen (N_2 ; $\delta^{15}N = 0\%$) into bioavailable nitrogen species (NH_4^+ , NO_3^-) is known as nitrogen fixation. This biological fixation is achieved using Fe, V or Mo based nitrogenase enzymes, which

cannot act in oxic conditions (Eady, 1991). Therefore, most of the cyanobacteria have morphological (heterocyst) or physiological (colony) adaptations to provide an anoxic environment within the cells for nitrogenase activity (Fay et al., 1968; Böhme, 1998). Isotopic fractionations for microbial nitrogen fixation have been recorded in a range of -3 to $+1\text{‰}$ (Fogel & Cifuentes, 1993).

2.8.2 Assimilation

The process responsible for the conversion of inorganic nitrogen to organic nitrogen via metabolic activity within living cells is known as assimilation. Similar to other biological process, here lighter isotopes (thermodynamically more efficient) are also preferred over heavy ones, causing N fractionation of -30 to 0‰ (Cifuentes et al., 1989; Montoya et al., 1991; Pennock., 1996; Waser et al., 1998; Altabet et al., 1999; Granger et al., 2004). During nitrate assimilation, $^{18}\text{O}:^{15}\text{N}$ enrichment ratio of ~ 1 have been observed in cyanobacteria, but in the heterotrophic α -protenobacteria, this ratio has been found to be ~ 2 (Granger et al., 2010).

2.8.3 Mineralisation and Nitrification

The release of inorganic NH_4^+ from organic matter during biological activity is known as mineralisation. This process usually causes a small N fractionation of $\sim \pm 1\text{‰}$ (Kendall et al., 2007). Oxidation of NH_4^+ to NO_3^- is known as nitrification, which takes in three steps, as shown in Figure 2.4.

- i. Oxidation of NH_4^+ to NH_2OH by the enzyme ammonia monooxygenase (AMO; a membrane bound enzyme). This step requires dissolved O_2 and an electron (which comes from the second step).

- ii. Oxidation of NH_2OH to NO_2^- by the enzyme hydroxylamine oxidoreductase (HAO; found in periplasm). In this step the oxygen atom required is taken from an H_2O molecule and additional electrons are generated.
- iii. Oxidation of NO_2^- to NO_3^- by the enzyme nitrite oxidoreductase (NOR; a membrane bound enzyme). The required oxygen for this step is also taken from H_2O molecules and an additional electron is generated.

The additional electrons produced in the second and third steps are used to gain energy for nitrifiers. The third oxidation step is generally very quick in nature. As the first and second oxidation steps are slower, they are considered as rate determining and responsible for isotope fractionation, ranging from -38‰ to -14‰ (Mariotti et al., 1981; Casciotti et al., 2003). However, in a nutrient limited environment, this significant fractionation effect might not be observed (Tye and Heaton, 2007). The reversibility of the above step also allows oxygen exchange between reacting nitrogen oxides and H_2O (Aleem et al., 1968).

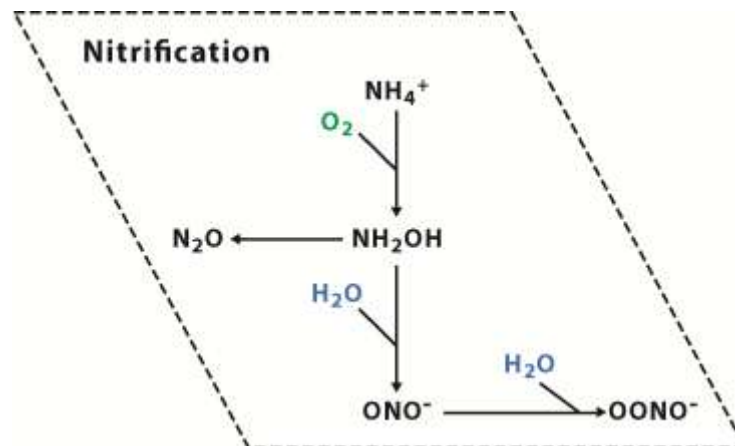


Figure 2.4. A schematic diagram of oxygenatom incorporation from O_2 and H_2O during nitrification (adapted from Kool et al., 2007).

2.8.4 Denitrification

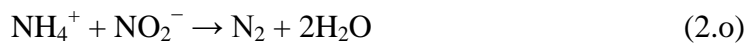
Assimilatory NO_3^- reduction to free molecular nitrogen (N_2) is known as denitrification. This process mostly takes place in hypoxic / anoxic conditions (Dissolved oxygen concentration $< 0.5 \text{ mg L}^{-1}$; Hübner 1986) where NO_3^- acts as an alternative electron acceptor for the oxidation of organic molecules. N isotope fractionation in this process is observed in a range from +15‰ to +30‰. The $\delta^{15}\text{N}$ and $\delta^{18}\text{O}$ of NO_3^- show a coupled isotopic effect during this process with fractionation ratio of 2:1 (Böttcher et al., 1990; Aravena & Robertson 1998; Mengis et al., 1999; Cey et al., 1999; Panno et al., 2006). All the steps in this process generate energy, of which the least amount is produced during NO_2 reduction. Therefore, this step is most likely to be reversed and so can promote the highest rates of oxygen exchange (Garber & Hollocher, 1982).

2.8.5 Dissimilatory nitrate reduction to ammonia (DNRA)

Reduction of NO_3^- to NH_4^+ without incorporation into organic molecules is known as dissimilatory nitrate reduction. This process mostly takes place in reduced and low nitrate environment (Myers, 1972; Gould and McCready, 1982; King and Nedwell, 1985; Adkins and Knowles, 1986). It has also been reported that high sulphide concentrations inhibit both nitrification and denitrification (Myers, 1972) and may fuel the DNRA by providing electrons through sulphate reduction (An and Gardner, 2002). Isotopic fractionation effects associated with this process vary between +13‰ and +20‰ (Granger et al., 2008).

2.8.6 Anammox

Anaerobic oxidation of NH_4^+ to N_2 is termed as anammox (Equation 2.o). This process is mostly observed in sewage system, ocean oxygen minimum zone (OMZ) and sediments (Kuypers et al., 2003; Dalsgaard et al., 2003, Jaeschke et al., 2007). However, isotope fractionation data for this process are yet to be established.



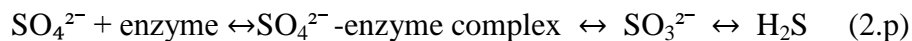
2.9 Sulphur based biological processes responsible for isotopic alterations

2.9.1 Sulphide oxidation

Sulphide oxidation is an energy yielding reaction which takes place by both biotic and abiotic pathways in oxic / anoxic conditions. Isotopic studies have suggested that sulphate formed via oxic sulphide oxidation should contain at least 25% atmospheric oxygen atom in its structure (Holt et al., 1981; Holt and Kumar 1991). However, recent studies have demonstrated that similar SO_4^{2-} produced in aerobic conditions may also be composed of more than 90% oxygen from H_2O (Balci et al. 2007; Kohl and Bao, 2011). It is evident that no isotopic effect happens when oxygen in sulphate comes from H_2O , while oxygen transfer from atmospheric O_2 to SO_4^{2-} during sulphide oxidation is very complicated to understand due to isotopic exchange between intermediate species and H_2O molecule (Lloyds, 1968; Betts and Voss, 1970). Once SO_4^{2-} is formed the chances of oxygen isotope exchange become insignificant (Llyods, 1968; Chiba and Sakai, 1985) under normal conditions.

2.9.2 Sulphate reduction

Under normal conditions, SO_4^{2-} reduction is generally a biological process which can be divided into two steps; first is an endergonic reaction, when SO_4^{2-} is reduced to SO_3^{2-} and the subsequent second step is an exergonic reaction when SO_3^{2-} is reduced to sulphide (Equation 2.p). SO_4^{2-} reduction to SO_3^{2-} is also a reversible process, and the isotopic values during this step may remain unchanged (Rees, 1973). Furthermore, dissimilatory reduction of SO_4^{2-} to sulphide causes smaller fractionation effects than the assimilatory pathway (Rees, 1973). The reported isotopic fraction associated with SO_4^{2-} reduction to sulphide in pure microbial environments ranges between -2% and -49% (Kaplan and Rittenberg, 1964; Kemp and Thode, 1968, McCready, 1975; Chambers and Trudinger, 1979; Bollinger et al., 2001). However, minimum fractionation effects associated with sediment SO_4^{2-} reduction rarely reaches below -10% , unless large amounts of organic substrate are available (Böttcher et al., 1997). Organic matter mineralisation by thermochemical reduction of SO_4^{2-} causes relatively lower $\delta^{34}\text{S}$ isotopic fractionation effect (0% to -25%) than the biological SO_4^{2-} reduction. This process mostly takes place at higher temperature during the sedimentary diagenetic process (Ohmoto and Rye, 1979; Ohmoto et al., 1990). Similarly, Brüchert et al., (2001) demonstrated that an increase in temperature decreases the ^{34}S fractionation associated with SO_4^{2-} reduction.



(Harrison and Thode, 1958).

CHAPTER 3: FIELD SITE AND METHODOLOGY

This chapter provides a description of the field site and methodology used for the study. Section 3.1 describes the field site location, climate, geology, ecology, glacial structure, mass balance and hydrology. Section 3.2 summarises snow sample collection, hydrological monitoring and stream sampling. Section 3.3 summarises the methodology used for chemical and isotope analysis in laboratory, whilst Section 3.4 summarises the rock dissolution and adsorption experiments undertaken to understand release of nitrogen and sulphur from the catchments rocks.

3.1 Svalbard climate and its importance in research context

Being situated between 74° and 81° N, the Svalbard archipelago comes under the classification of having a polar climate (Figure 3.1). Here average summer temperature usually ranges between 4° and 6°C and average winter temperature ranges between -12° and -15°C. Average annual precipitation is 386 mm water equivalent (Førland et al., 1997) at sea level with highest precipitation taking place in spring (February-April). Svalbard winter temperatures are often far higher than other land located at the same latitude (Russia and Canada) due to close contact with North Atlantic Current (a continuation of the warm Gulf Stream). Svalbard falls within the low pressure belt where cold polar air from the north and warm moisture laden air from the south encounter each other to produce a cyclonic condition. Hence, windy conditions are common in winter Polar night (Førland et al., 1997).

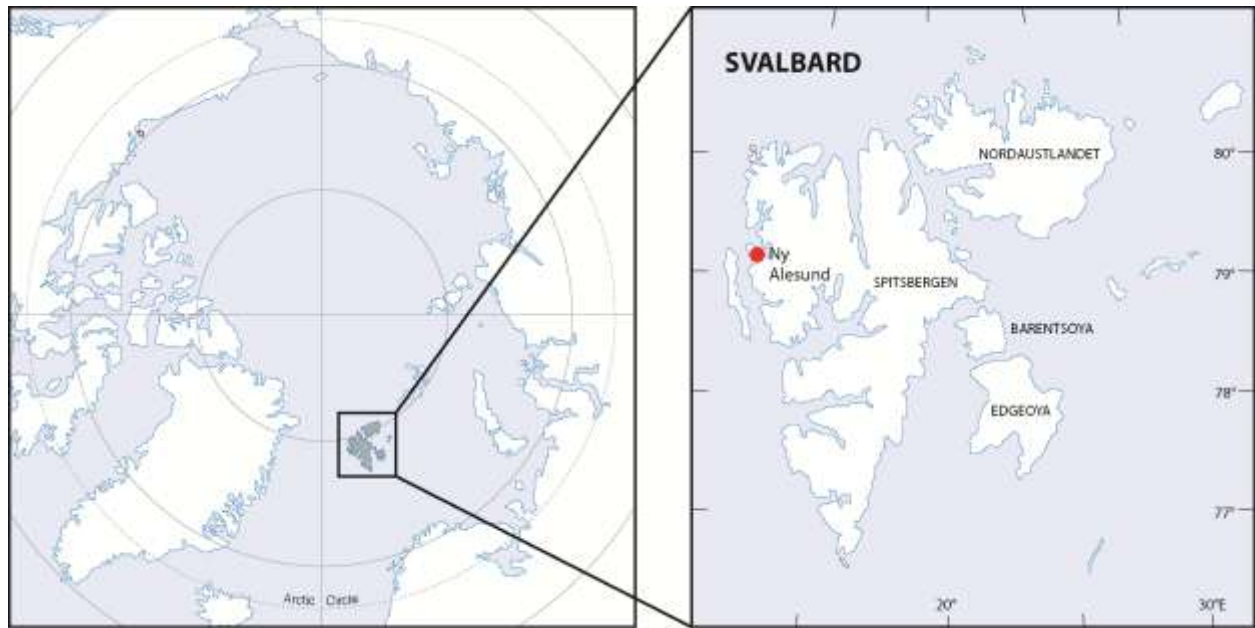


Figure 3.1. Svalbard Map and its position on globe.

During summer this archipelago experiences the Polar day, starting around 16-20 April and remaining for 131 to 132 days. In winter, Polar night starts around 23-25 October and stays for 116 to 124 days (24 hr dark) (Kupfer et al., 2006). Because of the axial tilt of the Earth, and its movement around sun, the amount of sunlight reaching at any given point on the surface varies over the course of the year. This creates a seasonal movement of the Arctic High pressure belt between 40° to 80° latitude north, being pushed southward during the winter, so that the main cyclone track is deflected into the industrialised areas of central Europe, Scandinavia and North-Western Russia (Barrie, 1986). Many of the industrial areas and other sources of pollutants all lie in the path of these moving cyclones and encounter the semi-permanent Siberian High pressure. As a consequence they are often deflected first towards the Kara and Barents Sea and then towards the Polar Basin. Svalbard is among the first landmasses in the pathway of these pollutant-laden air masses.

During summer, the Arctic high pressure belt retreats to a northerly position over Svalbard, or even farther north (up to 80° N). The cold dry Arctic air mass is then restricted to the Polar Basin and the circulation pattern in the Arctic becomes more

circumpolar, with moisture laden cyclones generally coming from North America via Iceland (Rahn et al. 1981). The cyclones in these areas can get loaded with ambient pollutants (mainly from industrial areas of north eastern America), but before reaching the Svalbard, they generally become greatly depleted due to precipitation over the ocean on the way. Consequently, the Barents and Kara Sea region is subject to a high influx of anthropogenic pollutants with a maximum in late winter-early spring (Bottenheim et al., 2004). Therefore, this generalised scenario show that each winter and spring, the Arctic troposphere receives anthropogenic pollution from various source regions (Ottar et al., 1986; Barrie, 1986; Jaffe et., 1991). Thereafter, pollution may have an influence on regional photochemistry (Jaffe. 1992), climate (Stamnes et al., 1995) and ecosystem dynamics (Lockhart, 1995).

Sometimes a deflection in the North Atlantic Current has been recorded due to the change in atmospheric pressure difference between the Iceland low and Azores high. This periodic deflection of atmospheric pressure difference (at sea level) between Iceland low and Azores high is known as North Atlantic Oscillation (NAO). Large differences between these places help to maintain the flow of the North Atlantic Current moving toward the north-western coastal part of Europe in the Arctic Ocean. This condition is called **NAO+** and strengthens the westerlies that cause the warm summers and mild wet winters in central and north-western Europe. When the atmospheric pressure is negative, a big portion of North Atlantic Current is deflected back towards eastern coast of North America, creating the **NAO-** conditions. It is clear from Figure 3.2 that during NAO- conditions, the High Arctic lacks proper temperature moderation by the North Atlantic Current. This suppresses the westerlies and causes cold winters.

North Atlantic Oscillation

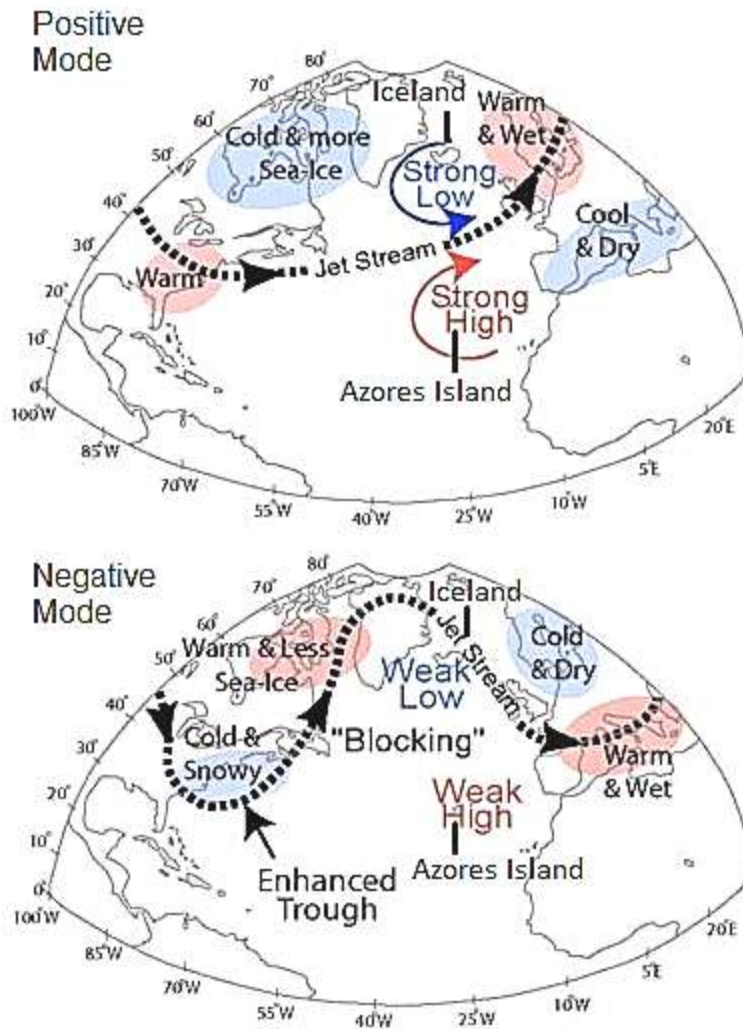


Figure 3.2. North Atlantic Oscillation showing positive and negative mode circulation pattern. (Adapted from <http://www.newx-forecasts.com/nao.html>)

3.2 Field Site: Glacier Midtre Lovénbreen

Midtre Lovénbreen (78.53°N and 12.04°E) is a small valley glacier located on the Brøggerhalvøya peninsula in North West Spitsbergen (Figure 3.3). Several small cirque basins feed into the main glacier tongue. The glacier is approximately 6 km long with an area of 5.5 km² and a maximum depth of 180 m. It ranges in elevation from 50 m at the snout to 600 m at the head wall. The equilibrium line altitude averages 395 m and the accumulation area ratio is known to average 0.35 of total glacier area (Björnsson et al., 1996; Rippin et al., 2003). Importantly, the thickness of ice and accumulation of snow means that much of the glacier bed lies at the pressure melting point. This allows delayed drainage through subglacial sediments during the summer (Hodson et al., 2005a). When these waters do emerge, artesian pressures can produce a small fountain or “upwelling”, as has been documented elsewhere in Svalbard (e.g. Wadham et al. 2004). Wynn et al. (2006) and Irvine-Fynn et al. (2010) show that sub-oxic conditions can dominate this outflow in the first instance, indicating that a proportion of the waters emerging from beneath the glacier are from anoxic environments, where denitrification is most likely (Wynn et al. 2006). However, changes in the dissolved oxygen status and electrical conductivity of these waters has shown that mixing between possible anoxic flowpaths and well-aerated, surface-derived meltwaters varies seasonally and, later in the summer, diurnally as well. Irvine-Fynn et al. (2010) showed that the diurnal oscillations in dissolved O₂ were greatest about 25 days after the upwelling emergence, suggesting that it takes some time before surface-derived meltwaters are able to force the development of a well-aerated rapid flowpath through the glacier bed. When this is achieved, rapid transfer of surface-derived meltwaters in the upper part of the glacier takes place (Irvine-Fynn et al. 2005), and so the potentially anoxic flowpaths are then assumed to be supplied by parts of the glacier bed not well connected to such drainage routes.



Figure 3.3. Glacier Midtre Lovénbreen situated on Ny Alesund, Svalbard.

3.2.1 Geology

The geological structure of Brøggerhalvøya peninsula is dominated by folding (during Silurian or early period) and thrusting that can be easily seen in stratified sedimentary and metamorphic sequences. The basement of Midtre Lovénbreen is mostly structured of Phyllite with beds of quartzite but the southern half glacier boundary is dominated by mica, schist with carbonate and quartzite beds (Hjelle, 1993). Sediment deposited fluviially in front of the glacier is mostly brought by supraglacial streams and from subglacial streams in the vicinity of subglacial outflows. The highest mountains are found in a series of a strata slightly dipping towards south in sequence; the southernmost being are mostly composed of mica-schist, quartz-carbonate-schist and marble, and the northernmost being the phyllite. Some isolated patches of silicious shale and chert are found in the proglacial region (Hjelle 1993; Roberson 2009).

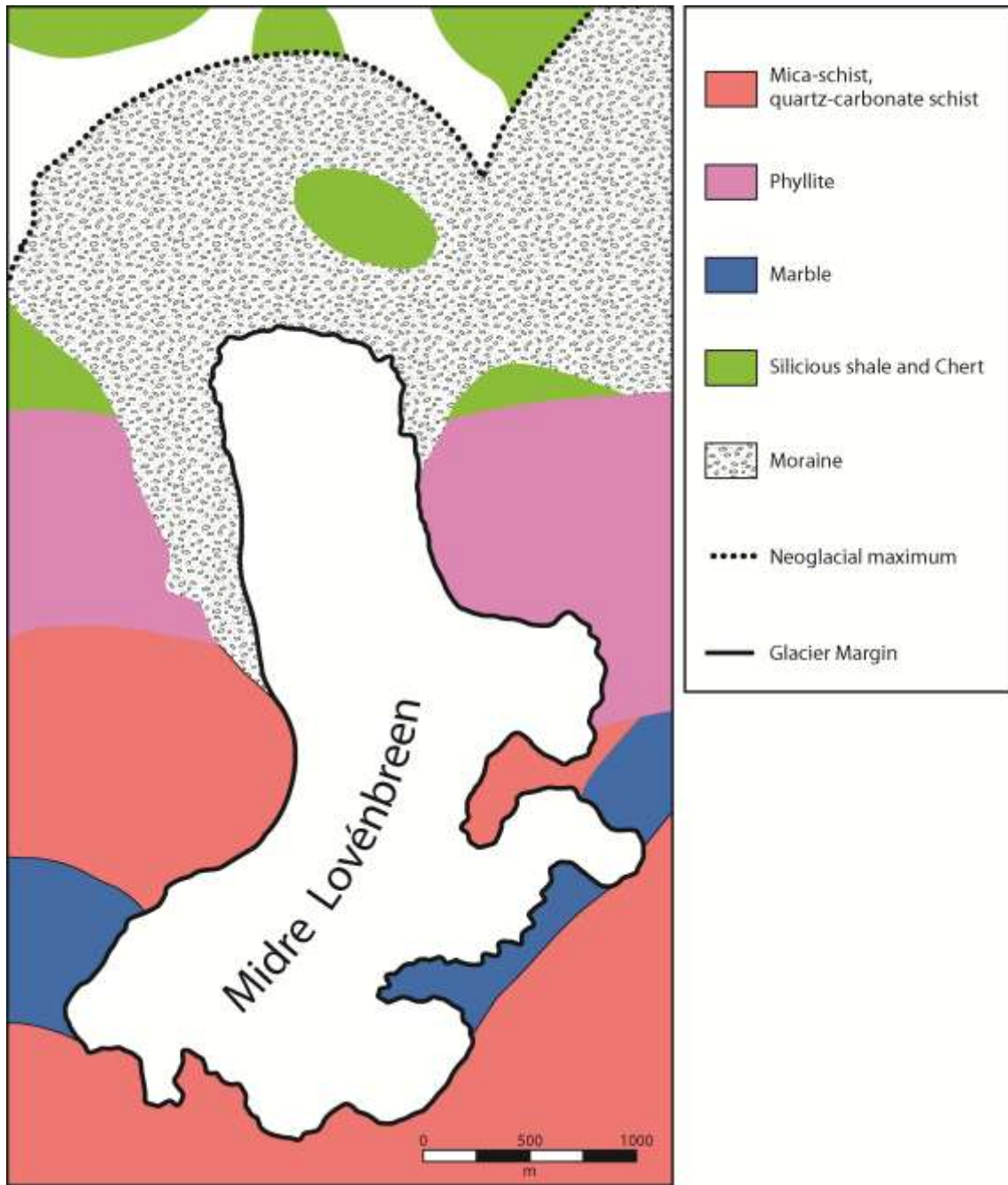


Figure 3.4. Geological map of the Midtre Lovénbreen Glacier (adapted from Roberson, 2009)

3.2.2 Ecology

Ecosystem productivity in the Arctic environment is highly dependent upon the temperature. During winter time when solar insolation becomes low, biological activity also reaches its annual minimum. During summer when polar region receive highest annual solar insolation increases, biological activity becomes visible upon deglaciated snow/ice free terrain, in the form of various flowering plants and shrubs that include *Cassiope retragona* (10-15%), *Salix polaris* (5-10%), the moss *Sanionia uncinata* (10-20%), *Oxyria digina*, *Bistorta vivipara*, *Saxifraga oppositifolia*, *Saxifraga cernua*, *Saxifraga hieracifolia*, *Saxifraga hirculus*, *Silene acaulis*, *Dryas octopetala*, *Cerastium arcticum*, *Alopecurus borealis*, *Poa Alpina*, *Carex misandra*, *Luzula confuse*, *Stereocaulon alpinum* and white crustose lichens (Ronning 1979). However, these flora are almost absent in front of Midtre Lovénbreen. This is due to the active runoff that takes place every summer and therefore glacial deposits remain too unstable for the above flora (Figure 3.5). In addition to above flora, ubiquitous microbes also exist in this area, some of which not only survive in extreme cold, but also maintain metabolic activity throughout the entire year, especially in subglacial sediments (Hodson et al., 2005a).

On the microbial scale, the subglacial and proglacial environments are inhabited by 25 species of chlorophytes and 23 species of cyanobacteria. Their abundance is generally highest in barren zone followed by vegetated then subglacial zone (Kaštovska et al., 2005). However, the highest number of bacteria are generally found in vegetated zone (ca. 13×10^{11} cells mg^{-1} of soil dry wt.) followed by barren soil (ca. 6×10^{10} cells mg^{-1} of soil dry wt.) and then subglacial till (ca. 8×10^9 cells mg^{-1} of soil dry wt.) (Kaštovska et al., 2005). Fungi are also reported in the vicinity of Midtre Lovénbreen with *Cryptococcus gastricus*, *Cryptococcus terricolus*, *Rhodotorula muscorum*, *Mrakia psychrophila*, *Mrakia gelida* and *Rhodotorula glacialis* being identified (Pathan et al., 2010).

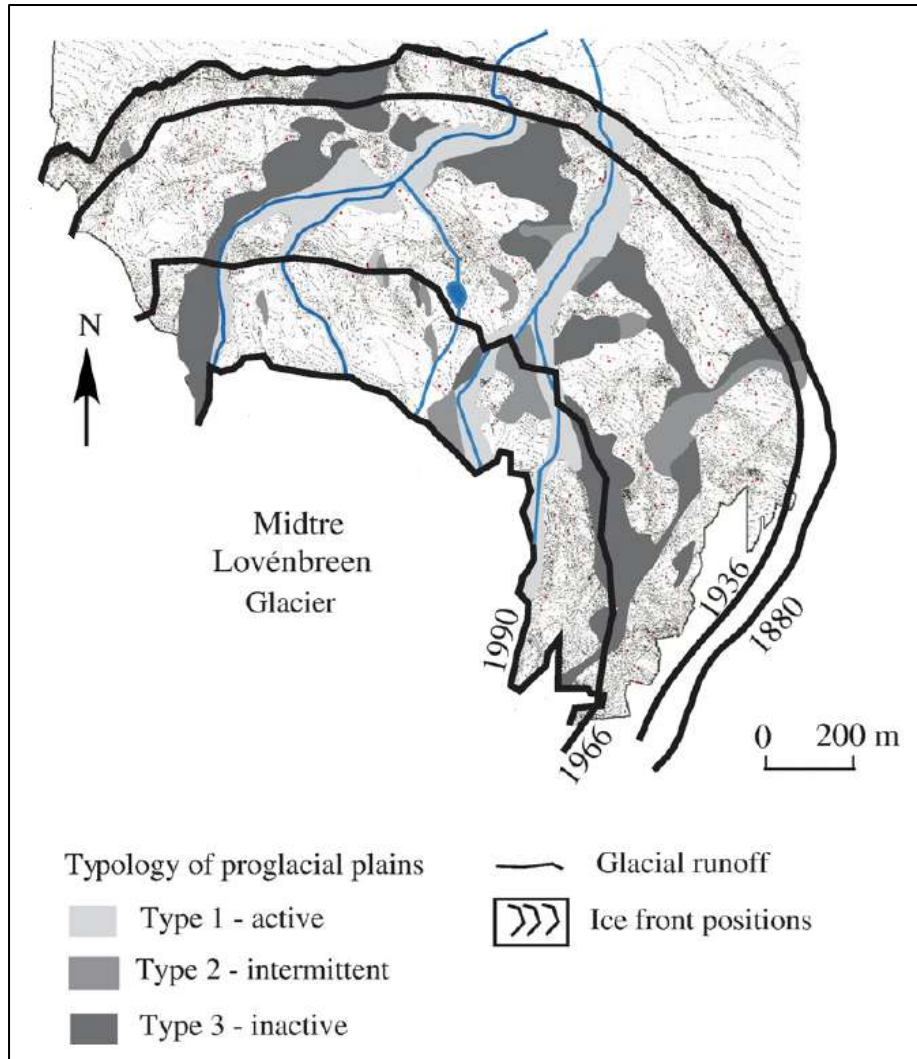


Figure 3.5. Physically active, intermittent and inactive zone in Midtre Lovénbreen catchment (adapted from Moreau et al., 2008).

The snowcover also holds a small fraction of microbial biomass, which is dominated by Proteobacteria classes; Alphaproteobacteria (mostly phototrophs), Betaproteobacteria (mostly aerobic or facultative organic degrading bacteria, some chemolithotrophs and phototrophs) and Gammaproteobacteria (facultative parasites, chemolithotrophs). Total bacterial abundance in the snow varies between 2×10^4 cells mL^{-1} and 2×10^5 cells mL^{-1} (Amato et al., 2007). These bacteria are sometimes

equipped with natural physiological abilities (for example spore formation, pigmentation etc) to survive and propagate in such extreme conditions. Cryoconite is another unique, small and biologically rich habitat generally found upon glacial surface, which is documented by cyanobacteria (mostly *Phormidium* species), bacteria (ca. 4×10^{11} cells mg^{-1} soil dry wt.; Kaštovska et al., 2005), viruses, nanoflagellates and also a small number of chlorophyte algae (*Chlorella*, *Cylindromonas* and *Chlamydomonas*) and ciliates (*Monodinium*, *Strombidium* and *Halteria*) (Sävström et al., 2002).

Invertebrates species identified in the Midtre Lovénbreen catchment include: 5% herbivores (Symphyta, Aphidoidea), 47% detritivore / omnivore (Collembola, Acarnia), 21% predators (Acarnia, Archnida, Diptera) and 26% parasitoids (Hymenoptera, Rhizopoda) (Hodkinson et al., 2004).

3.2.3 Glacier structure

Snow and ice upon the glacier are stratified in different layers which are altered by freeze-thaw cycles. During winter time a typical accumulation consists of: i) a layer of high density clear blue ice, which is formed by refrozen percolated meltwater at the base under gravitational force. This high density snow is covered by: ii) low density snow layers that are also known as firn and formed by partial melting and refreeze of deposited snow (Hambrey et al., 2005). Down the glacier, flow structures on the glacier ice surface can be seen in the form of arcuate fractures near glacier tongue. Longitudinal folding is also observed, which can be formed by stratified ice moving in opposite directions (Hambrey et al., 1999). Longitudinal foliation and a few open crevasses are well recorded in Midtre Lovénbreen (Hambrey et al., 2005). The latter convey meltwater into the subglacial drainage system (see Section 3.2.5).

Based upon seismic and radar data, King et al., (2008) suggested that the glacier bed is in places composed of a thin permafrost sediment layer (also called frozen talus) over bedrock. The thickness of the permafrost layer varies from 0.5 to 13 m with the greatest thickness observed on the southeast side of the glacier. This layer is also composed of 40–45% rock, 5–15% water and 45–50% ice, as a minimum, according to the geophysical data described by King et al., (2008). Elsewhere, the glacier is underlain by more typical glacial till, some of which is assumed to be at the pressure melting point. For example, based upon seismic, radar survey and borehole measurements, the central part of the glacier's bed has been identified among the pressure melting point zone (Björnsson et al., 1996; King et al., 2008).

3.2.4 Mass Balance

Similar to most non-surge type Svalbard glaciers. Midtre Lovénbreen's terminus has continuously receded since 1890 from its Neo-glacial maxima (Hambrey et al., 2005). Further, based on former margin positions, 1 km of retreat with an approximate volume loss of 25% has been observed in Midtre Lovénbreen glacier over last 100 years (Hansen, 1999).

The contribution of Svalbard glaciers to global sea level rise has been found to be significant (Dowdeswell and others, 1997; Van der Wal and Wild 2001). Glacier mass balance measurements are thus important to understand the hydrological cycle both at regional and global scales. Smaller glaciers in the Spitsbergen have been used for mass balance measurement for a long time, giving the longest mass balance series for this area (Hagen & Liestøl 1990). Austre Brøggerbreen and Midtre Lovénbreen in Kongsfjorden area of north-western Spitsbergen are two glaciers where mass balance measurements have been performed since 1967 and 1968. The average net mass balance loss for Midtre Lovénbreen is -0.35 ma^{-1} (up to 1999; Hagen et al., 2003).

3.2.5 Hydrology

Meltwater flow through glaciers is determined by meteorological forcing (atmospheric temperature, rainfall) as well its internal melting. Aufeis (icing) development in front of the terminus indicates the persistence of drainage in winter, often due to the polythermal nature of the glacier allowing basal melt (internal melting) and water storage throughout the winter (Hagen and Sætrang, 1991; Odegard et al., 1992; Bjornsson et al., 1996). Annual surface melting starts in late May and percolates into the snowpack, where a portion of it refreezes and releases latent heat. The contributing to internal snow pack warming and subsequently develops horizontal runoff channels (Repp, 1978)

Almost every summer (from middle or late May) glacial ablation results in three major proglacial streams in the Midtre Lovénbreen catchment. One stream emerges from the each eastern lateral (MLE) and western lateral side (MLW) of the glacial snout respectively and third one emerges from the middle of the glacial snout. The middle stream disappears before the other two during late summer. These streams receive discharge from supraglacial snowmelting and marginal ice melting and meander over short lateral distances, but follow the same incised flow path almost every year. As a result deep incisions of streams are typical over proglacial field. All the three streams discharge into Kongsfjorden, following a short interaction with the proglacial forefield (Figure 3.6).

Subglacial runoff takes place every summer in late May or early June after emerging from the glacier tongue as an artesian fountain or “upwelling” and merges into MLE. However, hydrological studies in last 1.5 decades demonstrated that subglacial upwellings have emerged on the eastern side of the glacial tongue most often, but in 1998 and 2005 it emerged on western side of the glacier (Irvine-Fynn et al., 2005). This movement of subglacial upwelling location reflects the structural changes in subglacial channels (Rippin et al., 2003), but the mechanism behind these

subglacial structural changes still needs to be explained. The opening time for subglacial upwelling also depends upon the amount of stored melt water under the glacial bed from previous seasons (Hodson et al., 2005b). Therefore, during summer ablation, the additional pressure due to snow and ice melt the glacial surface (over the pre-existing pressure by stored water from previous season), helps to pass the critical pressure limit required to open the subglacial runoff outlet. During this course of ablation subglacial channels become increasingly efficient (Vatne et al., 1995; Bingham 2003). Irvine-Fynn et al. (2005) suggested that during summer ablation, supraglacial meltwater supplies subglacial discharge via a moulin at 350 meter elevation on the eastern side of the glacier and three further moulins in the southern part ca. 400 m (Figure 3.6).

3.3 Sampling

3.3.1 Sampling sites and sampling frequency

During 2009, five bulk snowpack samples were collected from the centre line of the glacier surface at approximately 80 to 90 m elevation intervals on Day Of Year (DOY) 160 and before the start of snow melt (SG1 to SG5 in Figure 3.6). Melt water samples were then collected from the streams from DOY 184 at MLE1 and MLW1, and from DOY 198 at UPW, following subglacial upwelling emergence (Figure 3.6). Meltwater samples were collected every second or third day from DOY 184 to 205 and then approximately every week from DOY 233 to 250.

During 2010, winter deposition sampling was done in the last week of May (between DOY 143 to 149) from the five supraglacial sites. Subsequently, sampling was designed to investigate the downstream biogeochemical changes in the streams using 3 sites (MLW1, MLW2, MLW3) on the westernmost river and 4 sites (UPW, MLE1, MLE2, MLE3) on the easternmost river (Figure 3.6) on DOY 186. Five weekly profile samples were collected from the above stream sites throughout the summer until DOY 250. [Samples during 2010 were taken on behalf of the project (see acknowledgements)].

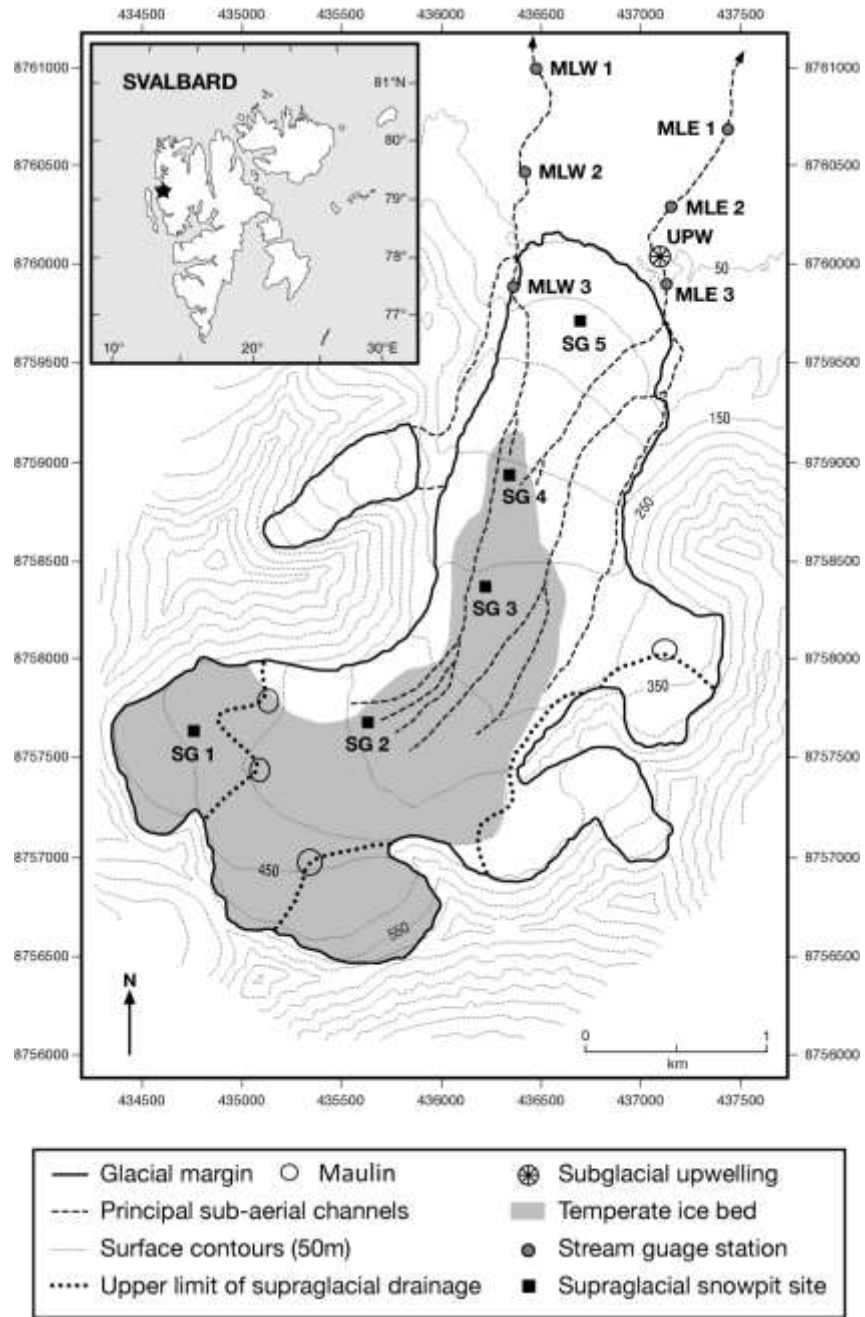


Figure 3.6. Midtre Lovénbreen map sampling set up, UPW is the upwelling site and MLE3, MLE2, MLE1 are downstream sampling sites on the eastern stream. MLW3 MLW2 and MLW1 are downstream sampling sites on the western stream. SG1-SG5 are supraglacial snowpit sites.



Figure 3.7. Data logging station at subglacial UPW site (a), at MLE1 (b), at MLW1 (c), July 2009.

3.3.2 Winter deposition sampling

Snowpack samples were collected using a pre-cleaned HDPE tube of known dimensions that was first cleaned at least three times with snow from near the site. Then it was inserted vertically into snow pack up to the glacial surface and excavated using a clean knife. The snow core was transferred into pre-cleaned polyethylene zip-lock bags (three times washed with snow) and weighed. Snow samples were then thawed at 4°C and filtered with 0.45 µm cellulose nitrate filter paper (nitrate elution from the filter paper was below detection limit). Filtered samples were stored in 60 mL polyethylene bottles refrozen at -20°C and transported back to laboratory for chemical and isotope analysis. Bottles were pre-rinsed with filtered sample water before sample transfer.

3.3.3 Summer stream sampling

Before sample collection each pre-rinsed bottle was cleaned with sample water at least three times. Stream water was used to wash sampling bottles and released downstream. Between 1 and 1.5 litres of meltwater sample was then collected from each stream sites in HDPE bottles. Samples were filtered using 0.45 µm pore size cellulose nitrate filter papers at the British NERC Arctic station lab facility (1-2 hour after sample collection). Then 3 × 60 mL samples were stored and frozen in polypropylene bottles and transported to Sheffield for further analysis. Between 0.5 and 1 litre samples were also stored separately for SO₄²⁻ isotope analysis.

3.3.4 Sample preservation

Following the most conventional method to separate dissolved and particulate in aquatic media, sample were filtered with 0.45 µm pore size filter. Substances that pass through the 0.45 µm pore size along with liquid were considered as solute. This assumption is not correct in all cases, because there are some picoplankton (0.2 – 2

μm) and femtoplankton ($< 0.2 \mu\text{m}$) (Sieburth et al., 1978; Stockner, 1991) that are small enough in size to pass the above $0.45 \mu\text{m}$ size. However, these genera are mostly reported in marine ecosystems and are sparsely found in atmospheric, terrestrial or glacial ecosystems. Therefore, any possible alteration in fresh water due to picoplankton and femtoplankton are considered to be negligible. Filtered samples were preserved at -20°C to stop any further biochemical activity.

3.3.5 Real time stream monitoring

Data loggers (Aqua TROLL[®] 200 from In-situ Inc.) were installed at two stream sites (MLE1 and MLW1) situated within the Little Ice Age moraines during 2009 and 2010 to monitor electrical conductivity, pressure and temperature (Figure 3.6). These data loggers were fixed and secured to a suitable position near the middle of the stream where sensors could face maximum flow in an appropriate depth of water using aluminium poles. Because the streams kept meandering, the data loggers were also shifted accordingly. Data loggers were configured to record the data at every 5 seconds and averaged every 1 hour. However, these systems were ill-equipped to deal with the dynamic, sediment-rich streams. Therefore, it was not possible to present data from UPW. Meltwater discharge at MLW1 and MLE1 was established after calibrating the pressure transducer records using the salt dilution method for salt dilution.

For each dilution, 300 to 500 g of NaCl was properly dissolved in half bucket ($\sim 6 \text{ L}$) of stream water and then injected at a distance of ~ 90 meter upstream allowing proper mixing of injection solution in the stream (Day, 1977). Following the salt dilution, change in EC was recorded to calculate the discharge using the equation 3.1 given below. Errors were ca, 15% according regression analysis of the results and the data logger readings.

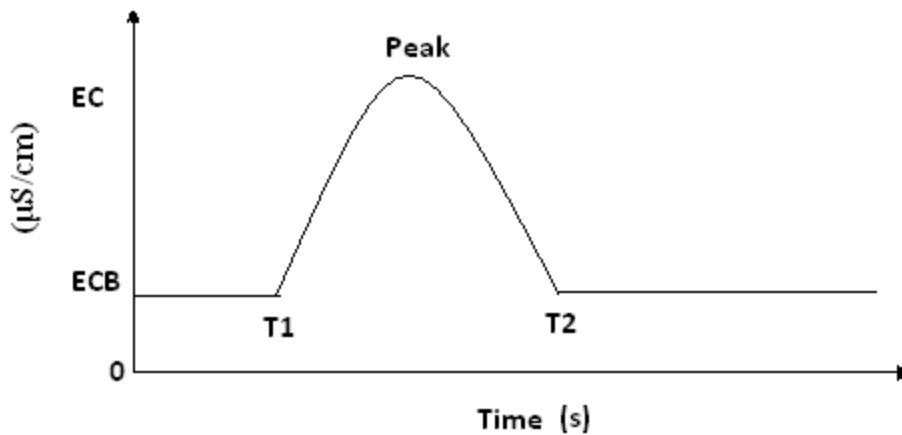


Figure 3.8. Salt wave peak in the stream during salt dilution gauging.

$$Q = KM / (T_2 - T_1) (EC - EC_B) \quad (3.1)$$

EC = Average conductivity of salt wave / time taken by salt wave to pass logging point ($T_2 - T_1$)

Where Q = discharge (m^3/s), M = mass of salt used for dilution, T_1 = time when salt wave starts, T_2 = time at which salt wave ends (all in seconds), EC = average conductivity ($\mu S/cm$), EC_B = Background conductivity ($\mu S/cm$) (Figure 3.8).

Putting the respective value in above equation gave discharge value in m^3/sec after coefficient “K” was determined by calibration of sensor with salt standards; 10, 20, 30 and 40 $mg L^{-1}$ of salt solution was prepared in stream water and EC of the calibration solutions were plotted against their concentration to obtain the “K” value (“K” is the slope of the salt concentration versus EC reading). This calibration was performed in the field to maintain the temperature of calibration solution close to the stream temperature.

3.4 Chemical analysis

To preserve SO_4^{2-} isotope samples, HCl was added to filtered water to give a pH between 3 and 4. Thereafter, the samples were shaken for a few minutes to release CO_2 and then 5 mL of 1 Molar BaCl_2 solution was added. The resulting solution was left undisturbed for 24 hours to allow BaSO_4 precipitate and settle down in the flask. After that the clear supernatant was poured off and remaining liquid filtered through 0.45 μm cellulose nitrate and washed using deionised water. The filter paper and white precipitate was then dried and packed into aluminium foil to transport it for analysis. NO_3^- isotope samples were transported frozen to UEA (University of East Anglia, Norwich, UK), SO_4^{2-} and H_2O isotope samples to NERC Isotope Geoscience Laboratory, Nottingham, UK. Samples for the analysis of major ions, TN and DOC were transported to the University of Sheffield, Sheffield, UK also in a frozen state. All water and snow samples were kept frozen for 3 to 6 months prior to analysis. It has been observed that solute chemistry of frozen samples does not change significantly for upto 12 months (Welch et al., 1996; Escobar and Randell, 2000; Gardolinski et al., 2001; Kaszyńska et al., 2003).

3.4.1 Dissolved Organic Carbon (DOC)

Dissolved organic carbon (DOC) determinations were undertaken on behalf of project (see acknowledgement) using a Thermalox total organic carbon / total nitrogen analyzer. Filtered samples were decanted into vials up to 1/3 of their volume limit and loaded into a vial rack of the autosampler-AS8000. In this method inorganic carbon (carbonates, bicarbonates, and CO_2) was removed by addition of 10% HCl and subsequent purging with carrier gas (CO_2 free O_2). This pretreated sample was then injected to the TC furnace through a carbon free septum where the organic carbon was oxidised to CO_2 through catalytic oxidation at 680°C. The generated CO_2 gas was measured by a Nondispersive Infrared CO_2 Detector (NDIR). These values were calibrated against known standard concentrations (potassium hydrogen phthalate;

KHP). Precision errors were <5% (Table 3.1). This is also known as the non purgeable organic carbon (NPOC) method.

Table 3.1. Operatic condition of the Thermalox TC/TN analyser.

Software	Lab View®
Carrier gas	O ₂
Carrier gas flow rate	180 mL minute ⁻¹
Sparge acid	10 % HCl
Sparge volume	45 µL
Furnace temperature	680°C
Oxidising agent	Platinum coated quartz rods
Sample injection volume	Low DOC (0 – 2 mg L ⁻¹) = 50 µL Mid DOC (2 – 15 mg L ⁻¹) = 30 µL High DOC (30 – 60 mg L ⁻¹) = 20 µL
Precision: Standard deviation	≤ 5% of full scale ranges to 3 mg L ⁻¹ ≤ 3% of full scale ranges to 500 mg L ⁻¹ ≤ 2% of full scale ranges to 40,000 mg L ⁻¹

3.4.2 Total dissolved nitrogen (TDN) and dissolved organic nitrogen (DON) by Thermalox analyser

To measure TDN, filtered sample was injected to a catalytic furnace for the oxidation of organics at a high temperature and the oxidised gas (NO_x) were swept by carrier gas through to a chemiluminescent detector (This detector works on chemiluminiscent reaction under heated vaccum chamber, where NO reacts with O₃). NO₂ also formed in oxidised gases was further reduced to NO in a reduction furnace. DON concentrations were calculated based upon the difference between the TDN and dissolved inorganic nitrogen (DIN= NO₃⁻ + NH₄⁺; detected using methods described in section 3.4.4). The detection range of the machine is 20 µg L⁻¹ to 200 mg L⁻¹.

NH₄Cl was used as a standard to calibrate the TN values and precision errors were ≤ 5% (see Table 3.2).

Table 3.2. Operatic condition of the Thermalox TC/TN analyser.

Software	Lab View®
Carrier gas	O ₂
Carrier gas flow rate	180 mL minute ⁻¹
Furnace temperature	1000°C
Oxidising agent	Platinum coated quartz rods
Sample injection volume	≤ 5% of full scale ranges to 3 mg L ⁻¹ ≤ 3% of full scale ranges to 200 mg L ⁻¹

3.4.3 Dissolved organic nitrogen (DON) by persulphate oxidation methed

In this method potassium per sulphate (K₂S₂O₈) was recrystalised thrice to improve its purity and then 6 g of it dissovved in 100 mL of 1.5 M NaOH solution. Two mL of the resulting solution (stable for 8 days) was added to 12 mL of filtered sample in a borosilicate tube and instantly closed tight with a teflon lined cap. For blank correction, three tubes were also filled with persulphate solution. These tubes were autoclaved at 120°C with a slow vent setting.

This oxidized NO₃⁻ was then analysed by the colorimetric method on an autoanalyser (SKALAR) equipped with SAN⁺⁺ colorimetric detector and 1050 automatic sampler (programmed on SAN⁺⁺ FlowAcess® software). To calculate the DON amount, inorganic nitrogen (NH₄⁺ + NO₃⁻) from respective non-oxidised samples was substracted from oxidised nitrogen (see Section 3.4.4). The precision for this method was ± 2%.

3.4.4 Major ions

Major ions (anions: NO_3^- , SO_4^{2-} , F^- , Cl^- , PO_4^{3-} ; cations NH_4^+ , Na^+ , K^+ , Ca^{2+} , Mg^{2+}) were measured using a Dionex DX 90 ion chromatograph, operated through a 4400 integrator and AS40 autosampler. Repeatability for standards was 1.6, 5.7, 2.8, 1.4, 6.5% for the anions listed above and 2.5, 0.06, 0.2, 0.08, 1.5% for the cations. HCO_3^- was determined by ion balance calculation.

The Dionex ion chromatographs use suppressed conductivity detection to perform isocratic ion analysis. This system consists of liquid eluent, high pressure pump, a sample injector, a separation column, a chemical suppressor and a conductivity cell.

Table 3.3. Operating conditions for cations

Software	Chromeleon®
Eluent	20 mM Methansulfonic acid
Eluent flow rate	0.5 mL minute ⁻¹
Injection volume	25 µL
Loop size	10 µL
Guard column	Ionpac® CG12A-5 µM
Analytical column	Ionpac® CG12A-5 µM
Detector	ECD

Table 3.4. Operating conditions for anions

Software	Chromeleon®
Reagent	1.0 mM NaHCO_3
Eluent	1.0 mM Na_2CO_3
Eluent flow rate	0.5 mL / min
Injection volume	25 µL
Loop size	10 µL
Guard column	Ionpac® AG14A-5µM
Analytical column	Ionpac® AG14A-5µM
Detector	ECD

3.4.5 Dissolved silicate (SiO₂)

Dissolved silicate was determined by the colorimetric method on an autoanalyser (SKALAR) equipped with SAN⁺⁺ colorimetric detector and 1050 automatic sampler (programmed on SAN⁺⁺ FlowAccess® software). In this method, an acidic solution of sample was treated with molybdate solution that formed a yellow coloured silicomolybdic acid. Based upon the absorptivity of formed yellow colour at 380 nm (Lambert-Beer's law valid for up to 200 µmol L⁻¹ of SiO₂ concentration), the concentration of silicate in the samples were measured against known standard solution with a precision error of < 6% according to the standard deviation of replicate measurements.

3.4.6 Total dissolved nitrogen flux measurement for the glacial streams

TDN (NH₄⁺, NO₃⁻, DON) concentrations in the snow and stream samples were integrated with discharge data to measure the downstream TDN changes. First, the mean discharge weighted concentration (MDC) for NH₄⁺, NO₃⁻ and DON was calculated by, $MDC = \frac{\sum_i^n (Q_i C_i)}{\sum_i^n Q_i}$ where Q_i is instantaneous discharge at the time of sampling (m³ s⁻¹) and C_i is instantaneous concentration at time of sampling (µg L⁻¹) and n, the number of samples (for whole sampling period), for each stream sites. Then the MDC values for NH₄⁺, NO₃⁻ and DON from each sampling sites were compared to its upstream and downstream sites to calculate the downstream changes. Assuming snow melt dominate the stream discharge, mean concentration of NH₄⁺, NO₃⁻ and DON in the snowpack were used in parallel to the stream's MDC values for the flux calculation.

3.5 Analysis of stable isotopic tracers

3.5.1 Denitrifier method for $\delta^{15}\text{N-NO}_3$ and $\delta^{18}\text{O-NO}_3$ analysis using GC-IRMS

This method is based on denitrification, developed by Sigman et al., (2001) and Casciotti et al., (2002) and then amended by Kaiser et al., (2007). It was rapid and fully automated and required only ≈ 10 nmole NO_3^- , 2-3 orders of magnitude less than the silver nitrate method, at a similar analytical precision (0.2‰ for $\delta^{15}\text{N}$, 0.5‰ for $\delta^{18}\text{O}$). It was based on denitrification of the NO_3^- by a specific denitrifier *Pseudomonas aureofaciens* to nitrous oxide (N_2O). This strain lacks active nitrous oxide reductase required for converting nitrous oxide to free nitrogen and showed little isotope exchange between water and intermediate species during denitrification. The N_2O $^{15}\text{N}/^{14}\text{N}$ and $^{18}\text{O}/^{17}\text{O}$ ratios of the N_2O was determined by mass spectrometry at the masses 44, 45, 46 (Sercon TGII/Geo) and corrected to $\delta^{15}\text{N}$ and $\delta^{18}\text{O}$ values versus atmospheric- N_2 and VSMOW respectively by comparison with the NO_3^- reference materials IAEA-NO-3, USGS-34 and USGS-35. [The samples were analysed on behalf of the project at UEA, Norwich (see acknowledgements Section)].

3.5.2 $\delta^{34}\text{S-SO}_4$ and $\delta^{18}\text{O-SO}_4$ analysis

For $^{34}\text{S}/^{32}\text{S}$ analysis, barium sulphate was combusted to SO_2 in an EA-1120 elemental analyser on-line to a Delta+XL isotope ratio mass spectrometer (ThermoFinnigan, Bremen, Germany), with $^{34}\text{S}/^{32}\text{S}$ ratios calculated as $\delta^{34}\text{S}$ values versus CDT by comparison with standards IAEA SO5 ($\delta^{34}\text{S} = +0.5\text{‰}$) and NBS-127 ($\delta^{34}\text{S} = +21.1\text{‰}$). Analytical precision of replicates was typically $< 0.3\text{‰}$ (1 SD).

For $^{18}\text{O}/^{16}\text{O}$ analysis, the barium sulphate was pyrolysed in a TC/EA elemental analyser on-line to a Delta+XL IRMS (ThermoFinnigan, Bremen, Germany), with $^{18}\text{O}/^{16}\text{O}$ ratios calculated as $\delta^{18}\text{O}$ values versus SMOW by comparison with standards IAEA SO6 ($\delta^{18}\text{O} = -11.3\text{‰}$) and NBS-127 ($\delta^{18}\text{O} = +8.6\text{‰}$). Analytical precision of replicates was typically $< 0.8\text{‰}$ (1 SD). [The samples were analysed on behalf of

project at NERC Isotope Geosciences Laboratory, Nottingham (see acknowledgements Section)]

3.5.3 $\delta^{18}\text{O}\text{-H}_2\text{O}$ Analysis

$^{18}\text{O}/^{16}\text{O}$ ratios were determined on CO_2 equilibrated water samples in an Isoprep 18 coupled to a SIRA mass spectrometer (Micromass, Middlewich, England). The ratios were reported as $\delta^{18}\text{O}$ values versus VSMOW, based on comparison with laboratory standards calibrated against IAEA standards VSMOW and SLAP, with analytical precision (1 S.D.) typically better than 0.05‰ for $\delta^{18}\text{O}$. The samples were analysed on behalf of project at NERC Isotope Geosciences Laboratory, Nottingham (see acknowledgements Section).

3.6 Rock dissolution experiments

Midtre Lovénbreen catchment is largely covered by quaternary moraines, most probably transported from higher altitude mountains such as Welderyeggen, which is composed of phyllite, mica and schist with carbonate and quartzite beds, Steenfjellet, which is further composed of gneiss and migmatite (Hjelle 1993) (Figure 3.4). All the three rocks used in the dissolution experiment were therefore either metamorphic or sedimentary rocks. **Phyllite** is a foliated metamorphic rock that mostly consists of quartz, mica and chlorite formed by low grade metamorphism of shale or pelite. **Gneiss** is common metamorphic rock that is mostly formed as a result of high grade regional contact metamorphism in igneous or sedimentary rocks. It is coarse to medium foliated in texture. **Conglomerate** was largely composed of quartz amalgamated with kaolinite, pyrite, aluminium silicate, calcium hydroxyapatite and manganese oxide. A small amount of jarosite, gypsum and iron oxy-hydroxide and oxide can also be detected from the rock surface (Borin et al., 2010).

Table 3.5, The content of nitrogen, sulphur and its respective isotope signature for the six major meta-sedimentary rocks collected from the Midtre Lovénbreen catchment (Wynn, 2004).

Sample	<i>n</i>	$\delta^{15}\text{N-NH}_4^+$ (‰)	Nitrogen content	$\delta^{34}\text{S}$ (‰)	Sulphur Content
		Vs Air	($\mu\text{g/g}$)	Vs CDT	($\mu\text{g/g}$)
Phyllite	2	+7.2	198.4	+17.9	1200
Green chert	1	+4.8	59.3	+14.7	2540
Gneiss	1	n.a.	b.d.	+8.2	350
Conglomerate	2	-1.6	167.8	+10.3	5020
Subglacial till	2	+7.7	52.0	+18.2	760
Quartzite	1	n.a.	b.d.	-4.1	50

Two type of rock experiments were done to understand the potential role of rock-N and S in the glacial catchment: in these experiments three different rocks [phyllite, gneiss, conglomerate] were collected from Midtre Lovénbreen catchment area. All three rocks were washed with hydrogen peroxide and crushed to make powder and then sieved through a 250 μm size mesh (Wynn, 2004).

3.6.1 Dissolution experiments

Simple lab-based rock dissolution experiments were carried out to understand the release of inorganic N and S from the rocks. The leaching or dissolution procedure involved the following steps:

- 5 g rock powder was suspended into 35 mL of respective MilliQ water (18Ω) in a precleaned centrifuge tube.
- The suspension was agitated on an end-over shaker for 24 hours.
- Solutions were centrifuged at 3500 rpm for 15 minutes and then the supernatant liquid was removed and filtered through a 0.45 μm size cellulose nitrate filter paper. Then analysed for Na⁺, K⁺, Ca²⁺, Mg²⁺, NH₄⁺, Cl and SO₄²⁻ NO₃⁻ and using the colorimetric method described in Section 3.4.4, was then conducted immediately.
- At the same time 45 mL of MilliQ water was added to a centrifuge tube and followed all the above procedure was used in parallel for blank correction.
- Increases in ions in leachate were then calculated (in μg g⁻¹ of rock powder).

All experiments were conducted in triplicate and repeated using the same powder to produce three successive data sets.

3.6.2 Adsorption experiment

The adsorption of inorganic nitrogen by the rocks were carried out in the following steps:

- 5g of rock powder was taken into a precleaned centrifuge tube and washed three times following the procedure described in Section 3.6.1.
- Washed and dried rock powders were equilibrated with 45 mL solutions of known NO₃⁻-N and NH₄⁺-N concentration for 30 minutes. The resulting suspensions were centrifuged at 3500 rpm for 15 minutes and then supernatant

liquid was filtered with 0.45 μm pore size cellulose nitrate filter paper. Filtrate was analysed for NO_3^- -N and NH_4^+ -N using the colorimetric method described in Section 3.4.4.

- At the same time 45 mL of MilliQ water was filled in a centrifuge tube and followed all the above procedures in parallel for blank correction.

- The change in the amount of inorganic nitrogen from solution was used to calculate for adsorption following the methodology described in Section 3.4.4.

CHAPTER 4: RESULTS

This chapter presents meteorological, hydrological and solute chemistry data collected during the two years of study. Section 4.1 presents the meteorological and Section 4.2 hydrological data. Sections 4.3 and 4.4 present the solute abundance, distribution and variability in snow and stream samples respectively. The isotopic characterisation of representative field samples are presented in Section 4.5, whilst Section 4.6 presents the data obtained from lab based rock experiments. A summary of major results follows in Section 4.7.

4.1 Ny Ålesund Meteorology

The local climate during 2009 experienced a moderate condition of NAO, where the index values ranged between -3.7 and $+1.7$ with an annual mean of -0.4 . The monthly mean air temperature of winter, spring, summer and fall, ranged from -11.8 to -7.8°C , -15.6 to -1.8°C , $+1.6$ to $+6^{\circ}\text{C}$ and -4.3 to $+1.2^{\circ}\text{C}$ respectively. The monthly precipitation during this year varied between 0.5 and 6.2 cm, of which larger amount took place during fall. However, snow accumulation reached a maximum of 67 cm depth (at an altitude of 17 m above sea level) during the winter-spring (Figure 4.1).

During 2010, the NAO was significantly negative, and so whilst the index value was $+2.4$ in January, which subsequently ranged between -4.6 and 0 for the rest of the year, with an annual mean of -1.8 . The monthly mean air temperature of winter, spring, summer and fall temperature varied from -13.9 to -4.3°C , -7.8°C to $+2.9$, $+1.2$ to $+5.7^{\circ}\text{C}$ and -11.6 to -3.4°C respectively. The monthly precipitation during this year varied between 0 and 12.2 cm and again, the larger fraction of precipitation occurred during fall. The maximum snow accumulation only reached 23 cm during this winter-spring interval (Figure 4.1).

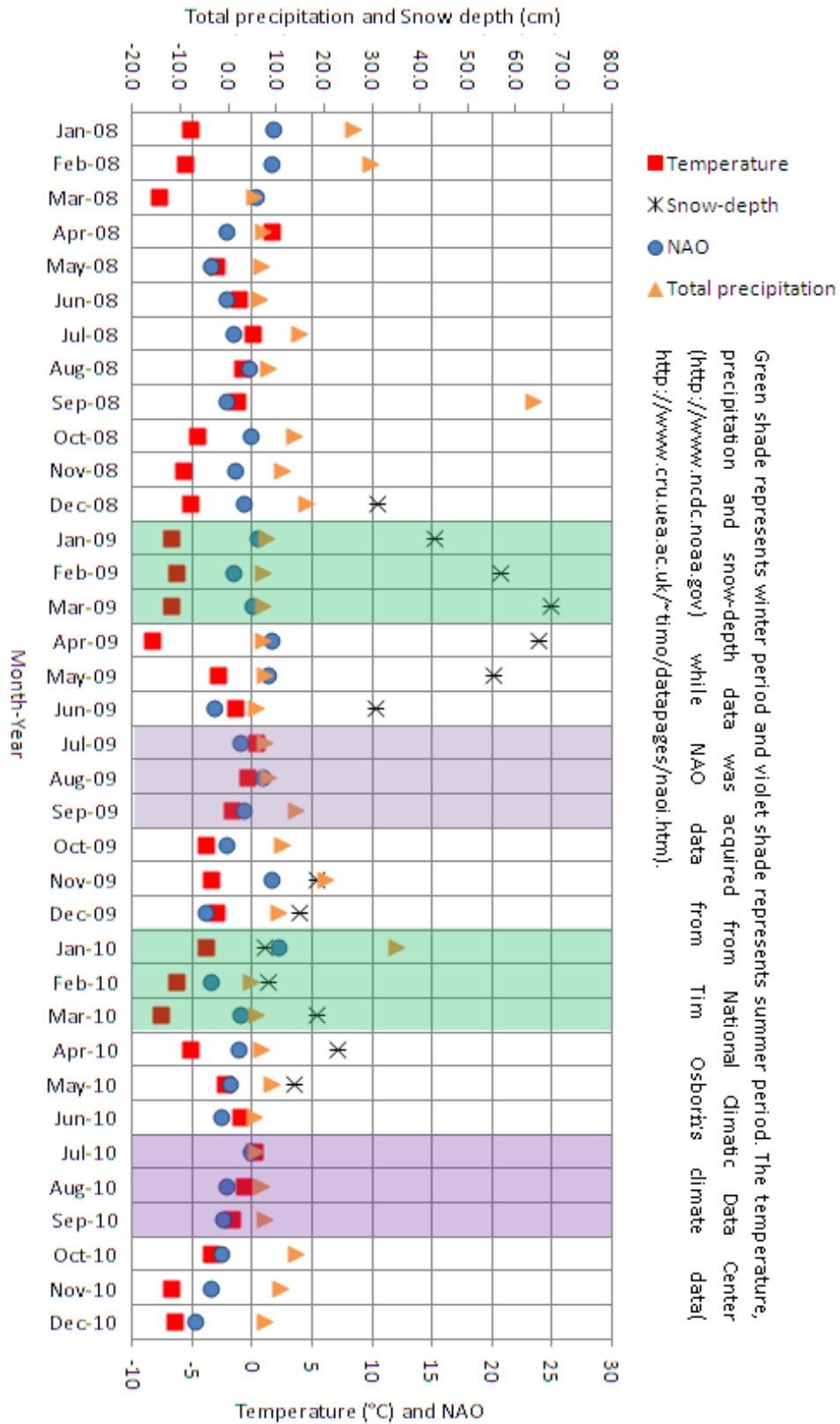


Figure 4.1. Meteorological conditions at the Ny Ålesund during 2009 and 2010.

4.2 Hydrological conditions

During summer 2009, initially (before DOY 196) when the eastern and the western stream received water directly from supraglacial snow and glacial marginal ice melt, discharges were similar at the two streams. After the subglacial outburst (DOY 196), which opened into the eastern stream, discharge at MLE1 increased to the seasonal maximum of $2.45 \text{ m}^3 \text{ s}^{-1}$ on DOY 213, and then slowly decreased to $0.21 \text{ m}^3 \text{ s}^{-1}$ with little diurnal variation in-between. However, during this period discharge at MLW1 (which remained sourced from supraglacial and glacial marginal ice melting only) showed a relatively small increase and then decreased to a value about $0.1 \text{ m}^3 \text{ s}^{-1}$ (Figure 4.2).

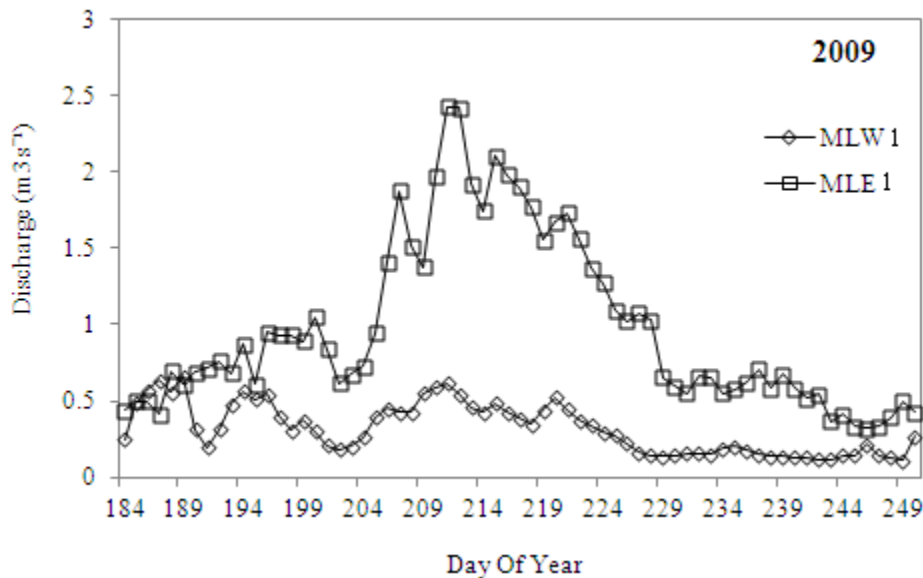


Figure 4.2. Daily average discharge variations at MLE1 and MLW1 during summer 2009.

During summer 2010, discharge observations were collected from DOY 184 to 238 at MLE1 and MLW1. This time, snowmelt started earlier (mid June) and so complete melt of proglacial snow (during late June) and the subsequent subglacial outburst (first week of July) occurred earlier than in 2009. Again the proglacial eastern

stream was fed by the two distinct sources of melt water: the eastern ice marginal stream (MLE3) and subglacial runoff (UPW). The MLW1 had no subglacial runoff, and so supraglacial snow and marginal ice melt remained the predominant source of water throughout the summer. The water discharge at MLE1 initially reached a maximum of $1.5 \text{ m}^3 \text{ s}^{-1}$ during early summer (on the DOY 194) and afterwards decreased to $0.13 \text{ m}^3 \text{ s}^{-1}$ during late summer (on the DOY 238). Similarly the water discharge at MLW1 also decreased from the early to late summer ($0.3 \text{ m}^3 \text{ s}^{-1}$ to $0.1 \text{ m}^3 \text{ s}^{-1}$) but the discharge and its variation was lower than at MLE1 (Figure 4.3).

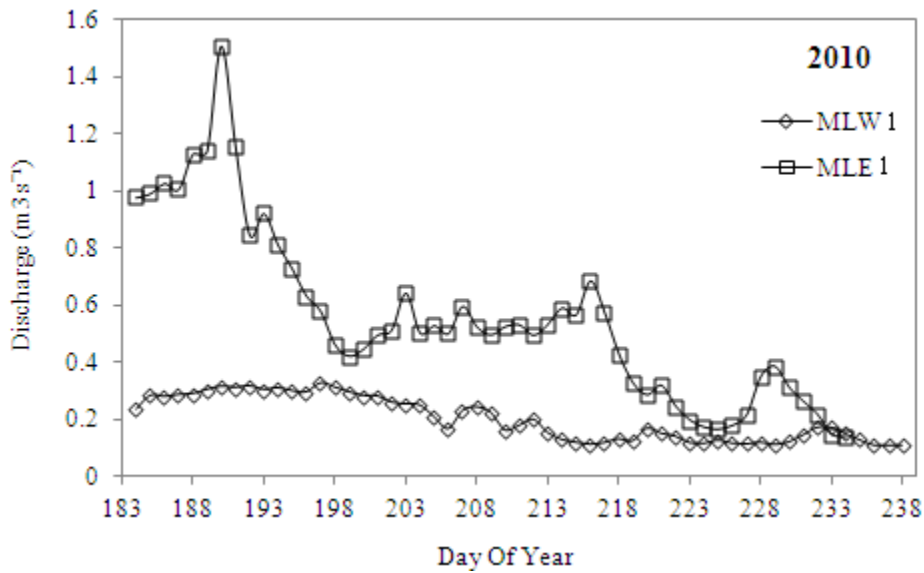


Figure 4.3. Daily average discharge variations at MLE1 and MLW1 during summer 2010.

4.3 Snow solute chemistry

(Complete data is given in appendix 1, Table I and II)

This section presents the abundance of solute in snow, their distribution along the glacier and variability on annual scale during the two years of study (see Section 3.2). Solute/ Cl^- ratios were used to split the sea-salt and non sea-salt deposition.

Table 4.1. Mean concentrations (\pm standard deviation) of solute and their ratio against Cl^- in snow [SSR = Sea Salt Ratio (Wilson, 1975) and n = number of samples].

Species	Snow (2009)	Snow (2010)	Solute/ Cl^-	SSR	Snow (2009)	Snow (2010)
Ca^{2+} (mg L^{-1})	0.81 \pm 0.26 (n = 5)	0.62 \pm 0.25 (n = 5)	$\text{Ca}^{2+} / \text{Cl}^-$	0.02	0.32 \pm 0.14 (n = 5)	0.53 \pm 0.11 (n = 5)
Mg^{2+} (mg L^{-1})	0.57 \pm 0.18 (n = 5)	0.40 \pm 0.05 (n = 5)	$\text{Mg}^{2+} / \text{Cl}^-$	0.06	0.21 \pm 0.05 (n = 5)	0.36 \pm 0.11 (n = 5)
Na^+ (mg L^{-1})	1.69 \pm 0.90 (n = 5)	0.80 \pm 0.19 (n = 5)	$\text{Na}^+ / \text{Cl}^-$	0.55	0.58 \pm 0.02 (n = 5)	0.73 \pm 0.29 (n = 5)
K^+ (mg L^{-1})	0.10 \pm 0.04 (n = 5)	0.06 \pm 0.01 (n = 5)	K^+ / Cl^-	0.02	0.04 \pm 0.01 (n = 5)	0.05 \pm 0.01 (n = 5)
$\text{NH}_4^+ \text{-N}$ ($\mu\text{g L}^{-1}$)	16.25 \pm 2.40 (n = 5)	21.07 \pm 3.60 (n = 5)	$\text{NH}_4^+ \text{-N} / \text{Cl}^-$	–	7.02 \pm 3.89 (n = 5)	19.27 \pm 6.08 (n = 5)
F^- (mg L^{-1})	–	–	F^- / Cl^-	–	–	–
Cl^- (mg L^{-1})	2.93 \pm 1.66 (n = 5)	1.14 \pm 0.22 (n = 5)	–	–	–	–
$\text{NO}_3^- \text{-N}$ ($\mu\text{g L}^{-1}$)	24.45 \pm 4.78 (n = 5)	34.15 \pm 15.87 (n = 4)	$\text{NO}_3^- \text{-N} / \text{Cl}^-$	0.103	9.58 \pm 2.75 (n = 5)	33.09 \pm 22.91 (n = 4)
SS-SO_4^{2-} (mg L^{-1})	0.41 \pm 0.23 (n = 5)	0.12 \pm 0.02 (n = 5)	$\text{SO}_4^{2-} / \text{Cl}^-$	0.14	0.17 \pm 0.06 (n = 5)	0.26 \pm 0.06 (n = 5)
NSS-SO_4 - (mg L^{-1})	0.14 \pm 0.04 (n = 4)	0.17 \pm 0.03 (n = 5)	$\text{NSS-SO}_4^{2-} / \text{Cl}^-$	0	0.048 (n = 4)	0.058 (n = 5)
Si (mg L^{-1})	–	0.02 \pm 0.01 (n = 3)	Si / Cl^-	–	–	0.01 \pm 0.01 (n = 3)
HCO_3^- (mg L^{-1})	36.58 \pm 11.16 (n = 8)	2.98 \pm 0.79 (n = 5)	$\text{HCO}_3^- / \text{Cl}^-$	0.0073	1.59 \pm 1.13 (n = 5)	2.07 \pm 1.02 (n = 5)
DOC (mg L^{-1})	0.33 \pm 0.06 (n = 3)	0.28 \pm 0.16 (n = 3)	DOC / Cl^-	–	0.28 \pm 0.17 (n = 5)	0.28 \pm 0.23 (n = 3)
DON ($\mu\text{g L}^{-1}$)	29.21 \pm 4.41 (n = 4)	86 \pm 9.38 (n = 2)	DON / Cl^-	–	10.96 \pm 6.71 (n = 5)	86 \pm 9.38 (n = 2)

4.3.1 Year 2009

The five snow pits (SG1 to SG5) were located at decreasing altitudes and had snow depths of 233, 207, 177, 152, 105 cm. Due to metamorphosis of different grain sizes of snow, ice layers could be easily seen in snowpack profiles. Different snow layers could represent different chemistries but here we assume that the overall snow signature gives an appropriate insight to all events during snowpack formation and runoff production.

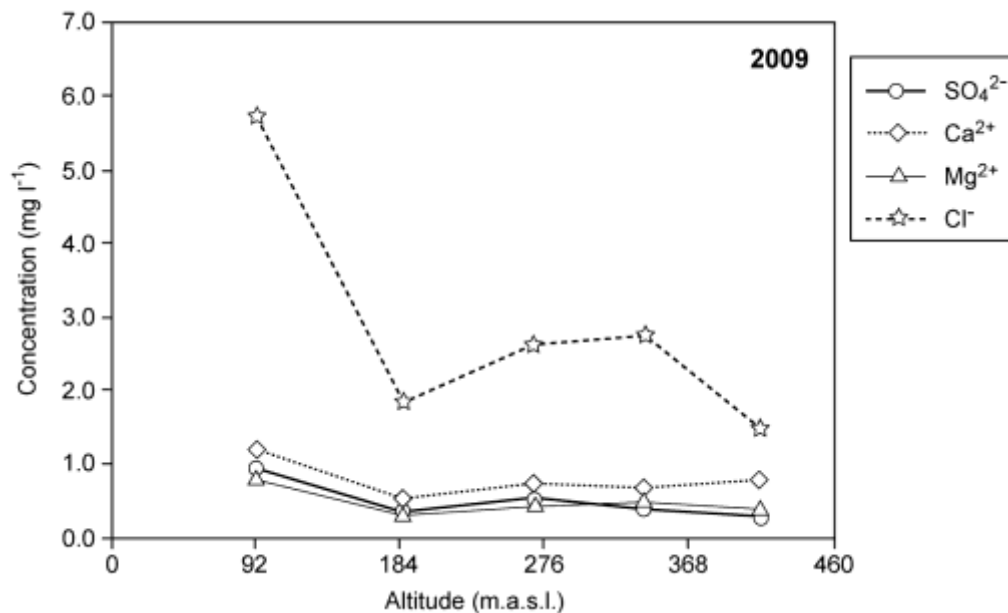


Figure 4.4. Altitudinal variations of four major ions in the 2009 snow.

Snow in Ny-Ålesund was dominated by sea salts which are obvious when the solute/Cl⁻ ratio in snow and standard sea salt are considered (Table 4.1). Higher amounts of K⁺, Ca²⁺ and Mg²⁺ relative to marine water were also found in the snow (Table 4.1), most likely representing dissolution of windblown terrigenous inputs. The SO₄²⁻ concentration in the snow gradually decreased from 0.98 mg L⁻¹ at lower altitude (92 m) to 0.34 mg L⁻¹ at higher altitude (413 m) (Figure 4.4). Cl⁻ concentration of snow (SG5, SG2, SG1) also showed the similar trend of gradually

decreasing with increasing altitude, while Ca^{2+} and Mg^{2+} did not show any significant relationship with altitude change. Sea salt SO_4^{2-} contributed about 61% of total snow SO_4^{2-} (assuming sea-salt $\text{SO}_4^{2-} = 0.103 \times \text{Cl}^-$, Wilson, 1975).

Dissolved inorganic nitrogen in snow samples was found in the form of NH_4^+ -N and NO_3^- -N, with a concentration range from 14 to 20 $\mu\text{g L}^{-1}$ and 18 to 29 $\mu\text{g L}^{-1}$ respectively. DON was also detected with a concentration range from 23 to 33 $\mu\text{g L}^{-1}$, which means it contributed the largest fraction to the soluble nitrogen pool of deposited snow in the Midtre Lovénbreen glacier catchment. Snow DOC concentrations varied from 0.22 to 0.39 mg L^{-1} , consequently DOC/DON ratio ranged between 12.56 and 16.06 with a mean value of 13.87 ± 1.91 ($n = 3$).

4.3.2 Year 2010

Snow depths at the five snow pits sites (SG1 to SG5) in 2010 were 203, 167, 148, 115, 65 cm respectively. Na^+ and Cl^- concentrations in these snow samples were lower than the 2009 snow (ca. half of 2009). Similarly, Ca^{2+} , Mg^{2+} , K^+ , SO_4^{2-} , HCO_3^- , DOC concentrations were also comparatively lower than 2009 snow (Table 4.1). However, NO_3^- -N, NH_4^+ -N and DON concentrations were comparatively higher in 2010 (Table 4.1). Among these annual changes in ionic loadings, solute/ Cl^- ratios in the 2010 snow were up to two fold higher than the 2009 snow.

Unlike 2009, non-sea-salt sources were the major contributor to the 2010 snow SO_4^{2-} (41% was sea-salt in origin and 59% was non sea-salt) and the SO_4^{2-} content of snow was not correlated with altitude on the glacier. Apparently, Ca^{2+} and Cl^- in 2010 followed a similar variation from site to site, whilst Mg^{2+} and SO_4^{2-} concentrations were relatively uniform (Figure 4.5). In addition, Si was also analysed during 2010 and its concentration in the snow ranged between 12 to 21 $\mu\text{g L}^{-1}$. DON in the 2010 snow was 2 to 3 time higher (80.3 to 93.6 $\mu\text{g L}^{-1}$) than the 2009 snow while DOC

(0.165 to 0.465 mg L⁻¹) was relatively lower. Consequently the DOC/DON ratio (3 to 5.8) in the 2010 snow was lower than the 2009.

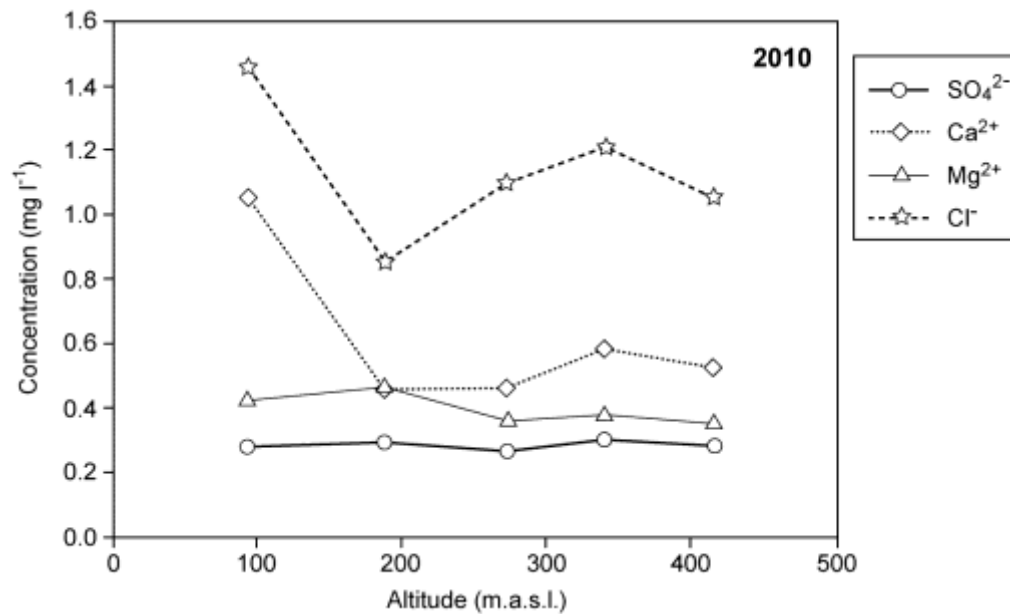


Figure 4.5. Ca²⁺, Mg²⁺, Cl⁻, SO₄²⁻ concentrations in the snowpack collected from different altitude during 2010 spring.

4.4 Stream nitrogen and sulphur dynamics

(Complete data is given in appendix 1, Table III and IV)

This section presents the solute abundance and variability at proglacial stream sites during summer 2009 and 2010. Here solute/Cl⁻ ratios are used to demonstrate snow-derived and non-snow derived solute provenance under the assumption that Cl⁻ is tracer of snowmelt.

Table 4.2. Mean concentration (\pm standard deviation) of solute and their ratio against Cl^- at UPW, MLE1 and MLW1 during summer 2009.

Species	UPW	MLE1	MLW1	Solute/ Cl^-	UPW	MLE1	MLW1
Ca^{2+} (mg L^{-1})	15.15 \pm 2.03 (n = 8)	13.14 \pm 2.90 (n = 14)	11.34 \pm 3.08 (n = 12)	$\text{Ca}^{2+} / \text{Cl}^-$	5.26 \pm 1.48 (n = 8)	5.92 \pm 3.16 (n = 14)	8.07 \pm 3.5 (n = 12)
Mg^{2+} (mg L^{-1})	3.55 \pm 0.34 (n = 8)	2.28 \pm 0.80 (n = 14)	1.68 \pm 0.64 (n = 12)	$\text{Mg}^{2+} / \text{Cl}^-$	1.23 \pm 0.31 (n = 8)	1.02 \pm 0.60 (n = 14)	1.21 \pm 0.61 (n = 12)
Na^+ (mg L^{-1})	2.34 \pm 0.27 (n = 8)	2.09 \pm 1.15 (n = 14)	1.17 \pm 0.29 (n = 12)	$\text{Na}^+ / \text{Cl}^-$	0.81 \pm 0.18 (n = 8)	0.70 \pm 0.14 (n = 14)	0.77 \pm 0.10 (n = 12)
K^+ (mg L^{-1})	1.52 \pm 0.16 (n = 8)	1.41 \pm 1.20 (n = 14)	0.74 \pm 0.24 (n = 12)	K^+ / Cl^-	0.53 \pm 0.13 (n = 8)	0.55 \pm 0.34 (n = 14)	0.53 \pm 0.26 (n = 12)
$\text{NH}_4^+\text{-N}$ ($\mu\text{g L}^{-1}$)	3.90 \pm 3.92 (n = 8)	11.35 \pm 20.21 (n = 14)	8.77 \pm 11.86 (n = 12)	$\text{NH}_4^+\text{-N} / \text{Cl}^-$	1.19 \pm 1.06 (n = 8)	4.22 \pm 6.58 (n = 14)	5.16 \pm 6.24 (n = 12)
F^- (mg L^{-1})	0.14 \pm 0.02 (n = 8)	0.05 \pm 0.03 (n = 14)	0.03 \pm 0.02 (n = 12)	F^- / Cl^-	0.05 \pm 0.02 (n = 8)	0.02 \pm 0.02 (n = 14)	0.02 \pm 0.01 (n = 12)
Cl^- (mg L^{-1})	3.03 \pm 0.73 (n = 8)	2.99 \pm 2.15 (n = 14)	1.57 \pm 0.53 (n = 12)	–	–	–	–
$\text{NO}_3^-\text{-N}$ ($\mu\text{g L}^{-1}$)	48.98 \pm 11.62 (n = 8)	38.39 \pm 35.39 (n = 13)	24.97 \pm 12.52 (n = 12)	$\text{NO}_3^-\text{-N} / \text{Cl}^-$	16.18 \pm 1.86 (n = 8)	15.29 \pm 9.16 (n = 14)	16.90 \pm 8.72 (n = 12)
SO_4^{2-} (mg L^{-1})	20.24 \pm 4.11 (n = 8)	13.91 \pm 5.39 (n = 14)	11.14 \pm 7.52 (n = 12)	$\text{SO}_4^{2-} / \text{Cl}^-$	7.13 \pm 2.63 (n = 8)	6.54 \pm 4.66 (n = 14)	8.31 \pm 6.02 (n = 12)
HCO_3^- (mg L^{-1})	36.58 \pm 11.16 (n = 8)	36.77 \pm 7.16 (n = 14)	31.56 \pm 6.53 (n = 12)	$\text{HCO}_3^- / \text{Cl}^-$	13.11 \pm 5.61 (n = 8)	16.11 \pm 7.36 (n = 14)	21.84 \pm 7.43 (n = 12)
DOC (mg L^{-1})	2.04 \pm 1.92 (n = 8)	2.56 \pm 1.60 (n = 11)	1.51 \pm 1.26 (n = 13)	DOC / Cl^-	0.80 \pm 0.84 (n = 8)	1.16 \pm 0.83 (n = 11)	1.27 \pm 1.35 (n = 13)
DON ($\mu\text{g L}^{-1}$)	4.79 \pm 5.89 (n = 8)	29.22 \pm 27.07 (n = 12)	30.40 \pm 38.56 (n = 8)	DON / Cl^-	2.56 \pm 2.62 (n = 8)	10.62 \pm 11.31 (n = 12)	2.56 \pm 2.62 (n = 8)

4.4.1 Year 2009

The chemistry of meltwater at MLE1, MLW1 and UPW was dominated by Ca^{2+} , HCO_3^- and SO_4^{2-} ions, and so median solute/ Cl^- ratio was higher than snow for these ions (Table 4.2). NO_3^- -N concentrations varied from below detection limit to $150 \mu\text{g L}^{-1}$, 37 to $67 \mu\text{g L}^{-1}$ and 4 to $51 \mu\text{g L}^{-1}$ at MLE1, UPW and MLW1 respectively. Median NO_3^- -N/ Cl^- ratio at these proglacial stream sites was significantly higher (> 1.5 times) than snow (Table 4.2). NH_4^+ -N concentrations in most of the samples from UPW, MLE1 and MLW1 were almost negligible, but they exceeded the average snow concentration of $16 \mu\text{g L}^{-1}$ concentration a few times at MLE1 and MLW1 during the early stage of the record. Mean NH_4^+ -N/ Cl^- ratios also mostly remained lower than those in snow. Mg^{2+} , Na^+ and Cl^- concentrations at the MLE1 were relatively higher than at UPW and MLW1 (Figure 4.6).

DOC concentrations at MLE1 and MLW1 were relatively high during initial and late summer melt. Similarly, at UPW the DOC concentrations increased during late summer melt. However, DON behaviour at all sites was very much independent and its concentration remained almost insignificant at UPW for whole sampling period. The median ionic ratio of these organic solute against Cl^- at proglacial sites, were also higher than the snow (Table 4.2).

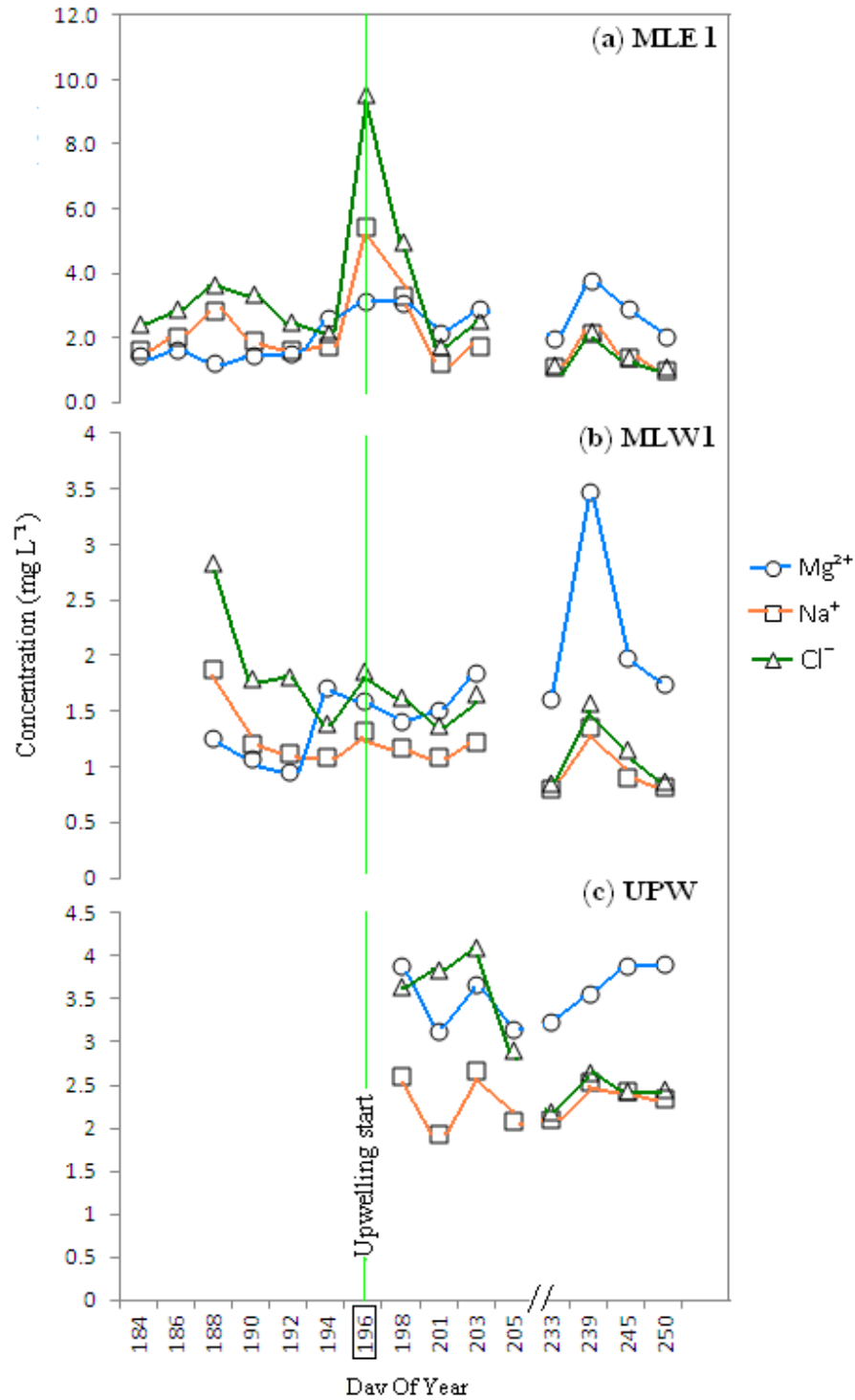


Figure 4.6. Panels (a), (b) and (c) shows the temporal variation of Mg²⁺, Na⁺, and Cl⁻ at MLE1, MLW1 and UPW sites respectively during summer 2009.

4.4.1.1 Spatio-temporal nitrogen dynamics

During the early summer melt when MLE1 was largely fed by supraglacial snowmelt (before DOY 196), NO_3^- -N and DOC were relatively high and NO_3^- -N reached its seasonal maximum value of $150 \mu\text{g L}^{-1}$ on DOY 188. At the same time Cl^- also reached a second maximum concentration on DOY 188 (Figure 4.7a). After the opening of subglacial upwelling (DOY 196), when the MLE1 was largely fed by UPW, concentrations of DOC and NO_3^- -N continued to decline at MLE1 but later increased on DOY 203. Furthermore, on the very first day of upwelling Cl^- reached its seasonal maximum concentration at MLE1 and thereafter decreased to a near constant value (Figure 4.7a). DOC and NO_3^- -N at MLW1 also showed an overall decrease from early summer melt until the day of the subglacial upwelling began when they increased. Similarly Cl^- showed an overall decrease from early to late summer at MLW1 (Figure 4.7b). UPW showed a different regime, where NO_3^- -N and Cl^- covaried and decreased following the outburst, while DOC mimicked MLE1 (Figure 4.7c) and generally increased. DON varied from below detection limit to $111 \mu\text{g L}^{-1}$. However, these data were too erratic for any temporal pattern to be established.

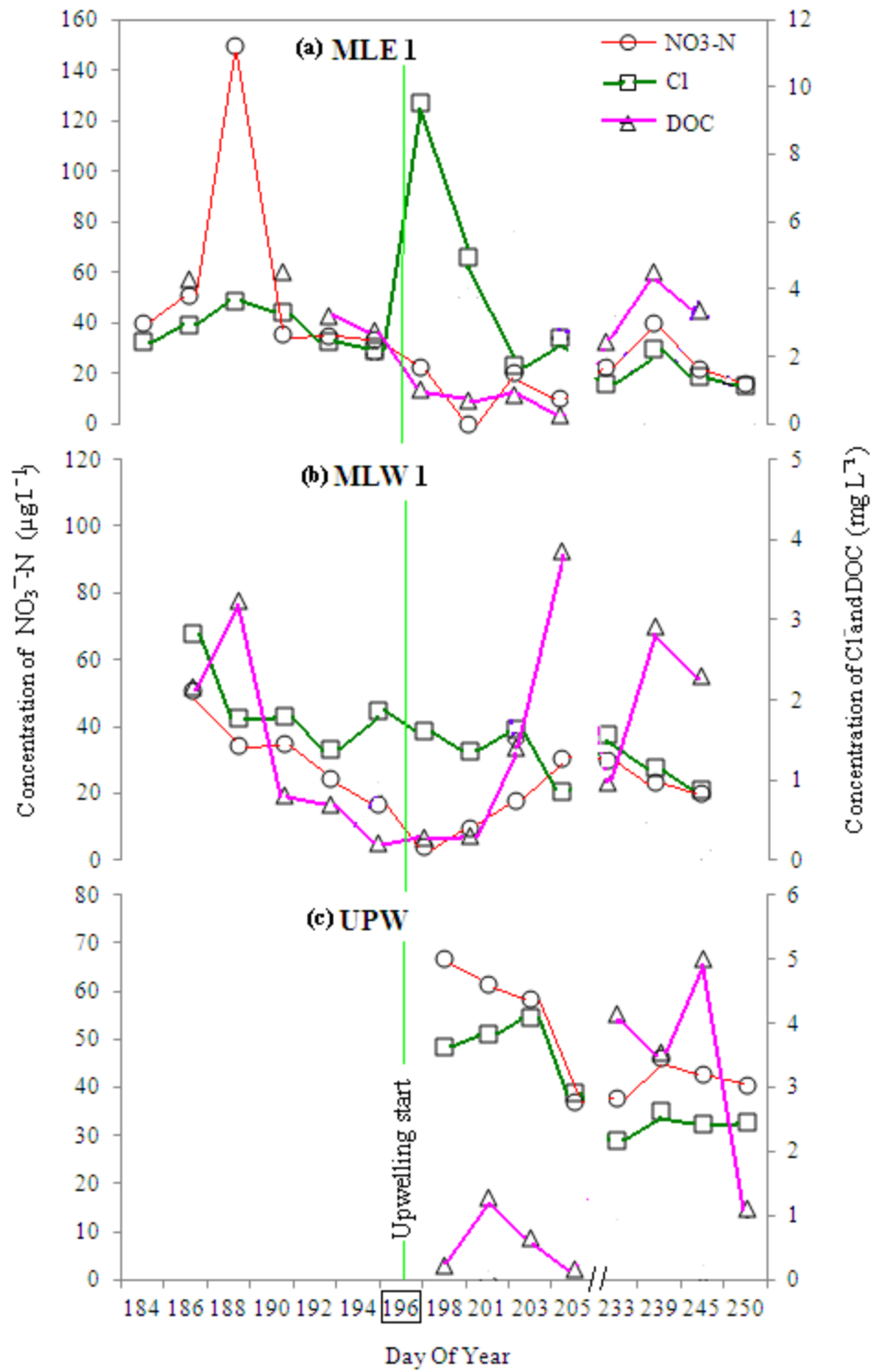


Figure 4.7. Panels (a), (b) and (c) shows the temporal variation of $\text{NO}_3^- \text{-N}$, Cl^- and DOC at MLE1, MLW1 and UPW sites respectively during summer 2009.

To study spatial NO_3^- -N variations in the two streams, the NO_3^- -N/ Cl^- ratios of UPW were compared with MLE1 and MLW1. The NO_3^- -N/ Cl^- ratios of water moving from UPW to MLE1 remained almost the same (Figure 4.8) whilst in the MLW1 (which did not have upwelling water) it was two times higher than both MLE1 water and snow (Figure 4.8). Therefore, NO_3^- -N enrichment at MLW1 from a non snowpack source was apparent and Figure 4.8 suggests it was most important in late summer samples (DOY 233 onwards).

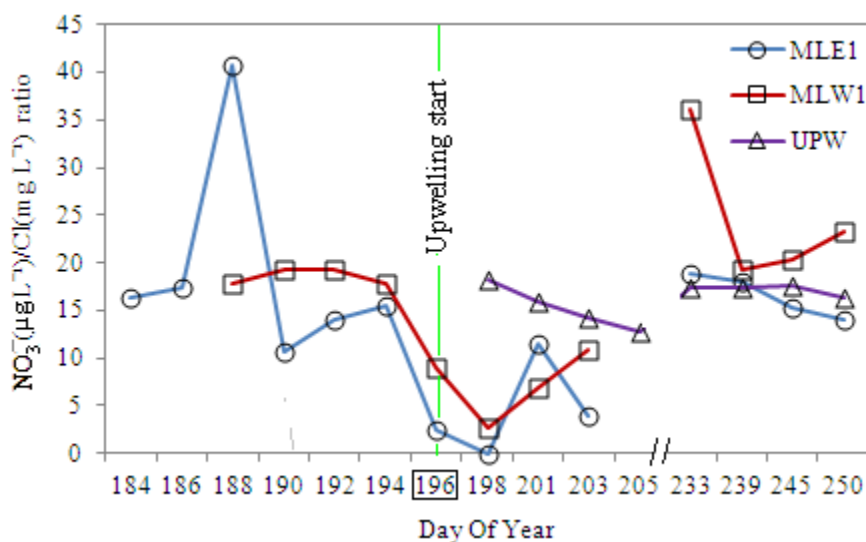


Figure 4.8. Spatial and temporal variatis of NO_3^- -N/ Cl^- concentration ratio in the stream water at MLE1, MLW1 and UPW during summer 2009.

4.4.1.2 Spatio-temporal sulphate dynamics

A separation between non-snow and snow derived SO_4^{2-} at MLE1, MLW1 and UPW was made by using the mean snow SO_4^{2-} / Cl^- ratio, according to which snowmelt contributed a small fraction of SO_4^{2-} at UPW (1.5% to 4%), MLE1 (1% to 12.6%) and MLW1 (0.8% to 11%) (Figure 4.9 a, b and c). Therefore, largest fraction of SO_4^{2-} at the three sites was non-snow in origin. The variability and the fraction of snow SO_4^{2-} at MLE1 and MLW1 was higher than UPW. However, non-snow SO_4^{2-} variation at the three stream stations was totally independent of snow SO_4^{2-} . Non

snow SO_4^{2-} increased at MLE1 (from 5 to 25 mg L^{-1}) and MLW1 (from 4 to 30 mg L^{-1}) from initial summer to the late summer, but at UPW it had an initial decrease (from 20 to 14 mg L^{-1}) from DOY 198 to DOY 205 and a subsequent increase (to 27 mg L^{-1}) during the later period. Except on DOY 239, non-snow SO_4^{2-} at MLE1 (influence by UPW water) remained higher than MLW1 during the whole summer (Figure 4.9a and b).

The Ca^{2+} and total SO_4^{2-} at all the three stream sites varied in similar fashion during the whole summer and showed an overall increase from early to the late summer (Figure 4.9 d, e and f). The rate of increase in total SO_4^{2-} concentration was higher than Ca^{2+} which caused a simultaneous decrease in $\text{Ca}^{2+}/\text{SO}_4^{2-}$ molar ratio at MLE1 (3.6 to 1.6), MLW1 (5.3 to 1.5) and UPW (2 to 1.5) (Figure 4.9 a, b and c). The K^+ concentration at MLW1 remained constant during the whole summer. However, at MLE1 it was constant during most of the summer except on DOY 188 and 190 when it increased by 2 to 4 fold. This peak event of K^+ at MLE1 was notable for its similarity with a simultaneous SO_4^{2-} peak (Figure 4.9d).

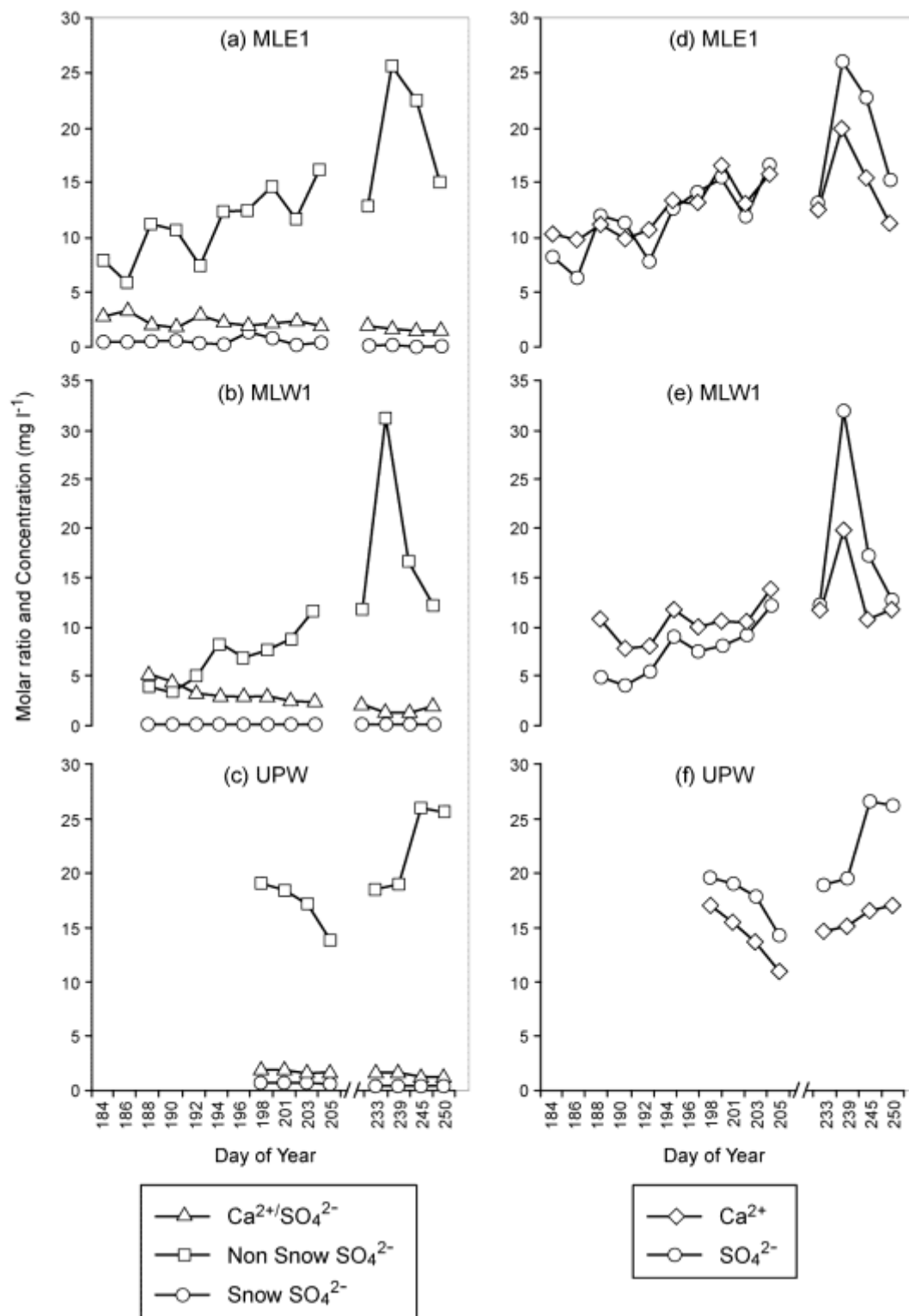


Figure 4.9. Temporal variations of Ca²⁺/SO₄²⁻ molar ratios and non-snow, snow SO₄²⁻ at the (a) MLE1, (b) MLW1 and (c) UPW and the temporal variations of Ca²⁺, K⁺, SO₄²⁻ at the (d) MLE1, (e) MLW1 and (f) UPW during summer 2009.

4.4.2 Year 2010

Although the snow major ion concentrations during the two consecutive years were different, the streams, major ion concentrations remained largely similar. Furthermore, like 2010 snow, the subglacial runoff and the streams also had significantly high DON (20 to 103 $\mu\text{g L}^{-1}$) and much more consistent DOC/DON ratio (3 to 10.9) than 2009. The Si concentration in the streams (during 2010) varied between 2.19 and 0.02 mg L^{-1} (Figure 4.10 and 4.12).

The eastern proglacial stream again received water from two sources: i) **ice marginal stream** (MLE3), mostly fed by glacial ice melt and ii) **subglacial runoff** opening at UPW (sometime before DOY 186). The two waters mixed before MLE2 (Figure 3.6). Solute concentrations at UPW were significantly higher than at MLE3 and subsequent mixing of the two waters resulted into a solute concentration between the two limits at MLE2. Water travelling from MLE2 to MLE1 either experienced a small increase in solute concentration or remained unchanged (Figure 4.10, 4.11, 4.14, 4.16 and 4.18). However, the source of water into the western stream was largely ice and snow melt which emerged from the glacier margin and travelled downstream via MLW3, MLW2 and MLW1. During this course, an increase in the major ions concentration was more obvious (Figure 4.12, 4.13, 4.17 and 4.19). Spatial and temporal changes in the proglacial streams K^+ and Si concentrations were insignificant relative to Ca^{2+} and SO_4^{2-} changes (Figure 4.10).

Table 4.3. Mean concentration of major ions, DOC and DON with standard deviation at the stream sites during summer 2010. (n is number of samples).

Site	Ca ²⁺ (mg L ⁻¹)	Mg ²⁺ (mg L ⁻¹)	Na ⁺	K ⁺	NH ₄ ⁺ -N (µg L ⁻¹)	F ⁻ (mg L ⁻¹)	Cl ⁻ (mg L ⁻¹)	NO ₃ ⁻ -N (µg L ⁻¹)	SO ₄ ²⁻ (mg L ⁻¹)	Si (mg L ⁻¹)	HCO ₃ ⁻ (mg L ⁻¹)	DOC (mg L ⁻¹)	DON (µg L ⁻¹)
UPW	10.19±6.0 9 (n=5)	3.20±0.7 8 (n=5)	1.73±0.4 7 (n=5)	1.30±0.3 9 (n=5)	4.64±4.27 (n=5)	0.15±0.0 3 (n=5)	1.89±0.5 4 (n=5)	33.47±12.5 4 (n=5)	23.07±8.94 (n=5)	0.90±0.7 3 (n=5)	13.73±10.4 8 (n=5)	0.81±0.9 2 (n=5)	69.88±24.9 0(n=5)
MLE3	8.61±2.34 (n=5)	0.75±0.6 3 (n=5)	0.41±0.2 7 (n=5)	0.48±0.3 0(n=5)	5.63±3.37 (n=5)	0.01±0.0 2(n=5)	0.71±0.4 5(n=5)	17.09±11.3 4(n=5)	5.87±6.39 (n=5)	0.38±0.6 2 (n=5)	12.49±4.23 (n=5)	0.33±0.4 6 (n=5)	75.27±20.3 6 (n=5)
MLE2	11.06±4.4 7 (n=5)	2.05±1.0 4(n=5)	1.06±0.5 0(n=5)	0.88±0.3 5(n=5)	3.89±2.29 (n=5)	0.11±0.0 3(n=5)	1.24±0.4 6(n=5)	28.94±16.4 4(n=5)	14.57±7.04 (n=5)	0.57±0.8 2(n=5)	15.72±6.74 (n=5)	0.25±0.3 5(n=5)	4.37±2.06 (n=5)
MLE1	12.34±6.5 0(n=5)	2.27±1.2 7(n=5)	1.16±0.5 2(n=5)	0.95±0.3 8(n=5)	5.93±3.73 (n=5)	0.10±0.0 3(n=5)	1.23±0.4 6(n=5)	26.08±12.6 9(n=5)	38.27±10.8 6(n=5)	0.38±0.2 1(n=5)	17.96±8.55 (n=5)	0.75±0.8 8(n=5)	65.98±33.4 8(n=5)
MLW3	5.91±3.39 (n=5)	0.50±0.4 7(n=5)	0.45±0.3 4(n=5)	0.25±0.1 9(n=5)	4.47±2.82 (n=5)	0.02±0.0 3(n=5)	0.67±0.4 4(n=5)	17.38±10.1 0(n=5)	2.12±3.16 (n=5)	0.39±0.6 9(n=5)	9.87±5.23 (n=5)	n.a. 0(n=5)	60.45±29.0 0(n=5)
MLW2	9.06±1.83 (n=5)	1.39±1.1 1(n=5)	0.70±0.3 2(n=5)	0.59±0.3 8(n=5)	3.90±2.40 (n=5)	0.05±0.0 3(n=5)	0.77±0.3 6(n=5)	17.09±10.7 2(n=5)	8.50±8.96 (n=5)	0.15±0.1 4(n=5)	13.95±2.39 (n=5)	n.a. 7(n=5)	59.00±21.4 7(n=5)
MLW1	14.27±4.8 5(n=5)	1.89±1.5 1(n=5)	0.76±0.5 2(n=5)	0.56±0.4 5(n=5)	5.20±1.69 (n=5)	0.05±0.0 3(n=5)	0.83±0.4 3(n=5)	17.38±10.6 1(n=5)	13.04±12.3 1(n=5)	0.21±0.1 8(n=5)	20.68±5.19 (n=5)	0.48±0.2 6(n=5)	57.41±17.0 9(n=5)

Table 4.3

Table 4.4. Mean of ionic ratios with standard deviation at the stream sites during summer 2010. (n is number of samples).

Site	Ca ²⁺ /Cl ⁻	Mg ²⁺ /Cl ⁻	Na ⁺ /Cl ⁻	K ⁺ /Cl ⁻	NH ₄ ⁺ -N/Cl ⁻	F ⁻ /Cl ⁻	NO ₃ ⁻ -N/Cl ⁻	SO ₄ ²⁻ /Cl ⁻	Si/Cl ⁻	HCO ₃ ⁻ /Cl ⁻	DOC/Cl ⁻	DON/Cl ⁻
UPW	5.81±4.29 (n = 5)	1.73±0.2 (n = 5)	0.92±0.0 (n = 5)	0.69±0.0 (n = 5)	2.25±1.40 (n = 5)	0.08±0.0 (n = 5)	18.81±7.77 (n = 5)	12.31±3.47 (n = 5)	0.44±0.2 (n = 5)	7.92±6.98 (n = 5)	0.49±0.6 (n = 5)	4.95±21.07 (n = 5)
MILE3	15.26±7.08 (n = 5)	0.99±0.1 (n = 5)	0.58±0.0 (n = 5)	0.69±0.1 (n = 5)	11.21±7.0 (n = 5)	0.01±0.0 (n = 5)	26.04±16.4 (n = 5)	7.06±3.65 (n = 5)	0.65±1.2 (n = 5)	22.98±11.9 (n = 5)	0.60±0.8 (n = 5)	131.00±65.6 (n = 5)
MILE2	10.69±7.32 (n = 5)	1.62±0.2 (n = 5)	0.84±0.0 (n = 5)	0.70±0.0 (n = 5)	3.80±2.48 (n = 5)	0.09±0.0 (n = 5)	22.02±7.73 (n = 5)	11.78±2.83 (n = 5)	0.36±0.4 (n = 5)	15.19±10.3 (n = 5)	0.18±0.1 (n = 5)	58.23±41.13 (n = 5)
MILE1	12.36±9.27 (n = 5)	1.79±0.3 (n = 5)	0.93±0.1 (n = 5)	0.76±0.0 (n = 5)	5.85±3.91 (n = 5)	0.09±0.0 (n = 5)	21.10±8.09 (n = 5)	12.67±3.66 (n = 5)	0.29±0.0 (n = 5)	17.96±12.8 (n = 5)	0.57±0.5 (n = 5)	59.51±37.28 (n = 5)
MILW3	9.50±2.55 (n = 5)	0.71±0.3 (n = 5)	0.65±0.1 (n = 5)	0.37±0.1 (n = 5)	9.18±6.37 (n = 5)	0.02±0.0 (n = 5)	27.97±19.1 (n = 5)	2.31±2.86 (n = 5)	1.05±1.2 (n = 5)	16.19±4.47 (n = 5)	n.a.	130.47±130. (n = 5)
MILW2	13.15±3.97 (n = 5)	1.69±0.5 (n = 5)	0.93±0.1 (n = 5)	0.75±0.1 (n = 5)	6.46±4.03 (n = 5)	0.06±0.0 (n = 5)	20.44±7.58 (n = 5)	9.48±5.44 (n = 5)	0.18±0.0 (n = 5)	20.96±7.90 (n = 5)	n.a.	90.27±45.66 (n = 5)
MILW1	18.56±3.52 (n = 5)	2.17±0.6 (n = 5)	0.89±0.1 (n = 5)	0.93±0.1 (n = 5)	7.16±3.56 (n = 5)	0.06±0.0 (n = 5)	21.13±12.5 (n = 5)	13.83±5.61 (n = 5)	0.24±0.0 (n = 5)	27.86±7.40 (n = 5)	0.76±0.7 (n = 5)	90.43±53.91 (n = 5)

Table 4.4

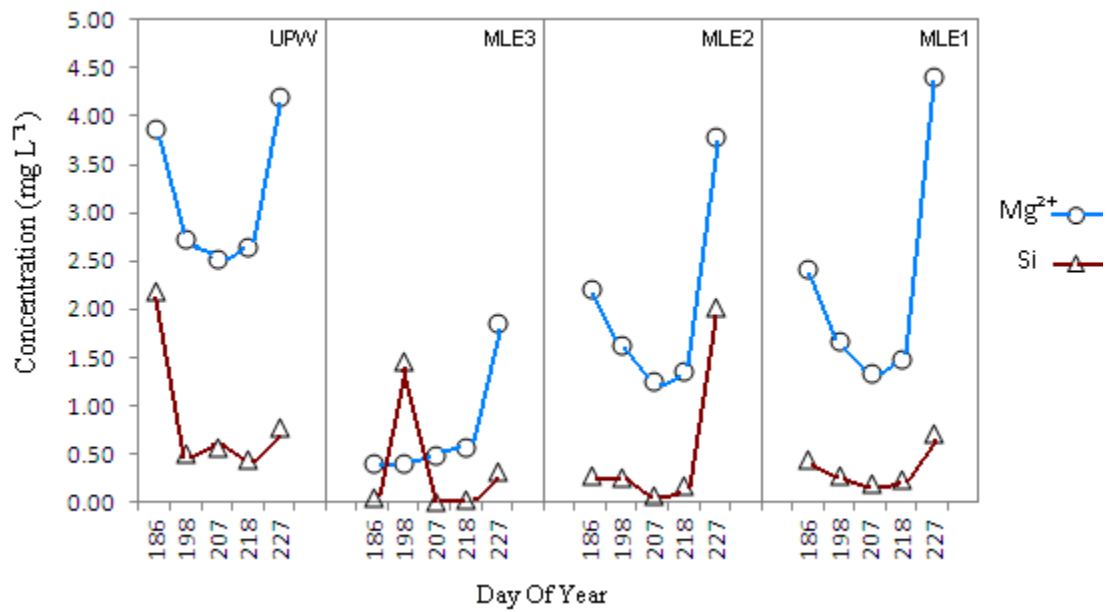


Figure 4.10. Spatial and temporal variations of Mg²⁺ and Si in the eastern stream during summer 2010.

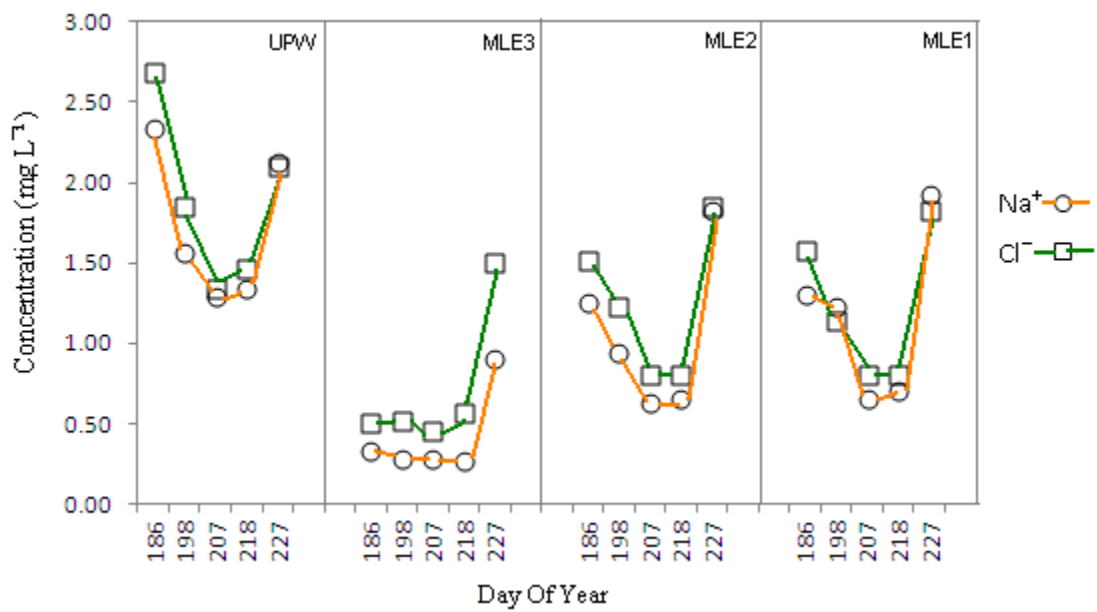


Figure 4.11. Spatial and temporal variations of Na⁺ and Cl⁻ in the eastern stream during summer 2010.

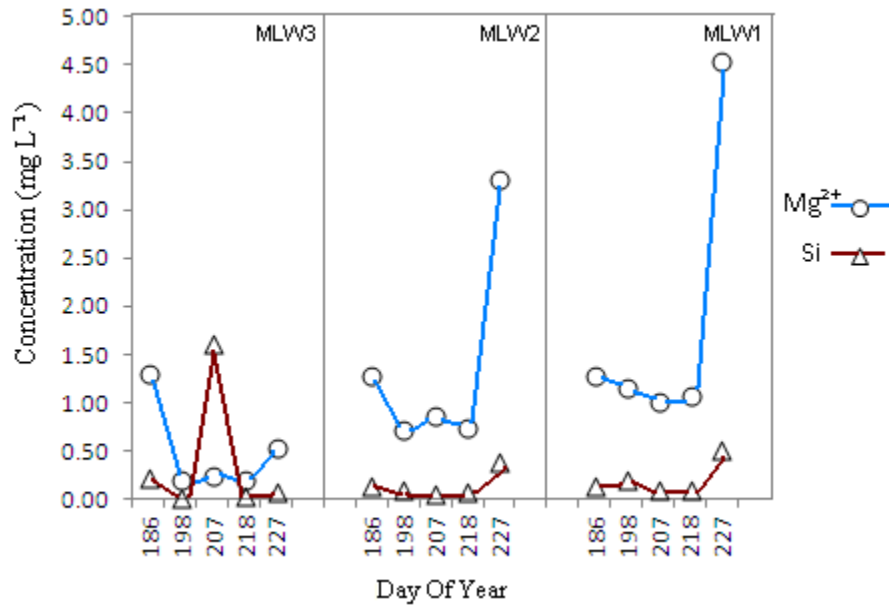


Figure 4.12. Spatial and temporal variations of Mg²⁺ and Si in the western stream during summer 2010.

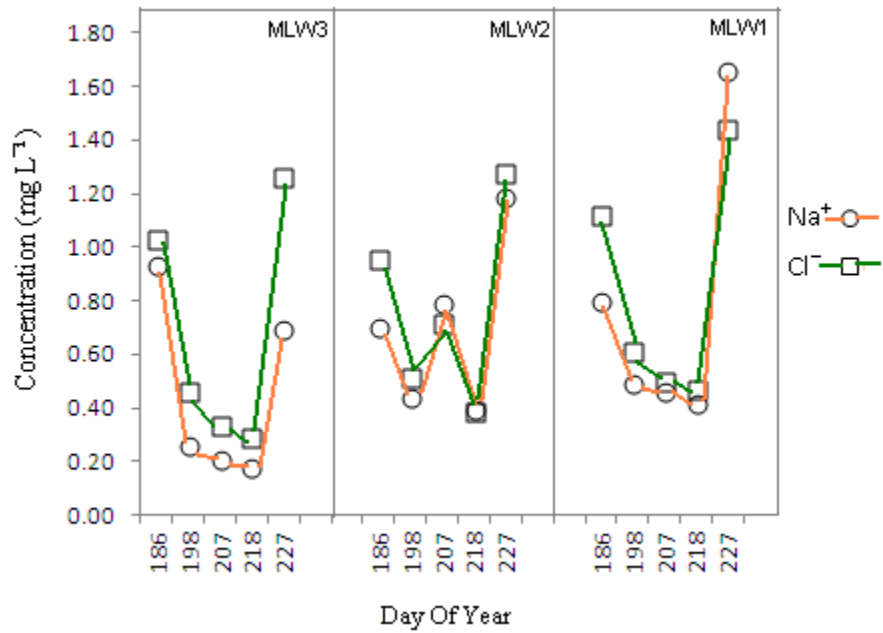


Figure 4.13. Spatial and temporal variations of Na⁺ and Cl⁻ in the western stream during summer 2010.

4.4.2.1 Spatio-temporal nitrogen dynamics

The temporal variations of $\text{NH}_4^+\text{-N}$, DON and DOC/DON ratio at the two sources of the eastern stream (i.e. UPW and MLE3) were different, whilst $\text{NO}_3^-\text{-N}$ behaved consistently. The temporal variation of nitrogen species at the two subsequent downstream sites MLE2 and MLE1 were then similar. Among all the nitrogen species, DON was the only species which increased clearly from early to the late summer sampling. $\text{NH}_4^+\text{-N}$ concentration remained low and the variations in its concentration were not significant (Figure 4.14).

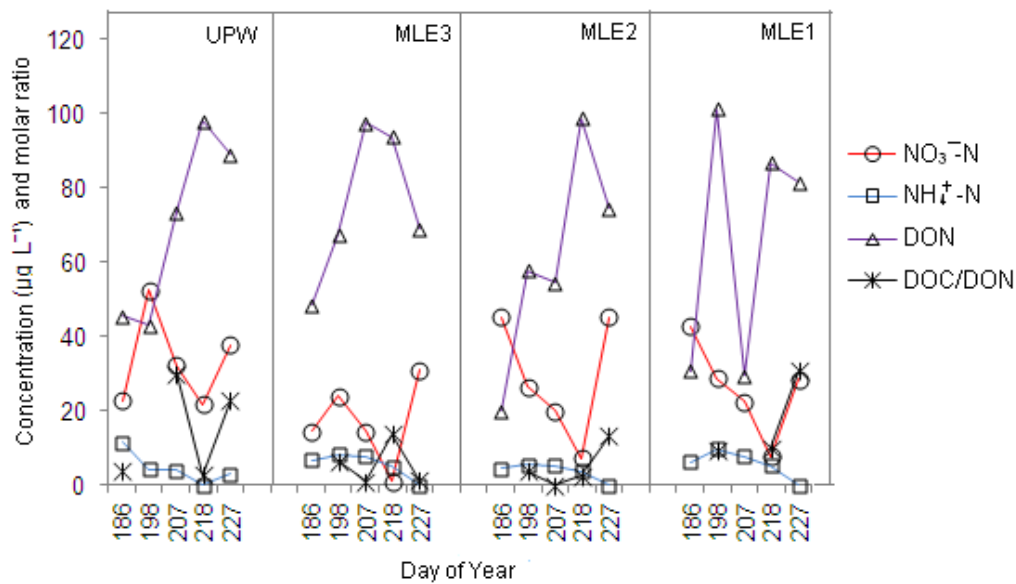


Figure 4.14. Spatial and temporal variations of $\text{NO}_3^-\text{-N}$, $\text{NH}_4^+\text{-N}$, DON and DOC/DON at UPW, MLE3, MLE2 and MLE1 during summer 2010.

In the western stream, temporal variations of nitrogen species at the first two sites (MLW3 followed by MLW2) were similar and $\text{NO}_3^-\text{-N}$ showed an overall increase towards the later summer. However, nitrogen variation at the last downstream site (MLW1) in the western stream showed an overall decrease in $\text{NO}_3^-\text{-N}$ towards later summer. $\text{NH}_4^+\text{-N}$ concentration at all three downstream sites remained low and

its variation was not significant, whereas DON concentration was significant but no straightforward trend was visible from its variations (Figure 4.15).

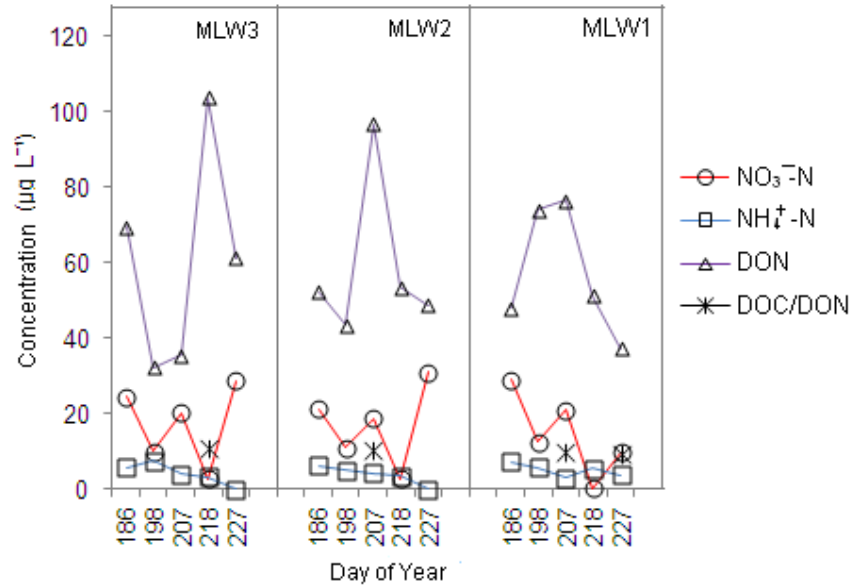


Figure 4.15. Spatial and temporal variations of NO₃⁻-N, NH₄⁺-N and DON in the western stream during summer 2010.

During 2010, the median ratio of NO₃⁻-N, NH₄⁺-N and DON against Cl⁻ in snow was significantly higher than the streams (Table 4.1 and 4.4). Furthermore, the mean NO₃⁻-N/Cl⁻ ratio in the western stream showed a significant downstream decrease, whilst in the eastern stream it remained more uniform (Table 4.4).

4.4.2.2. Spatio-temporal sulphate dynamics

Snow derived SO₄²⁻ in the eastern and western streams remained very low and so any temporal changes were outlined by variations in rock-derived SO₄²⁻. However, largest fraction of subglacial runoff and proglacial stream SO₄²⁻ was non-snow in

origin which had a clear temporal trend at all the stream sites (Figure 4.18 and 4.19). Non-snow SO_4^{2-} at UPW, MLE2 and MLE1 showed similar temporal variations and decreased from DOY 186 to 207, and increased afterwards until DOY 227. However, at MLE3, non-snow SO_4^{2-} experienced a continuous increase from DOY 186 to DOY 227 (Figure 4.18). The $\text{Ca}^{2+}/\text{SO}_4^{2-}$ molar ratio at MLE2 and MLE1 increased to ca. 3 and afterwards decreased back to the value greater than 1. At MLE3 most of the values were between 1 and 13 (Figure 4.18).

In the western stream at MLW3 non-snow SO_4^{2-} decreased to the snow SO_4^{2-} value (ca. 0.27 mg L^{-1}) and remained constant afterwards. However, non-snow SO_4^{2-} at MLW2 and MLW1 followed the similar temporal trend observed at UPW, MLE2 and MLE1 (Figure 4.18 and 4.19). Furthermore, the $\text{Ca}^{2+}/\text{SO}_4^{2-}$ molar ratio at MLW3, MLW2 and MLW1 also had similar temporal trend like observed at UPW, MLE2 and MLE1 but this ratio reached to an exceptionally high value (ca. 33 mg L^{-1}) at MLW3 (Figure 4.19).

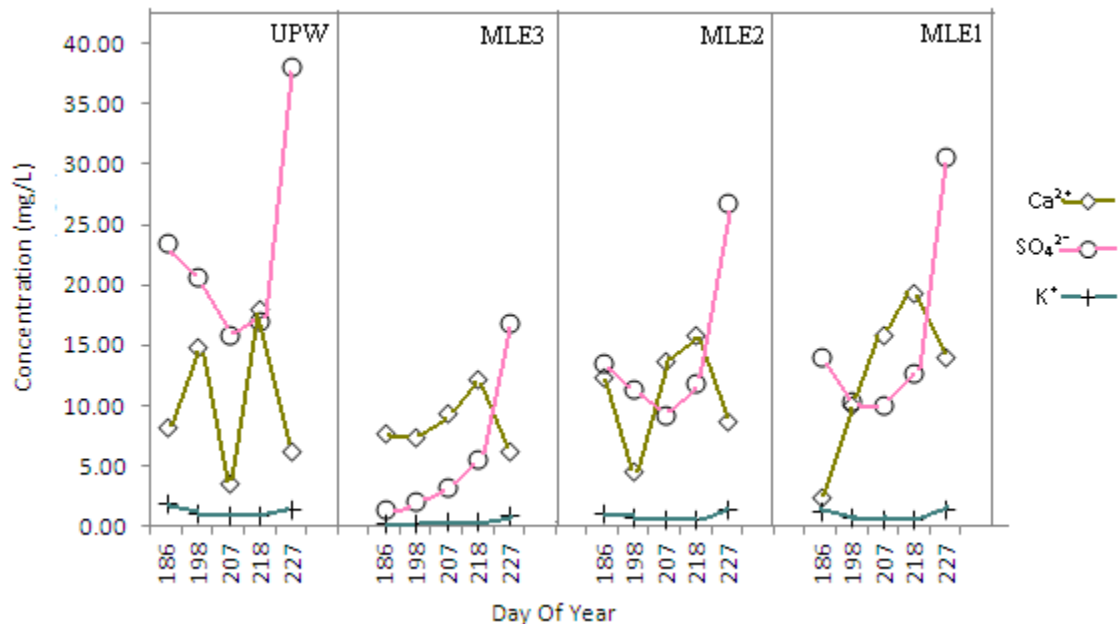


Figure 4.16. Spatial and temporal variations of Ca^{2+} , SO_4^{2-} and K^+ in the eastern stream during summer 2010.

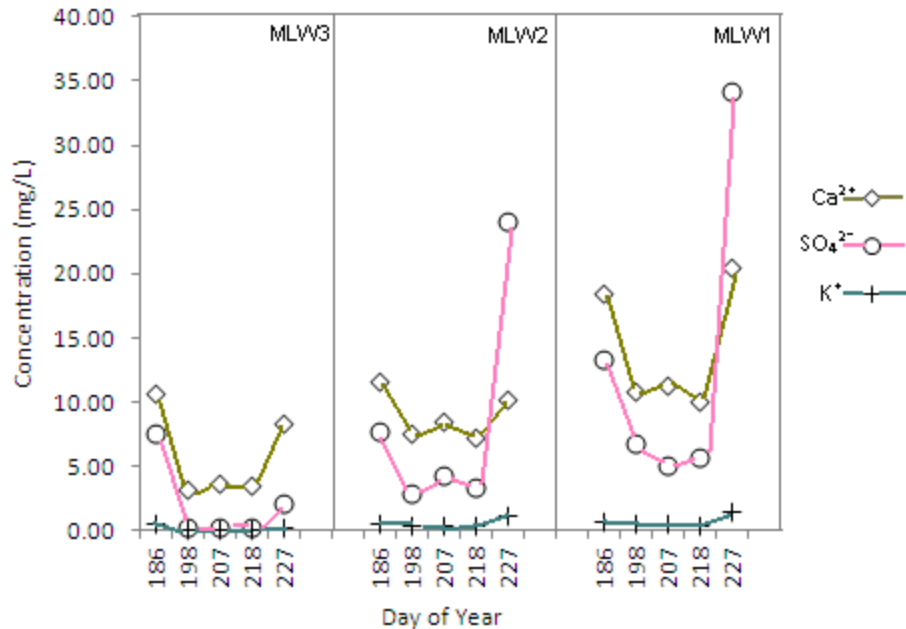


Figure 4.17. Spatial and temporal variations of Ca²⁺, SO₄²⁻ and K⁺ in the western stream during summer 2010.

In the eastern stream non-snow SO₄²⁻ remained almost constant when the water mixed whilst travelling downstream to MLE2. This trend was consistent throughout the whole summer stream sampling campaign. However, when the water travelled further downstream to MLE1, non-snowpack SO₄²⁻ increased during DOY 186, 207, 218 and 227, whilst it decreased on the DOY 198. The Ca²⁺/SO₄²⁻ molar ratio in the eastern stream also showed a downstream (MLE2 to MLE1) decrease on DOY 198 but, afterwards (from DOY 198 to 227) the ratio did not experience any significant downstream change (Figure 4.18).

In the western stream, non-snow SO₄²⁻ continuously increased from MLW3 to MLW2 to MLW1 throughout the stream sampling period although the increase on the DOY 227 was significantly higher than the previous days (DOY 186, 198, 207 and 218). The Ca²⁺/SO₄²⁻ molar ratio remained constant throughout the flowpath on DOY 186 however, later on DOY 198, 207 and 218, the ratio increased from MLW3 to MLW2 then either remained constant or experienced a decrease. On DOY 227 this

ratio had an initial decrease from MLW3 to MLW2 and remained almost constant afterwards (Figure 4.18).

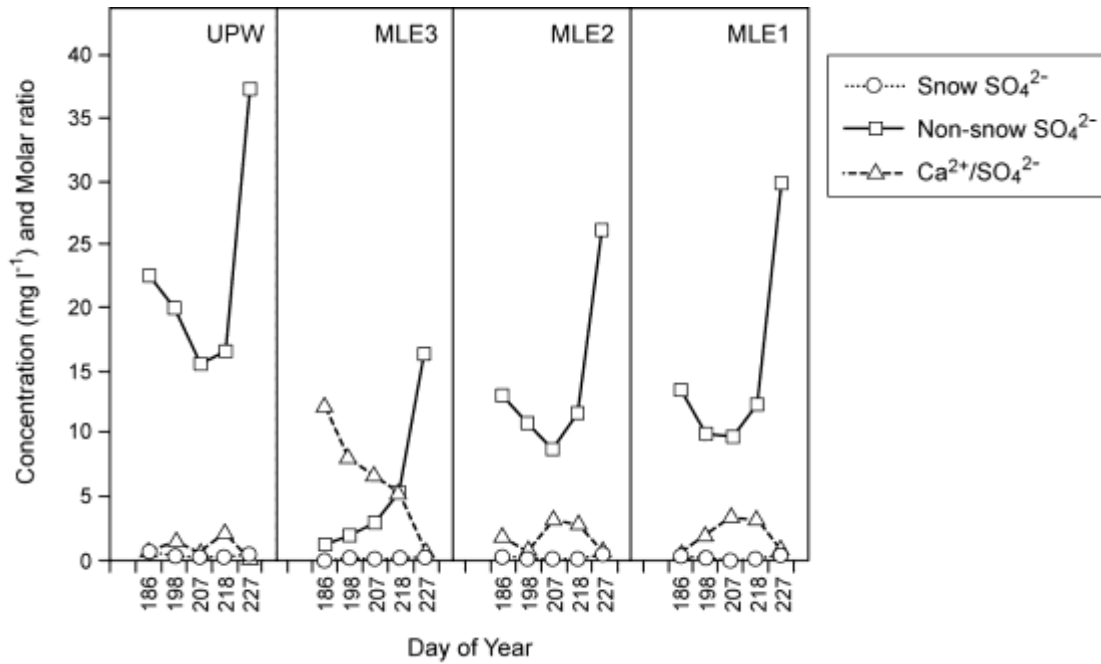


Figure 4.18. Spatial and temporal variations of snow, non-snow derived SO_4^{2-} and $\text{Ca}^{2+}/\text{SO}_4^{2-}$ molar ratio in the eastern stream during summer 2010.

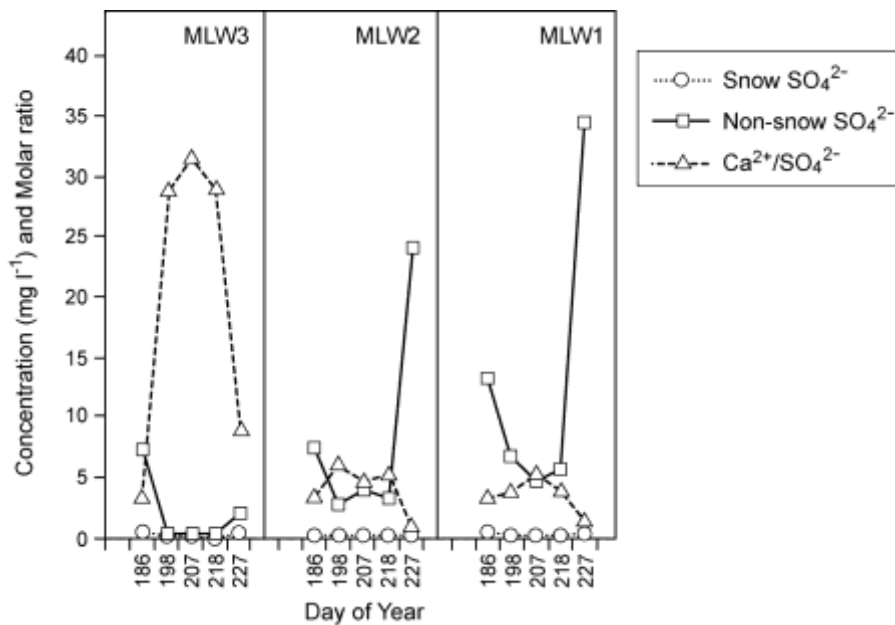


Figure 4.19. Spatial and temporal variations of snow, non-snow derived SO_4^{2-} and $\text{Ca}^{2+}/\text{SO}_4^{2-}$ molar ratio in the western stream during summer 2010.

On the temporal scale, SO_4^{2-} and Ca^{2+} did not show any significant co-variations in the eastern stream, whereas on spatial scale the two ions varied in similar fashion during the whole stream sampling period (Figure 4.16). In contrast, the western stream showed significant co-variations between the two ions both on temporal and spatial scales (Figure 4.17).

4.5 Isotopic characterisation

(Complete data is given in appendix 1, Table V, VI and VII)

This section presents the stable isotope composition of NO_3^- , SO_4^- and H_2O in representative samples (snow, streams), its distribution and variability during the two years of study.

4.5.1 Year 2009

4.5.1.1 $\delta^{15}\text{N}$, $\delta^{18}\text{O}$ - NO_3 and $\delta^{18}\text{O}$ - H_2O of snow and streams

Table 4.5. Mean of stable isotope composition (\pm standard deviation) of NO_3^- , SO_4^- and H_2O in snow and stream samples during 2009.

Site	$\delta^{15}\text{N}$ - NO_3 (‰)	$\delta^{18}\text{O}$ - NO_3 (‰)	$\delta^{34}\text{S}$ - SO_4 (‰)	$\delta^{18}\text{O}$ - SO_4 (‰)	$\delta^{18}\text{O}$ - H_2O (‰)
Snow	-8.73 ± 1.33 (n = 5)	$+78.14 \pm 1.48$ (n = 5)	n.a.	n.a.	-12.80 ± 0.42 (n = 4)
UPW	-4.17 ± 1.66 (n = 6)	$+26.49 \pm 7.41$ (n = 6)	$+15.7 \pm 0.08$ (n = 3)	-6.4 ± 0.41 (n = 3)	-13.1 ± 0.52 (n = 3)
MLE1	$+4.45 \pm 8.94$ (n = 9)	$+33.43 \pm 15.6$ 6 (n = 9)	$+11.74 \pm 2.41$ (n = 10)	-6.28 ± 4.28 (n = 10)	-13.05 ± 0.45 (n = 10)
MLW1	$+3.99 \pm 10.41$ (n = 9)	$+22.12 \pm 16.7$ 5 (n = 9)	$+15.06 \pm 1.84$ (n = 7)	-6.73 ± 2.15 (n = 7)	-12.87 ± 0.68 (n = 7)

Average $\delta^{15}\text{N-NO}_3$ and $\delta^{18}\text{O-NO}_3$ of pre-melt snow were $-8.7 \pm 1.33\text{‰}$ and $+78.1 \pm 1.48\text{‰}$ respectively (Table 4.5). Figure 4.20 shows that the lowest $\delta^{15}\text{N-NO}_3$ of -7.8‰ and highest $\delta^{18}\text{O-NO}_3$ of $+64.4\text{‰}$ of stream water were recorded prior to the subglacial outflow at MLE1 (i.e. prior to DOY 196). This interval is referred to as **Phase I**. During **Phase II** (post DOY 196) the $\delta^{15}\text{N-NO}_3$ at MLE1 increased to a seasonal maximum of $+14.9\text{‰}$, whilst $\delta^{18}\text{O-NO}_3$ decreased to a seasonal minimum of $+17.5\text{‰}$. MLW1 revealed similar results, the lowest $\delta^{15}\text{N-NO}_3$ of -7.4‰ and highest $\delta^{18}\text{O-NO}_3$ of $+46.8\text{‰}$ being recorded during Phase I then changing to a maximum $\delta^{15}\text{N-NO}_3$ of $+11.4\text{‰}$ and minimum $\delta^{18}\text{O-NO}_3$ of $+3.8\text{‰}$ during Phase II. At UPW, the $\delta^{15}\text{N-NO}_3$ varied from -7.3‰ to -3.8‰ and the $\delta^{18}\text{O-NO}_3$ varied from $+36.4\text{‰}$ to $+16.2\text{‰}$ (Figure 4.20). Further, $\delta^{15}\text{N-NO}_3$ at MLE1 and MLW1 were significantly greater than that found in snow during Phase II suggesting an influence from the glacier forefield not the subglacial alone, because no subglacial waters drain to MLW1. Lastly, the $\delta^{15}\text{N-NO}_3$ values increased in a downstream direction between UPW and MLE1 (Figure 4.20). The $\delta^{18}\text{O-H}_2\text{O}$ for most of the snowpack and stream samples was similar and in the range -13.7‰ to -12.2‰ (Table 4.5).

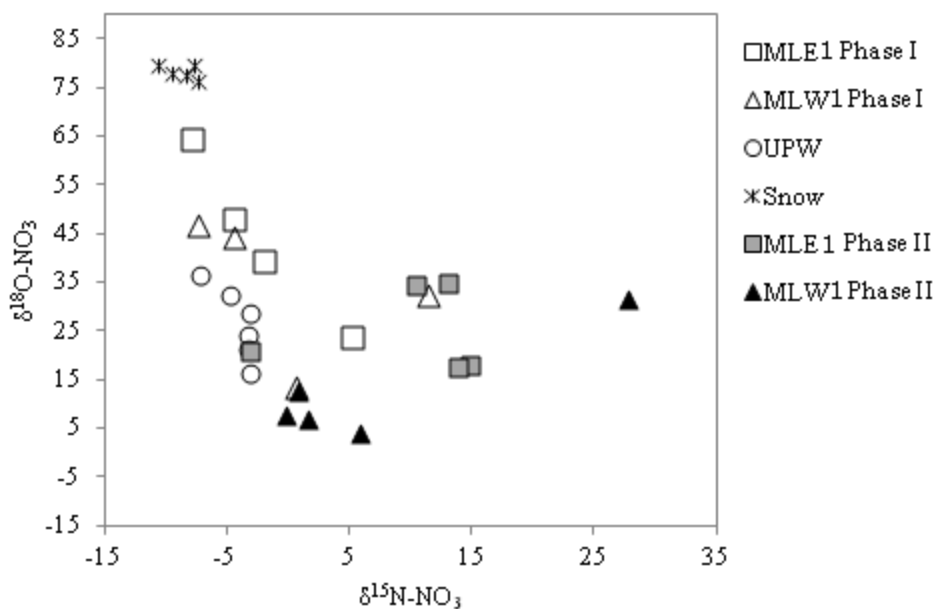


Figure 4.20. $\delta^{15}\text{N-NO}_3$ versus $\delta^{18}\text{O-NO}_3$ plot for the snow and stream samples during 2009.

4.5.1.2 $\delta^{34}\text{S-SO}_4$ and $\delta^{18}\text{O-SO}_4$ of streams

At the stream sites, MLE1 and MLW1, $\delta^{34}\text{S-SO}_4$ ranged from +7‰ to +15‰ and +11‰ to +16‰ respectively. Therefore $\delta^{34}\text{S-SO}_4$ variation at MLE1 was greater than at the MLW1. However, all the three available $\delta^{34}\text{S-SO}_4$ at UPW were similar (~+16‰) (Figure 4.21). At all the stream sites, $\delta^{18}\text{O-SO}_4$ remained significantly negative and below -3‰, with one exceptional positive value of +5‰ at MLE1 on DOY 188 (Figure 4.22). Generally, SO_4^{2-} concentrations and respective $\delta^{34}\text{S-SO}_4$ values at MLE1 were positively correlated with each other (Figure 4.21). The MLE1 $\delta^{34}\text{S-SO}_4$ values also follow the phase change like $\delta^{15}\text{N-NO}_3$ phases (see Section 4.5.1.1), during **Phase I** $\delta^{34}\text{S-SO}_4$ was lower than +13‰ at the MLE1 while during **Phase II**, $\delta^{34}\text{S-SO}_4$ was higher than +13‰. But this temporal differentiation was not discernable at MLW1 and UPW. Furthermore, a significant decrease of 2‰ in $\delta^{34}\text{S-SO}_4$ value was

observed in the eastern stream when the subglacial runoff travelled from UPW to MLE1 (Table 4.5).

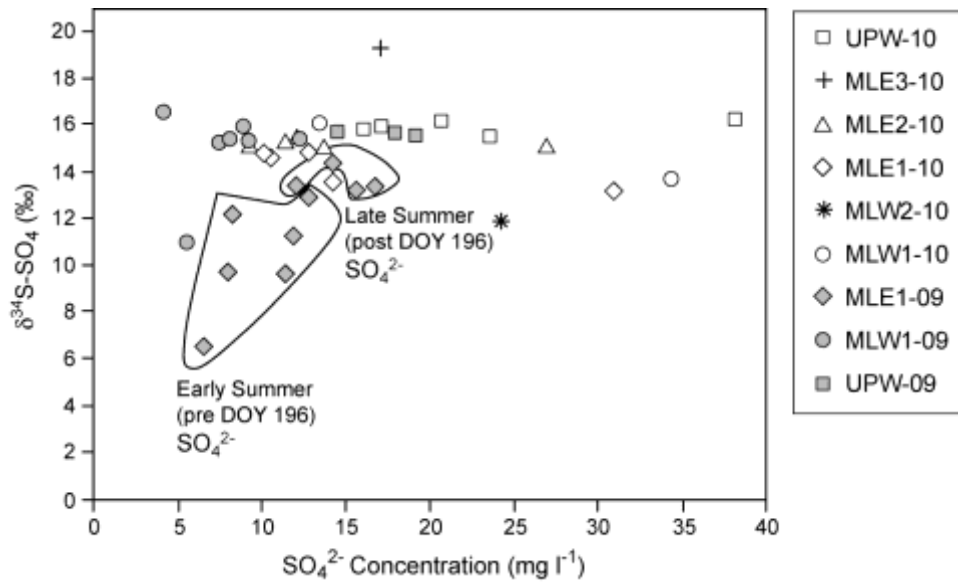


Figure 4.21. $\delta^{34}\text{S-SO}_4$ Vs SO_4^{2-} plot for 2009 and 2010 summer stream samples. The two circles represent the two types of SO_4^{2-} regime: one pre DOY 196 and other post DOY 196 during 2009 summer.

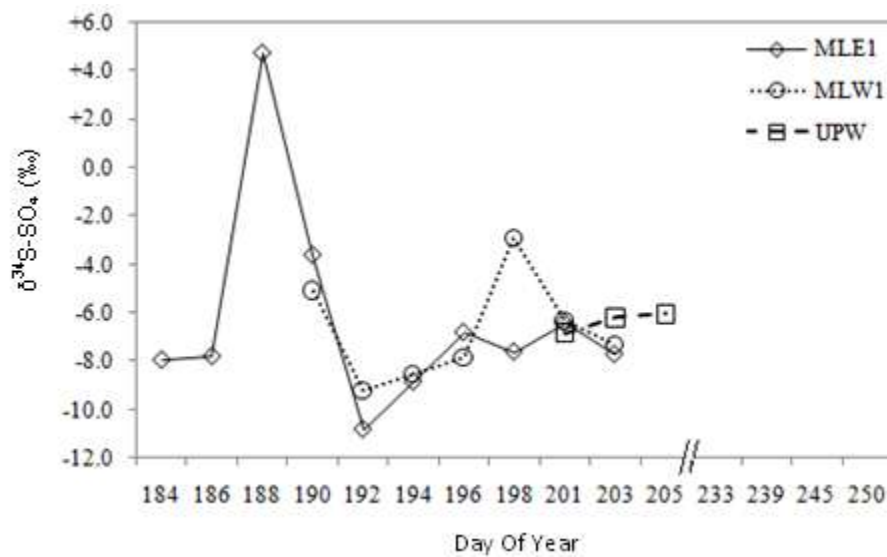


Figure 4.22. Temporal variations of stream's $\delta^{18}\text{O-SO}_4$ during summer 2009.

4.5.2 Year 2010

4.5.2.1 $\delta^{15}\text{N}$, $\delta^{18}\text{O}\text{-NO}_3$ and $\delta^{18}\text{O}\text{-H}_2\text{O}$ of snow and streams

Table 4.6. Mean stable isotope composition (\pm standard deviation) of NO_3^- , SO_4^- and H_2O in snow and stream samples during 2010.

Site	$\delta^{15}\text{N}\text{-NO}_3$ (‰)	$\delta^{18}\text{O}\text{-NO}_3$ (‰)	$\delta^{34}\text{S}\text{-SO}_4$ (‰)	$\delta^{34}\text{O}\text{-SO}_4$ (‰)	$\delta^{18}\text{O}\text{-H}_2\text{O}$ (‰)
Snow	-14.14 ± 0.82 (n = 5)	$+89.07 \pm 1.31$ (n = 5)	n.a.	n.a.	-10.90 ± 0.44 (n = 5)
UPW	-2.82 ± 5.18 (n = 5)	$+36.31 \pm 8.41$ (n = 5)	$+16 \pm 0.30$ (n = 5)	-5.00 ± 0.60 (n = 5)	-11.22 ± 0.38 (n = 5)
MLE3	-6.60 ± 3.66 (n = 3)	$+51.49 \pm 32.23$ (n = 3)	$+19.4 \pm 0.00$ (n = 1)	-5.10 ± 0.00 (n = 1)	-10.29 ± 0.46 (n = 5)
MLE2	-6.29 ± 1.36 (n = 5)	$+51.49 \pm 32.23$ (n = 5)	$+15.40 \pm 0.20$ (n = 5)	-5.30 ± 0.70 (n = 5)	-10.85 ± 0.52 (n = 5)
MLE1	-5.03 ± 2.46 (n = 5)	$+38.27 \pm 10.86$ (n = 5)	$+14.30 \pm 0.80$ (n = 5)	-3.80 ± 1.3 (n = 5)	-10.69 ± 0.51 (n = 5)
MLW3	-5.27 ± 2.46 (n = 4)	$+44.92 \pm 17.44$ (n = 4)	n.a.	n.a.	-10.43 ± 0.73 (n = 5)
MLW2	-4.69 ± 3.33 (n = 5)	$+31.83 \pm 18.19$ (n = 5)	$+11.90 \pm 0.00$ (n = 1)	-10.10 ± 0.00 (n = 1)	-10.39 ± 0.38 (n = 5)
MLW1	-3.64 ± 2.91 (n = 4)	$+31.83 \pm 18.19$ (n = 4)	$+15.00 \pm 1.70$ (n = 2)	-8.60 ± 1.30 (n = 2)	-10.32 ± 0.33 (n = 5)

In the 2010 snow $\delta^{15}\text{N}\text{-NO}_3$ and $\delta^{18}\text{O}\text{-NO}_3$ varied over a small range (-15‰ to -13‰ and $+87\text{‰}$ to $+90\text{‰}$ respectively). This time $\delta^{18}\text{O}\text{-H}_2\text{O}$ of the snow and streams was heavier than 2009 (by 1‰ to 2‰ ; see Table 5 and 6). During the following summer $\delta^{15}\text{N}\text{-NO}_3$ and $\delta^{18}\text{O}\text{-NO}_3$ in the UPW and the proglacial streams ranged from -9.6‰ to $+6\text{‰}$ and $+7\text{‰}$ to $+73.5\text{‰}$ respectively. However, the $+6\text{‰}$ was the only positive $\delta^{15}\text{N}\text{-NO}_3$ value observed at UPW on the first day of sampling (DOY 186). Over the summer, $\delta^{15}\text{N}\text{-NO}_3$ in the UPW and the proglacial stream showed a change of $+9.4\text{‰}$, whilst $\delta^{18}\text{O}\text{-NO}_3$ decreased by up to 66‰ between DOY 186 and DOY 227.

On a spatial scale, $\delta^{15}\text{N-NO}_3$ either remained constant or showed a significant increase (of, up to 4.7‰ over a course of ca. 1 km) between the ice marginal and downstream sites, whilst $\delta^{18}\text{O-NO}_3$ always experienced a significant decrease (by, up to 16‰) downstream on every sampling day (Figure 4.24).

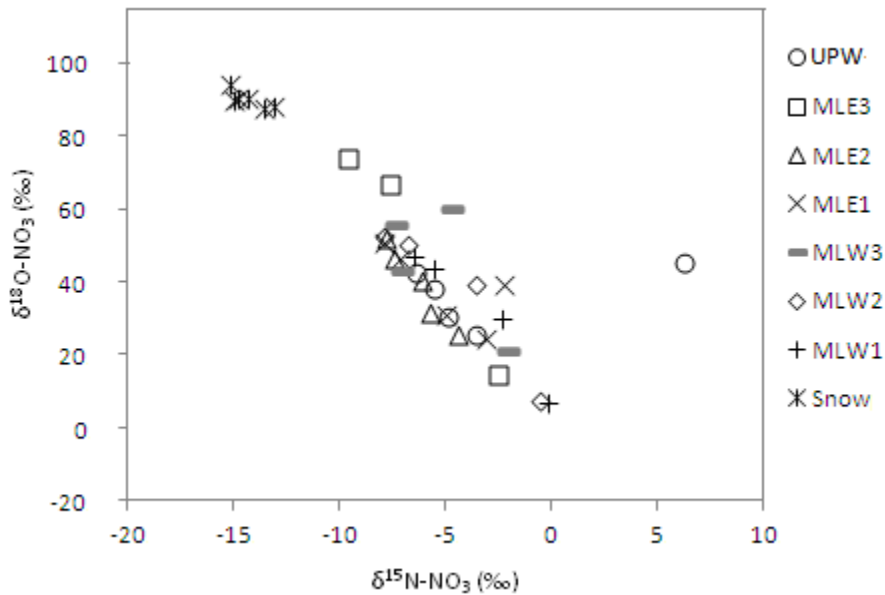


Figure 4.23. $\delta^{15}\text{N-NO}_3$ versus $\delta^{18}\text{O-NO}_3$ plot for the snow and stream samples during 2010.

The $\delta^{15}\text{N-NO}_3$ and $\delta^{18}\text{O-NO}_3$ from all the samples during 2010 were significantly correlated in which positive enrichment of $\delta^{15}\text{N-NO}_3$ and contemporary negative enrichment in $\delta^{18}\text{O-NO}_3$ formed an apparent linear relationship [excluding positive $\delta^{15}\text{N-NO}_3$ value, Pearson correlation coefficient for the rest was -0.95 ($p < 0.0001$, $n = 34$)] (Figure 4.23).

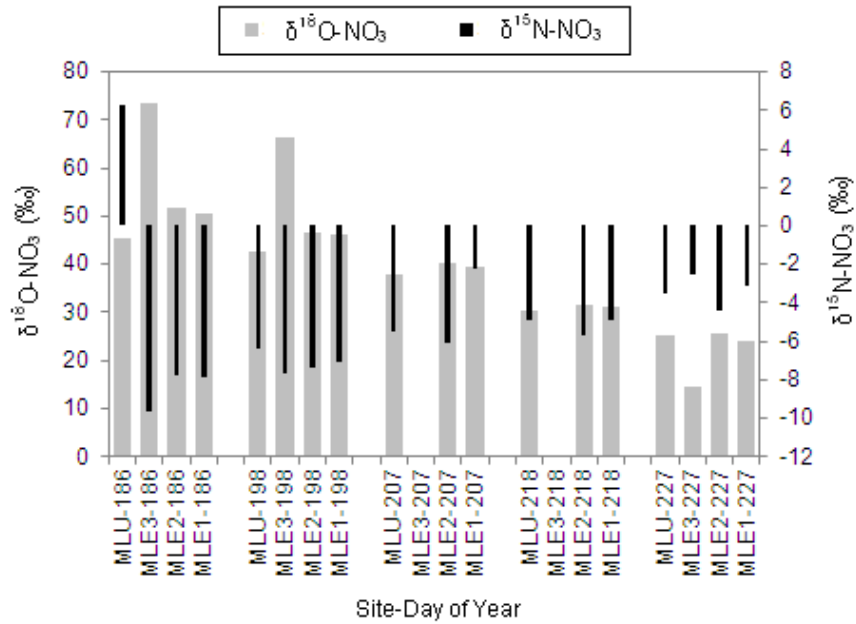


Figure 4.24. $\delta^{15}\text{N-NO}_3$ and $\delta^{18}\text{O-NO}_3$ spatial and temporal variation in the eastern stream during summer 2010.

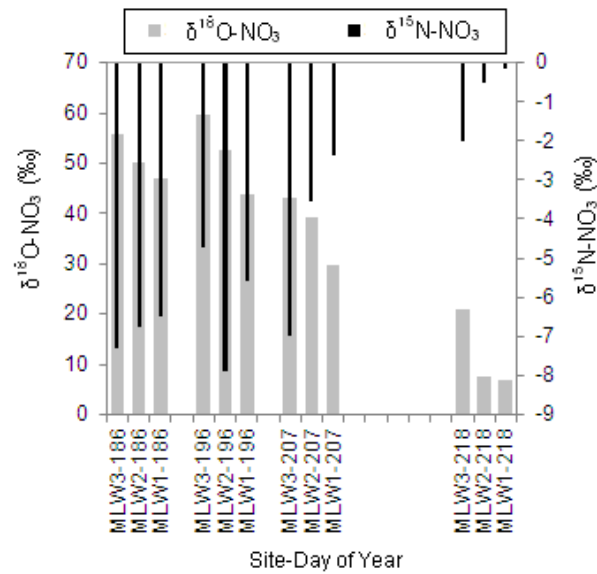


Figure 4.25. $\delta^{15}\text{N-NO}_3$ and $\delta^{18}\text{O-NO}_3$ spatial and temporal variation in the western stream during summer 2010.

4.5.2.2 $\delta^{34}\text{S-SO}_4$ and $\delta^{18}\text{O-SO}_4$ of streams

During summer 2010, $\delta^{34}\text{S-SO}_4$ in the eastern stream (+13.3‰ to +19.4‰) was slightly more enriched with ^{34}S than 2009. This pattern was also observed in the western stream (+11.9‰ to +16.3‰) (Figure 4.21). Again similar to 2009, $\delta^{34}\text{S-SO}_4$ at UPW remained constant during whole summer sampling period and the $\delta^{34}\text{S-SO}_4$ variation in the eastern stream was more than the western stream. This time $\delta^{18}\text{O-SO}_4$ in these streams ranged between -10.1‰ to -1.9‰ . Furthermore, unlike 2009, no relationship was observed between SO_4^{2-} concentration and respective $\delta^{34}\text{S-SO}_4$ in the eastern stream (Figure 4.21) and no temporal division was apparent in $\delta^{34}\text{S-SO}_4$.

An investigation of spatial variation of $\delta^{34}\text{S-SO}_4$ in the eastern stream showed that as the water moved downstream from MLE3 to MLE1, its $\delta^{34}\text{S-SO}_4$ experienced a significant decrease (ca. 0.9 to 5‰ over the course of ca. 1 km flowpath) (Figure 4.26). However, the $\delta^{18}\text{O-SO}_4$ showed an overall increase downstream (Figure 4.26).

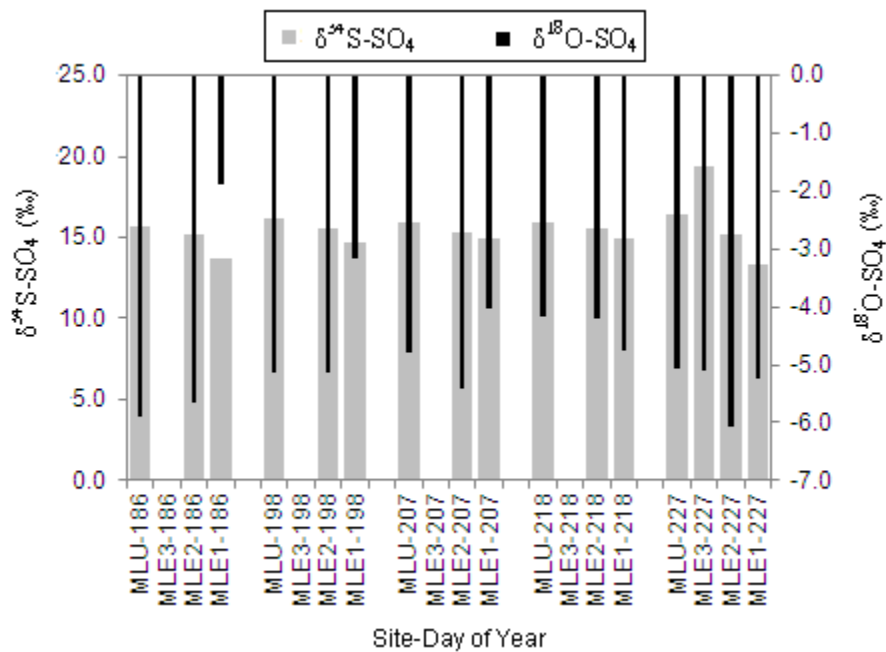


Figure 4.26. Spatial and temporal variations in $\delta^{34}\text{S-SO}_4$ and $\delta^{18}\text{O-SO}_4$ in the eastern stream during summer 2010.

4.6 Dissolution experiment results

4.6.1 Rock nitrogen, sulphur and their isotopic composition

In order to investigate geological nitrogen contribution in the catchment biogeochemistry here we used the data of rock nitrogen, sulphur content and their respective isotopic signature from the 6 major rocks collected from Midtre Lovénbreen catchment (see Table 3.4; Wynn 2004).

From the Table 4.7, it was obvious that phyllite (which covers largest part of the Midtre Lovénbreen catchment) contained a very significant amount of nitrogen, followed by conglomerate, green chert and subglacial till. However, largest amount of sulphur was recovered from conglomerate followed by green chert, phyllite, subglacial till and quartzite. Irrespective of being found in close vicinity to each other, these rock's nitrogen and sulphur content and respective isotopic signature varied by a significant margin. The nitrogen content in the gneiss and quartz, was below detection limit hence $\delta^{15}\text{N-NH}_4^+$ could not be obtained. The $\delta^{15}\text{N-NH}_4$ was positive for most of the rocks except for the conglomerate. Similarly, most of the rocks had positive $\delta^{34}\text{S}$ value except for the quartzite. There was no association found between the rock nitrogen / sulphur content variation and their respective isotopic signature variation.

4.6.2 Dissolved inorganic nitrogen and other ions release from rock dissolution

Dissolution of the three experimental rock powders with milliQ water (18 Ω) for 72 hrs released a considerable amount of inorganic nitrogen. NH_4^+ -N release was observed in the two out of the three rocks and amounted $0.34 \pm 0.06 \mu\text{g NH}_4^+\text{-N g}^{-1}$ of phyllite and $3.06 \pm 0.11 \mu\text{g NH}_4^+\text{-N g}^{-1}$ of conglomerate, whilst gneiss did not produce NH_4^+ -N at all during its dissolution. Further, NO_3^- -N release was also observed in all the three rock powders that amounted to $0.39 \pm 0.01 \mu\text{g NO}_3^-\text{-N g}^{-1}$ of phyllite, $0.43 \pm$

0.03 $\mu\text{g NO}_3^- \text{-N g}^{-1}$ of gneiss and $0.80 \pm 0.03 \mu\text{g NO}_3^- \text{-N g}^{-1}$ of conglomerates. Thus, overall releasable inorganic nitrogen through rock dissolution was highest in conglomerate followed by phyllite and gneiss. All the three rocks were analysed in triplicates, and looking at standard deviation it is obvious that repetitiveness is much better for $\text{NO}_3^- \text{-N}$ than $\text{NH}_4^+ \text{-N}$ release (Figure 4.27).

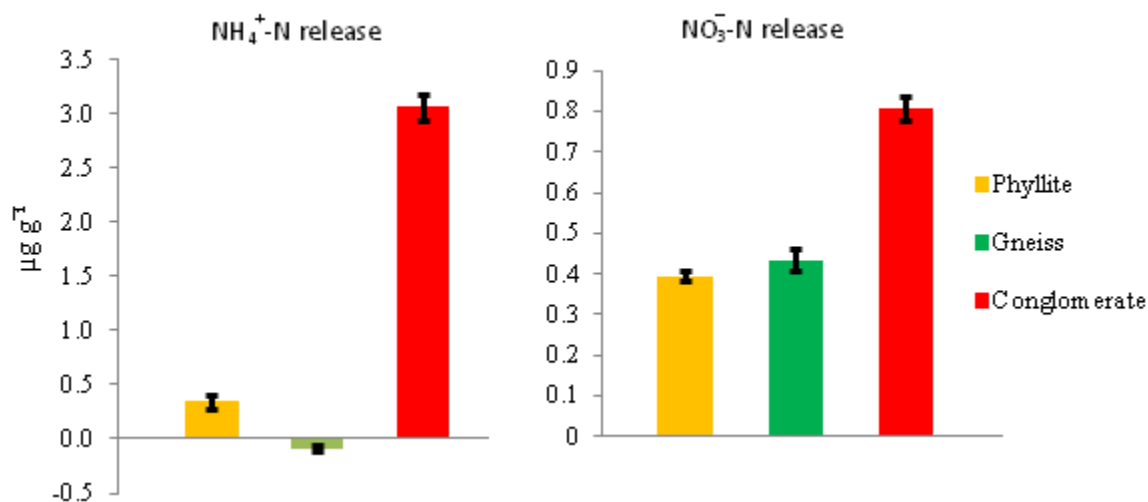


Figure 4.27. $\text{NH}_4^+ \text{-N}$ and $\text{NO}_3^- \text{-N}$ release from the three Midtre Lovénbreen rocks collected. Whiskers on each bars represents standard deviation.

Table 4.8, Mean of released major ions (\pm standard deviation) during the dissolution of three rocks from Midtre Lovénbreen.

Rock	Na^+ ($\mu\text{g/g}$)	K^+ ($\mu\text{g/g}$)	Ca^{2+} ($\mu\text{g/g}$)	Mg^{2+} ($\mu\text{g/g}$)	Si ($\mu\text{g/g}$)	SO_4^{2-} ($\mu\text{g/g}$)
Phyllite	19.9 \pm 1.6 (n = 3)	26.7 \pm 2.6 (n = 3)	148.3 \pm 17.0 (n = 3)	1.63 \pm 0.1 (n = 3)	24.8 \pm 0.8 (n = 3)	10.7 \pm 1.2 (n = 3)
Gneiss	76.0 \pm 5.7 (n = 3)	18.9 \pm 0.7 (n = 3)	158.4 \pm 11.4 (n = 3)	1.54 \pm 0.2 (n = 3)	44.5 \pm 2.3 (n = 3)	4.9 \pm 0.2 (n = 3)
Conglomerate	12.1 \pm 2.6 (n = 3)	16.9 \pm 6.7 (n = 3)	102.5 \pm 2.7 (n = 3)	1.94 \pm 0.9 (n = 3)	46.3 \pm 3.3 (n = 3)	34.8 \pm 6.4 (n = 3)

Releases of other major ions (Na^+ , K^+ , Ca^{2+} , Mg^{2+} , SO_4^{2-}) and silicawere also observed from rock dissolution experiment. Phyllite released relatively high amount of K^+ and relatively low amount of Si than the other two rocks (Table 4.8). Gneiss released relatively high amount of Na^+ and low SO_4^{2-} than the other two rocks, whereas conglomerate liberated a relatively large amount of SO_4^{2-} and low amount of Na^+ and Ca^{2+} compared with the other two rocks.

4.6.3 Nitrogen adsorption efficiency of the rocks

Regression models for NH_4^+ -N adsorption showed that adsorption by all the three rocks increased linearly up to a final concentration of $340 \mu\text{g L}^{-1}$ NH_4^+ -N. However, further higher concentrations showed a non-linear relationship typical of adsorption isotherm for other solutes and glacial sediments (Hodson et al., 2004). Initial NH_4^+ -N adsorption by conglomerate was substantially higher than the other two rocks. The phyllite regression curve remained relatively linear from 255 to $1020 \mu\text{g L}^{-1}$ NH_4^+ -N concentration however, whilst both gneiss and conglomerate showed adsorption maxima between 4.0 and $5.0 \mu\text{g NH}_4^+$ -N g^{-1} rock.

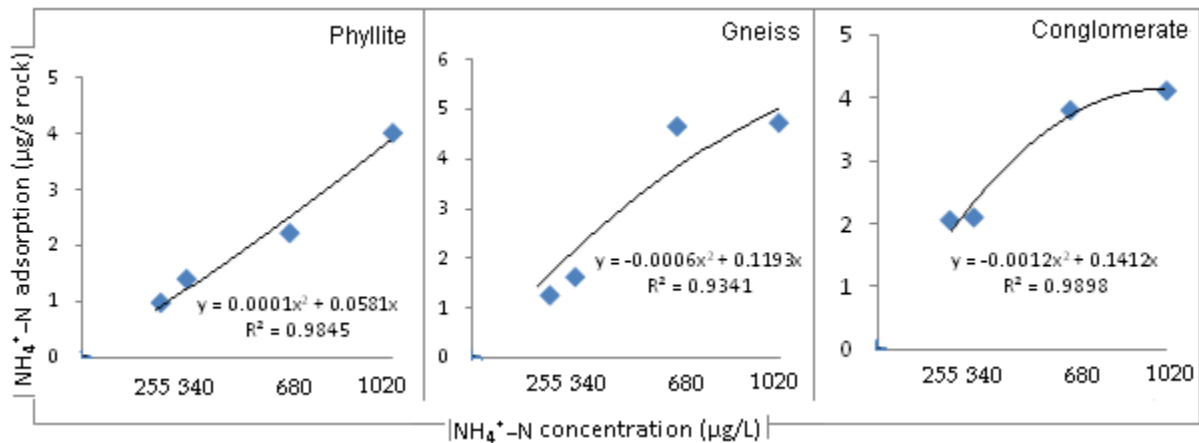


Figure 4.28, NH_4^+ adsorption isotherm curve for the three major rocks from the Midtre Lovénbreen glacier.

4.7 Summary

The major characteristics of the results are:

- Local climate condition during 2010 was slightly colder and drier than 2009. In addition snow accumulation during 2010 was lower than 2009 and the melt season commence much earlier.
- Snow solute content during 2009 was higher and more in marine origins than in 2010. However, the total dissolved nitrogen concentration in the 2010 snow was considerably higher. Both the years DON made the highest fraction of snow's total dissolved nitrogen pool.
- The average $\delta^{15}\text{N-NO}_3$ and $\delta^{18}\text{O-NO}_3$ in 2009 snow were $-8.7 \pm 1.3\text{‰}$ and $+78.1 \pm 1.5\text{‰}$ and in 2010 snow $-14.1 \pm 0.8\text{‰}$ and $89.0 \pm 1.3\text{‰}$ respectively.
- During both the years, the proglacial stream's ionic contents were dominated Ca^{2+} , HCO_3^- and SO_4^{2-} . Ionic ratios of these ions against Cl^- were higher than that in the snow.
- Similarly during both the years, median $\text{NO}_3\text{-N/Cl}^-$ and DOC/Cl^- ratios in the proglacial streams were higher whilst $\text{NH}_4^+\text{-N/Cl}^-$ were lower than that in the snow. During downstream transport the $\text{NO}_3\text{-N/Cl}^-$ ratios either remained invariable or experienced a decrease.
- During 2009, the $\delta^{15}\text{N-NO}_3$ values in the proglacial streams varied from -7.8‰ to $+14.9\text{‰}$ and $\delta^{18}\text{O-NO}_3$ from $+17.5$ to $+46.8\text{‰}$, whilst during 2010, the $\delta^{15}\text{N-NO}_3$ varied from -9.6‰ to $+6.0\text{‰}$ and $\delta^{18}\text{O-NO}_3$ from $+7.0\text{‰}$ to $+73.5\text{‰}$. With the passing summer the $\delta^{15}\text{N-NO}_3$ values either remained invariable or increased whilst $\delta^{18}\text{O-NO}_3$ significantly decreased. Similarly, during downstream transport $\delta^{15}\text{N-NO}_3$ values either remained invariable or increased whilst $\delta^{18}\text{O-NO}_3$ significantly decreased (over the ~ 1 km long flowpath).

- During both the years 88% to 99% of the proglacial stream SO_4^{2-} was non-snow in origin and concentration increased from early to late summer at all proglacial sites except UPW where it had an initial decrease and thereafter increase in later summer. In addition, spatiotemporal variation of SO_4^{2-} and Ca^{2+} was similar.
- During 2009, the $\delta^{34}\text{S-SO}_4$ in the proglacial streams varied from +7‰ to +16‰ and $\delta^{18}\text{O-SO}_4$ from -10‰ to +5‰ whilst during 2010, $\delta^{34}\text{S-SO}_4$ varied from +11.1‰ to +19.4‰ and $\delta^{18}\text{O-SO}_4$ from -10.1 to +1.9‰. Unlike $\delta^{15}\text{N-NO}_3$ and $\delta^{18}\text{O-NO}_3$ no clear temporal change was visible in $\delta^{34}\text{S-SO}$ and $\delta^{18}\text{O-SO}_4$. However, during downstream transport $\delta^{34}\text{S-SO}_4$ and $\delta^{18}\text{O-SO}_4$ either remained invariable or increased (over the ~ 1km long flowpath).
- Rock powders released significant amounts of dissolved inorganic nitrogen during dissolution experiments and adsorbed $\text{NH}_4^+\text{-N}$ after further re-suspending the powder into $\text{NH}_4^+\text{-N}$ solution.

CHAPTER 5: DISSCUSSION

This chapter presents a discussion of scientific findings based upon the results summarised in Chapter 4. Section 5.1 and 5.2 discusses the potential sources, depositional process, abundance and annual dynamics of nitrogen and then sulphur in the snow, as well as their likely sensitivity towards meteorological drivers. Similarly, Sections 5.3 and 5.4 discusses the sources, sinks and spatio-temporal variability of N and S respectively, in order to characterise microbial processes and their importance in local biogeochemical cycling. Section 5.5 and 5.6 discusses the rock generated N and S and their possible role in catchment scale biogeochemistry.

5.1 Snow nitrogen sources, abundance and their annual variability

5.1.1 Isotopic insights

Many previous studies have already established a connection between mid-latitude pollution and Arctic snow NO_3^- and SO_4^{2-} concentrations by using atmospheric circulation models (see Section 3.1.1). Further, researchers have used stable isotopic techniques successfully to demonstrate the link between atmospheric and snow NO_3^- . However, complete identification of NO_3^- point sources still needs to be improved by first developing better understanding of complex atmospheric chemical reactions and their associated isotopic effects on both temporal and spatial scales. In this study, the similarity of snow $\delta^{18}\text{O}-\text{NO}_3$ to tropospheric $\delta^{18}\text{O}-\text{O}_3$ (Johnston and Thiemens, 1997) (see Section 4.6.1) reaffirms the atmospheric origin of NO_3^- (Kendall et al., 2007) and show a good agreement with the previous studies conducted in the same catchment and nearby Ny Ålesund [$\delta^{18}\text{O}-\text{NO}_3 = +57$ to $+85\%$ and $\delta^{15}\text{N}-\text{NO}_3 = -15$ to -5% (Heaton et al., 2004; Tye and Heaton 2007; Wynn et al., 2006, 2007)] (Figure 5.1). However, $\delta^{18}\text{O}-\text{NO}_3$ during 2010 was a little higher than ever recorded for this region. The typical range of atmospheric $\delta^{15}\text{N}$ and $\delta^{18}\text{O}-\text{NO}_3$ can consequently be defined with some confidence for this site ($\delta^{15}\text{N}-\text{NO}_3 = -10.6\%$

to -7.4‰ , $\delta^{18}\text{O-NO}_3 = +76.1\text{‰}$ to $+79.6\text{‰}$ during 2009 and -13‰ to -15‰ and $+87\text{‰}$ to $+90\text{‰}$ respectively during 2010).

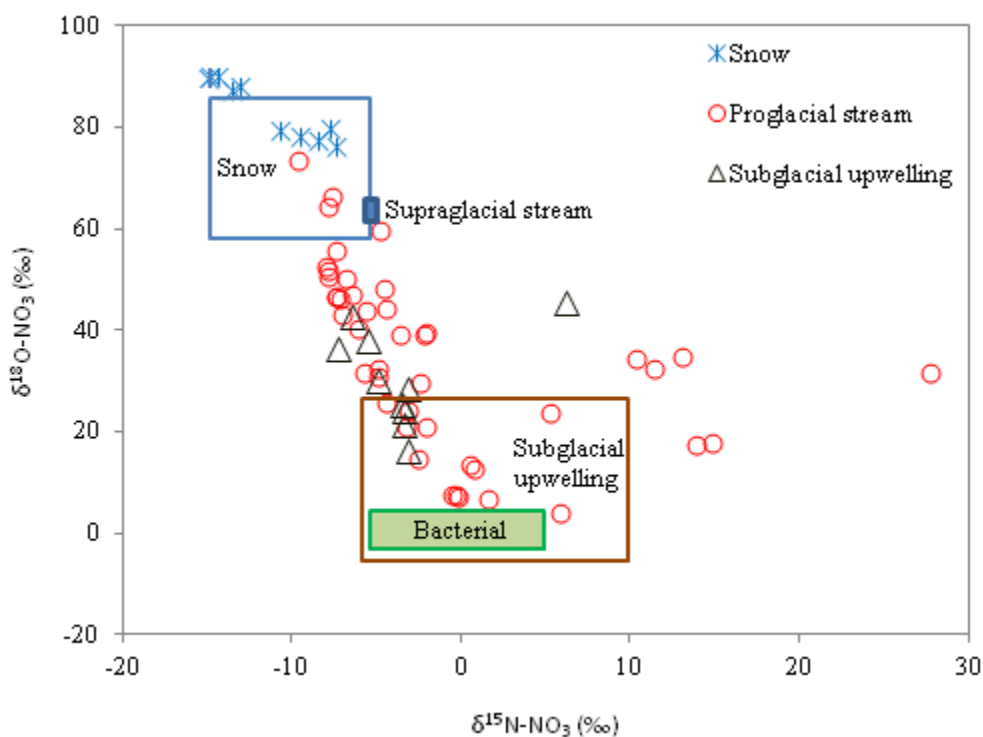


Figure 5.1. $\delta^{15}\text{N-NO}_3$ versus $\delta^{18}\text{O-NO}_3$ variation at Midtre Lovénbreen. Individual data points are from the present study, while the larger annotated rectangles represent the domain of the graph occupied by results from previous work at this site (“Snow”, “Supraglacial streams” and “Subglacial upwelling”). The shaded rectangle (“Bacterial”) depicts the predicted composition of microbially produced NO_3^- .

The significant difference in the snow accumulation (depth of snow during 2009 > snow during 2010) between the two years of study coincided with considerable changes in snow’s dissolved inorganic nitrogen and $\delta^{15}\text{N}$, $\delta^{18}\text{O-NO}_3$ (see Section 4.3 and 4.6.1). Many previous studies have reported an inverse relationship between snow accumulation and their NO_3^- concentrations (Herron, 1982; Legrand and Kirchner, 1990; Yang et al., 1995; Fischer et al., 1998) and suggested that during

low snow accumulation (wet deposition), dry deposition becomes the major mechanism of aerosol deposition in the polar region, which generally leads to higher solute concentration in snow. Thus, lower snow accumulation and higher dissolved inorganic nitrogen concentration in 2010 snow support this model. Dry deposition is generally composed of heavier $\delta^{15}\text{N-NO}_3$ than wet deposition (Heaton et al 1997; Elliott et al., 2009). In this study, the greater snow water equivalent accumulation in 2009 showed heavier $\delta^{15}\text{N-NO}_3$ than 2010, demonstrating that the mode of deposition is an unlikely control upon the $\delta^{15}\text{N-NO}_3$ signature of the bulk snowpack.

Significantly, negative $\delta^{15}\text{N-NO}_3$ (up to $\sim -36\text{‰}$; Michalski et al., 2005; Morin et al., 2008) in the polar atmosphere and snow is now a well known occurrence. However, the reasons for such negative values, for example, those found in this study are not properly understood. Presently there are three different mechanisms thought to explain the process that causes such negative $\delta^{15}\text{N-NO}_3$:

- 1) Mass dependent fractionation during long-range, trans-boundary transport (Heaton et al., 2004);
- 2) Stratospheric supply of ^{14}N enriched NO_3^- (Heaton, 2004) through PSC clouds; and
- 3) Photolytic recycling of snow NO_3^- (Morin et al., 2008).

In parallel, when we check the snow $\delta^{34}\text{S-SO}_4$ reported from Arctic snow (Mann, 2005; Wynn 2004), it does not show any significant ^{32}S depletion caused by long range transportation (see next Section). On this basis we consequently reject hypothesis (1) as major reason for highly negative $\delta^{15}\text{N-NO}_3$ observed in Arctic snow because SO_4^{2-} and NO_3^- share similar source area in many parts of Europe. Based upon Dubowski et al. (2001) lab experiment, photolysis seems to be effective only in upper few centimeters of the snow column and mostly takes place in liquid inclusions. Therefore, supply of ^{14}N enriched NO_3^- from stratospheric during PSC formation appears the most likely source of highly negative $\delta^{15}\text{N-NO}_3$ unless tropospheric SO_4^{2-} and NO_3^- are different and / or local sources of the latter are more important than the

former (Eckhardt et al., 2003). The NO_x supply to the stratosphere mostly takes place in the form of N_2O because of its long lifetime [ca. 120 year (Volk et al., 1997)] that allows it to drift from lower troposphere to the stratosphere. Therefore, ^{14}N enriched NO_3^- in stratosphere are assumed to be formed by N_2O photolysis by ultra-violet radiation. In a lab-based simulated study by Rahn et al., (1998) and later on Röckmann et al., (2000) showed that ultraviolet photolysis of N_2O produced a large $\delta^{15}\text{N}$ enrichment of up to -48.7% . However, OCS (carbonyl sulphide) is the most stable sulphur compound in atmosphere [(lifetime ~ 4 to 5 year) Johnson, 1981] and therefore is considered major sulphur compound to reach into the stratosphere but unlike N_2O , Hattori et al., (2011) demonstrated that OCS ultraviolet photolysis produced only a small $\delta^{34}\text{S}$ enrichment of $1.1 \pm 4.2\%$.

During this study, it was observed that more negative NAO conditions coincided with more negative $\delta^{15}\text{N}\text{-NO}_3$ and vice-versa. Although no study has yet reported any possible impact of NAO variations over atmospheric $\delta^{15}\text{N}\text{-NO}_3$, $\delta^{18}\text{O}\text{-NO}_3$, it has been suggested by some studies that NAO can directly / indirectly influence the atmospheric pollution distribution, its transport and direction in the northern hemisphere troposphere (Eckhardt et al., 2003; Christoudias et al., 2012). For example, the NAO index refers to the pressure gradient between the sub-polar high and polar low, and so the lower the index value, the lower the pressure gradient. Therefore, the more negative NAO during 2010 would have led to weaker movement of tropospheric airmass and consequently more deposition during transport to Arctic.

5.1.2 Dissolved organic nitrogen

Irrespective of annual variability in total nitrogen deposition, DON forms the largest fraction of snow's dissolved nitrogen pool. Because the removal processes for inorganic nitrogen are more effective than organic species, the latter is often accepted as a better long range carrier (Neff et al., 2002; Matsumoto and Uematsu, 2005). DON in the atmosphere most likely exists as small particulate or gaseous forms (Spokes et

al, 2000; Cornell et al., 2001) and is estimated to form 20% to 65% of atmospheric total dissolved nitrogen (Zhang and Anastasio 2001; Weathers et al., 2000). In addition, water soluble organic nitrogen species are generally more frequent in nitrogen deposition, which can contain many different compounds with different origins (Cornell et al., 2003). However, because of the lack of attention from the scientific community its sourcing and fate in this part of the world remains poorly understood. One reason for this lack of attention is that dissolved organic nitrogen was generally assumed as a product of locally recycled nitrogen. As a result, anthropogenic nitrogen became the major focus of research interest (Cornell, 2010).

Although in this study, two different methods were used to analyse the TN in the two sampling years, a remarkable difference in 2009 (persulphate method) and 2010 (high temperature oxidation method) snow DON values was observed. This may not necessarily reflect the methodological efficiency because the total nitrogen recovery by the persulphate ($93 \pm 13 \%$) and high temperature thermal oxidation ($87 \pm 14 \%$) are generally in very close agreement (Bronk et al., 1999). Therefore, the 3 to 4 times difference (Table 4.1) could possibly be a result of annual variability in production / deposition processes. The predominantly low DOC/DON ratio (<16) from the two year's snow samples (Figure 4.7 and 4.13) suggests that DON was largely composed of light nitrogen containing organic compounds (i.e. PAN and related alkyl nitrates, amines, aminoacids and urea) (Gorzelska and Galloway, 1990). This agrees with previous studies of atmospheric organic nitrogen that demonstrate atmospheric organic nitrogen to be largely composed of light weight molecules (Timperley et al., 1985; Mopper and Zika, 1987; Leuenberger et al., 1988; Gorzelska and Galloway, 1990; Anastasio and McGregor, 2000; Cornell et al., 2001; Zhang and Anastasio, 2001). However, understanding about organic nitrogen sourcing not only in the high Arctic but also on the global scale remains underdeveloped and needs more consideration.

In general, the most likely sources of atmospheric DON are the following:

- 1) **Biogenic release from the sea.** DON in sea water is produced by various biological processes, including its direct release from living cells and by putrefaction of dead cells (Bronk and Steinberg, 2008). The atmosphere over the sea and coastal regions are more likely to receive this kind of DON (Cornell et al., 2003). It is also evident that marine DON increases with latitude and becomes more dominant in the northern latitudes. Hence, their deposition can increase here as well (Gorzelska and Galloway, 1990). According to Gershey (1983) the C/N ratio of marine generated aerosols range between 6.7 to 9.7 which is significantly near to the dominant DOC/DON ratio observed from the 2010 snow samples (3 to 5.8) in this study.

- 2) **Anthropogenic pollution** (i.e. fossil fuel burning, fertiliser production). Direct DON release from local sources (including pollution by ships) and distant sources (pollution in the north western Eurasia and North-America, or secondary aerosol formation by reactions between released inorganic NO_x with organic molecules in suitable environments). PAN is thought to be the most important species that represents this section has dissolved organic nitrogen (Beine and Krogne, 2000), however due to low solubility (Holdren et al., 1984; Kames and Schurath, 1995) its persistence in snow is doubtful. Furthermore, it is generally assumed that most of the PAN decomposed to NO_x before deposition (Beine and Krogne, 2000).

- 3) **Aeolian dust.** Soils with humic substances can also have fair amount of DON, therefore, the release of such material in atmosphere by winds, can be considered as a source.

Thus DON dominated the total dissolved nitrogen content of snow, concentration ranging from 23 to 94 $\mu\text{g L}^{-1}$ (42 to 70%) and most of it was likely to come from marine biogenic sources. However, $\text{NH}_4^+\text{-N}$ and $\text{NO}_3^-\text{-N}$ were mostly sourced from anthropogenic activity at lower latitudes and constitute the second

largest source of total dissolved nitrogen, their concentration ranged between 14 to 26 $\mu\text{g L}^{-1}$ (17 to 24%) and 12 to 30 $\mu\text{g L}^{-1}$ (18 to 34%) respectively.

5.2 Snow sulphur sources, abundance and their annual variability

5.2.1 Isotopic insights

Sulphate in High Arctic glaciers can be derived from four possible sources:

- 1) **Sea salt SO_4^{2-}** ($\delta^{34}\text{S-SO}_4 = +21\text{‰}$; Böttcher et al., 2007) coming along with sea breeze.
- 2) **Biogenic SO_4^{2-}** , generated by oxidation of Di-Methyl Sulphide (DMS, $\delta^{34}\text{S-SO}_4 = +14\text{‰}$ to $+22\text{‰}$; Calhoun et al., 1991; Patris et al., 2000a) in the atmosphere (DMS is mostly generated by marine algae and is one of the dominant natural sources of sulphur to the atmosphere).
- 3) Dissolution of SO_4^{2-} containing **dust minerals** ($\delta^{34}\text{S-SO}_4 = -10\text{‰}$ to $+10\text{‰}$, Nielsen, 1974) transported by winds over glacier.
- 4) **Anthropogenic SO_4^{2-}** generated by oil refining, fossil fuel burning and metal smelting ($\delta^{34}\text{S-SO}_4 = -2\text{‰}$ to $+10\text{‰}$; Zhao, 1998; Novak et al., 2001; Tichomirowa et al., 2007).

In this study due to unavailability of $\delta^{34}\text{S-SO}_4$ data for the snow samples, snow non-sea-salt SO_4^{2-} could not be traced using the above isotopic signatures. However, according to a previous study on the same region $\delta^{34}\text{S-SO}_4$ of snow non-sea-salt SO_4^{2-} were variable on annual scale and ranged between -4.25 and $+2.6$ (Wynn, 2004). This indicated that anthropogenic sourcing of non-sea-salt SO_4^{2-} in the Midtre Lovénbreen snow samples were more discernable. However, recent studies show that SO_4^{2-}

sourcing in snow are more mixed (including sea-salt, DMS derived and anthropogenic) than one dominant source (Fisher et al., 2011) and further the contributions of these sources varies seasonally. The snowpacks SO_4^{2-} concentration during the two year of study were in the range reported in recent past studies in the same / nearby regions (Simoes and Zagorodnov, 2001; Wynn et al. 2006; Beaudon and Moore, 2009). NH_4^+ play a major in neutralising agent for the excess SO_4^{2-} in the snow and consequently moderates the snow acidity. In addition base cations associated with wind-blown dust can also neutralise excess sulphate in snow.

The significant difference between the ionic content of two years snowpack can primarily be related with snow accumulation and it may be inferred that high snow accumulation (wet deposition) generally increases ionic content of snowpack. However, during low snow accumulation dry deposition events are assumed to increase the SO_4^{2-} concentration (Herron, 1982; Fischer et al., 1998). In this study no such evidence of inverse relationship between snow accumulation and SO_4^{2-} suggests either dry deposition was not significant or snowpack ionic content was amended by postdepositional ionic displacement. Further, the difference in sea-salt and non-sea-salt ionic content of the two years snowpack was perhaps more influenced by climatic parameters (temperature, pressure, humidity, rain and wind) that controlled atmospheric transport and depositional process.

5.3 Spatio-temporal stream nitrogen dynamics

During 2009, this study largely emphasised temporal variability of related biogeochemical processes in the streams. However, during 2010, spatial variability was the focus of research. Therefore, to make a clear impression, the two years of data are discussed separately in the first instance.

5.3.1 Year 2009

Variations $\delta^{15}\text{N-NO}_3$ in both streams can be divided into two phases to explain the temporal biogeochemical changes: 1) **Phase I**: before the emergence of subglacial upwelling, when NO_3^- -N in stream water had a $\delta^{15}\text{N-NO}_3$ signature close to the snow; 2) **Phase II**: after the subglacial upwelling emergence, when NO_3^- -N in stream water had $\delta^{15}\text{N-NO}_3$ signature significantly higher than snow (Figure 4.20). Therefore, it is hypothesised that during Phase I, most of snow NO_3^- -N drained into the initial fraction of runoff at MLE1 and MLW1 by an elution process, leaving the remaining snow increasingly depleted in NO_3^- -N (e.g. Roberts et al, 2010). Hence, during Phase II, NO_3^- -N was increasingly produced by microbes that caused a further overall increase of NO_3^- -N and DOC in the MLE1 and MLW1. The basis for this hypothesis is further elaborated later in this section (Figure 5.3).

In addition to isotopic evidence, the relatively higher NO_3^- -N and Cl^- in two streams (Figure 4.7a and b) reaffirms that stream NO_3^- -N during phase I was predominantly derived from snow, considering snow as a major source of Cl^- for the catchment streams. This phenomenon is also known as an “ionic pulse”, in which the early part of snowmelt releases water having more concentrated chemical composition than its parent snow (Johansen and Henriksen, 1978; Williams et al., 1996; Goto-Azuma, 1998). According to Rasch et al. (2000), during the early melt season, water discharge in high Arctic streams is generally dominated by snowmelt. However, later on in the summer, hydro-chemical processes and subsequent stream chemical compositions are also controlled by active layer depth change, biogeochemical reactions, temperature and on a short time scale, rainfall as well (McNamara et al., 2008). Therefore, due to seasonal warming, air temperature reached 10°C for the first time just 2 days before DOY 196 (Figure 5.2) probably helped increasing active layer interflow and biological activity, assisting the leading transition to the phase II type conditions.

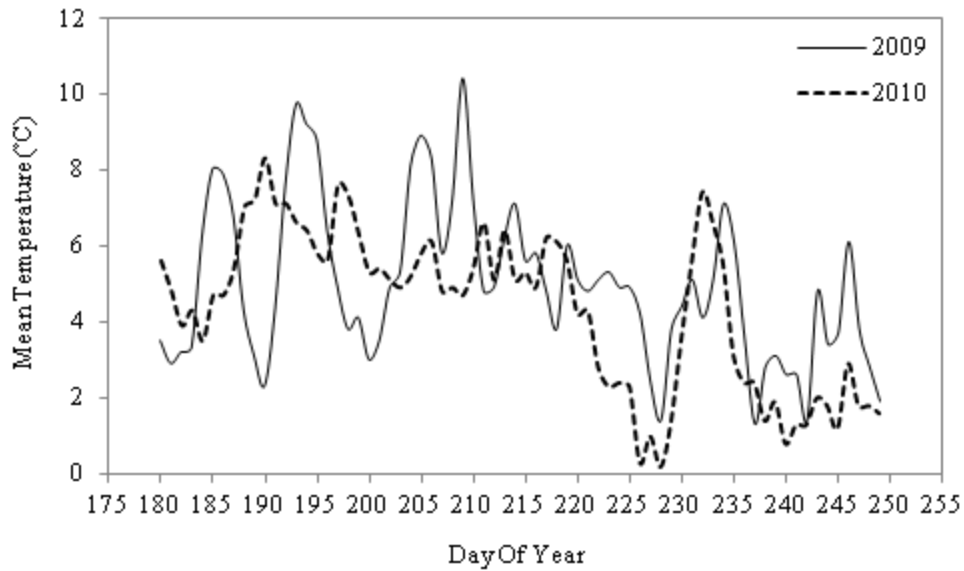


Figure 5.2. Mean atmospheric temperature variation in Ny Ålesund during summer 2009 and 2010.

During Phase II the streams had potentially more processes that significantly influenced their chemical composition, as is obvious from the $\delta^{15}\text{N-NO}_3$ variations across a significantly broader range (Figure 4.20). This view is further supported by the increase in ionic solutes normally released from rocks by weathering processes (SO_4^{2-} , HCO_3^- , Ca^{2+} , Mg^{2+}) and which reached their annual maximum concentrations during Phase II. However, the major limiting nutrients required for biological metabolic activity (NO_3^- -N, NH_4^+ -N, and DOC) decreased to minimum levels except at UPW where only NH_4^+ -N was depleted. This demonstrates a biogeochemical interaction between melt water and sediments, such that melt water which is able to access the deeper parts of the glacier shows signs of biological activity during Phase II. Another factor that can also influence the chemical composition of proglacial streams is snowline retreat to higher altitude, which generally increases the fraction of ice-melt derived water in total water discharge (Rasch et al., 2000; Hodson et al., 2005b). In this study the western stream was ideal for looking into stream chemical composition change caused by such a shift in snowline because, there was no subglacial runoff entering it during the summer.

Further, high Cl^- concentration in UPW waters clearly show that this water was predominantly derived from supraglacial snow throughout the entire summer. Therefore, UPW which mixed with MLE waters accessed the subglacial system via the stable crevasses and moulins situated at the 400 m altitude on the eastern lateral side of the glacier (Irvine-Fynn et al., 2005).

5.3.1.1 Subglacial nitrogen biogeochemical cycling

The presence of non-snowpack NO_3^- “excess nitrate” in the subglacial upwelling waters has already been reported in previous studies (Hodson et al 2005a; Wynn et al 2007) and offers a potential explanation for the shift from Phase I snow dominated NO_3^- -N toward microbial NO_3^- -N dynamics during Phase II. The sources of the excess NO_3^- -N remain unclear, although organic matter mineralisation and / or nitrification seem plausible given the presence of DON and NH_4^+ in these waters. According to Wynn et al. (2007) interacting sedimentary rocks can also provide an additional source of inorganic nitrogen, and so its relative contribution is considered in section 5.5.

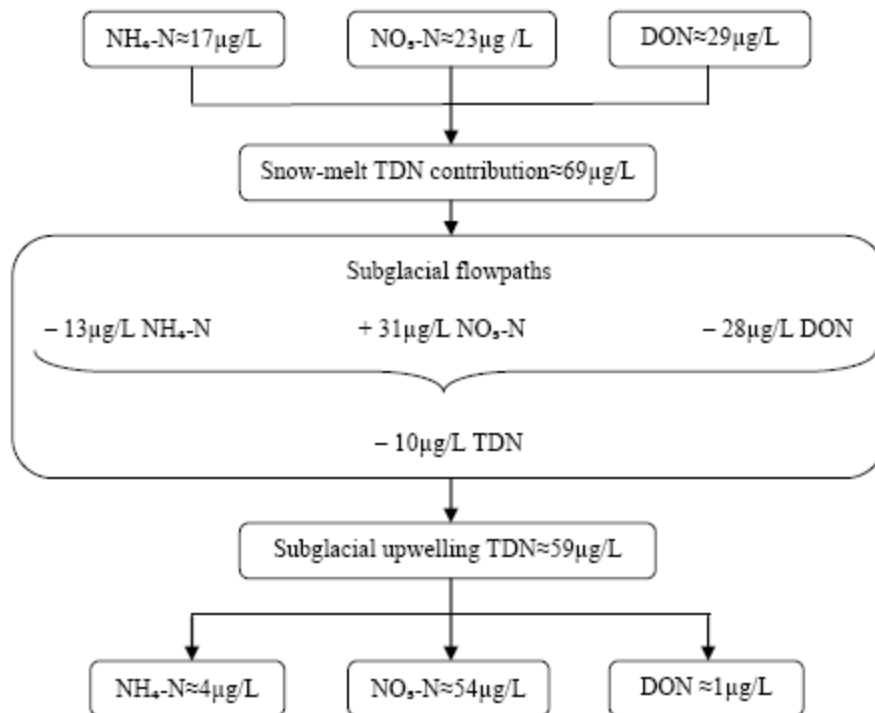


Figure 5.3. Schematic diagram of average discharge weighted total dissolved nitrogen (TDN) concentration in the subglacially routed eastern stream (between DOY 198 and DOY 250).

Williams et al. (1996) and Wynn et al. (2007) failed to find any significant nitrification in snow and therefore Wynn et al. (2007) suggested the subglacial system was a potential place for this process. In a recent study, Boyd et al. (2011) demonstrated significant presence and activity of nitrifiers and other microbes in subglacial sediments of a Canadian temperate glacier. Therefore, to understand and characterise the NO_3^- -N sources more precisely in the present study, average discharge weighted dissolved nitrogen values (DON, NO_3^- , NH_4^+) in snow and resulting subglacial upwelling waters were used as a tracer to identify net inter-species conversion (Figure 5.3). Since upwelling waters are predominantly supplied by snowmelt entering high altitude crevasses (Hodson et al, 2005b; Irvine Fynn et al, 2010), Figure 5.3 shows that the subglacial system was acting as a sink for both DON

and $\text{NH}_4^+\text{-N}$, but as a source of excess $\text{NO}_3^-\text{-N}$ during summer 2009. However, taking all three dissolved nitrogen species into account (TDN), overall, the subglacial system acted as a net sink for nitrogen. Therefore, mineralisation and / or nitrification of DON and $\text{NH}_4^+\text{-N}$ appear to be dominant processes resulting in excess $\text{NO}_3^-\text{-N}$ (57% of $\text{NO}_3^-\text{-N}$ leaving the subglacial system). Previous studies were not able to identify DON as a potential substrate for excess $\text{NO}_3^-\text{-N}$ due to lack of data (Hodson et al. 2005a; Wynn et al., 2007), although Hodson et al. (2005a) inferred the possibility for labile DON in atmospheric deposition and urged for its immediate research attention. Hence, this study reveals DON as an equally important species as $\text{NO}_3^-\text{-N}$ and $\text{NH}_4^+\text{-N}$ in High Arctic nitrogen biogeochemical cycling.

Dual isotope tracers have been widely used by nitrogen biogeochemists to understand and quantify the nitrification in both in-situ and ex-situ conditions (Hollocher and Nicholas, 1981; Anderson and Hooper, 1983; Anisfeld et al., 2007; Tye and Heaton 2007; Wexler et al., 2011). These studies were based on an assumed stoichiometry of NO_3^- formation, whereby one of the three oxygen atoms would be derived from O_2 and the other two atoms from H_2O . Any isotopic fraction or exchange effects are assumed insignificant, allowing simple calculation of the $\delta^{18}\text{O}\text{-NO}_3$ value for nitrification from:

$$\delta^{18}\text{O}\text{-NO}_3_{\text{nitrification}} = 2/3 \delta^{18}\text{O}\text{-H}_2\text{O} + 1/3 \delta^{18}\text{O}\text{-Atm.O}_2 \quad (5.2)$$

Where $\delta^{18}\text{O}\text{-H}_2\text{O}$ (ca. -13‰) was measured and $\delta^{18}\text{O}\text{-Atm.O}_2$ assumed equal to atmospheric O_2 [ca. 24‰ , (Luz and Barkan, 2011)]. However, the general application of Equation 5.2 is now questioned, owing to several experimental studies which have produced microbial NO_3^- with $\delta^{18}\text{O}$ values both lower and higher than would be calculated from Equation 5.2 (Mayer et al., 2001; Spoelstra et al., 2007; Snider et al., 2010; Buchwald and Casciotti, 2010; Casciotti et al., 2010). In addition, recent findings on O isotope exchange between NO_3^- and H_2O (Kool et al., 2011) have widened the knowledge gap and uncertainty associated with the use of $\delta^{18}\text{O}\text{-NO}_3$.

Therefore, any further use of $\delta^{18}\text{O}\text{-NO}_3$ requires more understanding on related isotopic fractionation and exchange in respective environment, which is obviously beyond the scope of this study.

Nitrogen fixing bacteria convert the atmospheric free N_2 ($\delta^{15}\text{N} \sim 0\text{‰}$) to NO_3^- with a $\delta^{15}\text{N}$ fractionation of -3‰ to $+2\text{‰}$ (Peterson and Fry, 1987; Fogel and Cifuentis, 1993). Mineralisation of organic matter generally produces a $\delta^{15}\text{N}$ fractionation of $\pm 1\text{‰}$ and for nitrification it ranges from -38 to -14‰ (Mariotti et al., 1981; Casciotti et al., 2003). However, in a nutrient limited environment, fractionation associated with nitrification has generally been found insignificant (Tye and Heaton, 2007). In addition, using the average snowpack $\delta^{15}\text{N}\text{-NH}_4 \approx -5\text{‰}$ from the previous study in the same region (Wynn, 2004) and marine $\delta^{15}\text{N}\text{-DON} \approx +4\text{‰}$ (Knapp et al., 2005), a likely range of bacterial nitrate $\approx +5\text{‰}$ to -5‰ , has been assumed in this study (Figure 5.4 and 5.6).

Greater NO_3^- -N concentrations in subglacial runoff suggested the presence of additional NO_3^- -N that was most likely derived from NH_4^+ and DON (Figure 5.3). Further, Figure 5.3 also showed that significant proportion of NH_4^+ and DON (reactant) converted to NO_3^- -N (product) consequently due to “reservoir effect” the isotopic composition of product should be very similar to the reactant. The snowpack $\delta^{15}\text{N}\text{-NH}_4$ value in this region varies from -1.7‰ to -2.8‰ and $\delta^{15}\text{N}$ of particulate organic nitrogen ranges between -3‰ and -5‰ (Wynn et al., 2007). Therefore, DON derived from the mineralisation of local particulate organic nitrogen would have the similar $\delta^{15}\text{N}$ signature (-3‰ to -5‰). However, as described earlier in section 5.1.2 snowpack DON were more likely in marine origin, ($\delta^{15}\text{N}\text{-DON} \sim +4\text{‰}$ Knapp et al., 2005) for that reason accumulative $\delta^{15}\text{N}$ composition of snowpack DON should be $< +4\text{‰}$. In this way $\delta^{15}\text{N}$ of NO_3^- -N produced from the above substrate (snowpack derived NH_4^+ and DON) is likely to range between -5‰ and $+4\text{‰}$. Mixing of this additional NO_3^- -N with snowpack derived NO_3^- -N ($\sim -8\text{‰}$) defines the final $\delta^{15}\text{N}\text{-NO}_3$ composition ranging between -8‰ and $+4\text{‰}$. Increase in the fraction of additional NO_3^- -N as a result increase accumulative $\delta^{15}\text{N}\text{-NO}_3$ often observed in

subglacial upwelling water (Figure 5.4). Furthermore, as demonstrated in the dissolution experiment (see Section 4.6.2) inorganic nitrogen contribution from the rock weathering can also be considered forming a proportion of additional NO_3^- -N, however, its quantitative significance remains unclear. Complete understanding of source apportionment and nitrification role, needs further characterisation of $\delta^{15}\text{N}$ -DON and established isotopic fractionation data.

An alternative mechanism, nitrogen fixation has recently been detected upon Midtre Lovénbreen (Telling et al., 2011), yet it mostly takes place in association with photosynthesis because of its high energy demand (Lindstorm et al., 1952; Carpenter et al., 1978; Joye & Paerl, 1994). This is unlikely to operate in the subglacial environment and so nitrification of other substrates seems most likely. Further, Telling et al., (2011) found that N_2 fixation occurred on the glacier surface (not in the snowpack) and was not significant when snow-derived NH_4 -N was present. In addition 14% loss of TDN in the subglacial flowpath also indicated its assimilation or conversion to particulate form with no or very small isotopic fractionation.

Wynn et al., (2006) study at Midtre Lovénbreen reported positive $\delta^{15}\text{N}$ - NO_3 associated with insignificant NO_3^- -N concentration and dissolved oxygen levels in early subglacial runoff and suggested denitrification occurred within the subglacial system. According to them this early subglacial runoff is generally dominated by old melt water stored from the last summer season and because the system stays closed during winter and spring, microbial O_2 consumption often leads to anoxia providing the platform for microbial denitrification. Since evidence for partial denitrification in UPW waters was lacking in 2009 (Figure 5.4), we contend that there are poorly understood temporal changes in the discharge of subglacial water from low redox environments. This is because evidence for subglacial denitrification was discernable during 1997, when nitrate “disappeared” from subglacial runoff (Hodson et al. 2005a); during 1999, when a nitrogen enriched, early summer polluted rainfall was stored at the glacier bed for ten days (Roberts et al. 2010), and during 2002 and 2003, when Wynn et al. (2006, 2007) captured the very first fractions of UPW emerging from the

glacier bed. Thus, it can be assumed that the intensity of denitrification signal in subglacial runoff is variable and perhaps determined by the amount of subglacial water stored over winter and its mixing with summer snowmelt before subglacial outburst in early summer. These were both subject to change due to apparent “carry-over” in the annual water budget according to Hodson et al., (2005b). The apparent lack of denitrification evidence during 2009 might therefore indicate low over-winter storage levels and significant replenishment by aerated snowmelt just prior to the subglacial outflow at UPW on DOY 196.

5.3.1.2 Proglacial nitrogen biogeochemical cycling

The MLE1 and MLW1 samples containing NO_3^- -N concentration lower than snow had significantly higher $\delta^{15}\text{N-NO}_3$ than both snow and UPW. In addition, enrichment of 0.2‰, 18‰, 17‰ in $\delta^{15}\text{N-NO}_3$ between UPW samples and their respective downstream MLE1 samples [DOY 239, 245, 250 respectively (Figure 5.4)] further reflected the existence of biological recycling in the streams. Although stream NO_3^- -N concentrations also decreased between UPW and MLE1, the NO_3^- -N/ Cl^- ratio during this course of downstream flow remained unaltered (Figure 4.8) and suggested no net loss of NO_3^- -N. This could have been caused by dilution through mixing of glacial marginal ice melt stream (MLE3) which had been often reported in previous hydrological studies on the same catchment (Hodson et al. 2005; Irvine-Fynn et al. 2005). In such a case, the $\delta^{15}\text{N-NO}_3$ can only be increased by replacement of lighter $\delta^{15}\text{N-NO}_3$ with heavier $\delta^{15}\text{N-NO}_3$. Therefore, replacement of UPW NO_3^- -N by in-stream proglacial source of NO_3^- -N can be justified. Considering the above observation two coexisting processes might have increased $\delta^{15}\text{N-NO}_3$ downstream. 1) Uptake or loss of NO_3^- -N (i.e. denitrification), and 2) addition of NO_3^- -N consistent with nitrification and / or mineralisation, and therefore not unlike that seen in UPW waters. Therefore, like the subglacial system, Midtre Lovénbreen’s proglacial zone is also dominated by phyllite and tills, which could have provided the heavier $\delta^{15}\text{N-NO}_3$ (see Section 5.5). In addition, DON recycling could represent another source, and both

types of NO_3^- -N can undergo denitrification. Parts of the glacier fore-field such as the stream's hyporheic zone provide the most obvious potential for reducing environments to support denitrification and nitrification (Hedin et al. 1998; Mcknight et al. 2004; Gooseff et al. 2004; 2010).

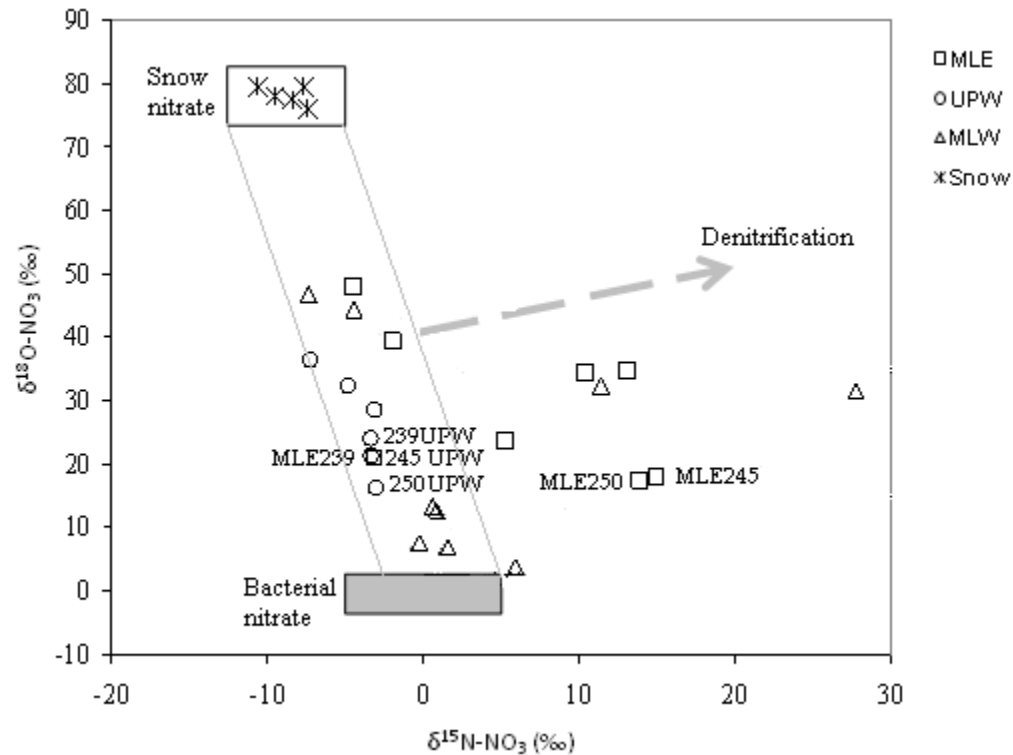


Figure 5.4. $\delta^{15}\text{N-NO}_3$ versus $\delta^{18}\text{O-NO}_3$ variation at the three stream sites and in the snowpacks. The shaded rectangle (“Bacterial nitrate”) depicts the predicted composition of microbially produced NO_3^- , while the grey arrow shows a hypothetical denitrification vector.

For example, the microbially-produced end-member signatures were defined as lying within the ranges of $\delta^{15}\text{N-NO}_3\text{-microbial}$ and $\delta^{18}\text{O-NO}_3\text{-microbial}$ those were established above and can be seen on Figure 5.4. Figure 5.4 also shows a broad “mixing zone” that joins the extremes of the snowpack and microbial $\delta^{15}\text{N-NO}_3$ and $\delta^{18}\text{O-NO}_3$ values. It is notable that during 2009, it was only the MLE1 and MLW1 samples whose nitrate isotope compositions lie outside the snowpack-microbial

mixing zone that were diagnostic of denitrification. Figure 5.4 shows that these samples were characterised by quite high, and in one case very high, $\delta^{15}\text{N}$ values (up to +28 ‰). This increase is a typical symptom of partial denitrification, which is commonly found to result in an increase in the $\delta^{15}\text{N}$ and $\delta^{18}\text{O}$ values of the residual nitrate by a factor of 2 to 1 respectively (Kendall et al. 2007). The implication therefore, is that like the glacier bed, ice marginal environments are also characterised by poorly understood variations in the relative importance of both nitrification and denitrification through time.

5.3.2 Year 2010

Unlike summer 2009, all the stream's $\delta^{15}\text{N-NO}_3$ values remained below 0‰ during 2010 except for one significant positive value (+6‰) at UPW on DOY 186. Therefore, in general the whole summer 2010 sampling period was similar to Phase I in 2009, when NO_3^- was closest to the snow signature. However, relatively small enrichment in ^{15}N and ^{16}O of NO_3^- relative to snowpack values still represented a biological contribution. This difference between the two year's catchment responses to the nitrogen cycling was probably due to the significant difference in climatic regime, since average summer 2009 was 0.5°C warmer (Figure 4.1 and 5.5). Consequently, it is logical to assume that biological activity during summer 2010 might be significantly diminished by relatively colder conditions. Similarly, recycling of other nutrient substrate (DOC, DON etc.) might have been lower in the proglacial active layer. For example, according to Mack et al. (2004) nitrogen mineralization can increase significantly as a result of small warming in un-manipulated tundra. Furthermore, microbial respiration is positively correlated with temperature (Mikan et al., 2002; Bardgette et al., 2007). Besides that, during the summer 2009, stream chemistry was investigated until DOY 250, while during 2010 it was done only up to DOY 227, making it possible that Phase II type were missed during summer 2010.

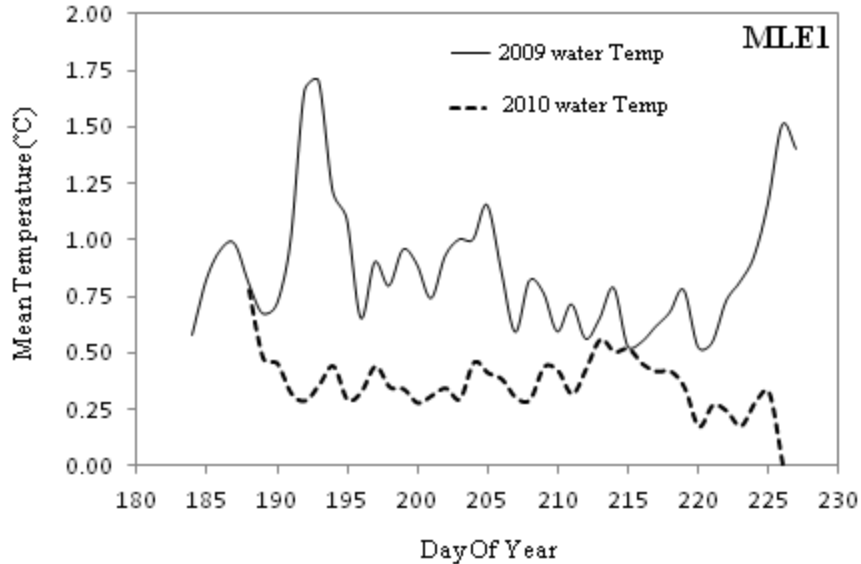


Figure 5.5. Daily mean temperature variation of eastern stream water during summer 2009 and 2010.

Mixing between the two NO_3^- -N sources: 1) **snow** and 2) **bacterial** was more obvious during 2010, as can be seen in Figure 5.6. Most of the $\delta^{15}\text{N-NO}_3$ and $\delta^{18}\text{O-NO}_3$ values therefore fall close to the line joining these end members. Therefore, it is apparent that during this period O exchange between NO_3^- and H_2O was insignificant. However, the positive $\delta^{15}\text{N-NO}_3$ observed in the initial subglacial runoff re-established the presence of denitrification activity in the subglacial system (see Section 5.3.1.1).

The enrichment in ^{15}N and ^{16}O of NO_3^- clearly shows that the relative fraction of biological NO_3^- -N in two streams increases from early to late summer. Given the temporal behaviour of DON and NO_3^- -N in the streams, melt water released from the glacier to the proglacial catchment can be divided into two groups: 1) ice marginal water directly released into proglacial catchment (MLE3 and MLW3), and 2) subglacial runoff at UPW and mixing upstream of MLE2 (Figure 3.6). In the first cases at MLE3 and MLW3, there was a similar temporal variation in DON and NO_3^- -N suggesting minimal NO_3^- production from DON. In the case of subglacial runoff an

inverse relation between DON and NO_3^- -N indicates that mineralisation and / or nitrification was most likely. Therefore, during summer, as NH_4^+ -N concentration became low due to assimilation (all surface and subsurface flowpaths) and also nitrification (subsurface flowpaths in talus, moraine and subglacial till) (Hodson et al., 2005a, 2008; Wynn et al., 2006, 2007; Robersts et al, 2010; Boyd et al., 2011), subglacial biota used DON and perhaps NH_4^+ -N as substrates for nitrification, which is the major nitrogen based bacterial process (see Section 5.3.1.1). Direct uptake of smaller organic nitrogen molecule (e.g. amino acids) by mycorrhizal plants in nitrogen poor tundra environments has already been reported (Schimel and Bennet, 2004 and references therein). However, this phenomenon hitherto is unknown for subglacial microbes.

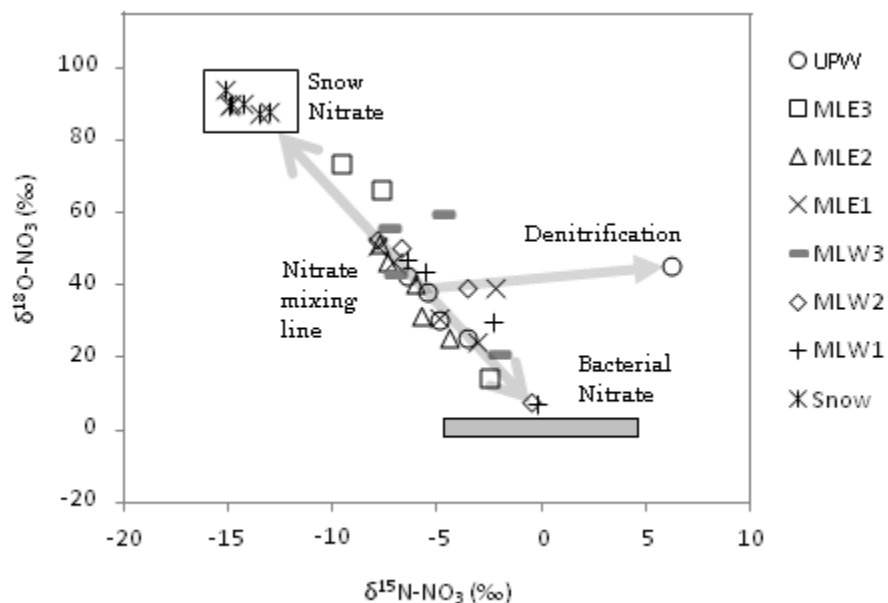


Figure 5.6. $\delta^{15}\text{N}$ versus $\delta^{18}\text{O}$ of snow and and stream NO_3^- during 2010. The grey line between snow and bacterial n member show the possible mixing of two NO_3^- sources, whilst the other grey line represents the possible denitrification of mixed NO_3^- in subglacial system.

5.3.2.1 Downstream nitrogen changes

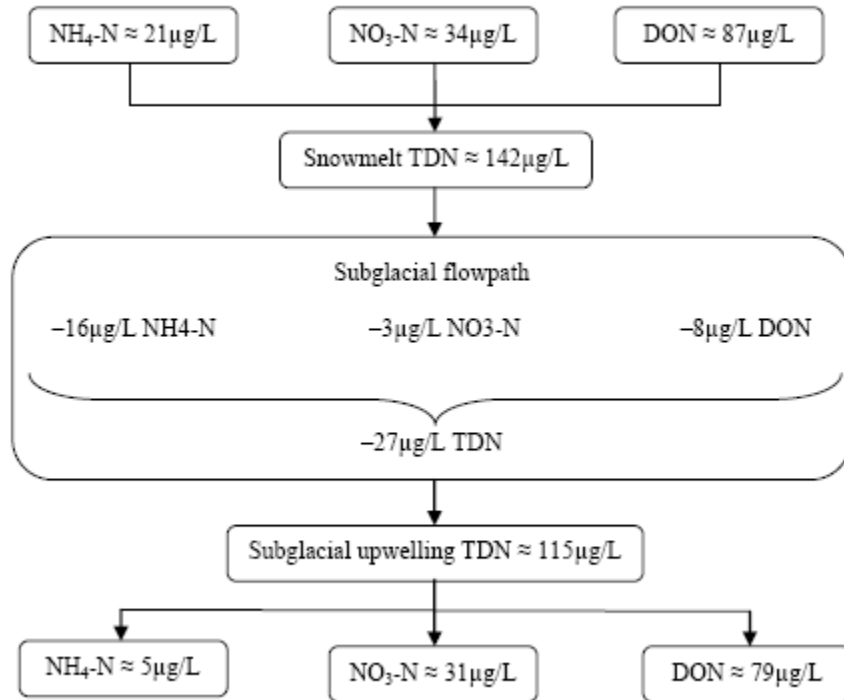


Figure 5.7. Schematic diagram of average discharge weighted total dissolved nitrogen (TDN) concentration in the subglacially routed eastern stream (between DOY 186 to DOY 227, 2010).

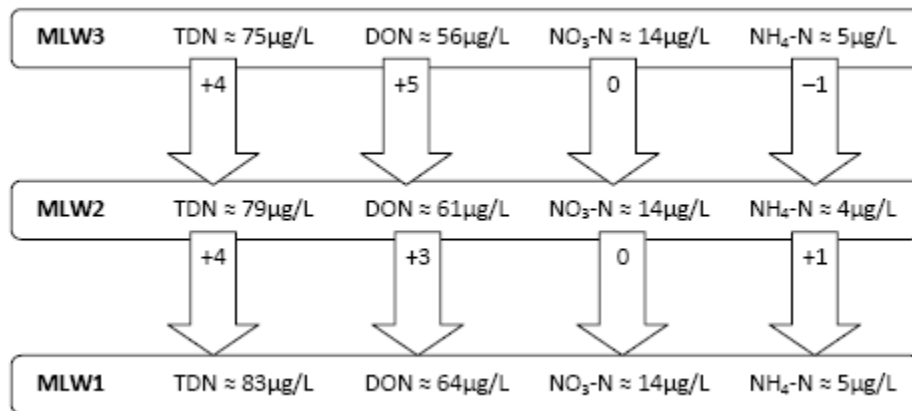


Figure 5.8. Schematic diagram of average discharge weighted total dissolved nitrogen (TDN) concentration in the western stream (between DOY 186 to DOY 227, 2010).

Spatial behaviour of nitrogen via different flowpaths was inconsistent during 2010. However, post DOY 198, a positive enrichment up to +3.2‰ in $\delta^{15}\text{N-NO}_3$ (Figure 4.24 and 4.25) at the downstream sites (MLE2 to MLE1 and MLW3 to MLW1) suggests that nitrogen recycling occurred. However, the $\text{NO}_3^- \text{-N/Cl}^-$ ratios remained largely unaltered which suggested both removal and production of $\text{NO}_3^- \text{-N}$ were balanced (see Section 5.3.1.2). Unlike summer 2009, no clear signature of proglacial stream denitrification surfaced this time. Further, whilst a clear subglacial loss of DON and $\text{NH}_4^+ \text{-N}$ occurred that was similar to 2009, no significant $\text{NO}_3^- \text{-N}$ production appeared this time. An overall loss of TDN can be seen on comparing the snow data with the subglacial runoff (Figure 5.7). Also unlike the stream at UPW, the proglacial streams produced significant amount of DON.

It is well evident that permafrost depth in Arctic is directly controlled by temperature, where increase in atmospheric temperature results into deepening of active layer depth (Hinkel and Nelson, 2003; Demchenko et al., 2006). Consequently, Arctic river biogeochemistry also changes with the changing permafrost depth (Frey and McClelland et al., 2009). For example, some studies suggest that increase in active layer depth leads to greater interaction of stream water with the hyporheic zone and subsequent retention of DON decreases its export (Frey and McClelland et al., 2009 and references therein; Townsend-Small et al., 2011). Therefore, it is logical to assume that even a small lowering of summer 2010 average air temperature (0.5°C) might have reduced dissolved organic matter removal comparative to summer 2009. Similarly, inorganic dissolved nitrogen might have gone through less downstream processing providing more conservative appearance of $\text{NO}_3^- \text{-N}$ and their isotopic signature in the catchment during summer 2010 (Figure 5.7 and 5.8).

In this way permafrost degradation is an effective biogeochemical driver in the Arctic rivers but, this as well as other biogeochemical drivers (i.e. living biomass, soil texture and content etc.) can vary on spatial scale (Frey and McClelland, 2009) and cause a non uniform changes in stream biogeochemistry. Spatial behaviour of the two streams DOC/DON ratio and DON (Figure 4.14 and 4.15) during summer 2010

therefore reveals the non-uniform set up of biogeochemical drivers in the Midtre Lovénbreen catchment.

5.3.3 Nitrogen release from rock weathering

Inorganic nitrogen release (Figure 4.27) observed from the rock powder dissolution experiment demonstrates that the conglomerate contains a significant and high amount of labile inorganic nitrogen, relative to phyllite and gneiss. However, total rock nitrogen in the phyllite was greater than conglomerate (Table 3.5). Gneiss formed via relatively high grade of metamorphism does not seem to contain considerable labile inorganic NH_4^+ -N, but NO_3^- -N. The labile inorganic nitrogen is potentially of great significance for the supply of labile nitrogen to biota that exists in the Midtre Lovénbreen catchment. During a study in the same area, Borin et al. (2010) found a significant microbial population with a gradient of biodiversity in a close vicinity of conglomerate rock clasts, and suggested that the leachates coming through the rock supplied nutrient for the biocoenosis. Furthermore, the three experimental rocks also adsorb NH_4^+ -N (Figure 4.28) which demonstrates that despite producing labile nitrogen these rocks could also be a sink for inorganic nitrogen ions. For example, during the early melt season, rocks and sediment may act as a source of inorganic nitrogen and as soon as NH_4^+ -N in rocks is depleted relative to surrounding solution via runoff, they start to act as a sink for any NH_4^+ -N that is not assimilated by microorganisms.

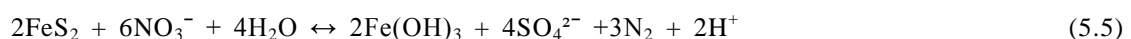
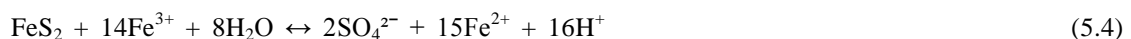
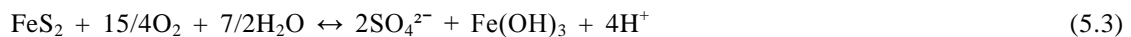
Table 5.1 Annual dissolved inorganic nitrogen yield (DIN; in Kg Km⁻² yr⁻¹) from suspended sediment (particle size < 125 µm) in midtre lovenbreen [calculated by multiplying rock dissolution data to annual suspended sediment yield; 2100 Kg Km⁻² yr⁻¹(from Hodson et al, 2004)]

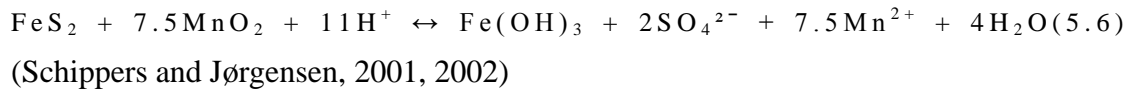
Rock Sample	NH ₄ ⁺ -N	NO ₃ ⁻ -N	DIN
Phyllite	0.714±0.126	0.819±0.021	1.533±0.128
Gneiss	b.d	0.903±0.239	0.903±0.063
Conglomerate	6.426±0.231	1.680±0.063	8.106±0.239

Thus suspended sediment derived DIN yield in Midtre Lovenbreen ranged between 0.903±0.063 and 8.106±0.239 Kg Km⁻² yr⁻¹ (Table 5.1) and therefore represented ~1.3% to 11% of atmospheric NO_x deposition (see Section 2.3). However, more accurate rock nitrogen release quantification needs better geological information which is not available yet for the study area. This nitrogen release from the rocks therefore could be one of the sources responsible for elevated NO₃⁻-N with positive isotopic signature often seen in subglacial system and proglacial streams. Ground water (pore water) is the place where concentrated rock derived nitrogen could be stored in large fraction and therefore any ground water-surface water exchange could lead the amendment in isotopic signature of surface water (stream) NO₃⁻-N as observed in this study (see Section 5.3).

5.4 Stream sulphur dynamics

The majority of the Midtre Lovénbreen glacier rocks (meta-sedimentary) contain high amount of sulphur therefore weathering of these rocks have potential to produce high amount of SO₄²⁻ via two well known pathways: 1) **biological** weathering, 2) **abiological** weathering.





5.4.1 Source and production pathways of sulphate

Snow-derived SO_4^{2-} (atmospheric) in the proglacial streams formed less than 90% of total SO_4^{2-} load and therefore similar to most other terrestrial system rock weathering supplied largest fraction of SO_4^{2-} load in the proglacial streams. The $\delta^{34}\text{S}$ - SO_4 values (+8‰ to +19‰) at the stream sites and their proximity to the catchment rock $\delta^{34}\text{S}$ (reduced sulphur) values (+8‰ to +18‰) indicated little or insignificant isotopic fractionation during sulphide oxidation. According to Toran and Harris (1989), mineral sulphide oxidation potentially produces no isotopic fractionation while oxidation of homogeneously dissolved sulphide is more likely to produce isotopic fractionation. Such processes can take place both in open and closed environment. However, sulphide dissolution before oxidation is unlikely to take place in open (aerobic) but closed (anaerobic) environment. Therefore, sulphide oxidation in closed (anaerobic) environment is likely to produce higher isotopic fractionation than open environment. In closed environment “reservoir effect” can also be observed, in which conversion of larger fraction of reactant to products leads to the isotopic signature of products increasingly closer to reactants. Thus, degree isotopic fractionation in closed environment can vary depending upon the product / reactant ratio. In Midtre Lovenbreen area closed environment potentially operate in subglacial and hyporheic zone.

Most of the $\delta^{18}\text{O}$ - SO_4 values in the subglacial system and proglacial streams were below -4.5‰ . This means that during the formation of these SO_4^{2-} molecules, out of the 4 oxygens present, less than one oxygen atoms was acquired from atmosphere (ca. $+24\text{‰}$) and more than three oxygen atom came from H_2O molecules (ca. -12‰). Such $\delta^{18}\text{O}$ - SO_4 signature in previous studies was commonly described as indicator of anoxic environment (Holt et al., 1981; Holt and Kumar 1991; Bottrell and

Tranter, 2002). However, based upon theoretical studies Luther (1987) suggested that oxidation of pyrite by Fe^{3+} is more energy efficient pathway than oxidation of paramagnetic FeS_2 by diamagnetic O_2 . Therefore, atmospheric O incorporation most likely takes place only during SO_3^{2-} oxidation (Balci et al. 2007) nevertheless, SO_3^{2-} - H_2O oxygen exchange can further decrease the percentage of atmospheric oxygen in the final SO_4^{2-} (Kohl and Bao, 2011). In addition, they also showed that SO_4^{2-} produced in aerobic conditions could also have all its 4 oxygen from H_2O molecule. Therefore, it is now suggested that due to similarity of $\delta^{18}\text{O}\text{-SO}_4$, produced in aerobic and anaerobic conditions, it can not be used to identify oxygen availability during sulphide oxidation (Balci et al., 2007; Kohl and Bao, 2011). This means that the redox conditions of subglacial weathering environments might not be as straight forward and easy to deduce from $\delta^{18}\text{O}\text{-SO}_4$ than initially proposed in the pioneering work of Bottrell and Tranter (2002). Similar oxygen sources and isotopic effects associated with the abiotic and biotic sulphide oxidation (-5% to $+2\%$; Fry et al., 1986) pathway render the isotope approach incapable of differentiating between them.

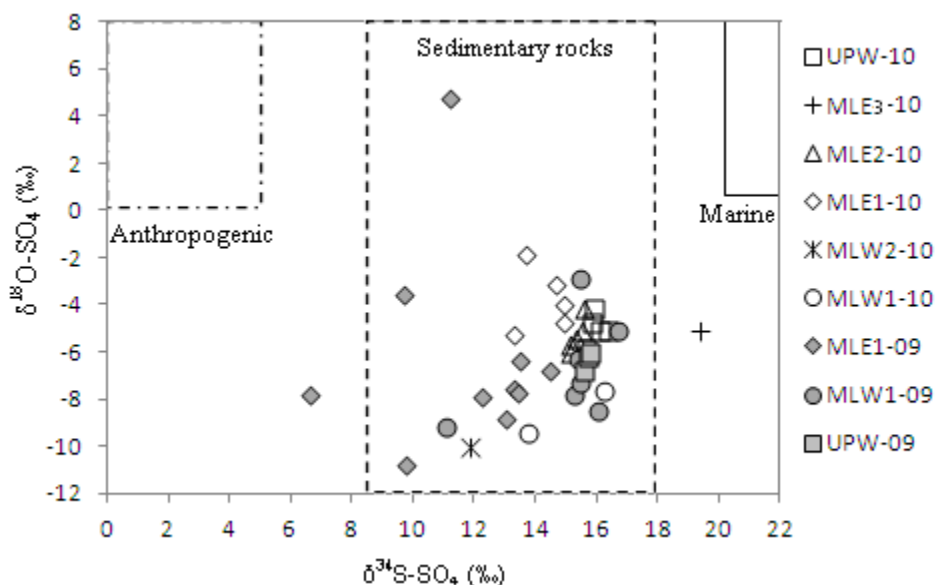


Figure 5.9. $\delta^{18}\text{O}\text{-SO}_4$ Vs $\delta^{34}\text{S}\text{-SO}_4$ plot for the stream sites during summer 2009 and 2010.

According to Schippers and Jørgensen (2002) abiotic oxidation of pyrite minerals by NO_3^- and Fe^{3+} may only take place in acidic conditions due to thermodynamic reasons, while Mn^{4+} can oxidise sulphide even at neutral or alkaline conditions (Böttcher and Thamdrup, 2001). During sulphide oxidation Mn^{4+} becomes reduced to Mn^{2+} which is a highly mobile species (Calvert and Petersen, 1996) and its recycling under anoxic conditions is very unlikely in the absence of Mn^{2+} oxidising bacteria. Since Fe^{2+} can be readily immobilised itself by reacting with sulphide in anoxic environments, Singer and Stumm (1970) hypothesised that biological oxidation of Fe^{2+} to Fe^{3+} in alkaline conditions could be the main process that can lead to high sulphide oxidation rate in anaerobic condition. However, in aerobic conditions, both metal oxidants have equal ability to catalyse sulphide oxidation. The isotopic effects associated with sulphide oxidation by Mn^{4+} are generally lower than the sulphide oxidation by Fe^{3+} (Böttcher and Thamdrup, 2001). Thus, the relative abundance and recycling of two metal oxidisers (Mn^{4+} , Fe^{3+}) play a significant role in defining the final signature of $\delta^{34}\text{S}\text{-SO}_4$. Moreover, SO_4^{2-} production in subglacial system and proglacial streams may predominantly proceed via the equations 5.4-5.6.

Laboratory culture experiments during a previous study had already demonstrated that abiological sulphide oxidation happens at a significantly slower rate than biological sulphide oxidation (Chen and Morris, 1972). Therefore, biological sulphide oxidation seems to be the last and best resort to explain the excess SO_4^{2-} generally observed in streams. The rate of the sulphide oxidation also depends upon pH of ambient environment and it has been found that biological oxidation of sulphide reaches to its maximum value around $\text{pH} \sim 7.5$, and decrease either on increase or decreases in pH (Krishanakumar and Manilal, 1999). However, the effect of pH on abiological sulphide oxidation is complex and shows two different optimum pH condition ($\text{pH} = 8$ and 11) for sulphide oxidation (Chen and Mossris, 1972).

The Figure 5.10 shows that $\text{Ca}^{2+} + \text{Mg}^{2+}$ and SO_4^{2-} release in the two proglacial streams were closely associated with each other and demonstrated that calcite weathering was enhanced by sulphide oxidation.

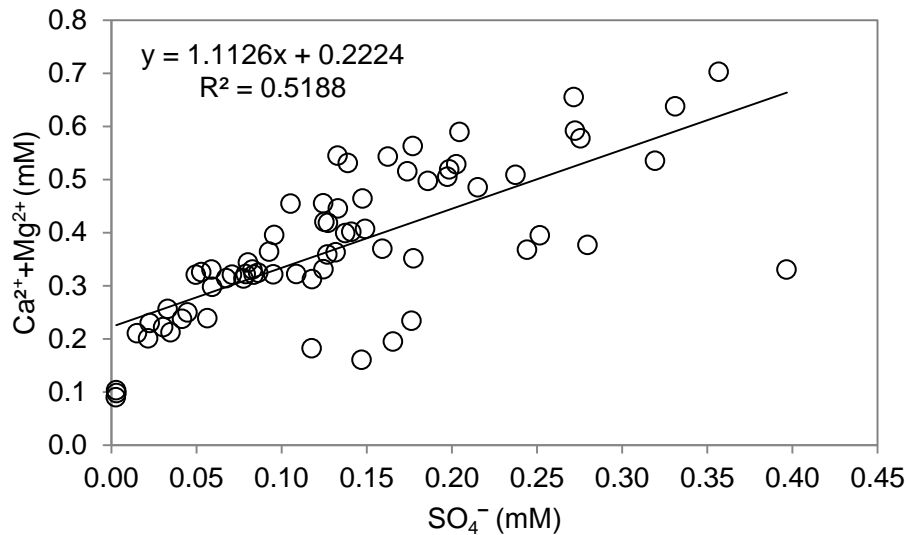
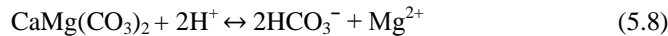
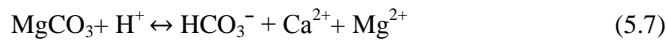
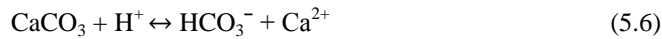


Figure 5.10. Relationship between $\text{Ca}^{2+} + \text{Mg}^{2+}$ and SO_4^{2-} of the Midtre Lovénbreen proglacial streams.

This coupling is performed by the H^+ ion production during sulphide oxidation and its consumption in CaCO_3 , $\text{CaMg}(\text{CO}_3)_2$, MgCO_3 weathering (Equation 5.6, 5.7 and 5.8). In these weathering processes one unit of H^+ produces one unit of Ca^{2+} or Mg^{2+} . Therefore, an indirect quantification of H^+ can be done from the available Ca^{2+} data and further assuming sulphide oxidation a predominant source of H^+ , the most likely sulphide oxidation pathway can be identified. As discussed in Section 5.4.1, there are three known sulphide oxidation pathways (Equation 5.3-5.5) which produce H^+ and in this study $\text{Ca}^{2+} + \text{Mg}^{2+} / \text{SO}_4^{2-}$ molar ratio ~ 1.1 (mostly >1.1 ; Figure 5.10) indicated each unit of SO_4^{2-} production was accompanied with one unit of H^+ . Out of the four sulphide oxidation pathways (Equation 5.3-5.5) Equation 5.3 and 5.5 produce the nearest $\text{H}^+ : \text{SO}_4^{2-}$ ratio (2 and 0.5 respectively) inferring them as predominant SO_4^{2-}

production pathway in the Midtre Lovenbreen. This indicates that coupled denitrification-sulphide oxidation were more likely in anaerobic condition.

The temporal decrease in the molar $\text{Ca}^{2+}/\text{SO}_4^{2-}$ ratios from early to late summer (Figure 4.9) indicates that alternative calcite weathering processes also took place (Equation 5.7). In addition, re-dissolution of evaporite salts deposited from last summer and winter (by evaporation and freeze concentration of ground water) would have mostly occurred during early snowmelt in the glacier fore-field (Cooper et al., 2002).



This well known coupling was more significant in proglacial streams than subglacial upwelling. Therefore, it can be assumed that in open system calcite weathering is more responsive and tightly associated with sulphide oxidation. Perhaps more efficient evaporite formation and their re-dissolution also play a key role to bring up tighter sulphide oxidation-calcite weathering coupling in proglacial zone than subglacial upwelling.

5.4.2 Spatio-temporal stream sulphate dynamics

An early decrease and later increase of SO_4^{2-} to higher concentrations in subglacial runoff was consistent during both the summer sampling years (Figure 4.9f and 4.18). Like with NO_3^- (Section 5.3.1) indicated that SO_4^{2-} elution in early snow melt led to a gradual decrease later on, before sulphide oxidation began to dominate. Early decrease in SO_4^{2-} at UPW was a result of dilution caused by increase in discharge (Figure 4.9c and 4.2). Furthermore, during summer 2009, unlike UPW, contemporary SO_4^{2-} at the proglacial site (MLE1 and MLW1) did not show the initial decrease in concentration (Figure 4.9), whereas during summer 2010 temporal

variation of SO_4^{2-} at the proglacial stream sites were similar to UPW (Figure 4.18). This further suggests that biological or in-stream moderation of stream solute chemistry was less during 2010 compared with 2009.

Low SO_4^{2-} concentration with lighter $\delta^{34}\text{S}\text{-SO}_4$ (below +13‰) during early summer 2009 (pre-DOY 196; Figure 10) therefore revealed that during this period proglacial field was dominated SO_4^{2-} produced in anaerobic condition (see Section 5.4.1; Balci et al 2007). Afterwards following the subglacial outburst, the increase in $\delta^{34}\text{S}\text{-SO}_4$ at MLE1 suggested increase in open or aerobic condition in the glacier forefield and subglacial zone. Further, a decrease in SO_4^{2-} concentration and $\delta^{34}\text{S}\text{-SO}_4$ following water travel from the UPW to MLE1 also suggests increase in the proportion of SO_4^{2-} produced in oxygen minimum condition. Absence of any significantly higher $\delta^{34}\text{S}\text{-SO}_4$ values ($> \text{rock-}\delta^{34}\text{S} = +18\text{‰}$) in the subglacial and proglacial streams preclude the possibility of SO_4^{2-} reduction process in these zones.

The 2010 summer study demonstrated the in-stream production of SO_4^{2-} . Unlike 2009, stream $\delta^{34}\text{S}\text{-SO}_4$ remained above +13‰ from the early summer melt indicating prevalent oxygen saturated condition in the proglacial field and subglacial zone, from the start of the stream sampling during 2010. Therefore, no distinct anaerobic condition was apparent from the stream's $\delta^{34}\text{S}\text{-SO}_4$ variations this time. It has generally been found that in sediments or hyporheic zone systems, denitrification processes are typically linked with sulphide oxidation (Sweerts et al., 1990; Krishnakumar and Manila, 1999; Cardoso et al., 2006) because NO_3^- acts as an electron acceptor. Under high sulphide conditions some bacteria reduce NO_3^- to NH_4^+ outside their cytoplasm which is known as dissimilatory nitrate reduction (Keith and Herbert, 1983; Brunet and Garcia-Gil, 1996). Therefore, as we know the Midtre Lovénbreen catchment rocks contains high amount of sulphide, this kind of linked sulphide oxidation – nitrogen removal process are plausible in anoxic hyporheic zone sediments in the catchment (see Section 5.4.1).

5.5 Summary

The major findings of discussion are:

- Mode of depositions was unlikely mechanism to controls the $\delta^{15}\text{N-NO}_3$ signature of bulk snowpack whilst supply of ^{14}N enriched NO_3^- from stratosphere appears most likely source of highly negative $\delta^{15}\text{N-NO}_3$.
- In the Midtre Lovénbreen snow depositions DON comprised the largest fraction of TDN and was largely composed of light nitrogen containing organic compounds from marine biogenic origin.
- The major sources of SO_4^- in Midtre Lovénbreen snow depositions were marine salt transported by breeze and anthropogenic production at lower latitude in Europe. However, the relative proportion of the two sourcing was significantly variable on annual scale.
- The proportion of microbially produced nitrate increased from the early to late melting period. At the same time increase in other microbial activities such as sulphide oxidation, demonstrated an increase in overall microbial activity in the Midtre Lovénbreen catchment. However, depending upon climatic conditions these microbial activities were significantly variable on time scale.
- Subglacial system hosts nitrification as major microbial activity adding nitrate in subglacial upwelling. DON and NH_4^+ were most likely substrate used in this process. However, subglacial system invariably performed as a TDN sink zone.
- In the proglacial streams of Midtre Lovénbreen both nitrogen consumption and production took place simultaneously whilst the variations in stream biogeochemistry on spatial scale demonstrated that biogeochemical driver in the catchment are spatially variable.

- The $\text{NO}_3\text{-H}_2\text{O}$ oxygen exchange in the study area appeared to be insignificant therefore use of isotope equation (equation 5.2) could be applied to deduce the microbial nitrification activity in the Midtre Lovénbreen streams.
- The rocks from Midtre Lovénbreen catchment also released significant N on dissolution. Therefore, in addition to snow derived DON and NH_4^+ , rock was also identified as to supply excess nitrogen in the subglacial upwelling and proglacial streams.
- Biological and abiological sulphide oxidation both took simultaneously in the subglacial and proglacial zone. Although, separating the biotic and abiotic SO_4^{2-} is unattainable by existing techniques. However, generally biotic sulphide oxidation is assumed to be major sulphide oxidation pathway.
- Sulphide oxidation took place via both aerobic and anaerobic pathway in Midtre Lovenbreen subglacial and proglacial streams and coupled denitrification-sulphide oxidation reaction was more likely in aneroobic condition. The sulphide oxidation-calcite weathering coupled reaction was most significant in the proglacial streams than subglacial upwelling demonstrating the possible re-dissolution of evaporite salts in proglacial streams.

CHAPTER 6: CONCLUSION

6.1 Summary comments and conceptual model

6.1.1 Nitrogen biogeochemical cycling

The majority of nitrogen deposited upon the Midtre Lovénbreen watershed came from atmospheric deposition during late winter and early spring. In this study, DON was identified as the major nitrogen reservoir of dissolved nitrogen pool (ca. 42-70%) in the snow, followed by NO_3^- -N (ca. 18-34%) and NH_4^+ -N (ca. 17-24%). However, the composition changed annually. NO_3^- -N and NH_4^+ -N in Arctic atmosphere are largely considered to be sourced from anthropogenic activity at lower latitude while during this study DON was probably of marine origin. Therefore, reveals that under current condition, non-sea-salt marine DON supply largest fraction of total dissolved nitrogen pool in snow. Furthermore, this study also demonstrates that stratosphere is the most likely source of highly negative snow $\delta^{15}\text{N}$ - NO_3 and by affecting the availability of NO_3^- -N in troposphere and stratosphere of Arctic region, climatic circulation (e.g. NAO) plays a cumulative role. After deposition photolysis and availability of salt forming cations determine the release of nitrogen back to atmosphere however their significance remain unclear.

During summer melt, release of both organic and inorganic nitrogen accelerated microbial activity to a significant level in the glacial and proglacial watershed. Moreover, meltwaters stored from previous summer season in subglacial environment had the potential to go through denitrification once dissolved redox conditions were established, which further depends upon the microbial dynamics, hydrological system and availability of nutrients (i.e. NO_3^- , NH_4^+ , organic matter etc.). However, these factors are subject to change, on spatial and temporal scale. For example, appearance of denitrification signature in early subglacial runoff also depends upon the mixing ratio of young meltwaters and old subglacial waters prior to

the opening of subglacial drainage system. Supraglacial meltwaters discharge through subglacial system re-oxygenates the environment that leads to more oxidative processes. For example, NO_3^- -N production in the subglacial system, associated with a stoichiometrically close amount of DON and NH_4^+ -N loss, revealed that mineralisation and / or nitrification were the dominant nitrogen cycling processes operating beneath the glacier. Thus, this study presented DON as a hitherto unknown source for the excess NO_3^- -N generally found in the subglacial water during summer melt. Overall, the combination of these processes meant that the subglacial system acted as sink for total dissolved nitrogen during both the years of study and demonstrated significant presence of biological nitrogen demand. Therefore, lost dissolved nitrogen presumably incorporated into biomass and / or converted to N_2 by denitrification.

Downstream enrichment in $\delta^{15}\text{N}$ - NO_3^- with either constant or increasing NO_3^- -N concentrations, allowed this study to identify addition NO_3^- -N sources and sinks in the proglacial streams and glacier forefield. Here, rapid microbial processing (i.e. assimilation, nitrification and denitrification) were found with similar characteristics to the glacier bed. The most likely additional nitrogen sources in such barren streams can be rock weathering which was evident from the significant release of inorganic nitrogen for experimental leaching of the catchment sedimentary rocks. The sedimentary rocks also have potential to retain fair amount of NH_4^+ from the ambient solution therefore, by determining the area of stream's hyporheic zone, microbial control and oxic / anoxic zone formation; permafrost degradation play important role in the stream biogeochemistry. Permafrost degradation and other biogeochemical drivers are spatially variable in the catchment that cause a non uniform changes in stream biogeochemistry. Overall, the proglacial streams acted as nitrogen source and thus highlighted its implications for the near shore marine ecosystem (in this case Kongsfjord, Svalbard).

Figure 6.1 presents a conceptual model of the biogeochemical cycling of N as revealed by this work and previous research. Atmospheric nitrogen deposition takes

place both by wet and dry deposition and a fraction of deposited nitrogen also return back to atmosphere by photolytic gaseous release. There is not much N processing or recycling occur within the snow however, during the melt season snow-derived organic and inorganic N are transported through various flowpaths over, beneath and within the glaciers to the proglacial streams. While undergoing the abovementioned transport meltwater also experience various N sources and sinks. For example, subglacial system is identified as hotspot of microbial mineralisation / nitrification and assimilation processes, also overall sink for N. Denitrification is also among the identified processes that often takes place in old melt water stored on subglacial system from previous season. Therefore, denitrification signature in subglacial upwelling is determined by the mixing ratio of old and fresh melt water. Proglacial streams also host similar microbial processes however, unlike subglacial system, identified as a net source of N. In Midtre Lovénbreen, sedimentary rocks also demonstrated significant release of nitrogen therefore considered as one of the source of additional nitrogen source often observed in same glacial catchment.

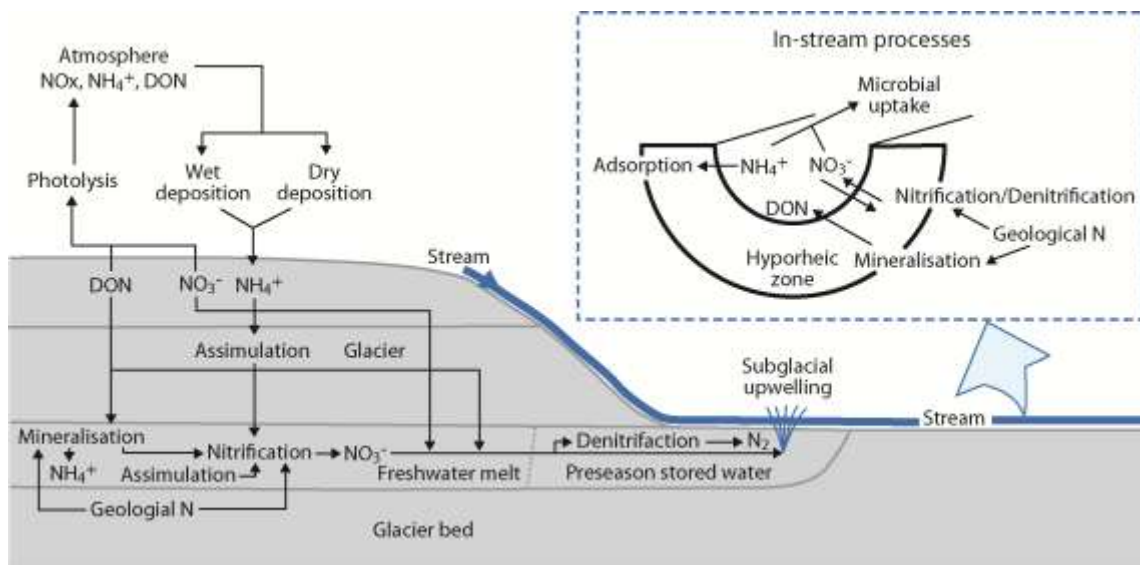


Figure 6.1. Conceptual model of nitrogen biogeochemical cycling in Midtre Lovénbreen

6.1.2 Sulphur biogeochemical cycling

Sulphate is a major ion responsible for snowpack acidity in the Arctic. In Midtre Lovénbreen, snow sea-salt SO_4^{2-} ranges between 43% and 61% of total SO_4^{2-} whilst non-sea-salt SO_4^{2-} ranges between 39% and 57% and appear to be largely anthropogenic during 2009. A more equal mix of anthropogenic and DMS derived SO_4^{2-} was proposed during 2010. Therefore, similar to nitrogen, SO_4^{2-} composition in snow also varied annually. Snow derived SO_4^{2-} made only a small fraction of the subglacial and proglacial streams SO_4^{2-} and large fraction (up to 99%) was supplied by sedimentary rock weathering. Although, existing isotope techniques are unable to distinguish between SO_4^{2-} produced by biological and abiological pathway, circumstantial evidence suggested biological oxidation of sulphide mineral via Fe^{3+} or Mn^{4+} pathway as most promising SO_4^{2-} production mechanism in these streams. Sulphide oxidation also produces H^+ , especially via Fe^{3+} pathway that catalyses the calcite weathering and result into high Ca^{2+} concentration thus bring this process in more important category by highlighting its implication in local / regional natural carbon cycle. This coupling between sulphide oxidation – calcite weathering was more significant in proglacial streams that also demonstrated the more significant re-dissolution of evaporite in the glacier forefield than the subglacial system. Most of the evaporite salts deposited in the proglacial streams pathway from previous season freeze-thaw cycles was washed by early meltwaters. Moreover, it is logical to assume that sulphur based chemoautotrophy prevail in the barren part of glacial catchment that probably support largest fraction primary production.

No observed signature for sulphate reduction in the catchment suggested that either organic matter in the environment rarely exceeded available NO_3^- and Fe^{3+} oxidising capacity or was masked by overwhelming amount of sulphide oxidation.

Figure 6.2 shows a conceptual model of sulphur biogeochemical cycling as revealed by this work and previous research. Similar to nitrogen deposition of

atmospheric deposition of SO_4^{2-} takes place both by wet and dry deposition. However, unlike nitrogen, knowledge about organic sulphur deposition and its significance for the study area is lacking. During melt season significant amount of SO_4^{2-} is produced by biotic and abiotic sulphide oxidation. Most of the deposited evaporite in stream flowpath are redissolved in the early fraction of meltwater. In addition, sulphide oxidation strongly influences the calcite weathering.

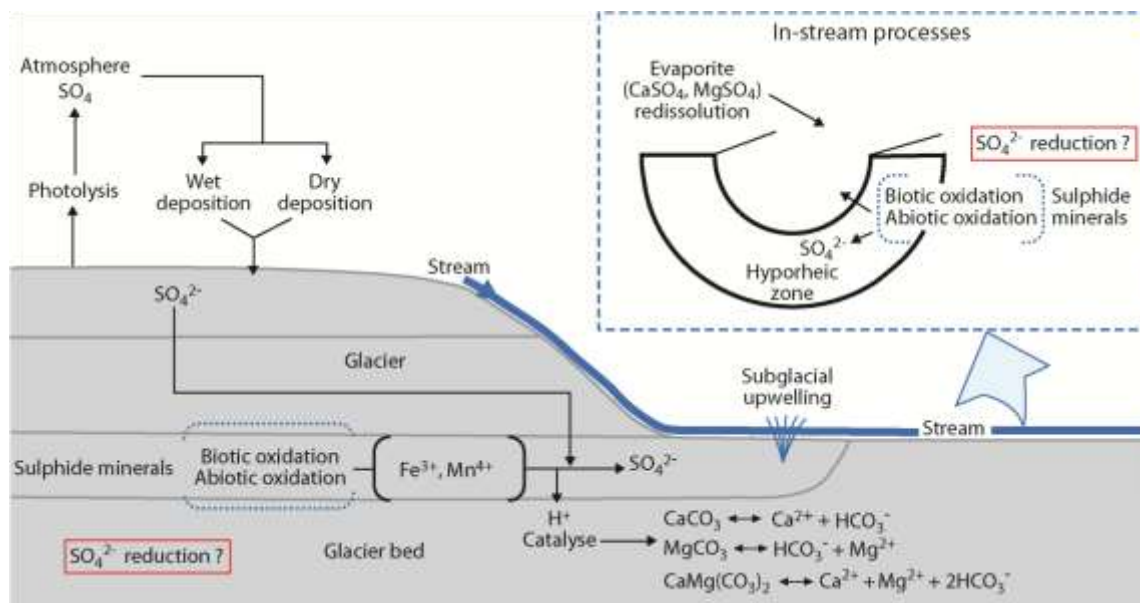


Figure 6.2. Conceptual model of sulphur biogeochemical cycling in Midtre Lovénbreen

6.2 Recommendations for future work

This study was successful in raising some scientific questions that require future studies. The most important questions are given below:

- *Do subglacial microbes use DON as preferential nitrogen substrate at low NH_4^+ concentration?*

This study has demonstrated possible recycling of DON in the glacial ecosystem and highlighted the importance to seek better understanding of DON provenances and isotopic composition in order to address the microbial processes which involve it. DON contains both N and C, therefore, its uptake may not be necessarily intentional for one element, but could instead be a strategy for obtaining both under nutrient deficient conditions. Addressing this question will be instrumental in understanding the mechanism of microbial nitrogen metabolism in subglacial environments.

- *Is rock weathering one of the major sources of nitrogen supply for biological metabolism in nitrogen-poor proglacial and subglacial habitats?*

In this study, release of inorganic nitrogen from rock powders suggested them to be a possible source of additional nitrogen seen in the proglacial streams. However, due to lack of knowledge about nitrogen flux through subglacial and hyporheic zones, the in-situ contribution of rock weathering have most likely been underestimated and ignored. Thus, there is a need to reveal the role of geological nitrogen in nitrogen poor Arctic ecosystems.

- *How to separate aerobic versus anaerobic sulphide oxidation?*

Stable isotope and solute studies have been proved unable to separate aerobic and anaerobic sulphide oxidation therefore remain a challenging job. Understanding the two type of SO_4^{2-} will be helpful to determine the oxic and anoxic zone in study area.

BIBLIOGRAPHY

Abbatt JPD, (1997). Interaction of HNO₃ with water-ice surface at temperatures of free troposphere, *Geophys. Res. Lett.*, 24, pp. 1479-1482#

Adkins AM and Knowles R, (1986). Denitrification, denitrifying bacteria, and iron reduction in a soil supplemented with sulfide and acetylene. *Canadian J. Soil Sci.*, 66, pp. 633-639.

Aleem MIH, (1968). Mechanism of oxidative phosphorylation in chemoautotroph *Nitrobacter agilis*. *Biochimica et Biophysica Acta* 162, pp. 338-347

Allègre C, Manhès G, Lewin É, (2001). Chemical composition of the Earth and the volatility control on planetary genetics. *Earth Planet. Sci. Lett.* 185, pp. 49-69

Altabet MA, Pilskaln C, Thunell R, Pride C, Sigman D, Chavez F, Francois R, (1999). The nitrogen isotope biogeochemistry of sinking particles from the margin of the eastern North Pacific. *Deep-Sea Res. Part I* 464, pp. 655-679

AMAP Assessment, (2006). Acidifying Pollutants, Arctic Haze, and Acidification in the Arctic. Arctic Monitoring and Assessment Programme (AMAP). xx+112 p.

Amato P, Hennebelle R, Magand O, Sancelme M, Delort AM, Barbante C, Boutron C, Ferrari C, (2007). Bacterial characterization of the snow cover at Spitzberg, Svalbard. *FEMS Microbiol Ecol* 59, pp. 255–264

Amato P, and Christner BC, (2009). Energy Metabolism Response to Low-Temperature and Frozen Conditions in *Psychrobacter cryohalolentis*. *Appl Environ Microbiol* 75, pp. 711–718

Amoroso A, et al., (2010). Microorganisms in dry polar snow are involved in the exchanges of reactive nitrogen species with the atmosphere, *Environ. Sci. Technol.*, 44(2), pp. 714–719, doi:10.1021/es9027309

An SM and Gardner WS, (2002). Dissimilatory nitrate reduction to ammonium (DNRA) as a nitrogen link, versus denitrification as a sink in a shallow estuary (Laguna Madre/Baffin Bay Texas). *Mar. Ecol., Prog. Ser.* 237, pp. 41– 50

Anastasio C and McGregor KG, (2000). Photodestruction of dissolved organic nitrogen species in fog waters. *Aerosol Science and Technology* 32, pp. 106–119

Anderson KK, Hooper AB, (1983). O₂ and H₂O are each the source in one O in NO₂⁻ produced from NH₃ by Nitrosomonas; ¹⁵NNMR evidence. *FEBS Lett* 164, pp. 236–240

Andreae MO, (1985). Dimethylsulfide in the water column and the sediment porewaters of the Peru upwelling areas. *Limnol. Oceanogr.* 30, pp. 1208-1218

Andreae MO, (1986). The ocean as a source of atmospheric sulfur compounds, p. 331-362. In P. Buat-Menard [ed.], *The role of air-sea exchange in geochemical cycling* by Reidel

Anesio AM, Hodson AJ, Fritz A, Psenner R, Sattler B, (2009). High microbial activity on glaciers: importance to the global carbon cycle. *Global Change Biol* 15, pp. 955–960

Anesio AM, Sattler B, Foreman C, Telling J, Hodson A, Tranter M, Psenner R, (2010). Carbon fluxes through bacterial communities on glacier surfaces. *Annals of Glaciology*, 51 (56), pp. 32-40

Anisfeld SC, Barnes RT, Altabet MA and Wu T, (2007). Isotopic apportionment of atmospheric and sewage nitrogen sources in two Connecticut rivers. *Environmental Science and Technology*, 41, pp. 6363-6369

Ansari AH, Hodson AJ, Heaton THE, Kaiser J, Marca-Bell A, (2012). Nitrogen Biogeochemical in a High Arctic glacier catchment, *Biogeochemistry*(in press)

Aravena R and Robertson WD, (1998). Use of multiple isotope tracers to evaluate denitrification in ground water: study of nitrate from a large-flux septic system plume. *Ground Water*, 36, pp. 975–982

Azmy K, Veizer J, Misi A, de Oliveira TF, Sanches AL, Dardenne MA, (2001). Dolomitization and isotope stratigraphy of the Vazante Formation, Sao Francisco Basin, Brazil. *Precambrian Research* 112, pp. 303– 329

Balci N, Shanks Iii WC, Mayer B, Mandernack KW, (2007). Oxygen and sulfur isotope systematics of sulfate produced by bacterial and abiotic oxidation of pyrite. *Geochim. Cosmochim. Acta* 71 (15), pp. 3796–3811

Bárcena TG, Yde JC, Finster KW, (2010). Methane flux and high-affinity methanotrophic diversity along the chronosequence of a receding glacier in Greenland. *Annals of Glaciology*, Vol. 51, No. 56, pp. 23-31

Bardgett RD, Richter A, Bol R, Garnett MH, Baumler R, Xu X, Lopez-Capel E, Manning DAC, Hobbs PJ, Hartley IR, Wanek W, (2007). Heterotrophic microbial communities use ancient carbon following glacial retreat. *Biology Letters* 3, pp. 487–490

Barkan E and Luz B, (2005). High-precision measurements of $^{17}\text{O}/^{16}\text{O}$ and $^{18}\text{O}/^{16}\text{O}$ in O_2 in H_2O . *Rapid Commun Mass Spectrom* 19, pp. 3737–3742

Barrie LA, and Hoff RM, (1984). Five years of chemistry observations in the Canadian Arctic. *Atmospheric Environment* 19, pp. 1995-2010

Barrie LA, (1985). Features of the atmospheric cycle of aerosol trace elements and sulfur dioxide revealed by baseline observations in Canada, *J. Atmos. Chem.* 3, pp. 139–152

Barrie LA,(1986). Arctic air pollution: an overview of current knowledge, *Atmospheric Environment* 20, pp. 643–663

Barrie LA, Bottenheim JW, Schnell RC, Crutzen PJ, Rasmussen RA, (1988). Ozone destruction and photochemical reactions at polar sunrise in the lower Arctic atmosphere. *Nature* 334, pp. 138-140

Barrie LA, den Hartog G, Bottenheim, JW, and Landsberger S, (1989). Anthropogenic aerosols and gases in the lower troposphere at Alert Canada in April 1986, *J. Atmos. Chem.* 9, pp. 101-127

Bates TS, Lamb BK, Guenther A, Dignon J, Stoiber RE, (1992). Sulfur emissions to the atmosphere from natural sources, *J. Atmos. Chem.*, 14, pp. 315-337

Beaudon E, and Moore JC, (2009). Frost flower chemical signature in winter snow on Vestfonna ice cap (Nordaustlandet, Svalbard), *The Cryosphere* 3, pp. 147-154

Beine HJ, and Krognæs T, (2001). The seasonal cycle of peroxyacetyl nitrate (PAN) in the European High Arctic Atmospheric Environment. 34, pp. 934–940

Beine HJ, Dominé F, Ianniello A, Nardino M, Allegrini I, Teinilä K, Hillamo R, (2003). Fluxes of Nitrates between Snow Surfaces and the Atmosphere in the European High Arctic, *Atmos. Chem. Phys.*, 3, pp. 335–346

Betts RH and Voss RH, (1970). The kinetics of oxygen exchange between sulfite ion and water. *Can. J. Chem.*, 48, pp. 2035–2041

Bhatia M, Sharp M, Foght J, (2006). Distinct Bacterial communities exist beneath a high Arctic polythermal glacier. *Appl Environ Microbiol* 72, pp. 5838–5845

Bingham RG, Nienow PW, Sharp MJ, (2003). Intra-annual and intra-seasonal flow dynamics of a High Arctic polythermal valley glacier, *Ann. Glaciology*, 37, pp. 181-188

Björnsson H, Gjessing Y, Hamran SE, Hagen JO, Liestøl O, Pálsson F, Erlingsson B, (1996). The thermal regime of sub-polar glaciers mapped by multi-frequency radio-echo sounding. *Journal of Glaciology* 42, pp. 23–32

Böhme H, (1998). Regulation of nitrogen fixation in heterocystforming cyanobacteria. *Trends Plant Sci.* 3, pp. 346–351

Bollinger C, Schroth MH, Bernasconi SM, Kleikemper J, Zeyer J, (2001). Sulfur isotope fractionation during microbial sulfate reduction by toluene-degrading bacteria. *Geochim Cosmochim Acta* 65, pp. 3289–3298

Borin S, Ventura S, Tambone F, Mapelli F, Schubotz F, Brusetti L, Scaglia B, D'Acqui LP, Solheim B, Turicchia S, Marasco R, Hinrichs KU, Baldi F, Adani F, Daffonchio D, (2010). Rock weathering creates oases of life in a high arctic desert. *Environmental Microbiology* 12, pp. 293–303

Böttcher J, Strebel O, Voerkelius S, Schmidt HL (1990). Using stable isotope fractionation of nitrate-nitrogen and nitrate-oxygen for evaluation of microbial denitrification in a sandy aquifer. *Journal of Hydrology*, 114, 413–424

Böttcher ME, Rusch A, Höpner T, Brumsack HJ (1997). Stable sulfur isotope effects related to local intense sulfate reduction in a tidal sandflat (southern North Sea). *Isotopes in Environmental and Health Studies*, 33, pp. 109–129.

Böttcher ME, Thamdrup B (2001). Anaerobic sulfide oxidation and stable isotope fractionation associated with bacterial sulfur disproportionation in the presence of MnO₂. *Geochim Cosmochim Acta* 65:1573–1581

Böttcher ME, Brumsack H-J and Dürselen CD (2007). The isotopic composition of modern seawater sulfate: I. Coastal waters with special regard to the North Sea. *Journal of Marine Systems* 67, 73-82.

Bottenheim JW, Daster A, Gong SL, Higuchi K, Li YF (2004). Long range transport of air pollution to the Arctic, in *Intercontinental Transport of Air Pollution*, edited by A. Stohl, pp. 12– 39, Springer, New York

Bottrell SH and Tranter M, (2002). Sulphide oxidation under partially anoxic conditions at the bed of Haut Glacier d’Arolla, Switzerland. *Hydrological Processes* 16, pp. 2363–2368

Boyd S R and Philippot P, (1998). Precambrian ammonium biogeochemistry: A study of the Moine metasediments, Scotland. *Chem. Geol.* 144, pp. 257–268

Boyd ES, Skidmore M, Mitchell AC, Bakermans C, Peters JW, (2010). Methanogenesis in subglacial sediments. *Environmental Microbiology Reports*, Vol. 2, pp. 685-692

Boyd ES, Lange RK, Mitchell AC, Havig JR, Hamilton TL, Lafrenière MJ, Shock EL, Peters JW, Skidmore M, (2011). Diversity, abundance, and potential activity of nitrifying and nitrate-reducing microbial assemblages in a subglacial ecosystem *Applied and Environmental Microbiology*, 77, pp. 4778–4787

Bremner JM, and Harada T, (1959). Release of ammonium and organic matter from soil by hydrofluoric acid, and effect of hydrofluoric acid treatment on extraction of soil organic matter by neutral and alkaline reagents. *J. Agric. Sci.* 52, pp. 137-146

Brewer AW, (1949). Evidence for a world circulation provided by the measurements of helium and water vapour distribution in the stratosphere, *Q. J. R. Meteorol. Soc.*, 75, pp. 351–363

Bronk DA and Ward BB, (1999). Gross and net nitrogen uptake and DON release in the euphotic zone of Monterey Bay, California. *Limnol Oceanogr* 44, pp. 573–585

Bronk DA and Steinberg DK, (2008). Nitrogen regeneration. In Capone, D. G., Bronk, D. A., Mulholland, M. M. et al. (eds), Nitrogen in the Marine Environment. *Academic Press, London*, pp.385–467

Bruchert V, Knoblauch C and Jørgensen BB, (2001). Controls on stable sulfur isotope fractionation during bacterial sulfate reduction in Arctic sediments. *Geochim. Cosmochim. Acta* 65, pp. 763–776

Brundet RC, and Garcia-Gil LJ, (1996). Sulfide-induced dissimilatory nitrate reduction to ammonia in anaerobic freshwater sediments. *FEMS Microbiol Ecol* 21, pp. 131–138

Buchwald C and Casciotti KL. (2010). Oxygen isotopic fractionation and exchange during bacterial nitrite oxidation, *Limnol. Oceanogr.*, 55(3), pp. 1064–1074, doi:10.4319/lo.2010.55.3.1064

Calhoun JA, Bates TS, Charlson RJ, (1991). Sulfur isotope measurements of submicrometer sulfate aerosol particles over the Pacific Ocean. *Geophys. Res. Lett.*, v. 18, pp. 1877-1880.

Calvert SE and Petersen TF, (1996). Sedimentary geochemistry of manganese. *Econ. Geol.*, 91 pp. 36–47

Cardoso RB, Sierra-Alvarez R, Rowlette P, Flores ER, Gomez J, Field JA, (2006). Sulfide oxidation under chemolithoautotrophic denitrifying conditions. *Biotechnol. Bioeng.* 95, pp. 1148–1157

Carpenter EJ, Van Raalte CD, Valiela I, (1978). Nitrogen fixation by algae in a Massachusetts salt marsh. *Limnol. Oceanogr.* 23, pp. 318-327

Carpenter EJ, Senjie L, Capone DG, (2000). Bacterial activity in South Pole snow. *Applied Environmental Microbiology* 66, pp. 4514–4517

Casciotti KL, Sigman DM, Galanter Hastings M, Böhlke JK and Hilkert A, (2002). Measurement of the oxygen isotopic composition of nitrate in marine and fresh waters using the denitrifier method. *Anal. Chem.* 74, pp. 4905–4912

Casciotti KL, Sigman DM, Ward BB, (2003). Linking diversity and stable isotope fractionation in ammonia-oxidizing bacteria, *Geomicrobiol. J.*, 20, pp. 1–19, doi :10.1080/01490450390219887

Casciotti KL, (2009). Inverse kinetic isotope fractionation during bacterial nitrite oxidation. *Geochim. Cosmochim. Acta* 73, pp. 2061–2076

Casciotti KL, McIlvin M, and Buchwald C, (2010). Oxygen isotopic exchange and fractionation during bacterial ammonia oxidation, *Limnol. Oceanogr.* 55, pp. 753-762

Cey EE, Rudolph, DL, Aravena R, Parkin G, (1999). Role of the riparian zone in controlling the distribution and fate of agricultural nitrogen near a small stream in southern Ontario. *Journal of Hydrology*. 37 pp. 45–67

Chambers LA, and Trudinger PA, (1978). Microbiological fractionation of stable sulphur isotopes. *Geomicrobiol. J.* pp. 249–293

Chambers LA, Trudinger PA, (1979). Microbiological fractionation of stable sulfur isotopes: a review and critique. *Geomicrobiol. J.* 1, pp. 249–293

Chapin DM and Bledsoe CS, (1992). Nitrogen fixation in Arctic plant communities. In: Chapin, D.M., et al. (Eds.), Arctic Ecosystems in a Change Climate. *Academic Press*, San Diego, pp. 301–319.

Chapin III FS, Bret-Harte MS, Hobbie S, Zhong H, (1996). Plant functional types as predictors of the transient response of arctic vegetation to global change. *J. Veg. Sci* 7, pp. 347–357.

Charlson RJ, Schwartz SE, Hales JM, Cess RD, Coakley JE, Hansen JAJ, Hoffman DJ, (1992). Climate forcing by anthropogenic aerosols. *Science* 255, pp. 423-430

Chen KY and Morris JC, (1972). Kinetics of oxidation of aqueous sulfide by oxygen. *Environ Sci Technol* 6(6), pp. 529–537.

Chiba H and Sakai H, (1985). Oxygen isotope exchange rate between dissolved sulfate and water at hydrothermal temperatures. *Geochim. Cosmochim. Acta*, 49, pp. 993–1000.

Chicarelli MI, Hayes JM, Popp BN, Eckardt CB, Max-well JR, (1993). Carbon and nitrogen isotopic compositions of alkyl porphyrins from the Triassic Serpiano oil shale. *Geochim. Cosmochim. Acta* 57, pp. 1307–1311

Choulaton TW, Gay MJ, Jones A, Fowler D, Cape JN, Leith ID, (1988). The influence of altitude on wet deposition. Comparison between field measurements at Great Dun Fell and the predictions of a seeder-feeder model. *Atmospheric Environment* 22, pp. 1363-1371

Christner BC, Mosley-Thompson E, Thompson LG, Reeve JN, (2003). Bacterial recovery from ancient glacial ice. *Environ. Microbiol.* 5, pp. 433–436

Christner BC, Skidmore ML, Priscu JC, Tranter M & Foreman CM ,(2008). Bacteria in subglacial environments. Psychrophiles: From *Biodiversity to Biotechnology* (Margesin R, Schinner F, Marx J-C & Gerday C, eds), pp. 51–71. Springer, Berlin

Christensen JH, (1997). The Danish eulerian hemispheric model: A three-dimensional air pollution model used for the *Arctic*, *Atmos. Environ.*, 31, pp. 4169– 4191.

Christoudias T, Pozzer A, and Lelieveld J, (2012). Influence of the North Atlantic Oscillation on air pollution transport, *Atmos. Chem. Phys.*, 12, 869–877, doi:10.5194/acp-12-869-2012

Cifuentes LA, Fogel ML, Pennock JR, Sharp JH, (1989). Biogeochemical factors that influence the stable nitrogen isotope ratio of dissolved ammonium in the Delaware Estuary. *Geochim. Cosmochim. Acta* 53,pp. 2713-2721

Clilverd H, Jones J, Kielland K, (2008). Nitrogen retention in the hyporheic zone of a glacial river in interior Alaska. *Biogeochemistry* 88, pp. 31–46

Colbeck SC, (1987). Snow metamorphism and classification. In *Seasonal Snowcovers: Physics, Chemistry and Hydrology* (edited by Jones H. G. and Orville-Thomas W. J.), pp. 1-35. D. Reidel, Dordrecht

Cofala J, Amann M, Klimont Z, Kupiainen K, and Höglund-Isaksson L, (2007). Scenarios of global anthropogenic emissions of air pollutants and Methane until 2030, *Atmos. Environ.*, 41, pp. 8486–8499

Conrad R, (1996). Anaerobic hydrogen metabolism in aquatic sediments. *Mitt. Internat. Verein. Limnol.* 25, pp. 15–24

Cooper RJ, Wadham JL, Tranter M, Hodgkins R, Peters NE, (2002). Groundwater hydrochemistry in the active layer of the proglacial zone, Finsterwalderbreen, Svalbard. *Journal of Hydrology* 269, pp. 208–223.

Cornell S, Mace K, Coeppicus S, Duce R, Huebert B, Jickells T, Zhuang L-Z, (2001). Organic nitrogen in Hawaiian rain and aerosol. *Journal of Geophysical Research–Atmospheres* 106, pp. 7973–7983

Cornell SE, Jickells TD, Cape JN, Duce RA, (2003). Organic nitrogen deposition on land and coastal environments: A review of methods and data, *Atmos. Environ.*, 37, pp. 2173– 2191

Cornell SE, (2010). Atmospheric nitrogen deposition: revisiting the question of the importance of the organic component. *Environmental Pollution*, Special Issue INI, in press. doi:10.1016/j.envpol.2010.11.014

Cragin JH, Hewitt AD, and Colbeck SC, (1993). Elution of ions from melting snow: chromatographic versus metamorphic processes. U.S.A. Cold Regions Research and Engineering Laboratory *CRREL Report* 93-8, 20 pp.

Cragin JH, Hewitt AD, and Colbeck AC, (1996). Grainscale mechanisms influencing the elution of ions from snow. *Atmospheric Environment* 30, pp. 119-127

Curtis CJ, Evans C, Goodale CL, and Heaton THE, (2011). What have stable isotope studies revealed about the nature and mechanisms of N saturation and nitrate leaching from semi-natural catchments? *Ecosystems*, 10.1007/s10021-011-9461-7.

Dalsgaard TDE and Thamdrup B, (2002). Factors controlling anaerobic ammonium oxidation with nitrite in marine sediments. *Appl. Environ. Microbiol.* 68, pp. 3802-3808.

D'Amico S, Collins T, Marx JC, Feller G & Gerday C, (2006). Psychrophilic microorganisms: challenges for life. *EMBO Rep* 7: pp. 385–389

Davidson EA, Janssens IA, (2006). Temperature feedback of soil carbon decomposition and feedbacks to climate change. *Nature*, 440, pp. 165-173

Davies TD, Vincent CE, and Brimhoxombe P, (1982). Preferential elution of strong acids from a Norwegian ice cap. *Nature* 300, pp. 161-163

Day TJ, (1977b). Observed mixing lengths in mountain streams. *Journal of hydrology* (35) pp. 125-136

Demchenko PF, Eliseev AV, Arzhanov MM, Mokhov II, (2006). Impact of global warming rate on permafrost degradation. *Izvestiya Atmospheric and Oceanic Physics* 42(1), pp. 32–39

Dickson DMJ, Kirst GO, (1986). The role of fl-dimethylsulfoniopropionate, glycine betaine and homarine in the osmoacclimation of *Platymonas subcordiformis*. *Planta* 167, pp. 536-543

Dowdeswell JA et al., (1997). The mass balance of circum-Arctic glaciers and recent climate change. *Quat. Res.*, 48(1), pp. 1–14

Duc L, Noll M, Meier BE, Burgmann H, Zeyer J, (2009). High diversity of diazotrophs in the forefield of a receding alpine glacier. *Microbial Ecology*, 57, pp. 179–190

Eckhardt S, Stohl A, Beirle S, Spichtinger N, James P, Forster C, Junker C, Wagner T, Platt U, Jennings SG, (2003). The North Atlantic Oscillation controls air pollution transport to the Arctic, *Atmos. Chem. Phys.*, 3, pp. 1769–1778

Eisinger, M. and Burrows J, (1998). ‘Tropospheric Sulfur Dioxide observed by the ERS-2 GOME instrument’. *Geophys. Res. Lett.* 25, 4177–4180

Elliott EM, Kendall C, Boyer EW, Burns DA, Lear GG, Golden HE, Harlin K, Bytnerowicz A, Butler TJ, Glatz R, (2009). Dual nitrate isotopes in dry deposition: utility for partitioning NO_x source contributions to landscape nitrogen deposition. *Journal of Geophysical Research*, 114, G04020. doi:10.1029/2008JG000889

Escobar IC, Hong SK, Randall AA, (2000). Removal of assimilable organic carbon and biodegradable dissolved organic carbon by reverse osmosis and nanofiltration membranes, *J. Membrane Sci.* 175, pp. 1–17

Fahey D, Gao RS, Carslaw KS, (2001). The detection of large HNO₃-containing particles in the winter Arctic stratosphere, *Science*, 291, pp. 1026–1031

Ferek RJ, Hobbs PV, Radke LF, Herring JA, Sturges WT, Cota GF, (1995). Dimethyl sulfide in the arctic atmosphere, *J. Geophys. Res.*, 100, 26, pp. 093-104,

Fellman JB, Spencer RGM, Hernes PJ, Edwards RT, Amore DVD, Hood E, (2010). The impact of glacier runoff on the biodegradability and biochemical composition of terrigenous dissolved organic matter in near-shore marine ecosystems, *Marine Chemistry*, In Press, Corrected Proof, Available online 31 March 2010, ISSN 0304-4203, DOI: 10.1016/j.marchem.2010.03.009

Fischer H, Wagenbach D and Kipfstuhl J, (1998). Sulfate and nitrate firm concentrations on the Greenland ice sheet: 2. Temporal anthropogenic deposition changes, *J. Geophys. Res.*, 103(D17), 21, pp. 935- 942

Frey KE, and McClelland JW, (2009). Impacts of permafrost degradation on arctic river biogeochemistry. *Hydrological Processes*, 23 (1), pp. 169–182

Fogel MA, and Cifuentes LA, (1993). Isotopic fraction- ation during primary production, p. 73-98. In M. H. Engel and S. A. Macko [eds.], *Organic geochemistry*. Plenum

Fogg GE, (1974). Nitrogen fixation In:*Algal physiology and biochemistry*, pp 560-582. Ed. by W. D. P. Stewart. Oxford: Blackwell

Foght J, Aislabie J, Turner S, Brown CE, Ryburn J, Saul DJ, and Lawson W, (2004). Culturable bacteria in subglacial sediments and ice from two Southern Hemisphere glaciers. *Microbial Ecol.* 47, pp. 329–340

Førland EJ, Hanssen-Bauer I, Nordli PØ, (1997). ‘Climate Statistics and Long-Term Series of Temperature and Precipitation at Svalbard and Jan Mayen’, Norwegian *Meteorol. Inst. Report 21/97 KLIMA*, p. 72

Fowler D, Cape JN, Leith DI, Choularton TW, Gay MJ, Jones A, (1988). The influence of altitude on rainfall composition at Great Dun Fell. *Atmos. Environ.*, 22, 1355-1417

Farquhar J, Bao HM, Thiemens M, (2000). Atmospheric influence of Earth’s earliest sulfur cycle. *Science*, 289, pp. 756-758

Galloway JN, Schlesinger WH, Levy H, Michaels A, Schnoor JL, (1995). Nitrogen fixation: Anthropogenic enhancement-environmental response, *Global Biogeochem. Cycles*, 9(1), pp. 235–252

Gambarotta S, (1995). Dinitrogen fixation and activation after 30 years: a puzzle still unsolved. *J. Organomet. Chem.* 500 (1995) 117

Garber EAE, Hollocher TC, (1982). ^{15}N , ^{18}O tracer studies on the activation of nitrite by denitrifying bacteria. *The Journal of Biological Chemistry*, 257, pp. 8091–8097

Gardolinski PCFC, Hanrahan G, Achterberg EP, Gledhill M, Tappin AD, House WA, Worsfold PJ, (2001). Comparison of sample storage protocols for the determination of nutrients in natural waters. *Water Research* 15, pp. 3670–3678

Garrels RM & Thompson ME, (1960). Oxidation and pyrite in ferric sulfate solution. *Am. J. Sci.* 268, pp. 57–67

Gellatly AM and Lyons TW, (2005). Trace sulfate in mid- Proterozoic carbonates and the sulfur isotope record of biospheric evolution. *Geochim. Cosmochim. Acta* 69, 3813–3829. (doi:10.1016/j.gca.2005.01.019)

Gleisner M, Herbert RB Jr, and Kockum PCF, (2006). Pyrite oxidation by *Acidithiobacillus ferrooxidans* at various concentrations of dissolved oxygen: *Chemical Geology*, v. 225, pp. 16–29, doi: 10.1016/j.chemgeo.2005.07.020.

Gooseff MN, McKnight DM, Runkel RL, Duff JH, (2004). Denitrification and hydrologic transient storage in a glacial meltwater stream, McMurdo Dry Valleys, Antarctica. *Limnology and Oceanography*, 49: pp. 1884–1895

Gooseff MN, (2010). Defining hyporheic zones – advancing our conceptual and operational definitions of where stream water and groundwater meet. *Geography Compass* 4, 945–955

Gorzelska K, Galloway JN, (1990). Amine nitrogen in the atmospheric environment over the North Atlantic Ocean. *Global Biogeochemical Cycles* 4, pp. 309–333

Goto-Azuma K, (1998). Changes in snow pack and melt water chemistry during snow melt. In Nakawo, M., Hayakawa, N., and Goodrich, L. E. (eds.), *Snow and Ice Science in Hydrology*. Nagoya: Nagoya University, pp. 119-133

Gounot AM (1986). Psychrophilic and psychrotrophic microorganisms. *Experimentia* 42, pp. 1192–1197.

Granger J, Sigman DM, Needoba JA, Harrison PJ, (2004). Coupled nitrogen and oxygen isotope fractionation of nitrate during assimilation by cultures of marine phytoplankton, *Limnol. Oceanogr.*, 49(5), pp. 1763– 1773

Granger J, Sigman DM, Lehmann MF, Tortell PD, (2008). Nitrogen and oxygen isotope fractionation during dissimilatory nitrate reduction by denitrifying bacteria, *Limnol. Oceanogr.*, 53(6), pp. 2533–2545

Granger J, Sigman DM, Rohde MM, Maldonado MT, Tortell PD, (2010). N and O isotope effects during nitrate assimilation by unicellular prokaryotic and eukaryotic plankton cultures, *Geochim. Cosmochim. Acta.*, 74, pp. 1030–1040

Haendel D, Muñhale K, Nizsche H-M, Stiehl G, Wand U, (1986). Isotopic variations of the fixed nitrogen in metamorphic rocks. *Geochim. Cosmochim. Acta* 50, pp. 749–758

Hagen JO, and Liestol O, (1990). Long-term mass-balance investigations in Svalbard, 1950-88. *Annals of Glaciology*, 14: pp. 102-106

Hagen JO and Sñtrang A, (1991). Radio-echo soundings of sub-polar glaciers with low frequency radar. *Polar Research*, 26, 15Ð57

Hagen JO, Kohler J, Melvold K, Winther JG, (2003). Glaciers in Svalbard: mass balance, runoff and freshwater flux, *Polar Research*22, pp. 145–159

Hall A, Pereira MD, Bea F, (1996). The abundance of ammonium in the granites of central Spain, and the behaviour of the ammonium ion during anatexis and fractional crystallization. *Mineral. Petrol.* 56, pp. 105–123

Hambrey MJ, Bennett MR, Dowdeswell JA, Glasser NF, Huddart D, (1999). Debris entrainment and transfer in polythermal valley glaciers. *Journal of Glaciology*, 45, pp. 69–86.

Hambrey M, Murray T, Glasser N, Hubbard A, Hubbard B, Stuart G, Hansen S, Kohler J, (2005). Structure and changing dynamics of a polythermal valley glacier on a centennial timescale: Midre Lovénbreen, Svalbard. *Journal of Geophysical Research*, 110, F01006, doi:10.1029/2004JF000128

Hansen S, (1999). A photogrammetrical, climate-statistical and geomorphological approach to the post Little Ice age changes of the Midtre Lovénbreen glacier, Svalbard. Master thesis, Univ. Copenhagen-The University Courses on Svalbard (UNIS)-University of Tromsø, Norway

Harder SL, Warren SG, Chadson RJ, Covert DS, (1996). Filtering of air through snow as a mechanism for aerosol deposition on the Antarctic ice sheet, *J. Geophys. Res.*, 101, 18, pp. 729-743

Harrison AG and Thode HG, (1958). Mechanisms of the bacterial reduction of sulfate from isotope fractionation studies. *Trans. Faraday Soc.* 53, pp.84–92

Hastings MG, Steig EJ, Sigman DM, (2004). Seasonal variations in N and O isotopes of nitrate in snow at Summit, Greenland: Implications for the study of nitrate in snow and ice cores, *J. Geophys. Res.*, 109, D20306, doi: 20310.21029/22004JD004991

Hattori S, Danielache S, Johnson M, Schmidt J, Kjaergaard H, Toyoda S, Ueno Y, Yoshida N, (2011): Ultraviolet absorption cross sections of carbonyl sulfide isotopologues OC32S, OC33S, OC34S and O13CS: isotopic fractionation in photolysis and atmospheric implications, *Atmos. Chem. Phys.*, 11, pp. 10293–10303, doi:10.5194/acp-11-10293-2011, 2011

Heaton THE, (1986). Isotopic studies of nitrogen pollution in the hydrosphere and atmosphere: a review. *Chem. Geol.* 59, pp. 87–102

Heaton THE, Spiro B, Madeline S, and Robertson C(1997). Potential canopy influences on the isotopic composition of nitrogen and sulphur in atmospheric deposition. *Oecologia*, 109, pp. 600-607

Heaton THE, Wynn P, Tye AM, (2004). Low 15N/14N ratios for nitrate in snow in the high Arctic (79° N). *Atmospheric Environment*, 38, pp. 5611–5621

Hedin LO, von Fischer JC, Ostrom NE, Kennedy BP, Brown MG & Robertson GP, (1998). Thermodynamic constraints on nitrogen transformations and other biogeochemical processes at soil-stream interfaces. *Ecology*, 79, pp. 684–703

Heidenreich JE, and Theimens MH, (1986). A non-mass-dependent oxygen isotope effect in the production of molecular oxygen: the role of molecular symmetry in isotopic chemistry, *J. Chem Phys.*, 84, pp.2129-2136,

Herron MM, (1982). Impurity sources of F⁻, Cl⁻, NO₃⁻ and SO₄⁻ in Greenland and Antarctic precipitation. *J. Geophys. Res.* 87: pp. 3052-3060

Hewitt AD, Cragin JH, Colbeck SC, (1989). Does snow have ion chromatographic properties? *Proc. 46th Ann. Eastern Snow Conf.*, Quebec City, Quebec, pp. 165-171

Hinkel KM, and Nelson FE, (2003). Spatial and temporal patterns of active layer thickness at Circumpolar Active Layer Monitoring (CALM) sites in northern Alaska, pp. 1995–2000, *J. Geophys. Res.*, 108(D2), 8168, doi:10.1029/2001JD000927

Hjelle A, (1993). *Geology of Svalbard*. Norsk Polarinstitut, Oslo, 162 pp

Hodkinson ID, Coulson SJ, Webb NR, (2004). Invertebrate community assembly across proglacial chronosequences in the high Arctic. *Journal of Animal Ecology* 73, pp. 556–568

Hodson, AJ and Tranter M, (1999). CO₂ Drawdown by Contemporary Glacial Meltwater Fluxes in High Arctic Svalbard, IAHS-AISH publication, pp. 259–265

Hodson AJ, Mumford PN, Kohler J, Wynn PM, (2005a). The High Arctic glacial ecosystem: new insights from nutrient budgets. *Biogeochemistry*, 72: pp. 233–256

Hodson AJ, Kohler J, Brinkhaus M, (2005b). Multi-year water and surface energy budget of a high latitude polythermal glacier: evidence for overwinter water storage in a dynamic subglacial reservoir, *Annals of Glaciology* 42 (1), pp. 42–46

Hodson AJ, Anesio AM, Tranter M, Fountain AG, Osborn AM, Priscu J, Laybourn-Parry J, Sattler B, (2008). Glacial ecosystems. *Ecol Monogr* 78, pp. 41–67

Hodson AJ, Roberts T, Engvall AC, Holmén K, Mumford PN, (2010a). Glacier ecosystem response to episodic nitrogen enrichment in Svalbard, European High Arctic. *Biogeochemistry* 98, pp. 171–184

Hodson A, Heaton THE, Langford H, Newsham K, (2010b). Chemical weathering and solute export by meltwater in a maritime Antarctic glacier basin. *Biogeochemistry*. doi:10.1007/s10533-009-9372-2

Hoefs J, (2009). *Stable Isotope Geochemistry*, Springer-Verlag, Berlin Heidelberg, 285 pp

Hole LR, JH Christensen, Ruoho-Airola T, Tørseth K, Ginzburg V, and Glowacki P, (2009). Past and future trends in concentrations of sulphur and nitrogen compounds in the Arctic. *Atmospheric Environment* 43, pp. 928–939.

Hollocher TC, Tate ME, Nicholas DJD, (1981). Oxidation of ammonia by *Nitrosomonas europaea*. *J Biol Chem* 256, pp. 10834–10836

Holloway JM, Dahlgren RA, Hansen B, Casey WH, (1998). Contribution of bedrock nitrogen to high nitrate concentrations in stream water. *Nature* 395, pp. 785–793

Holloway JM, and Dahlgren RA, (1999). Geologic nitrogen in terrestrial biogeochemical cycling, *Geology*, 27, pp. 567–570

Holloway JM, Dahlgren RA, Casey WH, (2001). Nitrogen release from rock and soil under simulated field conditions, *Chem. Geol.*, 174, 403–414

Holloway JAM and Dahlgren RA, (2002). Nitrogen in rock: occurrences and biogeochemical implications. *Global Biogeochem. Cycles* 16, 1118. doi:10.1029/2002GB001862.

Holt BD, Kumar R, (1991). Oxygen isotope fractionation for understanding the sulphur cycle. In *SCOPE 43: Stable Isotopes in the Assessment of Natural and Anthropogenic Sulphur in the Environment*, Krouse HR, Grinenko VA (eds). Wiley: Chichester; pp. 27–41.

Holt BD, Kumar R, Cunningham PT, (1981). Oxygen-18 study of the aqueous-phase oxidation of sulphur dioxide. *Atmospheric Environment* 15, pp. 557–566

Holton JR, Haynes PH, McIntyre ME, Douglass AR, Rood RB, Pfister L, (1995). Stratosphere-troposphere exchange, *Rev. Geophys.*, 33, pp. 403–439

Hood E and Scott D, (2008). Riverine organic matter and nutrients in southeast Alaska affected by glacial coverage. *Nature Geosci*, pp. 583-587

Hood E and Berner L, (2009). Effects of changing glacial coverage on the physical and biogeochemical properties of coastal streams in southeastern Alaska, *J. Geophys. Res.*, 114, G03001, doi:10.1029/2009JG000971

Hurtgen MT, Arthur MA, Suits NS, Kaufman AJ, (2002). The sulfur isotopic composition of Neoproterozoic seawater sulfate; implications for a snowball Earth? *Earth and Planetary Science Letters*, 203, 413– 429.

Hurtgen MT, Arthur MA, Prave AR, (2004). The sulfur isotopic composition of carbonate associated sulfate in Mesoproterozoic to Neoproterozoic carbonates from Death Valley, California. In: Amend, J.P., Edwards, K.J., Lyons, T.W. (Eds.), *Sulfur Biogeochemistry—Past and Present: Geological Society of American Special Paper*, vol. 379. *Geological Society of America*, Boulder, Colorado, pp. 177– 194

Hutchinson GE, (1944). Nitrogen in the biogeochemistry of the atmosphere. *Amer. Scientist*, 32, pp. 178-195

Hutterli MA, Crueger T, Fischer H, Andersen KK, Raible CC, Stocker TF, Siggaard-Andersen ML, McConnell JR, Bales RC, Burkhardt J, (2007). The influence of regional circulation patterns on wet and dry mineral dust and sea salt deposition over Greenland. *Climate Dynamics* 28, pp. 635–647

Irvine-Fynn TDL, Hodson AJ, Kohler J, Porter P, Vatne G, (2005). Dye tracing experiments at Midtre Lovénbreen, Svalbard: preliminary results and interpretations. In: Mavlyudov, B.R. (Ed.), *Proceedings of the 7th Glacier Caves and Glacial Karst in High Mountains and Polar Regions*. Institute of the Russian Academy of Sciences, Moscow, pp. 36–43

Irvine-Fynn TDL and Hodson AJ, (2010). Biogeochemistry and dissolved oxygen dynamics at a subglacial upwelling, Midtre Lovénbreen, Svalbard. *Ann. Glaciol.*,51(56),pp. 41–46

Itihara Y, and Suwa K, (1985). Ammonium contents of biotites from Precambrian rocks in Finland: The significance of NH_4^+ as a possible chemical fossil. *Geochim. Cosmochim. Acta*49, pp.145–151

Jaeschke A, Hopmans E, Wakeham S, Schouten S, Damste J, (2007). The presence of ladderanes lipids in the oxygen minimum zone of the Arabian Sea indicates nitrogen loss through anammox. *Limnol Oceanogr* 52,pp. 780–786

Jaffe DA, Honrath RE, Herring JA, Li SM, (1991). Measurement of nitrogen oxides at Barrow, Alaska during spring: evidence for regional and northern hemispheric sources of pollution, *J. Geophys. Res.* 96, pp. 7395–7405

Jaffe DA, (1992). The nitrogen cycle. In: S.S. Butcher, R.J. Charlson, G.H. Orians and G.V. Wolfe (Editors), *Global Biogeochemical Cycles*. Academic Press, London.

Jaffe DA, (2000) The nitrogen cycle. In Earth System Science. Jacobsen MC, Charlson RJ, Rodhe H, and Orians GH (eds). San Diego, CA, USA: *Academic Press*, pp. 322–342

Johannessen M, and Henriksen A, (1978). Chemistry of snowmelt: changes in concentration during melting. *Water Resour. Res.*14, pp. 615-619

Johnson JE and Harrison H, (1986). Carbonyl sulfide concentrations in the surface waters and above the Pacific Ocean, *J. Geophys. Res.* 91, pp. 7883–7888

Johnston JC, and Thiemens, MH, (1997). The isotopic composition of tropospheric ozone in three environments, *J. Geophys. Res.*102, 25, pp. 395-404

Joye SB & Paerl HW, (1994). Nitrogen cycling in microbial mats: rates and patterns of denitrification and nitrogen fixation. *Mar. Biol.* 119, pp. 285–295

Kah LC, Lyons TW, Frank TD, (2004). Low marine sulphates and protracted oxygenation of the Proterozoic biosphere. *Nature* 431, pp. 834–838

Kaplan IR and Rittenberg SC, (1964). Microbiological fractionation of sulfur isotopes. *J. Gen. Microbiol.*, 34, pp. 195–212.

Kemp ALW and Thode HG, (1968). The mechanism of the bacterial reduction of sulfate and of sulfide from isotope fractionation studies. *Geochim. Cosmochim. Acta*, 32, pp. 71–91

Kämäri, J, and Joki-Heiskala P, (1998). Acidifying Pollutants, Arctic haze, and Acidification in the Arctic. Arctic Monitoring and Assessment Programme. *AMAP Assessment Report* ch. 9, pp. 621–658

Kaiser J, Hastings MG, Houlton BZ et al., (2007). Triple oxygen isotope analysis of nitrate using the denitrifier method and thermal decomposition of N₂O. *Analytical Chemistry*, 79, pp. 599–607

Kaštovská K, Stibal M, Šabacká M, Cerná B, Šantrùèková H, Elster J, (2007). Microbial community structure and ecology of subglacial sediments in two polythermal Svalbard glaciers characterized by the epifluorescence microscopy and PLFA. *Polar Biol* 30, pp.277–287

Kendall C, (1998). Tracing nitrogen sources and cycling in catchments. In C. Kendall and J.J. McDonnell (Eds.), *Isotope Tracers in Catchment Hydrology*. Elsevier Science B.V. (Amsterdam), pp. 519-576.

Kendall C, Elliott EM, Wankel SD, (Eds) (2007). Tracing anthropogenic inputs of nitrogen to ecosystems, *Stable isotopes in ecology and environmental science*, pp. 375-449

Khalil MAK, and Rasmussen RA, (1990). Atmospheric methane: recent global trends. *Env. Sci. Technol.* 24, pp. 549–553

Keith SM, and Herbert RA, (1983). Dissimilatory nitrate reduction by a strain of *Desulfovibrio desulfuricans*. *FEMS Microbiol Lett* 18, pp. 55-59

King E, Smith A, Murray T, Stuart G, (2008). Glacier-bed characteristics of midtre Lovenbreen, Svalbard, from highresolution seismic and radar surveying. *Journal ofGlaciology*, 54, pp. 145–156

Kinjo T and Pratt PF, (1971). Nitrate adsorption: I. In some acid soils of Mexico and South America. *Soil Sci. Soc. Am. Proc.* 35, pp. 722–725

Kirchman DL, (1994). The uptake of inorganic nutrients by heterotrophic bacteria. *Microb. Ecol.* 28, pp. 255-271

Kirk GJD, and Kronzucker HJ, (2005). The potential for nitrification and nitrate uptake in the rhizosphere of wetland plants: a modelling study. *Annals of Botany* 96: 639–646

Kirst GO, Thiel C, Wolff H, Nothnagel J, Wanzek M, Ulmke R, (1991). Dimethylsulfoniopropionate (DMSP) in ice-algae and its possible biological role. *Mar. Chem.* 35, pp. 381-388

Knapp AN, Sigman DM, and Lipschultz F, (2005). N isotopic composition of dissolved organic nitrogen and nitrate at the Bermuda Atlantic time-series study site, *Global Biogeochem. Cycles*, 19, GB1018, doi:10.1029/2004GB002320

Knobeloch L, Salna B, Hogan A, Postle J, Anderson H, (2000). Blue babies and nitrate contaminated well water. *Environ Health Perspect*, 108, pp. 675–683

Kohl I and Bao H, (2011). Triple-oxygen-isotope determination of molecular oxygen incorporation in sulfate produced during abiotic pyrite oxidation (pH; 2–11), *Geochimica et Cosmochimica Acta*, Volume 75, Issue 7, 1 April 2011, pp. 1785-1798

Kool DM, Wrage N, Oenema O, Dolfing J, Van Groenigen JW, (2007). Oxygen exchange between (de)nitrification intermediates and H₂O and its implications for source determination of NO₃⁻ and N₂O: a review. *Rapid Communications in Mass Spectrometry* 21, pp. 3569–3578

Kool, DM, Müller C, Wrage N, Oenema O, Van Groenigen JW, (2009a). Oxygen exchange between nitrogen oxides and H₂O can occur during nitrifier pathways. *Soil Biology and Biochemistry* 41, pp. 1632-1641

Kool, DM, Wrage N, Oenema O, Van Kessel C, Van Groenigen JW, (2011). Oxygen exchange with water alters the oxygen isotopic signature of nitrate in soil ecosystems. *Soil Biol. Biochem.* 43, pp. 1180-1185

Krohn MD, Evans J, Robinson Jr. GR, (1988). Mineral-bound ammonium in black shales of the Triassic Cumnock Formation, Deep River Basin, North Carolina. U.S. *Geol. Surv. Bull.* 1776, pp. 86–98

Krauskopf KB, (1979). Introduction to Geochemistry. McGraw-Hill, New York

Kreutz KJ and Sholkovitz ER, (2000). Major element, rare earth element, and sulfur isotopic composition of a high-elevation firn core: sources and transport of mineral dust in Central Asia. *Geochemistry, Geophysics, Geosystems* (G3), 1, paper 2000GC000082

Krishnakumar B and Manila BV, (1999). Bacterial oxidation of sulphide under denitrifying conditions. *Biotechnol Lett* 21, pp. 437–440

Kupfer H, Herber A, König-Langlo G, (2006). Radiation Measurements and Synoptic Observations at Ny-Ålesund, Svalbard, *Ber. Polarforsch. Meeresforsch.*, 538, 104 pp

Kuypers MMM, Sliemers AO, Lavik G, Schmid M, Jørgensen BB, Kuenen JG, Sinninghe Damste JS, Strous M, Jetten MSM, (2003). *Nature* 422, pp.608–611

Lanoil B, Skidmore M, Priscu JC, Han S, Foo W, Vogel SW, Tulaczyk S & Engelhardt H, (2009). Bacteria beneath the West Antarctic ice sheet. *Environ Microbiol* 11: pp. 609–615

Larose C, Berger S, Ferrari C, Navarro E, Dommergue A, Schneider D, Vogel TM, (2010). Microbial sequences retrieved from environmental samples from seasonal Arctic snow and meltwater from Svalbard, Norway. *Extremophiles* 14, pp. 205-212

Law KS and Stohl A, (2007). Arctic air pollution: origins and impacts, *Science*, 315, pp. 1537–1540

Leck C and Persson C, (1996). The central Arctic Ocean as a source of dimethyl sul_de. Seasonal variability in relation to biological activity. *Tellus*, 48B, pp. 156–177

Lee, C., et al. (2011). SO₂ emissions and lifetimes: Estimates from inverse modeling using in situ and global, space-based (SCIAMACHY and OMI) observations, *J. Geophys. Res.*, 116, D06304, doi:10.1029/2010JD014758

Leggett DC & Hogan AW, (1994) A preliminary experiment to examine chemical exchange at the soil-snow interface. *The Science of the Total Environment* 160/161, pp. 403-407

Legrand M, and Kirchner S, (1990). 'Origins and variation of nitrate in south polar precipitation', *J. Geophys. Res* 95, D4, pp. 3493-3507

Legrand M and Mayewski PA, (1997). Glaciochemistry of polar ice cores: a review. *Rev. Geophys.* 35 Ž3., pp. 219–243

Lehmann S and Conrad R, (1996). Characteristics of turnover of OCS in four different soils. *Journal of Atmospheric Chemistry* 23, pp. 193-207

Lelieveld J, Dentener FJ, Peters W and Krol MC, (2004). On the role of hydroxyl radicals in the self-cleansing capacity of the troposphere, *Atmos. Chem. Phys.*, 4, pp. 2337– 2344

Leuenberger C, Czuczwa J, Tremp J, Giger R, (1988). Nitrated phenols in rain–atmospheric occurrence of phytotoxic pollutants. *Chemosphere* 17, pp. 511–515

Li SM and Barrie LA, (1993). Biogenic sulphur aerosols in the Arctic troposphere: I contributions to sulphate. *Journal of Geophysical Research* 98D, pp. 20613–20622

Lindstrom ES, Newton JW, Wilson PW, (1952). The relationship between photosynthesis and nitrogen fixation, *Proc. natn. Acad. Sci., U.S.A.* 38, pp. 392–396

Lloyd RM, (1968). Oxygen isotope behaviour in the sulfate–water system. *Journal of Geophysical Research* 73: pp. 6099–6110

Lockhart WL, Wilkinson P, Billeck BN, Hunt RV, Wagemann R, Brunskill GJ, (1995). Current and historical inputs of mercury to highlatitude lakes in Canada and to Hudson Bay. *Water Air Soil Pollut*, 80: pp. 603–613

Lovely DR and Klug MA, (1983). Sulfate reducers can outcompete methanogens at freshwater sulfate concentrations. *Applied Environmental Microbiology* 45 (1), 187-192

Lovett GM Kinsman JD, (1990). Atmospheric pollutant deposition to high-elevation ecosystems. *Atmospheric Environment* 24A, pp. 2767–2786

Luecke W& Nielsen H, (1972). Isotopenfraktionierung des Schwefels im Blasenspriih. *Foytsehr. Min.* 50 (Beiheft 3), pp. 36-37

Luther GW III, (1987). Pyrite oxidation and reduction: molecular orbital theory considerations. *Geochim. Cosmochim. Acta*, 51, pp. 3193-3199

Luz B and Barkan E, (2011). The isotopic composition of atmospheric oxygen. *Global Biogeochemical Cycles*, 25, GB3001, doi:10.1029/2010GB003883

Mack MC, Schuur EAG, Bret-Harte MS, Shaver GR, Chapin FS, (2004). Ecosystem carbon storage in arctic tundra reduced by long-term nutrient fertilization. *Nature* 431: pp. 440–443

Mackin JE and Aller RC, (1984). Ammonium adsorption in marine sediments. *Limnol. Oceanogr.* 29, pp. 250-257

Macko SA, Engel MH, and Parker PL, (1993). Early diagenesis of organic matter in sediments. Assessment of mechanisms and preservation by the use of isotopic molecular approaches. In *Organic Geochemistry*(ed. M. H. Engel and S. A. Macko), pp. 211–224. Olenum

Magdalena S'liwka-Kaszyńska, Agata Kot-Wasik, Jacek Namieśnik, (2003). Preservation and Storage of water samples, Critical Reviews in *Environmental Science and Technology*, Vol. 33, Iss. 1

Mann JL, (2005). Determination of sulphur isotope composition in sulphate from two high elevation snowpits by multi-collector thermal ionisation mass spectrometry using a double spike. PhD Thesis, University of Maryland, Maryland, 220p.

Mancinelli RL and McKay CP, (1988). The evolution of nitrogen cycling. *Orig. Life* 18, *Biosphere* 18, pp. 311–325

Mariotti A, Germon JC, Hubert P, Kaiser P, Letolle R, Tardieux A, Tardieux P, (1981). Experimental determination of nitrogen kinetic isotope fractionation: some principles; illustration for the denitrification and nitrification processes. *Plant Soil* 62: pp. 413–441

Mariotti A, (1983). Atmospheric nitrogen is a reliable standard for natural ($\delta^{15}\text{N}$) abundance measurements, *Nature* 303, pp. 685-687

Matsuhisa Y, Goldsmith JR, Clayton RN, (1978). Mechanisms of hydrothermal crystallization of quartz at 250°C and 15 kbar. *Geochim. Cosmochim. Acta* 42, 173–182

Matsumoto K, and Uematsu M, (2005). Free amino acids in marine aerosols over the western North Pacific Ocean, *Atmos. Environ.*, 39, pp. 2163–2170

Mayer B, Bollwerk SM, Mansfeldt T, Hutter B, and Veizer J, (2001.) The oxygen isotope composition of nitrate generated by nitrification in acid forest floors. *Geochimica et Cosmochimica Acta*, 65, pp. 2743-2756

McArdle NC and Liss PS, (1995). Isotopes and atmospheric sulphur. *Atmos. Environ.*, 29, pp. 2553-2556.

McCready RGL,(1975). Sulphur isotope fractionation by *Desulfovibrio* and *Desulfotomaculum* species. *Geochim. Cosmochim. Acta*39, pp. 1395–1401

McKnight DM, Runkel RL, Tate CM, Duff JH and Moorhead DL, (2004). Inorganic N and P dynamics of Antarctic glacial meltwater streams as controlled by hyporheic exchange and benthic autotrophic communities, *J. N. Am. Benthol. Soc.*, 23, pp. 171–188

McNamara JP, Kane DL, Hobbie J, Kling GW, (2008). Hydrologic and biogeochemical controls on the spatial and temporal patterns of nitrogen and phosphorus in an Arctic river. *Hydrological Processes* 17, pp. 3294–3309

Mengis M, Schiff SL, Harris M, English MC, Aravena R, Elgood RJ, MacLean A, (1999). Multiple geochemical and isotopic approaches for assessing ground water NO₃⁻ elimination in a riparian zone. *Ground Water* 37, pp. 448–457

Michalski G, Scott Z, Kabling M, Thiemens M, (2003). First measurements and modeling of $\Delta^{17}\text{O}$ in atmospheric nitrate. *Geophys.Res. Lett.* 30[16], ASC14–1.

Michalski G, Bockheim JG, Kendall C. and Thiemens M, (2005). Isotopic composition of Antarctic Dry Valley nitrate: Implications for NO_y sources and

cycling in *Antarctica*, *Geophys. Res. Lett.*, 32(13), L13817, doi: 13810.11029/12004GL022121

Mikan CJ, Schimel JP, Doyle AP, (2002). Temperature controls of microbial respiration above and below freezing in Arctic tundra soils. *Soil Biology & Biochemistry* 34, pp. 1785–1795

Miteva V, Sowers T, Brenchley J, (2007). Production of N₂O by ammonia oxidizing bacteria at subfreezing temperatures as a model for assessing the N₂O anomalies in the Vostok ice core. *Geomicrobiol J* 24, pp.451–459

Monteil PO and Cowan DA, (1993). Possible role of soluble carbohydrates and polyols as cryoprotectants in Antarctic plants, pp. 119–125. In R. B.n Heywood (ed.), *Proceedings of University Research in Antarctica*. British Antarctic Survey, Cambridge, United Kingdom

Montoya JP, Horrigan SG, McCarthy JJ, (1991). Rapid, storm-induced changes in the natural abundance ¹⁵N in a planktonic ecosystem. *Geochim. Cosmochim. Acta*, Vol. 55, pp. 3627–3638

Moore J, Kekonen T, Grinsted A, Isaksson E, (2006). Sulfate source inventories from a Svalbard ice core record spanning the industrial revolution. *J Geophys Res* 111:D15307. doi:10.1029/ 2005JD006453

Morin S, Savarino J, Frey MM, Yan N, Bekki S, Bottenheim JW, Martins JMF, (2008). Tracing the Origin and Fate of NO_x in the Arctic Atmosphere Using Stable Isotopes in Nitrate, *Science* 322 (5902), 730

Monteil PO, and Cowan DA, (1993). Possible role of soluble carbohydrates and polyols as cryoprotectants in Antarctic plants, pp. 119–125. In R. B. Heywood (ed.),

Proceedings of University Research in Antarctica. British Antarctic Survey, Cambridge, United Kingdom

Mopper K and Zika RG, (1987). Free amino acids in marine rain: Evidence for oxidation and potential role in nitrogen cycling. *Nature* 325, pp. 246-249

Mosier AR, (2001). Exchange of gaseous nitrogen compounds between agricultural systems and the atmosphere, *Plant Soil*, 228, pp. 17–27

Moreau M, Mercier D, Laffly D, Roussel E, (2008). Impacts of recent paraglacial dynamics on plant colonization: a case study on Midtre Lovénbreen foreland, Spitsbergen (79°N). *Geomorphology* 95, pp. 48–60

Mulvaney R and Wolff EW, (1993). Evidence for winter/spring denitrification of the stratosphere in the nitrate record of Antarctic ice cores. *J. Geophys Res.*, 98, pp. 5213-5220

Myers RJK, (1972). The effect of sulfide on nitrate reduction in soil. *Plant Soil* 37, pp. 431-433

Neff JC, Holland EA, Dentener FJ, McDowell WH, Russell KM, (2002). The origin, composition and rates of organic nitrogen deposition: a missing piece of the nitrogen cycle? *Biogeochemistry* 57/58, pp. 99–136

Neubauer J, and Heumann KG, (1988). Nitrate trace determination in snow and firn core samples of ice shelves at the Wedell Sea, Antarctica, *Atmos. Environ.*, 22, pp. 537-545

Newman L, Krouse HR, Grinenko VA, (1991). Stable isotopes. In Natural and Anthropogenic Sulphur in the Environment. *SCOPE 43* (edited -by Krause- H. R. And Grinenko V. A.). DD. 133-176. John Wiley. New York.

Nielsen H, (1974). Isotopic composition of the major contributors to atmospheric sulfur. *Tellus*, v. 26, pp. 213-221

Nielsen H, Pilot J, Grinenko LN, Grinenko VA, Lein A Yu., Smith JW, Pankina RG, (1991). Lithospheric sources of sulfur. In: H.R. Krouse and V.A. Grinenko (Eds), *Stable Isotopes: Natural and Anthropogenic Sulphur in the Environment, SCOPE 43*, John Wiley and Sons, Chichester, pp. 65-132

Norman AL, Barrie LA, Toom-Sauntry D, Sirois A, Krouse HR, Li SM and Sharma S, (1999). Sources of aerosol sulphate at Alert: Apportionment using stable isotopes. *J. Geophys. Res.*, v. 104, n. D9, p. 11, pp. 619-631.

Novak M, Jackova I, Prechova E, (2001). Temporal trends in the isotope signature of air-borne sulfur in Central Europe. *Environ. Sci. Technol.* 35, pp. 255–260

Nriagu, JO, Coker RD and Barrie LA, (1991). Origin of sulphur in Canadian Arctic Haze from isotope measurements. *Nature*, v. 349, pp. 142-145.

Odegard R, Hamran SE, BO PH, Etzelmüller B, Vatne G, Sollid JL, (1992). Thermal regime of a valley glacier, Erikbreen, northern Spitsbergen. *Polar Research*, 11(2), pp. 69-79

Olson GJ, (1991). Rate of pyrite bioleaching by *Thiobacillus ferrooxidans*: results of an interlaboratory comparison. *Appl. Environ. Microbiol.* 57, pp. 642–644.

Ohmoto H and Rye RO, (1979). Isotopes of sulfur and carbon. In: H.L. Barnes, Ed., *Geochemistry of Hydrothermal Ore Deposits*, Wiley, New York, pp. 509–567

Ohmoto H, (1986). Systematics of metal ratios and sulfur isotopic ratios in low-temperature basemetal deposits. *Terra Cognita* 6, pp. 134-13

Ohmoto H, Kaiser CJ, and Geer KA, (1990). Systematics of sulphur isotopes in recent marine sediments and ancient sediment-hosted basemetal deposits. In *Stable Isotopes and Fluid Processes in Mineralization*. Vol. 23 (ed. H. K. Herbert and S. E. Ho), pp. 70–120, Geology Department & University Extension, The University of Western Australia

Ottar BO, Pacyna JM, Berg TC, (1986). Aircraft measurements of air pollution in the Norwegian Arctic. *Atmospheric Environment* 20, pp. 87-100.

Pacyna JM, and Ottar B, (1989). Origin of natural constituents in the arctic aerosol. *Atmos. Environ.*, 23, pp. 809-815.

Panno SV, Hackley KC, Kelly WR, Hwang HH, (2006). Isotopic evidence of nitrate sources and denitrification in the Mississippi River, Illinois. *J. Environ. Qual.* 35, pp. 495–504

Papineau D, Mojzsis SJ, Kahru JA, and Marty B, (2005). Nitrogen isotopic composition of ammoniated phyllosilicates: case studies from Precambrian metamorphosed sedimentary rocks. *Chemical Geology*, v. 216, pp. 37–58

Parmer KA, Uriyo AP, and Singh BR, (1980). Adsorption of nitrate and chloride in some Tanzanian andept soils. *Agrochimica* 24, pp. 492-499

Parwel A, Ryhage R, Wickman FE, (1957). Natural variations in the relative abundances of the nitrogen isotopes. *Geochim. Cosmochim. Acta* 11, pp. 165–170

Pathan AAK, Bhadra B, Begum Z, Sisinthy Shivaji S, (2010). Diversity of yeasts from Puddles in the vicinity of Midre Love´nbreen Glacier, Arctic and Bioprospecting for enzymes and fatty acids. *Curr Microbiol* 60, pp. 307–314

Patris Nicolas, Delmas Robert J and Jouzel Jean, (2000a). Isotopic signatures of sulphur in shallow Antarctic ice cores. *J. of Geophys. Res.*, v. 105, n. D6, pp. 7071-7078.

Patris N, Mihalopoulos N, Baboukas ED and Jouzel J, (2000b). Isotopic composition of sulfur in size-resolved marine aerosols above the Atlantic Ocean. *J. Geophys. Res.* 105, pp. 14449–14457

Patris N, Delmas RJ, Legrand M, De Angelis M, Ferron FA, Stievenard M, Jouzel J, (2002). First sulfur isotope measurements in central Greenland ice cores along the preindustrial and industrial periods. *J. of Geophys. Res.*, v. 107, n. D11, p. ACH 6-1 – ACH 6-13

Pennock JR, Velinsky DJ, Ludlan JM, Sharp JH, Fogel ML, (1996). Isotopic fractionation of ammonium and nitrate during uptake of *Skeletonema costatum*: implications for d15N dynamics under bloom conditions. *Limnol Oceanogr* 41, pp. 451–460

Peterson BJ, Fry B, (1987). Stable isotopes in ecosystem studies. *Annu Rev Ecol Syst* 18, pp. 293-320

Plumb RA, (1996). A "tropical pipe" model of stratospheric transport. *J. Geophys. Res.*, 101, pp. 3957-3972

Porazinska D, Fountain AG, Nylén T, Tranter M, Virginia RA, Wall DH, (2004). The biodiversity and biogeochemistry of cryoconite holes from McMurdo dry valley glaciers, Antarctica. *Arctic, Antarctic, and Alpine Research* 36, pp. 84–91

Price PB and Sowers T, (2004). Temperature dependence of metabolic rates for microbial growth, maintenance and survival. *PNAS* 101, pp. 4631–4636

Pruett LE, Kreutz KJ, Wadleigh M, Aizen V, (2004). Assessment of sulfate sources in high-elevation Asian precipitation using stable sulphur isotopes. *Environ. Sci. Technol.*, 38, pp. 4728– 4733

Rahn KA, (1981). Relative importances of North America and Eurasia as sources of Arctic aerosol. *Atmospheric Environment* 15, pp. 447-1455

Rahn T, Zhang H, Wahlen M, Blake GA, (1998). Stable isotope fractionation during ultraviolet photolysis of N₂O. *Geophys. Res. Lett.* 25, pp. 4489–4492

Rasch M, Elberling B, Jakobsen BH, Hasholt B, (2000). High resolution measurements of water discharge, sediment, and solute transport in the River Zackenbergelven, Northeast Greenland. *Arctic, Antarctic, and Alpine Research* 32(3), pp. 336–345

Rau GH, Arthur MA, Dean WE, (1987). ¹⁵N/¹⁴N variations in Cretaceous Atlantic sedimentary sequences: Implications for past changes in marine nitrogen biogeochemistry. *Earth and Planetary Science Letters* 82, pp. 269–279

Rayleigh L, (1939). Nitrogen, argon and neon in the earth's crust with application to cosmology, *Proc. Roy. Soc.* A170, pp. 451-464

Rees CE, (1973). A steady-state model for sulphur isotope fractionation in bacterial reduction processes. *Geochim. Cosmochim. Acta* 37, pp. 1141–1162

Repp K, (1978). The hydrology of Bayelva, Spitsbergen, *Nordic Hydrology*, 19, pp. 259–268.

Rohde RA and Price PB, (2007). Diffusion-controlled metabolism for long-term survival of single isolated microorganisms trapped within ice crystals. *PNAS* 104, pp. 16592–16597

Rinsland CP, Gunson MR, Ko MKW, Weisensten DW, Zander R, Abrams MC, Goldman A, Sze ND, Yue GK, (1995). H₂SO₄ photolysis: A source of sulfur dioxide in the upper stratosphere, *Geophys Res.Lett.*, 22 (9), pp. 1109-1112

Rippin D, Willis I, Arnold N, Hodson A, Moore J, Kohler J, Björnsson H, (2003). Changes in geometry and subglacial drainage of Midre Lovénbreen, Svalbard, determined from digital elevation models. *Earth Surface Processes and Landforms* 28: pp. 273 –298. DOI: 10.1002/ esp.485

Roberson S, (2009). Characterization and quanti_cation of glacial sediment transport in two small valley glaciers. Aberystwyth University, pp 1-235

Roberts TJ, Hodson AJ, Evans CD, Holmen K, (2010). Modelling the impacts of a nitrogen pollution event on the biogeochemistry of an Arctic glacier. *Ann. Glaciol.*, 51(56), pp. 163–170

Röckmann TC, Brenninkmeijer AM, Wollenhaupt M, Crowley JN, Crutzen PJ, (2000). Measurement of the isotopic fractionation of ¹⁵N¹⁴N¹⁶O, ¹⁴N¹⁵N¹⁶O, and ¹⁴N¹⁴N¹⁸O in the UV photolysis of nitrous oxide. *Geophys.Res. Lett.* 27, pp. 1399–402

Rønning OI, (1979) Svalbards Flora. Norsk Polarinstitut, Oslo

Rothlisberger R, et al. (2002). Nitrate in Greenland and Antarctic icecores: A detailed description of post-depositional processes, *Ann.Glaciol.*, 35, pp. 209–216

Rysgaard S, Thastum P, Dalsgaard T, Christensen PB, Sloth NP, (1999). Effects of salinity on NH₄⁺absorption, nitrification, and denitrification in Danish estuarine sediments. *Estuaries* 22(1): pp. 21–30

Sakai H, des Marais DJ, Ueda A and Moore JG, (1984). Concentrations and isotope ratios of carbon, nitrogen and sulphur in ocean-floor basalts, *Geochim. Cosmochim. Acta*, 48, pp. 2433-2441

Sasaki A, Arikawa Y and Folinsbee R, (1979). Kiba reagent method of sulfur extraction applied to isotopic work. *Bulletin Geological Survey of Japan*, 30, pp. 241-245.

Sawstrom C, Mumford P, Marshall W, Hodson A, Laybourn-Parry J, (2002). The microbial communities and primary productivity of cryoconite holes in an Arctic glacier (Svalbard, 79-N). *Polar Biol* 25, pp. 591–596

Scalen RS, (1959). The isotopic composition, concentration and chemical state of the nitrogen in igneous rocks. PhD thesis, University of Arkansas. “University Microfilms”, *Ann Arbor, Michigsn Microfilm* No. 59-1379.

Schimel JP, and Bennett J, (2004). Nitrogen mineralization: Challenges of a changing paradigm. *Ecology* 85, pp. 591–602

Schippers A, and Jørgensen BB, (2001). Oxidation of pyrite and iron sulfide by manganese dioxide in marine sediment. *Geochim. Cosmochim. Acta* 65, pp. 915–922

Schippers A and Jørgensen BB, (2002). Biogeochemistry of pyrite and iron sulfide oxidation in marine sediments. *Geochim. Cosmochim. Acta*, 66, pp. 85–92.

Schlesinger WH, (1997). Biogeochemistry: An Analysis of Global Change. *Academic Press*, ed. 2, San Diego, CA

Schuur EAG, et al., (2008). Vulnerability of permafrost carbon to climate change: Implications for the global carbon cycle. *BioScience*, 58, pp. 701–714, doi:10.1641/B580807

Sharp M, Tranter M, Brown GH and Skidmore M, (1995). Rates of chemical denudation and CO₂ drawdown in a glacier-covered alpine catchment. *Geology* 23, pp. 61–64.

Sigler WV and Zeyer J, (2002). Microbial diversity and activity along the forefields of two receding glaciers. *Microb. Ecol.*, 43, pp. 397–407

Sigler WV, Crivii S and Zeyer J, (2002). Bacterial succession in glacial forefield soils characterised by community structure, activity and opportunistic growth dynamics. *Microb Ecol* 44,pp. 306–316

Singer PC and Stumm W, (1970). Acidic mine drainage: the rate determining step. *Science* 167, pp. 1121-1123

Singh BR and Kanehiro Y, (1969). Adsorption of nitrate in amorphous and kaolinitic Hawaiian soils. *Soil Sci. Soc. Am. Proc.* 33, pp. 681-683

Singh HB and Hanst PL, (1981). Peroxyacetylnitrate (PAN) in the unpolluted atmosphere: An important reservoir for nitrogen oxides, *Geophys. Res. Lett.*, 8, pp. 941– 944

Sigman DM, Casciotti KL, Andreani M, Barford C, Galanter M and Bohlke JK, (2001). A bacterial method for the nitrogen isotopic analysis of nitrate in seawater and freshwater, *Anal. Chem.*, 73(17), pp. 4145–4153

Simoës JC, and Zagorodnov VS, (2001). The record of anthropogenic pollution in snow and ice in Svalbard, Norway. *Atm. Environ.* 35, pp. 403–413

Sieburth JMcN, Smetacek V and Lenz J, (1978). Pelagic ecosystem structure: heterotrophic compartments of the plankton and their relationship to plankton size fractions. *Limnol. Oceanogr.*, 23 (6)pp. 1256-1263

Skidmore ML, Foght JM, Sharp MJ (2000). Microbial life beneath a High Arctic glacier. *Appl Environ Microbiol*, 66,pp. 3214–3220

Skidmore M, Anderson SP, Sharp M, Foght J, Lanoil BD (2005). Comparison of microbial compositions of two subglacial environments reveals a possible role for microbes in chemical weathering processes. *Appl Environ Microbiol* 71,pp. 6986–6997

Skidmore M, Tranter M, Tulaczyk S, & Lanoil B, (2010). Hydrochemistry of ice stream beds – evaporitic or microbial effects? *Hydrological Processes*, Vol. 24, pp. 517-523

Smil V, (1997). Global population and the nitrogen cycle. *Scientific American*, July,pp. 76–81

Snider DM, Spoelstra J, Schiff SL, Venkiteswaran JJ, (2010). Stable oxygen isotope ratios of nitrate produced from nitrification: ¹⁸O-labeled water incubations of agricultural and temperate forest soils. *Environmental Science and Technology*, 44, pp. 5358-5364

Solberg S, Schmidbauer N, Sembm A, Stordal F, (1996). Boundary-layer ozone depletion as seen in the Norwegian Arctic in spring, d. *Atmos. Chem.*, 23, pp. 301-332

Solheim B, Endal A and Vigstad H, (1996) Nitrogen fixation in Arctic vegetation and soils from Svalbard, Norway, *Polar Biol.*,16, pp. 35-40

Solomon S, (1999). Stratospheric ozone depletion: a review of concepts and history. *Reviews of Geophysics* 37, pp. 275–316

Solorzano L & Sharp JH, (1980). Determination of total dissolved nitrogen in natural waters. *Limnol. Oceanogr.* 25 (4), pp. 751–754

Spoelstra J, Schiff SL, Hazlett PW, Jeffries DS, and Semkin RG, (2007). The isotopic composition of nitrate produced from nitrification in a hardwood forest floor. *Geochimica et Cosmochimica Acta*, 71, pp. 3757-3771

Spokes LJ, Yeatman SG, Cornell SE, Jickells TD, (2000). Nitrogen deposition to the eastern Atlantic Ocean: the importance of southeasterly flow. *Tellus* 52B, pp. 37–49

Stamnes K, Zak B and Shaw GE, (1995) The atmospheric radiation measurements (ARM) program: ARM's window on the Arctic. *Sci. Total Envir.* 160/161, pp. 825-829

Stevenson FJ, (1962). Chemical state of nitrogen in rocks. *Geochim. Cosmochim. Acta* 26, pp. 797- 809

Stockner, JG & KS Shortreed, (1991). Autotrophic picoplankton: community composition abundance and distribution across a gradient of oligotrophic British Columbia and Yukon Territory lakes. *Int. Revue ges. Hydrobiol.*, 76, pp. 581-601

Stohl A, (2006). Characteristics of atmospheric transport into the Arctic troposphere, *J.Geophys. Res.*, 111, D11306, doi: 10.1029/2005JD006888

Strom J, Umegard J, Tørseth K, Tunved P, Hansson H-C, Holmen K, Wismann V, Herber A, Konig-Langlo G, (2003). One year of particle size distribution and aerosol chemical composition measurements at the Zeppelin Station, Svalbard, March 2000–March 2001, *Phys. Chem. Earth*, 28, pp. 1181–1190

Stumm W, and Morgan J, (1970). *Aquatic Chemistry*. Wiley Interscience, New York.

Sweerts, JP, De Beer D, Nielsen LP, Verdouw H, Van den Heuvel JC, Cohen Y and Cappenberg TE, (1990). Denitrification by sulphur oxidizing Beggiatoa spp. mats on freshwater sediments. *Nature* 344, pp. 762–763

Taylor BE, (1986). Magmatic volatiles: isotopic variation of C, H and S. In: Valley JW, Taylor HP, Jr, O~JR (eds) Stable isotopes in high temperature geological processes. *Mineralogical Society of America*, Washington, pp. 185-255

Telling J, Anesio AM, Tranter M, Irvine-Fynn T, Hodson A, Butler C, Wadham J, (2010) Nitrogen fixation on Arctic glaciers, Svalbard. *J. Geophys. Res.*, 116, G03039, 8 PP., 2011, doi:10.1029/2010JG001632

Telling J, Anesio AM, Hawkings J, Tranter M, Wadham J, Hodson A, Irvine-Fynn T, Yallop ML, (2010). Measuring rates of gross photosynthesis and net community production in cryoconite holes: a comparison of field methods. *Annals of Glaciology* 51(56), pp. 135-144

Thiemens MH, (1999). Mass-independent isotope effects in planetary atmospheres and the early Solar system. *Science* 283, pp. 341–345

Tichomirowa M, Haubrich F, Klemm W, and Matschullat J, (2007). Regional and temporal (1992–2004) evolution of air-borne sulphur isotope composition in Saxony, southeastern Germany, central Europe, *Isotopes Environ. Health Stud.*, 43, pp. 295–305,

Timperley MH, Vigor-Brown RJ, Kawashima M, and Ishigami M, (1985). Organic nitrogen compounds in atmospheric precipitation: Their chemistry and availability to phytoplankton. *Can. J. Fish. Aquat. Sci.* 42: pp. 1171-1177

Townsend-Small A, McClelland J, Max RH, Peterson B, (2011). Seasonal and hydrologic drivers of dissolved organic matter and nutrients in the upper Kuparuk River, Alaskan Arctic, *Biogeochemistry*, Vol 1-3, pp. 109-124, DOI: 10.1007/s10533-010-9451-4

Tranter M, Brown GH, Hodson A, Gurnell AM, (1996). Hydrochemistry as an indicator of the nature of subglacial drainage system structure: a comparison of Arctic and Alpine environments. *Hydrol. Process.* 10, pp. 541– 556

Tranter M, Sharp MJ, Lamb H, Brown GH, Hubbard BP, Willis IC, (2002). Geochemical weathering at the bed of Haut Glacier d’Arolla, Switzerland - a new model. *Hydrolog. Process.* 16,pp. 959–993

Tranter M, Skidmore M, Wadham J, (2005). Hydrological controls on microbial communities in subglacial environments. *Hydrol Process* 19,pp. 995–998

Tye AM, Young SD, Crout NMJ, West HM, Stapleton LM, Poulton PR, Laybourn-Parry J, (2005) The fate of N-15 added in high Arctic tundra to mimic increased inputs of atmospheric nitrogen released from a melting snowpack. *Glob Change Biol* 11:1640–1654

Tye, AM, and Heaton THE, (2007). Chemical and isotopic characteristics of weathering and nitrogen release in non-glacial drainage waters on Arctic tundra. *Geochimica et Cosmochimica Acta*, 71, pp. 4188-4205

Vaida V, Kjaergaard HG, Hintze PE, Donaldson DJ, (2003). Photolysis of sulfuric acid vapor by visible solar radiation, *Science*, 299, pp. 1566– 1568

Vairavamurthy A, Andreae MO, Iverson RL, (1985). Biosynthesis of dimethylsulfide and dimethylpropiothetin by *Hymenomonas carterae* in relation to sulfur source and salinity variations. *Limnol. Oceanogr.*,30, pp. 59-70

van de Wal RSW, Wild M, (2001). Modelling the response of glaciers to climate change, applying volume-area scaling in combination with a high resolution GCM. *Clim Dyn* 18, pp. 359–366

Vatne G, Etzelmiiller B, Sollid JL and OdegSrd. RS, (1995). Hydrology of a polythermal glacier, Erikbreen, northern Spitsbergen. *Nordic Hydrology*26, pp. 169-190

Wadham JL Bottrell S, Tranter M and Raiswell R, (2004), Stable isotope evidence for microbial sulphate reduction at the bed of a polythermal high Arctic glacier, *Earth Planet. Sci. Lett.*, 219, pp. 341–355, doi:10.1016/S0012-821X(03)00683-6.

Wadham JL, RJ Cooper, Tranter M, and Bottrell S, (2007). Evidence for widespread anoxia in the proglacial zone of an Arctic glacier, *Chem. Geol.*, 243, pp. 1–15, doi:10.1016/j.chemgeo.2007.04.010.

Wadham JL, Tranter M, Tulaczyk S and Sharp M, (2008). Subglacial methanogenesis: a potential climatic amplifier? *Global Biogeochem. Cycles* 22, GB2021

Wadham JL, Tranter M, Skidmore M, Hodson AJ, Priscu J, Lyons WB, Sharp M, Wynn P & Jackson M, (2010). Biogeochemical weathering under ice: Size matters. *Global Biogeochemical Cycles*, Vol. 24, GB3025, doi:10.1029/2009GB003688

Waddington ED, Cunningham J, Harder S, (1996). The effects of snow ventilation on chemical concentrations. In: Wolff, E.W., and R.C. Bales (editors). *Chemical Exchange Between the Atmosphere and Polar Snow. NATO ASI Series Vol. 143*, Springer, pp. 403–451

Waser NAD, Harrison PJ, Nielsen B, Calvert SE, Turpin DH, (1998). Nitrogen isotope fractionation during the uptake and assimilation of nitrate, nitrite, ammonium, and urea by a marine diatom. *Limnol Oceanogr* 43, pp. 215–224

Watts JE, (1969). Climates of China and Korea. In: Climates of Northern and Eastern Asia(ed. H. Arakawa). *World Survey of Climatology*. Vol. 8. Amsterdam: Elsevier Scientific Publishing Company, pp. 1–74

Weathers KC, Lovett GM, Likens GE, Caraco NFM, (2000). Cloudwater inputs of nitrogen to forest ecosystems in southern Chile: forms, fluxes and sources. *Ecosystems* 3, pp. 590–595

Weitemeyer K and Buffett BA, (2006). Accumulation and release of methane from clathrates from below the Laurentide and Cordilleran ice sheets. *Glob Planet Change* 53, pp. 176–187

Welch KA, Lyons WB, Graham E, Neumann K, Thomas JM, Mikesell D, (1996). Determination of major element chemistry in terrestrial waters from Antarctica by ion chromatography. *J. Chromatogr.* A739, pp. 257– 263

Weston RE, (1999). Anomalous or mass-independent isotope effects. *Chem. Rev.* 99, pp.2115–2136

Wexler SK, Hiscock KM and Dennis PF, (2011). Catchment-scale quantification of hyporheic denitrification using an isotopic and solute flux approach. *Environmental Science and Technology*, 45, pp. 3967-3973

Williams LB and Ferrell RE, (1991). Ammonium substitution in illite during maturation of organic matter. *Clays CZay Minerals* 39, pp. 400-408.

Williams LB, Wilcoxon BR, Ferrell Jr, RE, Sassen R, (1993). Diagenesis of ammonium during hydrocarbon maturation and migration, Wilcox Group, Louisiana, USA. *Appl. Geochem.* 7, pp. 123–134

Williamson MA and Rimstidt JD, (1994). The kinetics and electrochemical rate-determining step of aqueous pyrite oxidation. *Geochimica et Cosmochimica Acta* 58, pp. 5443–5454.

Williams MW, Brooks PD, Mosier AR & Tonnessen KA, (1996). Mineral N transformations in and under seasonal snow in a high elevation catchment, Rocky Mountains, USA. *Water Resources Research* 32, pp.3175–3185

Wilson TRS, (1975). Salinity and the major elements of seawater. In “Chemical Oceanography” 2nd edn, Vol. I. (J.P. Riley and G. Skirrow, eds) *Academic press*, London.

Wynn PM, (2004). The provenance and fate of nitrogen in Arctic glacial melt waters: an isotopic approach. PhD Thesis, The University of Sheffield, Sheffield, 247p.

Wynn PM, Hodson AJ, Heaton THE, (2006). Chemical and isotopic switching within the subglacial environment of a High Arctic glacier. *Biogeochemistry* 78:173–193

Wynn PM, Hodson AJ, Heaton THE, Chenery SR, (2007). Nitrate production beneath a High Arctic glacier, Svalbard, *Chemical Geology*, 244 (1-2), pp. 88-102

Xiang SR, Shang TC, Chen Y, Yao TD, (2009b). Deposition and post-deposition mechanisms as possible drivers of microbial population variability in glacier ice. *FEMS Microbiol. Ecol.* 70, pp. 165-176.

Xue D, Botte J, De Baets B, Accoe F, Nestler A, Taylor P, Van Cleemput O, Berlund M and Boeckx P, (2009) Present limitations and future prospects of stable isotope

methods for nitrate source identification in surface- and groundwater. *Water Research*, 43, pp. 1159-1170

Yamagata S, Kobayashi D, Ohta S, Muraio N, Shiobara M, Wada M, Yabuki M, Konishi H, Yamanouchi T, (2009). Properties of aerosols and their wet deposition in the arctic spring during ASTAR2004 at Ny-Alesund, Svalbard. *Atmospheric Chemistry and Physics* 9, 261-270

Yang Q, Mayewski PA, Whitlow S, Twickler M, Morrison M, Talbot R, Dibb JE, Linder E, (1995). Global perspective of nitrate flux in ice cores, *J. Geophys. Res.*, 100(D3), pp. 5113–5121

Yao T, Xiang S, Zhang X, Wang N, Wang Y, (2006). Microorganisms in the Malan ice core and their relation to climatic and environmental changes, *Global Biogeochem. Cycles*, 20, GB1004, doi:10.1029/2004GB002424

Yung YL and Miller CE, (1997). Isotopic fractionation of stratospheric nitrous oxide. *Science* 278, pp. 1778-1780

Zhang Q and Anastasio C, (2001). Chemistry of fog waters in California's Central Valley, 3, Concentrations and speciation of organic and inorganic nitrogen, *Atmos. Environ.*, 35, pp. 5629– 5643

Zhao, FJ, Spiro B, Poulton PR, McGrath SP, (1998). Use of sulfur isotope ratios to determine anthropogenic sulfur signals in a grassland ecosystem. *Environmental Science and Technology*, 32, pp. 2288–2291

APPENDIX

Table AI. Solute chemistry of five supraglacial snow-pit samples collected in early June 2009 (n.a = data not available).

Site	Na ⁺ (mg/L)	K ⁺ (mg/L)	Ca ²⁺ (mg/L)	Mg ⁺² (mg/L)	NH ₄ ⁺ -N (µg/L)	NO ₃ ⁻ -N (µg/L)	DON (µg/L)	DOC (mg/L)	DOC/DON (molar ratio)	SO ₄ ²⁻ (mg/L)	HCO ₃ ⁻ (mg/L)	Cl ⁻ (mg/L)	F ⁻ (µg/L)
SG1	0.89	0.07	0.85	0.43	19.8	17.8	23.3	0.26	13.01	0.34	3.49	1.52	< 1
SG2	1.62	0.10	0.68	0.58	17.3	26.0	28.3	0.39	16.07	0.47	2.97	2.82	< 1
SG3	1.57	0.11	0.74	0.56	13.6	28.8	32.7	1.41	50.30	0.55	2.97	2.65	< 1
SG4	1.13	0.07	0.55	0.42	15.6	21.2	32.5	0.35	12.56	0.13	3.16	1.89	< 1
SG5	3.20	0.16	1.22	0.86	14.8	28.4	n.a.	n.a.	n.a.	0.98	5.36	5.74	6

Table AII. Solute chemistry parameters of five supraglacial snow-pit samples collected in early late May 2010 (n.a = data not available)

Sites	Na ⁺ (mg/L)	K ⁺ (mg/L)	Mg ²⁺ (mg/L)	Ca ²⁺ (mg/L)	NH ₄ ⁺ -N (µg/L)	NO ₃ ⁻ -N (µg/L)	DON (µg/L)	DOC (mg/L)	DOC/DON (molar ratio)	SO ₄ ²⁻ (mg/L)	Cl ⁻ (mg/L)	F ⁻ (mg/L)
SG1	0.929	0.080	0.429	1.059	19.4	20.3	80.3	0.206	3.0	0.280	1.470	1.47
SG2	1.082	0.055	0.473	0.456	23.6	12.9	93.6	0.465	5.8	0.300	0.860	0.86
SG3	0.677	0.053	0.361	0.463	26.1	n.a.	n.a.	0.165	n.a.	0.260	1.100	1.10
SG4	0.690	0.043	0.383	0.591	17.8	30.0	n.a.	n.a.	n.a.	0.308	1.218	1.22
SG5	0.636	0.049	0.358	0.527	18.4	29.3	n.a.	n.a.	n.a.	0.282	1.060	1.06

Table AIII. Solute chemistry parameters of the MLE1, MLW1 and UPW during summer 2009 (n.a = data not available).

DOY	Na ⁺ (mg/L)	K ⁺ (mg/L)	Ca ²⁺ (mg/L)	Mg ⁺² (mg/L)	NH ₄ ⁺ -N (µg/L)	NO ₃ ⁻ -N (µg/L)	DON (µg/L)	DOC (mg/L)	DOC/DON (molar ratio)	SO ₄ ²⁻ (mg/L)	HCO ₃ ⁻ (mg/L)	Cl ⁻ (mg/L)	F ⁻ (µg/L)
MLE Site													
184	1.640	0.62	10.50	1.440	14.4	40.1	n.a.	n.a.	n.a.	8.30	29.80	2.44	22
186	2.010	0.76	9.84	1.630	73.3	50.9	n.a.	4.30	n.a.	6.48	39.70	2.92	27
188	2.830	5.29	11.20	1.210	37.5	149.8	n.a.	n.a.	n.a.	11.90	34.60	3.67	26

190	1.900	234	10.00	1.470	4.4	35.9	61.9	4.51	84.95	11.30	26.40	3.35	19
192	1.610	0.59	10.70	1490	3.2	34.8	7.6	3.25	501.18	7.97	30.80	2.48	16
194	1.740	1.25	13.40	2.630	3.7	33.7	27.5	2.78	117.93	12.70	40.50	2.16	56
196	5.420	1.21	13.30	3.130	3.4	23.0	50.3	1.02	23.67	14.10	37.60	9.53	50
198	3.330	1.26	16.50	3.110	< 0.1	< 0.1	70.3	0.71	11.32	15.60	48.00	4.97	70
201	1.210	0.86	13.10	2.180	1.9	20.4	34.3	0.89	30.25	12.00	37.10	1.76	73
203	1.760	1.18	15.70	2.890	1.5	10.0	42.8	0.29	7.88	16.70	43.20	2.57	80
233	1.110	1.00	12.60	1.960	4.9	22.4	n.a.	2.47	n.a.	13.20	34.00	1.19	52
239	2.180	1.40	19.80	3.790	2.7	40.3	< 0.1	4.56	n.a.	26.00	50.20	2.22	144
245	1.420	1.08	15.40	2.920	4.4	21.9	52.6	3.37	74.50	22.80	35.60	1.43	73
250	1.010	0.78	11.30	2.050	3.6	15.8	0.4	< 2	n.a.	15.20	27.30	1.13	29
MLW Site													
188	1.88	0.91	10.70	1.25	28.0	50.8	n.a.	2.17	n.a.	4.78	39.30	2.84	22
190	1.21	0.49	7.72	1.07	7.7	34.7	n.a.	3.25	n.a.	3.99	24.60	1.79	22
192	1.12	0.36	7.95	0.95	4.9	34.9	1.6	0.83	593.28	5.43	22.30	1.80	28
194	1.09	0.73	11.60	1.71	1.8	24.9	20.8	0.71	39.76	8.90	34.30	1.39	67
196	1.32	0.68	9.88	1.59	4.0	16.8	< 0.1	0.22	n.a.	7.46	29.90	1.86	14
198	1.17	0.59	10.40	1.41	1.9	4.5	111.7	0.29	3.02	8.05	40.10	1.62	31
201	1.08	0.64	10.30	1.50	2.9	9.6	36.0	0.31	10.04	9.14	28.80	1.37	13
203	1.22	0.76	13.60	1.84	38.9	17.9	< 0.1	1.41	n.a.	12.20	36.90	1.65	38
233	0.80	0.80	11.60	1.60	4.2	30.8	n.a.	3.86	n.a.	12.10	29.90	0.85	27
239	1.36	1.31	19.60	3.48	2.9	30.4	11.3	0.98	100.9	31.80	40.00	1.58	40
245	0.91	0.83	10.70	1.98	3.6	23.6	3.0	2.94	1162.7	17.00	22.70	1.16	17
250	0.82	0.80	11.60	1.74	4.4	20.5	58.7	2.31	45.88	12.60	29.90	8.80	17
UPW Site													
198	1.61	0.59	17.10	1.49	3.2	66.8	n.a.	0.30	n.a.	19.60	13.40	3.64	141
201	2.10	1.47	15.50	3.14	10.2	61.6	<0.1	1.30	n.a.	19.00	25.90	3.85	119
203	2.67	1.51	13.70	3.67	0.3	58.6	< 0.1	0.67	n.a.	17.80	39.50	4.09	117
205	1.93	1.25	11.00	3.13	1.1	37.3	< 0.1	0.19	n.a.	14.30	46.40	2.91	142
233	2.10	1.47	14.80	3.22	4.6	38.0	10.8	4.16	449.87	18.90	40.80	2.19	153
239	2.53	1.45	15.10	3.56	< 0.1	46.2	n.a.	3.57	n.a.	19.40	43.20	2.65	177
245	2.43	1.60	16.60	3.88	< 0.1	42.8	1.4	5.03	4188.55	26.40	40.80	2.44	142
250	2.33	1.60	17.10	3.90	< 0.1	40.5	11.6	1.13	113.35	26.10	42.60	2.46	148

Table AIV. Solute chemistry at the seven proglacial stream sites during summer 2010 (n.a = data not available).

Date (DOY)-Sites	Na ⁺ (mg/L)	K ⁺ (mg/L)	Mg ²⁺ (mg/L)	Ca ²⁺ (mg/L)	NH ₄ ⁺ -N (μg/L)	NO ₃ ⁻ -N (μg/L)	DON (μg/L)	DOC (mg/L)	DOC/DON (molar ratio)	SO ₄ ²⁻ (mg/L)	Cl ⁻ (mg/L)	F ⁻ (mg/L)
MLU-186	2.34	1.91	3.87	8.24	11.6	22.7	45.7	0.165	4.2	23.44	2.68	0.17
MLU-198	1.57	1.15	2.73	14.85	4.4	52.4	43.1	<0.02	n.a.	20.68	1.85	0.15
MLU-207	1.29	1.01	2.53	3.56	4.1	32.4	73.5	1.890	30.0	15.88	1.33	0.12
MLU-218	1.34	0.98	2.64	18.10	0.0	21.9	98.1	0.237	2.8	17.01	1.46	0.14
MLU-227	2.13	1.45	4.22	6.18	3.0	37.9	89.1	1.735	22.7	38.09	2.10	0.20
MLE3-186	0.33	0.30	0.41	7.75	6.8	14.7	48.5	<0.02	n.a.	1.47	0.51	0.00
MLE3-198	0.28	0.27	0.41	7.34	8.3	24.1	67.6	0.382	6.6	2.09	0.52	0.00
MLE3-207	0.28	0.38	0.48	9.45	7.8	14.6	97.6	0.093	1.1	3.20	0.45	0.01
MLE3-218	0.26	0.46	0.58	12.24	5.2	1.0	93.8	1.115	13.9	5.66	0.56	0.01
MLE3-227	0.90	1.00	1.87	6.25	0.0	31.0	69.0	0.082	1.4	16.93	1.51	0.06
MLE2-186	1.25	1.15	2.22	12.35	4.6	45.2	20.2	<0.02	n.a.	13.55	1.51	0.11
MLE2-198	0.95	0.74	1.64	4.56	5.7	26.6	57.7	0.186	3.8	11.32	1.23	0.10
MLE2-207	0.62	0.56	1.25	13.73	5.4	20.1	54.6	0.010	0.2	9.20	0.81	0.08
MLE2-218	0.66	0.59	1.37	15.91	3.8	7.4	98.8	0.217	2.6	11.95	0.80	0.09
MLE2-227	1.82	1.34	3.78	8.76	0.0	45.4	74.6	0.857	13.4	26.86	1.85	0.16
MLE1-186	1.31	1.23	2.43	2.36	6.4	42.9	30.7	<0.02	n.a.	14.13	1.57	0.10
MLE1-198	1.22	0.81	1.67	10.09	10.0	28.8	101.2	0.816	9.4	10.44	1.14	0.09
MLE1-207	0.66	0.61	1.35	15.94	7.8	22.5	29.7	<0.02	n.a.	10.12	0.81	0.08
MLE1-218	0.70	0.62	1.49	19.32	5.4	7.7	86.8	0.754	10.1	12.77	0.80	0.08
MLE1-227	1.93	1.46	4.42	14.02	0.0	28.5	81.5	2.158	30.9	30.66	1.83	0.15
MLW3-186	0.93	0.56	1.29	10.71	5.8	24.6	69.6	<0.02	n.a.	7.59	1.03	0.06
MLW3-198	0.26	0.11	0.20	3.26	7.5	10.2	32.3	<0.02	n.a.	0.27	0.46	0.00
MLW3-207	0.21	0.13	0.24	3.73	4.1	20.4	35.5	<0.02	n.a.	0.29	0.34	0.00
MLW3-218	0.18	0.13	0.21	3.55	3.4	3.0	103.7	0.971	10.9	0.30	0.29	0.00
MLW3-227	0.69	0.32	0.54	8.29	0.0	28.8	61.2	<0.02	n.a.	2.18	1.26	0.05
MLW2-186	0.70	0.62	1.28	11.59	6.3	21.4	52.2	<0.02	n.a.	7.73	0.96	0.06
MLW2-198	0.44	0.35	0.72	7.66	5.2	11.1	43.7	<0.02	n.a.	2.94	0.51	0.05

MLW2-207	0.79	0.39	0.86	8.56	4.3	18.9	96.8	0.867	10.5	4.30	0.72	0.05
MLW2-218	0.39	0.35	0.74	7.24	3.7	2.8	53.5	<0.02	n.a.	3.36	0.39	0.01
MLW2-227	1.18	1.23	3.32	10.26	0.0	31.2	48.8	<0.02	n.a.	24.17	1.28	0.08
MLW1-186	0.79	0.74	1.67	18.45	7.4	24.6	48.0	<0.02	n.a.	13.34	1.12	0.02
MLW1-198	0.49	0.52	1.16	10.87	5.8	10.2	74.0	<0.02	n.a.	6.81	0.61	0.05
MLW1-207	0.46	0.51	1.01	11.34	3.1	20.4	76.5	0.661	10.1	5.09	0.50	0.05
MLW1-218	0.42	0.49	1.07	10.13	5.7	3.0	51.4	<0.02	n.a.	5.69	0.47	0.01
MLW1-227	1.66	1.55	4.54	20.53	4.0	28.8	37.3	0.299	9.4	34.27	1.44	0.09

Table AV. Isotopic compositions of five supraglacial snow-pit samples collected in late spring 2009 and 2010.

Snow sites	2009			2010		
	$\delta^{15}\text{N-NO}_3$	$\delta^{18}\text{O-NO}_3$	$\delta^{18}\text{O-H}_2\text{O}$	$\delta^{15}\text{N-NO}_3$	$\delta^{18}\text{O-NO}_3$	$\delta^{18}\text{O-H}_2\text{O}$
SG1	-7.7	+79.6	n.a.	-13.05	+88.08	-10.71
SG2	-7.4	+76.1	-12.6	-14.31	+90.19	-10.85
SG3	-9.5	+78.0	-12.4	-13.55	+87.28	-10.40
SG4	-8.4	+77.4	-12.8	-14.83	+90.08	-10.91
SG5	-10.6	+79.5	-13.4	-14.95	+89.71	-11.61

Table AVI. Isotopic compositions of stream samples during summer 2009.

DOY	MLE					MLW					UPW				
	$\delta^{15}\text{N-NO}_3$	$\delta^{18}\text{O-NO}_3$	$\delta^{34}\text{S-SO}_4$	$\delta^{34}\text{O-SO}_4$	$\delta^{18}\text{O-H}_2\text{O}$	$\delta^{15}\text{N-NO}_3$	$\delta^{18}\text{O-NO}_3$	$\delta^{34}\text{S-SO}_4$	$\delta^{34}\text{O-SO}_4$	$\delta^{18}\text{O-H}_2\text{O}$	$\delta^{15}\text{N-NO}_3$	$\delta^{18}\text{O-NO}_3$	$\delta^{34}\text{S-SO}_4$	$\delta^{34}\text{O-SO}_4$	$\delta^{18}\text{O-H}_2\text{O}$
	(‰)	(‰)	(‰)	(‰)	(‰)	(‰)	(‰)	(‰)	(‰)	(‰)	(‰)	(‰)	(‰)	(‰)	(‰)
184	+5.3	+23.6	+12.2	-7.9	-13.6	n.a.	n.a.	n.a.	n.a.	n.a.	n.a.	n.a.	n.a.	n.a.	n.a.
186	-4.5	+48.0	+6.6	-7.8	-12.8	n.a.	n.a.	n.a.	n.a.	-13.6	n.a.	n.a.	n.a.	n.a.	n.a.
188	n.a.	n.a.	+11.2	+4.7	-12.7	-7.4	+46.8	n.a.	n.a.	-12.6	n.a.	n.a.	n.a.	n.a.	n.a.
190	n.a.	n.a.	+9.7	-3.6	-13.0	-4.5	+44.3	+16.7	-5.1	-14.0	n.a.	n.a.	n.a.	n.a.	n.a.
192	-7.8	+64.4	+9.8	-10.8	-13.5	+0.6	+13.4	+11.1	-9.2	-12.4	n.a.	n.a.	n.a.	n.a.	n.a.
194	-2.0	+39.4	+13.0	-8.8	-13.6	+11.4	+32.3	+16.1	-8.5	n.a.	n.a.	n.a.	n.a.	n.a.	n.a.
196	n.a.	n.a.	+14.5	-6.8	-12.6	n.a.	n.a.	+15.3	-7.8	-13.1	n.a.	n.a.	n.a.	n.a.	n.a.
198	n.a.	n.a.	+13.3	-7.6	-13.5	n.a.	n.a.	+15.5	-2.9	-13.5	-4.8	+32.3	n.a.	n.a.	n.a.
201	+13.1	+34.7	+13.5	-6.4	-12.6	n.a.	n.a.	+15.4	-6.3	-12.2	n.a.	n.a.	+15.6	-6.8	-12.8
203	+10.4	+34.4	+13.4	-7.7	-12.6	n.a.	n.a.	+15.5	-7.3	-12.3	n.a.	n.a.	+15.8	-6.2	-13.7
205	n.a.	n.a.	n.a.	n.a.	n.a.	n.a.	n.a.	n.a.	n.a.	n.a.	-7.3	+36.4	+15.8	0.60	-12.8
233	n.a.	n.a.	n.a.	n.a.	n.a.	+0.8	+12.6	n.a.	n.a.	n.a.	-3.3	+21.3	n.a.	n.a.	n.a.
239	-3.2	+21.0	n.a.	n.a.	n.a.	-0.3	+7.5	n.a.	n.a.	n.a.	-3.6	+24.0	n.a.	n.a.	n.a.
245	+14.9	+17.9	n.a.	n.a.	n.a.	+1.6	+6.8	n.a.	n.a.	n.a.	-3.1	+28.5	n.a.	n.a.	n.a.
250	+13.9	+17.5	+12.2	-7.9	n.a.	+5.9	+3.8	n.a.	n.a.	n.a.	-3.1	+16.2	n.a.	n.a.	n.a.

Table VII. Isotopic compositions of streams during summer 2010.

Date (DOY)-Sites	$\delta^{15}\text{N-NO}_3$ (‰)	$\delta^{18}\text{O-NO}_3$ (‰)	$\delta^{34}\text{S-SO}_4$ (‰)	$\delta^{34}\text{O-SO}_4$ (‰)	$\delta^{18}\text{O-H}_2\text{O}$ (‰)
MLU-186	+6.24	+45.37	+15.7	-5.9	-11.74
MLU-198	-6.42	+42.66	+16.2	-5.1	-11.35
MLU-207	-5.51	+37.96	+15.9	-4.8	-10.76
MLU-218	-4.91	+30.21	+15.9	-4.2	-10.95
MLU-227	-3.51	+25.33	+16.4	-5.1	-11.32

MLE3-186	-9.62	+73.53	n.a.	n.a.	-10.57
MLE3-198	-7.65	+66.43	n.a.	n.a.	-10.16
MLE3-207	n.a.	n.a.	n.a.	n.a.	-9.54
MLE3-218	n.a.	n.a.	n.a.	n.a.	-10.48
MLE3-227	-2.53	+14.50	+19.4	-5.1	-10.69
MLE2-186	-7.81	+51.63	+15.1	-5.7	-11.39
MLE2-198	-7.41	+46.49	+15.5	-5.1	-10.83
MLE2-207	-6.07	+40.31	+15.3	-5.4	-10.16
MLE2-218	-5.74	+31.56	+15.6	-4.2	-10.54
MLE2-227	-4.42	+25.51	+15.2	-6.1	-11.33
MLE1-186	-7.85	+50.71	+13.7	-1.9	-11.10
MLE1-198	-7.11	+46.21	+14.7	-3.2	-10.62
MLE1-207	-2.19	+39.31	+14.9	-4.0	-9.89
MLE1-218	-4.93	+30.99	+15.0	-4.8	-10.66
MLE1-227	-3.07	+24.12	+13.3	-5.2	-11.17
MLW3-186	-7.32	+55.68	n.a.	n.a.	-10.75
MLW3-198	-4.73	+59.81	n.a.	n.a.	-9.89
MLW3-207	-7.01	+43.20	n.a.	n.a.	-9.51
MLW3-218	n.a.	n.a.	n.a.	n.a.	-10.64
MLW3-227	-2.01	+21.00	n.a.	n.a.	-11.36
MLW2-186	-6.77	+50.09	n.a.	n.a.	-10.71
MLW2-198	-7.92	+52.51	n.a.	n.a.	-10.25
MLW2-207	-3.56	+39.17	n.a.	n.a.	-9.80
MLW2-218	n.a.	n.a.	n.a.	n.a.	-10.47
MLW2-227	-0.52	+7.58	+11.9	-10.1	-10.73
MLW1-186	-6.47	+46.87	+16.3	-7.7	-10.54
MLW1-198	-5.58	+43.81	n.a.	n.a.	-10.23
MLW1-207	-2.36	+29.67	n.a.	n.a.	-9.78
MLW1-218	n.a.	n.a.	n.a.	n.a.	-10.55
MLW1-227	-0.17	+6.98	+13.8	-9.5	-10.52